UTILISATION OF NATURAL RUBBER LATEX WASTE AS A POTENTIAL FILLER IN SYNTHETIC ELASTOMERS AND PLASTICS

THESIS SUBMITTED TO
THE MAHATMA GANDHI UNIVERSITY
IN PARTIAL FULFILMENT OF THE REQUIREMENTS FOR
THE AWARD OF THE DEGREE OF

DOCTOR OF PHILOSOPHY

IN POLYMER CHEMISTRY
UNDER THE FACULTY OF SCIENCE

BY

GEORGE MATHEW

DEPARTMENT OF CHEMISTRY
CMS COLLEGE, KOTTAYAM
KERALA, INDIA

MAY 2002

Dedicated to My Beloved Parents

राष्ट्रीय रासायनिक प्रयोगशाला (वैज्ञानिक तथा औद्योगिक अनुसंधान परिषद) पुणे - 411 008.

NATIONAL CHEMICAL LABORATORY (COUNCIL OF SCIENTIFIC & INDUSTRIAL RESEARCH) PUNE 411 008 (INDIA)

टेलीफोन 91-020-5893315-18 तार : केमेस्ट्री टेलेक्स 0145 - 7266 फैक्स 91-020-5893355 ई-मेल prs @ ems ncl res in
TELEPHONE 91-020-5893300 GRAM : CHEMISTRY TELEX 0145 - 7653 FAX : 91-020-5893761 E-MAIL : rh @ ems ncl res in
91-020-5893619
91-020-5893212

CERTIFICATE

This is to certify that the thesis entitled 'UTILISATION OF NATURAL RUBBER LATEX WASTE AS A POTENTIAL FILLER IN SYNTHETIC ELASTOMERS AND PLASTICS' is an authentic record of the research work carried out by Mr. George Mathew under my supervision and guidance, in partial fulfillment of the requirements for the award of the degree of Doctor of Philosophy in Polymer Chemistry, under the Faculty of Sciences, Mahatma Gandhi University, Kottayam. The work presented in this thesis has not been submitted for any other degree or diploma earlier. It is also certified that Mr. George Mathew has fulfilled the course requirements and passed the qualifying examination for the Ph.D. degree of Mahatma Gandhi University.

February 2001

(R.P.Singh)
Scientist E – II
Polymer Chemistry Division
Tel. & Fax: 020-5893234
E-mail : singh@poly ncl res in

MAHATMA GANDHI UNIVERSITY

Dr. SABU THOMAS B.Tech., Ph.D., CChem FRSC
Reader in Polymer Science & Technology
SCHOOL OF CHEMICAL SCIENCES
MAHATMA GANDHI UNIVERSITY
Priyadarshini Hills P.O.
Kottayam - 686 560
Kerala, India

E-mail : sabut@vsnl.com (Off.)
E-mail : sabuthom@satyam.net.in (Res.)
Phone Off. : 91-481 598303 (Direct)
91-481 598015
Res. : 91-481 590357
91-481 597914
Fax : 91-481 561190
91-481 561800

CERTIFICATE

This is to certify that the thesis entitled **Utilisation of Natural Rubber Latex Waste As A Potential Filler In Synthetic Elastomers and Plastics** is an authentic record of the research work carried out by **Mr. George Mathew** under the joint supervision of Dr. R.P.Singh and myself in partial fulfilment of the degree of **Doctor of Philosophy in Polymer Chemistry** under the Faculty of Science, Mahatma Gandhi University. The work presented in the thesis has not been submitted for any other degree or diploma earlier. It is also certified that Mr. George Mathew has fulfilled the course requirements and passed the qualifying examination for the Ph.D degree of the university.

Priyadarshini Hills
April 2002

Dr. Sabu Thomas

DECLARATION

I, George Mathew, hereby declare that the thesis entitled **Utilisation of Natural Rubber Latex Waste As a Potential Filler in Synthetic Elastomers and Plastics** is a bona fide record of the research work done by me and that no part of this thesis has not been presented earlier for any degree or diploma of any other university.

GEORGE MATHEW
Research Fellow
Dept. of Chemistry
C.M.S. College, Kottayam

Kottayam
May 2002

ACKNOWLEDGEMENTS

Thanks to all the scholarly professors and the colleagues who have creatively involved in this humble work and shared me their vast knowledge for the development of this thesis.

George Mathew

GLOSSARY OF TERMS

α	-	Swelling coeffecient
β	-	Lattice constant
χ	-	Interaction parameter
ε	-	Elongation at break
δ_p	-	Solubility parameter of polymer
δ_s	-	Solubility parameter of solvent
ρ_s	-	Density of solvent
$\Im$	-	Shear stress
σ	-	Stress
γ	-	Shear rate
η	-	Viscosity
υ_{phys}	-	Crosslink density from stress-strain curves
ρ_p	-	Density of polymer
ϕ	-	Volume fraction of filler
λ	-	Extension ratio
∂	-	Crosslink density from swelling studies

ASTM	-	American Society of Testing Materials
CBS	-	N-cyclohexyl-2-benzothiazyl sulphenamide
CGR	-	Cryoground rubber
ClLW	-	Dichlorocarbene modified latex waste
CRI	-	Cure rate index
CS	-	Contact surface
CTAB	-	Cetyl trimethyl ammonium bromide
CV	-	Conventional vulcanisation system
DCP	-	Dicumyl peroxide
DSC	-	Differential scanning calorimetry
DTA	-	Derivative thermogravimetry
DMA	-	Dynamic mechanical Analysis
DPG	-	Diphenyl guanidine
ENR	-	Epoxidised natural rubber
EPDM	-	Ethylene propylene diene terpolymer
E'	-	Storage modulus
E"	-	Loss modulus
ELW	-	Epoxidised latex waste
EV	-	Effecient vulcanisation system
FTIR	-	Fourier transform infrared spectroscopy
HAF	-	High abrasion furnace black
HDPE	-	High density polyethylene
HSR	-	High styrene resin

IRHD	-	International rubber hardness degrees
ISNR – 5	-	Indian standard natural rubber – 5 grade
LDPE	-	Low density polyethylene
LLDPE	-	Linear low density polyethylene
LED	-	Light emitting diode
LW	-	Latex waste
MA-PP or PP-g-MA	-	Maleic anhydride grafted PP
MBTS	-	Mercaptobenzothiazyl sulphenamide
Mc	-	Molecular weight between crosslinks
MFI	-	Melt flow index
MIR	-	Mid IR
NBR	-	Acrylonitrile-co-butadiene rubber
NCS	-	Non contact surface
NRT	-	National Recovery Technologies
NR	-	Natural rubber
Ph-PP or PP-g-Ph	-	Phenolic grafted PP
PP	-	Polypropylene
PS	-	Polystyrene
PET	-	Polyethylene terepthalate
PE	-	Polyethylene
php	-	Parts per hundred plastic
phr	-	Parts per hundred rubber
PP	-	Polypropylene
PVC	-	Poly vinyl chloride
Qt	-	Mole % uptake
$Q\alpha$	-	Equilibrium mole % uptake
SDT	-	Simultaneous difference temperature
SEM	-	Scanning electron microscopy
SBR	-	Styrene butadiene rubber
SMC	-	Sheet moulding compound
SSSE	-	Solid state shear extrusion
TDQ	-	2, 2, 4 – trimethyl -1,2-dihydroquinoline
Tg	-	Glass transition temperature
TMTD	-	Tetra methyl thiuram disulphide
TGA	-	Thermogravimetric analysis
TPE	-	Thermoplastic elastomer
tan δ	-	Dissipation factor
tan δ_{max}	-	Damping maximum
UTM	-	Universal testing machine
VYDAR	-	Vinyl detection and removal
Vi	-	Volume fraction of component i
XRF	-	X-ray flourascence
XRD	-	X-ray flourascence
ZDEC	-	Zinc diethyl dithio carbamate

CONTENTS

Chapter 2
Materials and Experimental Details 39

Chapter 1

CHAPTER 1

INTRODUCTION

ABSTRACT

Owing to strict regulations in the quality of most of the polymer products, the formation of rejects from polymer industries is considerably high. Since, these materials are stable to most common degrading agencies, their decomposition is a very slow process. The open burning of these rejects creates serious environmental problems due to the release of zinc compounds into the atmosphere. This introduction chapter addresses the issue of accumulated polymer rejects, the need of their recycling and the methods to recycle them successfully. The metamorphosis of the polymer recycling in the world, different aspects of recycling and various steps for recycling such as sorting, separation, size reduction etc. have been described. Special emphasis has been given to plastic recycling by various methods, rubber recycling by reclamation process and tyre recycling. As this thesis is mainly concerned with the recycling of natural rubber condom rejects, a review of previous research works in the recycling of gloves rejects, micro cellular solid waste / latex form etc. also have been included. Besides, a brief note which describes the work in this thesis has been included for a quick reference.

CHAPTER 1

INTRODUCTION

Polymers touch us often in our everyday life and activities in the form of several industrial / handmade products. Generally, the fate of an industrial product is decided by its efficiency to satisfy some conditions such as, it must be efficient (fit for the purpose), worthy of its price (value for money) and safe with an emotional factor (feel good factor). Polymers have the outstanding ability and attraction to fulfil these conditions and therefore a large number of polymer products are currently in use, ranging from footwear to space vehicles. Owing to strict regulations in the quality of most of these polymer products, the formation of rejects from these industries is considerably high. Since these materials are stable to the common degrading agencies such as heat, light, chemicals and weathering conditions, their decomposition takes several decades to complete. Simple dumping of such wastes in some free lands will debase the quality of the soil while their open burning will create serious ecological problems such as release of zinc compounds to the atmosphere[1]. Therefore it is a necessity of the present time that these polymer rejects must be recycled. The huge disposal of waste that pours annually into municipal solid waste streams is a major problem in industrial countries worldwide[2]. This can be visualized in **Figure 1.1**, which shows the massive stockpiles of scrap tires. Such as accumulation of waste tires provides ideal breeding grounds for rats and disease carrying mosquitoes. A fire hazard leading to enormous environmental pollution also is a possibility. Therefore, the most important objective of recycling is saving of resources.

In the present days of raw material shortage, the polymer industries should consider the polymer rejects as a raw material rather than as a disposal problem. Over the past two decades, the polymer community had been uttering and hearing the words 'recover', 'recycle' and 'reuse' frequently. Even though most polymer industries were in favour of recycling polymer rejects, only a minority of the polymer waste could be recycled. This is because the success of recycling mainly depends on the willingness of the citizens to accept changes in their life styles. Most of the citizens on an individual basis are happy to burn any amount of oil for their enjoyment but they normally refuse to accept

that 4% of a barrel should be burned after a useful service to the society. The willingness of the citizens of a country for recycling is dependent on several factors such as the physical conditions of the citizens which is certainly related to the population density and the geographic / climatic conditions of the country. As an example, the people of New Jersey with a heavy population will feel more need for recycling compared to Wyoming which is less populated. Similarly for a country such as India or China with thick population and Singapore, which reclaims land from sea, polymer recycling is equally important.

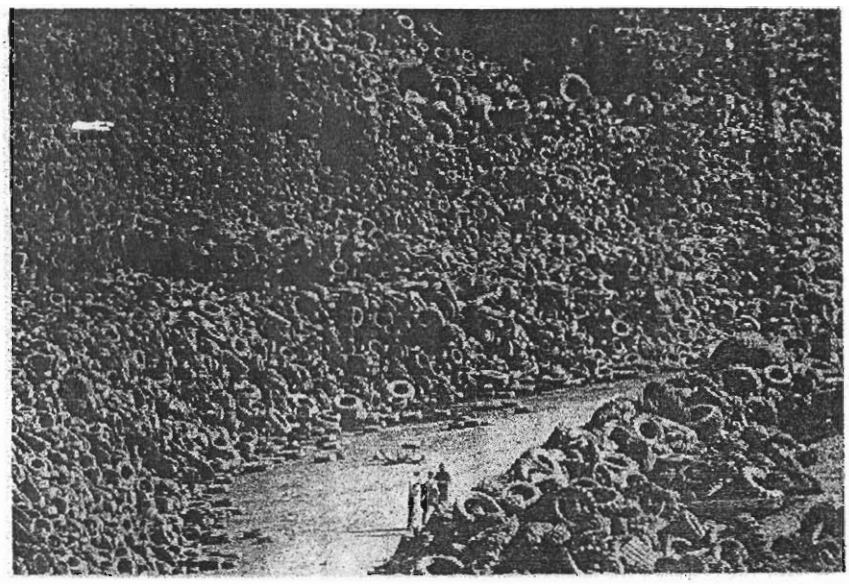

Figure 1.1. Massive stockpiles of scrap tires[3]

[Reference: J.R.Gunnigle., Proc.Conf. Rubber Div., Amer. Chem. Soc., Pittsburgh, PA, paper #68,Oct.11-14, 1994]

Even though environmental pollution by accumulated waste is so severe in many countries, it is not so severe in some other countries such as Germany. According to the Head of the Waste and Water Department of German Federal Environmental Agency (UBA)[4], only 0.5 % of the environmental pollution comes from waste. This is because of the effective measures taken on this problem by the government, spending a lot of money for the same. The present time is probably the right time to think of polymer recycling due to the rapidly changing political and economic realities. One can consider the present packaging technology. The modern packaging is of course convenient and efficient but less recyclable. In practical terms, the recyclability of a material decreases with reducing

weight of the package. Normally, a thin lightweight plastic pouch is difficult to recycle compared to a thick and heavy plastic bottle. It is this practical aspect of recycling which creates the main barrier to recycling than the variety of packing materials.

1.1. Metamorphosis of polymer recycling

The present day recycling movement in the world is 25 years old. It is during the second world war (1935-1945) that people first thought about recycling in general. The recycling of metal, paper and other materials needed for the war became necessary during the war time. By 1960, this situation intensified and the people began to use polymers more, mainly plastics. By the end of 1960's, people began to realize that using recycled materials instead of virgin materials could conserve enormous amounts of energy and resources. Community based recycling programs sprouted in cities and college campuses. Recycling and antilitter activities grew and finally people celebrated the first national earth day in 1970. During 1970's and early 1980's, public awareness of garbage disposal increased. Still people didn't feel the disposal as much expensive. In 1980's, the tide turned with several incidents which caused a sharp increase in the disposal costs. These incidents compelled the media to use the word "Solid Waste Crisis". According to a European survey[5], 7.6% of the plastic waste was recovered by mechanical recycling, 0.6% by chemical recycling and 17% was used for energy recovery.

1.2. Aspects of recycling

In addition to the support from social and political forces, the success of recycling depends on certain conditions of recycling. They are the following.

(i) The recycling process must have scientific and technological support. Then only it can attract business people.

(ii) The practice of recycling must be acceptable to the public.

According to modern concepts, recycling and energy recovery must be parts of the same equation. Recycling is not necessarily the preferable waste management solution as it is limited by the second law of thermodynamics and obeys the law of diminishing returns. Therefore, recycling should be performed at an optimum rate considering both economic and environmental aspects[6]. There are four cycles for recycling. In the first cycle, the waste from the production process is directly transformed into reusable material (in-plant

recycling). In the second cycle, potential waste is used in a new or another product, e.g., use of a worn car tires as a fender at the quay of a harbour. The third cycle (mechanical recycling) includes production and product usage as well as preparation of wastes and reuse as secondary material. The fourth one, called conversion cycle, involves the chemical feedstock recycling of wastes and their new usage as secondary materials.

1.2.1. Sorting and separation of polymer rejects

The majority of polymer rejects are blends of two or more polymers. It is already known that even 1% of an incompatible polymer can degrade the properties of the entire batch of recyclates. Therefore mixed plastics apart from being cheap, produce products withinferior properties. Owing to these reasons, the sorting and separation of polymer rejects is an unavoidable step in polymer recycling. The sorting process generally exploits either a unique property of the polymer, for e.g., density, hydrophobicity, and presence of chlorine or a change in the property with temperature, for e.g., melting point or solubility. For a sorting process to be successful commercially, it should be fast, reliable, economical and flexible enough to cope with various forms of impurities. The different types of sorting and separation methods are given below.

1.2.1.1. Manual sorting (PVC-PET separation)

This is done by the sorting with the help of persons with a "trained eye" and with the help of semi automated low cost lighter systems. For e.g., they can easily distinguish PVC from PET bottles in having a slight blue tint, a horizontal 'crescent' marking on the bottle base at the parison pinch-off[7]. Also the presence of whitish areas in PVC bottles due to stress whitening during crushing is helpful.

1.2.1.2. Density based sorting methods

(a). Wet separation

This technique of sink-float separation is mainly used in the case of mixed plastic flake. One main application is in the separation of PVC films from other polyethylene rejects. The mixture of plastics is put into a fluid medium to effect separation based on density. The liquid mediums commonly used are water [to separate polyolefins from non polyolefins (PET and PVC)], water / methanol mixture [to separate polymers with specific gravities less than unity such as polyolefins], NaCl / $ZnCl_2$ solutions – to separate

polymers with specific gravities greater than unity. Modified methods of this sort[8] are effective to separate TPE's from polyolefins. Owing to the similar density with polyolefins, TPE's are otherwise difficult to separate. Here the use of heavy liquid medium (dispersion of $CaCO_3$ in water) is practiced.

(b). Dry separation

In this case[9], an air separation process is used to remove coarse materials such as metal fragments, glass and heavy thick walled plastics. It can be used to separate polyamide flakes from ground HDPE fuel tanks, and to separate paper from ground bottle flake.

(c). Centrifugal sorting

Since this method is based on the principle of centrifugal acceleration, it can process even the most contaminated polymers to get a high purity stream. The hydrocyclone used for this is given in **Figure 1.2.**

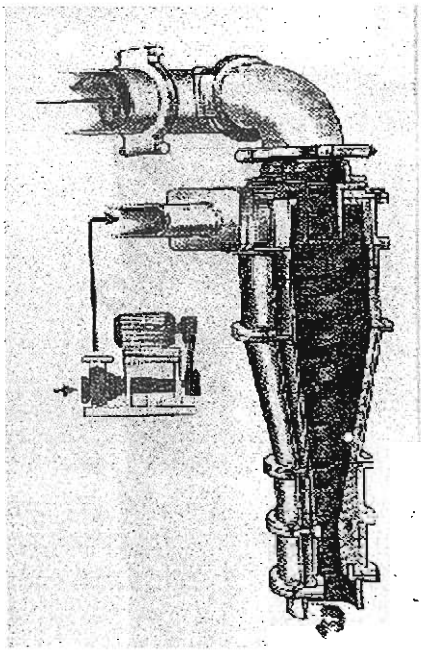

Figure 1.2. Cut-away view of a hydrocyclone for the separation of recycled plastics[10]

[Reference: K.H. Unkelbach., 'High duty plastics recycling with centrifugal force' (document available from KHD Humboldt Wedag AG, Koln, Germany)]

A modified equipment of this sort called 'CENSOR'[10] developed by KHD Humboldt Wedag (Cologne, Germany) can identify plastics differing in densities even by

0.005g/cc. By the proper selection of the separating medium, it can separate most of the difficult systems such as PE/PP, PS/PVC/Nylon etc. The advantages are the ability of the process to remove adhering air bubbles and fast and high selectivity of the separation process. A comparative assessment of the three methods discussed so far is given in **Table 1.1.**

Table 1.1. Data concerning acceleration, settling and floating velocities and retention times of CENSOR® sorting centrifuge compared to hydrocyclone and sink-float process[10]

Parameter	Sorting centrifuge			Hydrocyclone			Sink-float process		
Mean acceleration, m/s^2	1100			<100			1		
Retention time, s	25			1			400		
Particle size, mm	0.5	2	10	0.5	2	10	0.5	2	10
Mean settling velocity, mm/s	860	1550	4000	140	500	1200	6	30	120
Settling/floating time, s	0.11	0.06	0.025	0.6	0.18	0.07	300	67	15
Selectivity factor	227	416	1000	1.7	5.6	14	1.3	6	27

[Reference: K.H. Unkelbach., 'High duty plastics recycling with centrifugal force'(document available from KHD Humboldt Wedag AG, Koln, Germany)]

(d). Sorting with near critical and super critical fluids

This method uses a near and supercritical fluid such as liquid carbon dioxide as the separation medium[11-14]. This method can distinguish between plastic flakes differing by densities as small as 0.001 g/cc. The advantages are;

(i) easily and precisely controllable fluid density by changing the pressure.

(ii) it can save time for particle rise or settlement due to the very low fluid viscosity.

(iii) CO_2 medium is inexpensive, readily available, non-toxic and non-flammable.

(e). Preferential solvent absorption

This method[15] also is used for the separation of PVC and PET. The added solvent (alcohol, ketone, ester) or alcohol mixed with NaOH solution to get a density < 0.95 g/cc) is preferentially absorbed by PVC and this decreases its density. This is then separated

from the denser PET flake by floatation or centrifugation.

(f). Froth floatation

This method[16] originated from a similar process in metallurgy and is useful to separate PP from PE and PVC/PET. Since PVC readily absorbs plasticising chemicals, it is possible to change hydrophilic / hydrophobic properties of PVC. The process is shown in **Figure 1.3.**

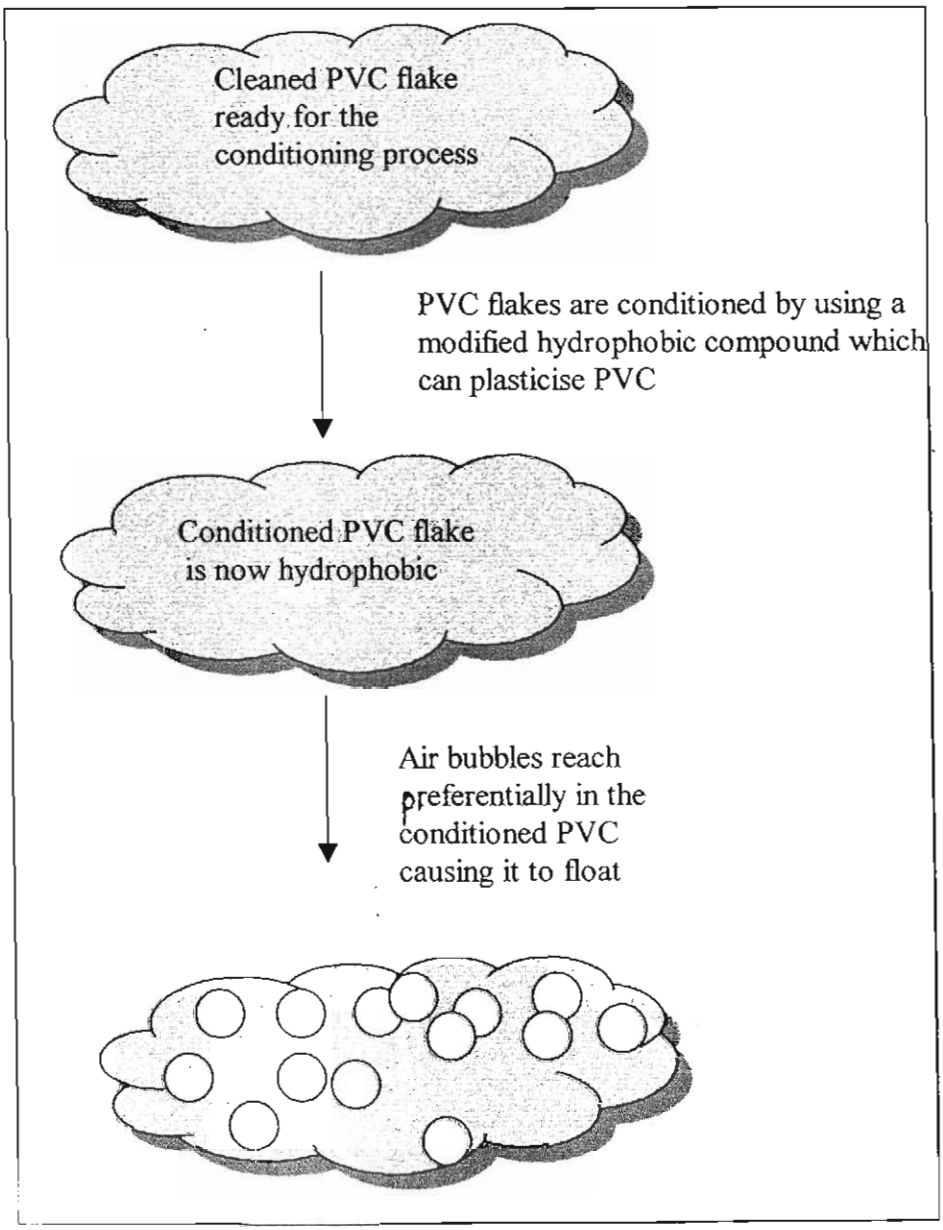

Figure 1.3. Schematic illustration of froth floatation process for the separation of PVC

[Reference: J.H. Schut, Plastic World, p.33, Nov 1994]

The bubbling of air through a suspension of plastic in water can facilitate the separation of PVC from PET. This is possible because air bubbles have high affinity for water repellent surfaces. Finally PVC floats while PET sinks.

1.2.1.3. Optical sorting

The method of optical sorting is based on the colour of the polymer waste. For e.g., separation of coloured PET from colourless PET, separation of different types of HDPE wastes. Since for food contact applications, PET of extremely high purity was needed, the separation of PVC was most necessary. As PVC discolours the whole system and becomes light brown when heated to 240 ^{0}C while PET crystallizes and turns white, this method is successful for their separation. Modern methods include the use of special filters, colour cameras, IR or CCD cameras[17].

1.2.1.4. Spectroscopic sorting methods

The identification of plastics can be successfully done also by using mid-IR reflection spectroscopy (MIR) (4000-700 cm^{-1}) since this region is directly related to specific chemical bonds in the polymer. An MIR spectrometer developed by Bruker Analytische Gmbh, Germany[18] can even identify plastics including the fillers or flame-retardants within 5 seconds with a rate of upto 10 items per minute. The operator has to simply place the plastic sample in the sampling head and press the foot pedal. The MIR light reflected off the sample identifies the material and reports it with a confidence factor. The most important advantage is that it is very fast that it takes only less than 10 sec for identification[19] and can identify dark plastics also.

Compared to MIR, near infra red (NIR) method (14300-4000 cm^{-1}) is rapid and reliable and can identify the material within milliseconds. It can penetrate deeper into the polymer than MIR and it therefore suffers less from surface paint/dirt etc. The peaks are most useful for the identification of C-H, O-H, N-H and C-O. When PET shows three characteristic peaks in the region 2100-2200 nm, HDPE shows a peak at 1200 nm, which is absent in PET. Rapid online identification systems by Eisenreich[20] Fraunhofer Institute for Chemical Technology, Pfinztal, Germany (100 spectra and 20 bottles /sec) and Opt Research Inc, Tokyo, Japan[21] are also very useful.

1.2.1.5. X-ray fluorescence (XRF) method

Atoms with a high molecular weight such as those in PVC emit a characteristic X-ray signature which is detected by the XRF analyzer while polyolefins with comparatively low molecular weight atoms emit a lower backscattering. Here the fluorescence detector identifies the presence of chlorine in the bottle and then the computer-timed airburst separates them. This process[22] is developed by National Recovery Technologies (NRT), Nashville, TN. One of the advantages of NRT-XRF technique is that it needs no singulation.

An instrument in this category is VYDAR (Vinyl detection and removal) [23] developed by Magnetic Separation systems, Nashville, TN, USA. The schematic of the instrument is shown in **Figure 1.4.**

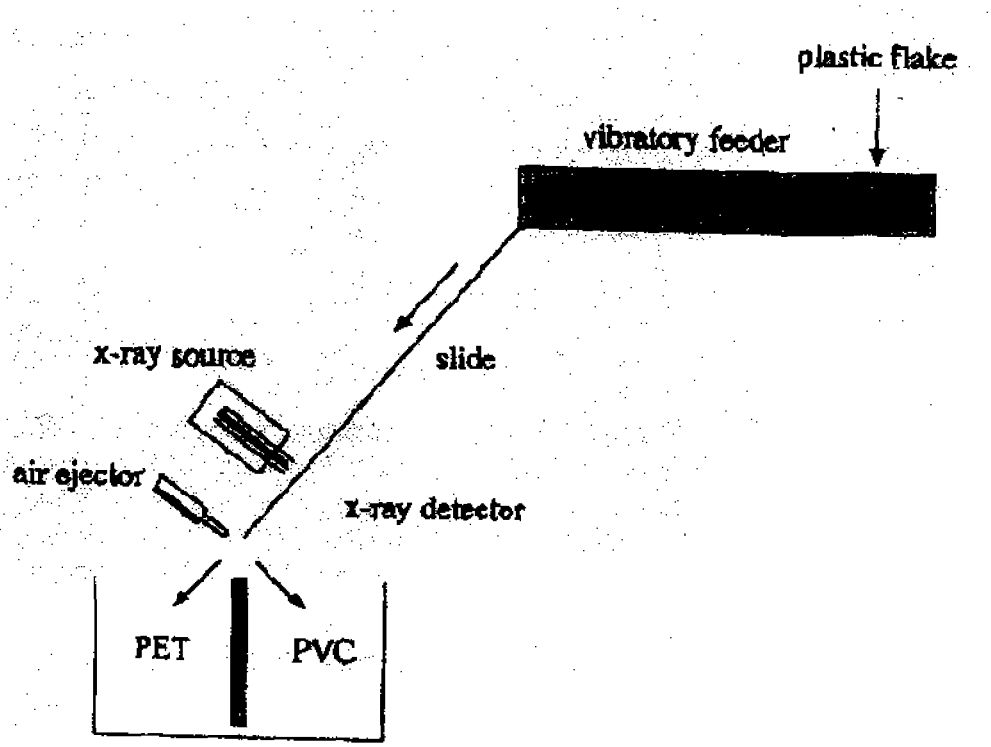

Figure 1.4. Schematic of XRF-based PVC flake sorting system (Vydar®)

[Reference: D.Vaughan and G.R.Kenny., New Challenges in Plastic Sorting' proc. SPE, 3rd Annual Recycling Conf, Chicago, IL, Nov, p.311 (1996)]

The capacity of the instrument is 1820 Kg flake/h, efficiency 97.5%. The disadvantage noted is the failure of the system to identify and remove PVC flakes hidden

in the aluminium caps.

1.2.1.6. Electrostatic methods

The underlying principle here is that when two dissimilar materials are brought into contact, there is an exchange of charge across the interface and owing to this, one body becomes positive and the other negative. When they separate, one polarity predominates leading to tribocharging. The device called triboelectric pen measures this tribocharge to identify the plastic.

Triboelectric pen

Tribopen resembles a fountain pen and is a compact hand-held device with sensor heads capable to distinguish the triboelectric charge produced by different plastics[24]. The sensor heads contain specially selected materials which generate either positive or negative electrostatic charge when it is rubbed against the plastic. The combination of positive and negative charges thus produced is characteristic of the electrostatic property of the plastic. **Figure 1.5a** is the photo of a triboelectric pen developed by Faculty of Engineering and Applied Sciences, University of Southampton, Southampton, UK. **Figure 1.5b** is its structural sketch. A tribopen with three sensor heads can identify four different types of plastics. The LED at the top of the pen indicates the plastic.

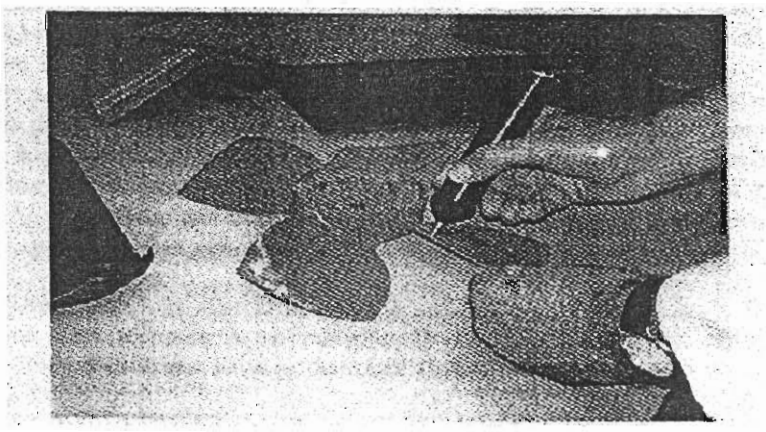

Figure 1.5a. The hand held Tribopen

[Reference: P.E.Mucci, British Patent PCT/GB94/00101(1994)]

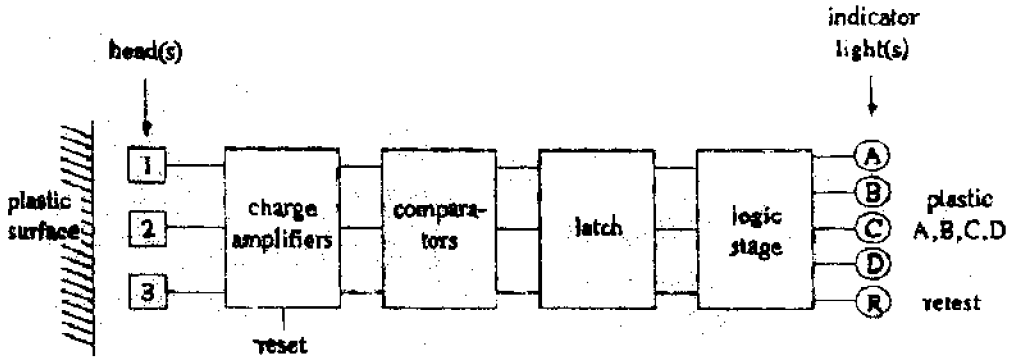

Figure 1.5b. The structural sketch of tribopen

[Reference: P.E.Mucci, British Patent PCT/GB94/00101(1994)]

In addition to this portable device, continuous electrostatic based sorting process is also available. The principle here is that if two different non-conductive materials are brought into frictional contact, charges are produced on the surface which will remain there for sometime. According to Cohen in the reference[25], the material with higher dielectric constant will be charged positive. According to their polarity, they can then be separated.[26,27]

1.2.1.7. Differential melting method

As PVC and PET differ in their melting point by 60^0C, they can be separated using a hot belt separator where PVC softens and adhere to the belt. When the belt turns upside down, PET falls from it. PVC is scraped off at another point[28].

1.2.1.8. Selective dissolution

The principle behind this technique[29,30] is that the thermodynamic differences between the six major polymers (LDPE, HDPE, PP, PET, PVC and PS) cause each one to dissolve in a given solvent only at different temperatures (**Table 1. 2**).

The respective polymer solutions are pumped to a devolatilising extruder. The solvents used are also recycled.

Table 1.2. Solvent and temperature conditions for the selective dissolution sorting process[29]

Polymer	Solvent	Temperature, ^{0}C	Solution Conc. %
PS	Xylene	15	6
LDPE	Xylene	75	10
HDPE	Xylene	105	10
PP	Xylene	120	10
PVC	Xylene/cyclohexane	120	10
PET	Xylene/cyclohexane	180	10

[Reference: E.B. Nauman, J.C.Lynch and S. Norwalk., 'Overcoming challenges in recycling high value plastics from durable goods' presented at the University of North Carolina at Charlotte Symposium on Plastics Recycling, September, 1996]

1.2.2. Size Reduction Methods

The primary aim of size reduction is to reduce the bulk density of the material, to ease transportation. This step converts the waste material into a regular and consistent form which can be easily metered and fed into recycling process. The main size reduction techniques are shredding, granulation, densification, compaction, agglomeration and pulverization.

(a). Cutting processes

1. Shredding

The process involves tearing and cutting and is meant for the recycling of films, sheet, hollow products and cable[31]. The operating principle is based on two asynchronised or four synchronized contra rotating shafts equipped with cutting discs and distance collars. The schematic diagram of a plastic shredder is given in **Figure 1.6**.

2. Rotary grinding.

The process involves the working with steel blocks (of 2.5-5 cm in size) mounted on a rotor which can chip fragments from the feed as it is forced into teeth by a ram[32].

3. Granulation

This process is effected by the rotation of rotating knifes (fly knives) with 3 or 4 stationary knives (bed knives). In order to ensure a constant cutting nip across the knife

width, the fly knives are kept at a slight angle with respect to the rotor shaft. The bed knives also are at the same angle but in opposite direction.

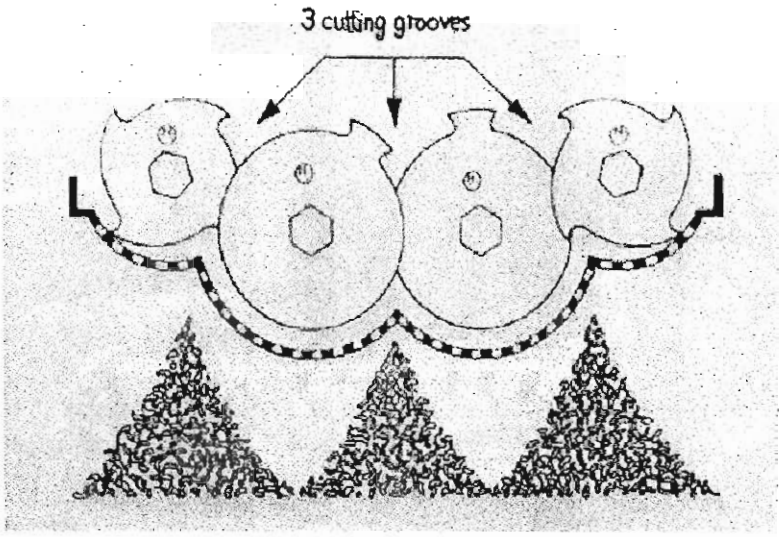

Figure 1.6. Schematic illustrating principle of operation of a plastic shredder with four cutting shafts[31]

[Reference: C.Spankuch and M.Fass., Kunststoffe, 84,8 (1994)]

4. Slicing

Slicers or guillotine shears[31] are meant for waste fibres, rolled up web and rubber bales. The difference from a shredder is that the slicer operates in a clockwise manner and the slicing knife cuts the material from the top and works its way downward.

5. Screw cutting

The cutting is effected by independently rotating screw shafts with tearing teeth and is for over sized plastic products. Compared to earlier described methods for films, normal plastic wastes, the separation of polymer laminates is difficult as simple grinding yields only an intimately mixed product. A method developed by Result Technology AG, Australia[33] works on the difference in the behaviour of laminate materials when subjected to acceleration and vortices in a specially designed unit. This causes the delamination along the interfacial boundaries. The varying morphologies after the treatment on an accelerator can be shown as in **Figure 1.7.** When aluminum foil tends to roll into globular particles, PE changes to flakes, PS to chips and PVC to cubic shape.

(b). Densification

In order to facilitate transportation, conveying, metering and feeding, the density of the waste materials such as films, foams and fibres must be increased from the range of 20-40 kg/m^3 to 400 kg/m^3 range. This is done by an agglomeration or densification process which softens the material with out melting it. Here the material undergoes a caking phenomena[31,34,35].

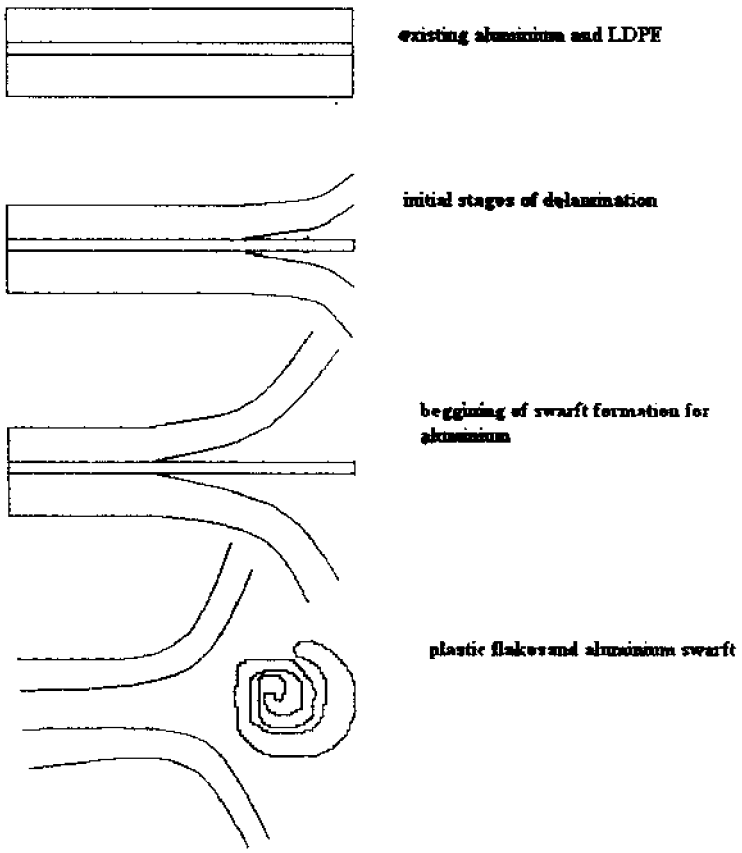

Figure 1.7. Schematic illustrating principle of laminate separation by high-speed rotation[33]

[Reference: C.Muther., 'Separation of laminates using Result Technology' Proc. SPE 3 rd Ann, Recycling Conf, Chicago, IL, Nov 7-8, p 37 (1996)]

(c). Pulverisation

This process is used to convert waste polymer to a powder which can then be used for sintered powder coatings, molding powders, fillers etc. The process is ideal for polyolefins, polyamides, polyesters, polyurethanes and PVC (rigid/flexible). An advantage of this process is that in the case of painted plastics, the foreign impurities also will be ground to finer particles which simply act as fillers. The main disadvantage is the development of temperature, and sticking of polymer on the cutting blades. This reduces the efficiency of cutting. Another method is SSSE[36] (solid state shear extrusion) or elastic deformation grinding developed by Berstoffe Maschinenbau GmbH, Hannover, Germany, (works by creating a larger free surface by the simultaneous action of high pressure and shear deformation[37]). The advantage is the formation of very fine powder, for e.g., wood particles of 50 μm could be produced by SSSE while normally it is 20 times higher than this. This method can convert low performance commingled post consumer recycled plastics into useful blends with out use of any compatibiliser[38]. It is the only technology that can collectively take the six most common plastics in the waste stream (HDPE, LDPE, PP, PET, PS and PVC) and convert them to a useful powder product. Despite the fine particle size of SSSE powder, they give no bridging problems in the feed zone of injection molding machines[39].

1.2.3. Melt Filtration

As most recycled polymers are characterised by the presence of contaminants such as dirt, cellulose material, aluminium foil, metal fragments, fibre glass and incompatible high melting polymers, melt filtration is an important step in polymer recycling and reprocessing. The process improves the quality of the product by trapping adventitious contamination, removing infused material, eliminating gels, homogenising the melt and minimising pressure spikes and clogs.

The proper selection of melt filtration technique is an important aspect in polymer recycling. This is made by considering several technological aspects[40] such as type, size, hardness and level of contaminants (vol %), material factors such as polymer type, additive package, melt viscosity at the processing temperature and throughputs and degree of wall adhesion.

1.3. Plastic Recycling.

Plastics are a product of the current century. Initially plastics were mimicking and replacing natural products but now they are considered as substitutes for metals, which are made from extremely inexpensive but non-renewable resource, crude oil.

Plastic waste management can be divided into three.

1. Mechanical or material recycling which preserves their molecular structure.
2. Chemical recycling, which converts plastics to monomers, oil refinery or petrochemical, feed stock.
3. Energy recycling where plastics are subjected to incineration.

Recycling methods for used plastics can be classified according to the **Figure 1.8.** The selection of the process is done based on the degree of sorting, degree of contamination and the amount of material to be recovered.

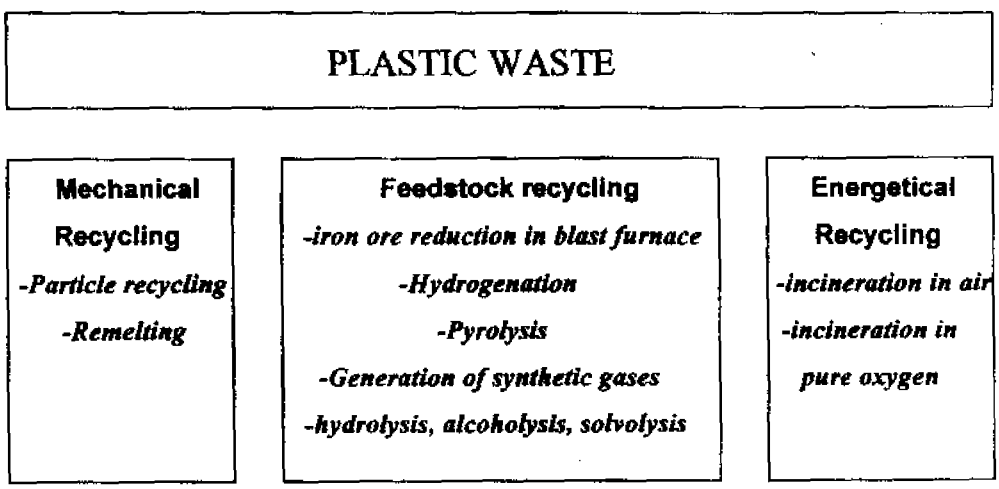

Figure 1.8. Possibilities of plastic recycling[41]

[Reference: W. Michaeli and K. Breyer, Macromol.Symp., 135, 83 (1998)]

1.3.1. Mechanical recycling

Mechanical recycling means a remelting of the polymer, production of new pellets and conversion into a new product. This is meant for well-sorted material in huge quantities. One of the best examples for this is the SMC (sheet molding compound) recycling done by ERCOM, Germany. It is known that the molecular degradation during the mechanical recycling process affects the properties.[42]

Plastic waste containing mixed and foreign substances are much problematic and the purification /separation process is uneconomical. The reason for such a difficulty can be made clear from the spectrum of processing temperature[43] given in **Table 1.3.** This necessitates the need of good sorting. The poor compatibility of the individual polymers can also be another reason.

Table 1.3. Selected processing temperatures for injection moulding[43]

Plastic	**Processing range**	**Melt temperature, ^{0}C**
Polystyrene	Wide	180-280
Polyethylene soft	Wide	160-260
Polyethylene hard	Wide	200-300
Polypropylene	Medium	230-270
Poly (vinylchloride)	Very narrow	180-210
Polyamide, PA6	Narrow	230-280
Polyamide, PA66	Very narrow	260-320
Polycarbonate, PC	Narrow	280-320

[Reference: H. Saechtling, Kunststoff Taschenbuch, Hanser, Munchen-Wien, 1986]

The mechanical recovery of plastics consists of general steps such as identification, sorting, grinding, washing, drying, extrusion and the final pelletizing[44]. The upgradation of the recycled material[45] is done by the addition of fibres, fillers, stabilizers, pigments, processing aids, compatibilisers etc. A novel approach of upgrading the recyclate by the addition of additives is developed by Pfaender et al[46]. This approach of restabilisation and repair of molecules by the development of appropriate formulation for targeted application can make recycled plastics good substitutes for virgin materials. The restabilisation is the most effective approach to improve the quality of any recyclate.[47,48]

The research group called MARECK[49] (material recycling of non reinforced thermoplastics), Aachen University of Technology, RWTH Aachen, covers all the processes of recycling from beginning to end. They developed, characterized and still practicing the methods for identification, separation, upgradation and analysis of the

plastics in recycling field. Their studies[50] emphasise the need of an analysis of all the mechanical properties of recycled materials.

1.3.2. Chemical recycling technologies.

The main options for chemical recycling are the following.

1. **Hydrogenation**

This is carried out at 300- 500 ^{0} C and at 100-400 atm. pressure to get low molecular weight oils, gases etc.

$$\text{Plastics waste} \xrightarrow{300\text{-}500^0\ C,\ 100\text{-}400\ atm.} \text{low molecular weight oils, gases}$$

2. **Pyrolysis-absence of O_2**

$$\text{Plastics waste} \xrightarrow{500\text{-}900\ ^0C,\ \text{absence of } O_2} \text{gaseous, liquid or waxy hydrocarbons}$$

3. **Pyrolysis-presence of O_2**

$$\text{Plastics waste} \xrightarrow{450^0\ C,\ \text{presence of } O_2} \text{synthesis gas} \longrightarrow \text{methanol, ammonia, energy generation, and other products}$$

4. **Hydrolysis, alcoholysis, glycolysis**

$$\text{Plastics waste} \longrightarrow \text{original substances}$$

5. **Degradative extrusion**

$$\text{Plastic waste} \longrightarrow \text{low molecular weight gases, liquids}$$

1.3.3. Incineration of Plastic Waste

The case of energy recovery comes when the plastic waste is highly crosslinked or contaminated with problematic substances. The plastic wastes are then burnt to produce steam and electricity.

Plastic wastes must be considered as an alternative source of energy and as a chemical raw material[51]. According to the present concepts of recycling in France, the recycling of a material can be considered only if it has a very small combustion value and it is feasible for recycling. Keeping the energy production from waste as an important strategy of energy policy[52], France could save about 1 million ton of crude oil by the burning of 8 million ton of municipal waste[53] (which is 40% of the total waste). But the

local residents will accept this idea of incineration only if it is combined with recycling and composting efforts in that area. A good example for such as activity is the integrated waste management in Hampshire, UK[54].

As the recycling of complex mixtures of polymers is practically difficult, the copyrolysis of waste polymers with coal was tried by Straka et al[55]. The coke can be used as a smokeless low sulphur fuel[56,57]. A stepwise pyrolysis of plastic mixtures (PVC, PS and PE) carried out by Bockhorn et al[58] indicates that the dehydrochlorination takes place quantitatively in the first reactor. The chlorine balance indicates a rate of conversion of 99.6%. Even though the feed was of high chlorine content, the product gases from the third reactor contain only negligible amount of chlorine (0.0044%). Polystyrene and polyamide –6, gave monomers in high yields in second reactor while polyethylene gave parafins and olefins in the third reactor.

The tertiary recycling of polyethylene by thermolysis and reactive distillation was carried out by Caffrey et al.[59]. Nitrogen atmosphere at 440^0 C was employed for the reaction to get a higher conversion of polyethylene into a condensable liquid compared to any other conventional pyrolysis.

1.4.Rubber Recycling.

1.4.1. Reclaimed Rubber or 'Reclaim'

'Reclaim' is defined as a type of rubber prepared from waste or worn out manufactured rubber articles and the process of reclaiming is concerned with imparting the necessary degree of plasticity to vulcanised rubber and thereby enabling it to be blended with uncured material or synthetic rubber.[60] The earliest effort to recycle polymer rubber rejects was by the process of reclamation[61]. Several excellent historical records and descriptions of rubber reclaiming processeare available in the literature.[62-65] The most important processes of reclaim manufacture are digester (Neutral or alkali)[66-69], pan or heater[70], acid[71,72], reclamator or dip[73], thermal[74], thermodynamic or hot banbury[75] and palmer or high pressure steam[76]. These processes mainly involve the heat plasticisation, fabric removal and mechanical treatment. Short description of these methods is given below.

1. Digester (alkali or neutral) process.

Here the ground scrap is heated at 180-205^0 C for 3-15 hours in autoclaves along with necessary plasticisers and solutions for destroying fabric. The plasticised rubber without any fabric is discharged into dump tanks, washed, dewatered and dried in hot air currents. In the alkali process, the scrap rubber is heated under pressure in caustic alkali solution to destroy fabric and to plasticise the rubber. This method is not in active use now due to scorch problems with certain type of accelerators. In the neutral process, zinc chloride solution is used instead of caustic alkali solution. The advantages here are the cheap fibre destruction, suitability for SBR scrap and less scorchy reclaim.

2. Pan or Heater process.

In this method, the ground scrap rubber is heated in large horizontal single-shell autoclaves at pressures of 100-300 lb./in.^{2} for varying periods of time. It is then air-dried. Reclaiming is completed in the conventional manner. The method is usually used for fabric free scrap.

3. Acid process

Here the fibre containing scrap is treated with hot dil. sulphuric acid in open tanks. Washing with the use of riffler with baffles removes stones, metal etc. The scrap is then nutralised with alkali, plasticised in live steam, milled and strained.

4. Reclamator or Dip process

This is considered as the best reclaiming process and was patented by the US Rubber Reclaiming Company in 1946. Reclamator is a screw extruder with a hopper at one end into which a premixed crumb/oil blend is automatically fed at a predetermined rate. The machine generates its own heat for devulcanisation by the mechanical working of the blend under pressure. The temperature of the rubber is controlled by heating and cooling jackets around the machine. After five minutes, the reclaim is discharged from the machine. It is cooled by water sprays and passed to a screw conveyor where it is mixed with required fillers. It is finally extracted through a perforated die, cut into small pieces by a rotating knife and conveyed to the refining section.

5. Thermal process

In this method, tire scrap is loaded into steam autoclaves with electric heaters. The conjoint destruction of fibres and softening of vulcanised rubber is done in a medium of superheated steam. One disadvantage is the nonsuitability of the method to SBR and certain other synthetic scrap.

6. Thermodynamic or Hot Banbury process

In hot banbury process, the raw cracked waste is loaded into the machine with plasticisers, reclaiming agents, carbon black etc. and subjected to intense shearing action by means of high pressure (180 lb./in.$^{2)}$ and temperature 500^0 F for 3-12 minutes. The batch is cooled before discharge.

7. Palmer or High Pressure Steam process

Fibre-free waste with reclaiming agents is charged into a specially constructed closed container. Then live steam at 800-1000 lb./in.^{2} is admitted into the container and maintained for 10 minutes. Then the pressure is suddenly released. The blown out and disintegrated reclaim is finally finished in the conventional manner.

1.4.1.1. Processes during reclamation

There are 6 main processes during reclamation.

1. Reduction in molecular weight to a lower level than that of a new rubber
2. Chain scission brings about reduction in gel content (g) and increase in gel swelling(s). The degree of devulcanisation is proportional to s/g ratio.
3. The product of reclamation process is a heterogeneous system of crosslinked fragments dispersed in a plastic component. If a reinforcing filler such as carbon black is present in the system, some portion of the fragment will be bound to it.
4. The chemical unsaturation of the rubber hydrocarbon of reclaimed rubber will be essentially unchanged from that of original vulcanised scrap.
5. In order to minimise the reduction in tensile strength and to impart satisfactory processability and speed of reclamation to the final product, the recommended dosage of reclaiming agent is 0.5-20% of the scrap weight.
6. Since natural rubber is more susceptible to depolymerisation than SBR and NR, the plasticity increases as reclamation progresses. But in the case of SBR, after an

initial increase of plasticity, the material will begin to reharden. Therefore the behaviour of a blend of SBR and NR cannot be predicted unless the composition is known.

1.4.1.2. Steps in a reclaiming process

The reclaiming process can be divided into 4 major parts, some of which are mechanical and others chemical. The different steps are grinding, defibering and depolymerisation, refining and recovery of reclaiming oils.

1. Grinding

When natural rubber is the only component in the scrap, this step can be avoided. But if SBR also is present, grinding step is necessary because of the lower absorption efficiency of SBR for the reclaiming agents and catalysts.

2. Defibering and depolymerisation

The use of caustic soda as a defibering agent for tire scrap was well established in reclaiming industry. Since caustic soda has adverse effect on the plasticity of vulcanised SBR, its use was abandoned later. The successive method was the use of a metal chloride solution (Ca) as defibering agent. The reclamation process using metal chlorides as defibering agents is called digester process, the steam heating of mechanically defibered ground scrap is called heater process and the most important is the reclamator process patented by the US rubber reclaiming company in 1953. It is a development of the banbury process.

3. Refining

This step in reclamation has not undergone much major development. One interesting development noted was the extensive use of the refines to get 'premixes'. Premixes are complete compounds (but without curatives) produced by co-refining the vulcanized scrap after the depolymerisation step with various fillers, softeners, and many other compounding ingredients. Therefore the physical properties of the vulcanised compounds could be improved considerably.

4. Recovery of reclaiming oils

Since some of the reclaiming oils are steam distillable, they will be easily removed from the reclaims during the release of pressure at the end of the devulcanising period.

The vapours of these oils can be condensed and reused.

1.4.1.3. Testing of reclaim[77-93]

The testing of the reclaim is done by examination during the course of manufacture and that of the finished product. The workability of the batches after digesting, pan treatment etc. is determined by milling and refining small lots. Frequent tests for specific gravity, Mooney viscosity etc. are needed during mill room operations to control the quality of the reclaim. Frequent testing of various agents used in the processing, testing of the final effluents can help to remove suspended solids. Examination of finished reclaim is to be done giving emphasis to three factors namely composition of the reclaim (especially the rubber content, presence of synthetic, copper, manganese etc), physical condition of unvulcanised reclaim (plasticity, colour, cleanliness, degree of tackiness, "body" and "nerve") and rate of cure/ageing characteristics.

1.4.1.4. Advantages and disadvantages of reclaimed rubber

Since,during manufacture, the reclaimed rubber undergoes thorough plasticisation and since it contains all the fillers in the original compound, it breaks down easily and mixes quickly than a new rubber. Another advantage is the comparatively lower power consumption during mixing and breakdown. Also it is important to note that stokes containing reclaimed rubber can usually be processed at a lower temperature. This is an advantageous fact when heat history and processing safety are concerned. The compound containing reclaimed rubber has greater processability since it is less nervy than a new rubber and hence it builds up less internal heat in the calender bank. Hence such a stock will be safer on calender even though it has shorter Mooney scorch time than a compound without reclaim. Stokes containing reclaim permits high speed calendering, resulting in uniform and smooth coating. Compound containing reclaim tend to hold their tack for prolonged time with less tack variations with climatic changes.

But during the reclamation process, the scrap rubber may undergo some degradation which will make their mechanical properties inferior to those stokes with a new rubber. Therefore use of reclaim remains at only 4% of US rubber consumption. Another disadvantage is the lower scorch safety resulting from the faster curing process. But altering the recipe of ingredients can properly control this.

1.4.1.5. Selection of reclaim for various applications[94-96]

The most important characteristics to be considered in the selection of reclaim for various purposes are the following.

1. Composition (rubber, carbon content and amount of extractable organic matter)
2. Price
3. Reclaiming process employed.
4. Degree of smoothness
5. Plasticity, nerve, body, tackiness and other characteristics (which affect milling, calendaring and extrusion) and the behaviour of uncured stock on maturing.
6. Tendencies for migratory staining.
7. Resistance to water absorption
8. Influence of the reclaim on rate of cure, tensile strength, elongation, modulus, flex cracking etc.

Peel reclaim (tire tread) in which filler is mainly channel or furnace black is preferred for compounds requiring high abrasion resistance. Reclaim has a high value when used for hard rubber battery containers but due to its inferior abrasion resistance, it cannot be used in first quality tire treads.

1.4.2. Problems with reclaimed rubber

1.4.2.1. Staining of reclaim

Stain is due to the presence of certain staining compounding oils in the vulcanised scrap, certain staining reclaiming oils, certain antioxidants and antiozonants. The effect will be intensive for nitrogen containing compounds such as amines. If the vulcanised scrap itself is staining, the use of adsorptive carbons prepared from the waste liquor (obtained from an alkaline pulping process) is recommendable.

1.4.2.2. Mooney growth

The phenomenon of increase in reclaim viscosity with age and storage temperature is commonly called Mooney growth. It was reported that Mooney growth could be controlled to a great extent by adding reducing sugars, polyalcohols and sodium nitrite.

1.4.3. Reclaiming agents

Some of the active classes of reclairning agents are the following.

1. Phenol and alkyl sulphides and disulphides

These reclaiming agents are the most effective of all the four classes. They catalyse the oxidative breakdown of polymer chain and disrupt the sulphur crosslinks. They work better in sulphur-cured vulcanisates than in non-sulphur cured ones. The effect is found to be intense in the presence of oxygen which promotes the production of low molecular weight polymer fragments even under mild conditions.

2. Aliphatic and aromatic mercaptans

The aromatic mercaptans are more effective than their aliphatic counterparts. More over it was found that when naphthalene group replaced the phenyl group, reactivity increased.

3. Amino compounds

These compounds are very effective reclaiming agents with an advantage that their activity does not depend on oxygen. Their efficiency is higher for non-sulphur cured vulcanisates than sulphur cured ones.

4. Unsaturated compounds

One example in this class is coal tar or naphtha. Its fractional distillation releases some materials such as indene, dicyclopentadiene, coumarone and others which are effective in the depolymerisation technique.

5. Reclamation using De Link

A novel technique for the reclamation is by the use of De Link[97]. The process can be represented as in **Figure 1.9**.

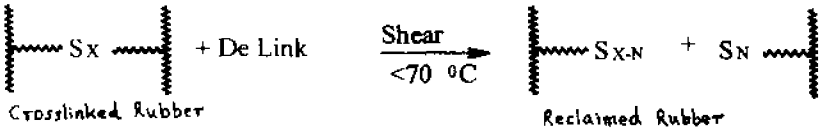

Figure 1.9. Reclamation process using De Link

The process is very easy as it consists of the mastication of rubber rejects with De Link and some other compounding ingredients such as virgin natural rubber and processing aids in a two roll mill.

1.4.4. Ultrasonic devulcanisation

Another advancement in the field of recycling is the ultrasonic devulcanisation[98]. Here, an ultrasonic field creates high frequency extension-contraction stresses. In the case of ultrasonic devulcanisation of polymer solutions[99], the acoustic cavitation of solvent accompanied by fast movement of tiny resonating bubbles effects breakage of macromolecules. A number of studies in this field of crosslinked elastomers are reported by Tukachinsky et al.[100], Levin et al[101] and Isayev et al. [102,103] The main contributions from these works are the optimisation of conditions of devulcanisation and the achievement in improving the selectivity of the process to network breakage than degradation.

1.4.5. Tire Recycling

The formation of waste tire is a great problem, which needs much attention. The waste formed in US alone is 250 million tires per year. It is estimated that presently more than 2.5 billion scrap tires are stockpiled in US[104]. Even though their percentage is less (2%) in municipal waste stream, they produce a lot of disposal and environmental problems due to their durability and shape. The main environmental issue resulting from the accumulation is that they provide ideal breeding grounds for rats, insects mainly mosquitoes. This is much more severe than what happens in natural habitats[3]. The main environmental issue in burning and clearing this waste is environmental pollution, both atmospheric and geological due to the formation of aromatic compounds such as benzene and toluene. The presence of fillers, textile fibre, steel wire together with the tightly crosslinked network in tires and its resilient nature, intensifies this problem especially when attempting size reduction for recycling.

In Germany, around 6,00,000 tons of tires are recycled each year[105]. One method to reuse the waste tires is by their size reduction, because proper recycling is possible by this route only due to their resilient nature and shape. Due to the presence of a higher content of textiles in passenger tires, their reprocessing is much more difficult than truck tires. The methods for the size reduction are shredding, mechanical grinding & cryogrinding. Most of the processes for the reuse of scrap tire involve its disintegration. Even though several chemical processes for the recycling of scrap rubber was proposed, the main

difficulty noted was the difference in the response of polymer blend components to devulcanisation process. The process of destructive distillation was proposed for converting scrap tires to useful products. This involved the pyrolysis of scrap rubber at 500-900 ^{0} C to get gases oils and a solid residue which mainly contained recovered carbon black and compounding ingredients. This residue was found to be only weakly reinforcing.

Another possibility is the use of recycled tire rubber for the modification of asphalt[106]

The higher initial costs of pavements made with asphalt rubber binder, in comparison with the costs of conventional pavements may be offset by their much greater durability and the resultant longer service life and the possibility of using thinner layers. Also, the break down of tire waste to low molecular weight components[107] by supercritical and subcritical oxidation[108,109] is reported in the literature. A destruction efficiency of greater than 0.9 could be obtained in these studies which claims this method as an alternative solution to waste tire crisis.

1.5. Previous research works on the reuse of latex waste

It is an acceptable fact that industrialisation and urbanisation have resulted in a large-scale generation of waste. The solid waste management is becoming increasingly difficult as traditional landfills are becoming scarce. The ever-increasing volume of polymer waste is a severe problem deserving serious attention. Of this polymer waste, only 8-12 % is plastic while the rest lion's share is elastomer waste. Tires whose life span has ended constitute the major portion of this waste. The recycling of tires and other rubber waste by the process of reclamation is suggested as a solution to the problem of rubber waste accumulation. But the use of reclaimed rubber constitutes only a few percentage of raw rubber consumption. This is due to the deterioration in technological properties[110-114]. In comparison with tire and other filled rubber wastes, scrap latex rejects such as gloves and condom rejects are better potential candidates for recycling. This is because of the huge rejection in the latex based industries (10-15% of the rubber consumed) and the lightly crosslinked and high quality nature of the rubber hydrocarbon.

Many efforts are made to recycle natural rubber latex waste by the way of reclamation. The Rubber Research Institute of India[115] and of Malaysia[116,117] have developed techniques to reclaim latex waste mainly gloves rejects. Reena et al. [118-120] also

have independently developed a novel and economic procedure to convert latex waste into a processsable form. The use of reclaimed latex waste in virgin natural rubber is reported by Reena et al. [118]. A gradual reduction in the optimum cure time and scorch time is noted with the addition of latex reclaim to natural rubber. It is found that such a reduction is due to the presence of crosslinking precursors and/or unreacted curatives in the latex reclaim. An increase in the maximum torque also is noted due to the increased crosslink density of the sample with the addition of latex reclaim. The good bonding between natural rubber and latex reclaim is reflected in the increased tensile strength, tear strength and ageing resistance of NR vulcanisates containing latex reclaim. Increase in crosslink density is found to increase the hardness and modulus of the samples with a corresponding decrease in elongation at break and compression set. The fractographic analysis also is supporting the improvement in technological properties. Similar addition of latex reclaim in styrene butadiene rubber[119] also is found to be reducing the optimum cure time and scorch time of the rubber compounds. Tensile and tear strength values also are increased upto a latex reclaim loading of 60% and then they decreased. This is examined to be due to the formation of a continuous phase by latex reclaim. Increase in crosslink density is found to be increasing the modulus and hardness while decreasing elongation at break and compression set. Only a marginal initial increase is reflected in the results of abrasion resistance which dropped with further loading of latex reclaim. An inverse relation between resilience and heat build up of the samples are noted in the study. Processability studies revealed the high pseudoplasticity of the samples. It is also important to note that no change in the viscosity is noted with the addition of latex reclaim upto 20%. Increase in temperature is found to be making the blends more Newtonian. The activation energy of the blends is observed to be intermediate between that of the components.

The detailed rheological analysis of natural rubber containing latex reclaim is carried out by Reena et al.[120]. They observed that the viscosity decreased marginally on the addition of latex reclaim while it is almost unaffected with the variation in shear rate. The estimate of energy of activation revealed that the temperature sensitivity of the blends is not affected with the addition of latex reclaim. Addition of upto 50 wt. % latex reclaim is found to be producing smooth extrudates.

In addition to the use of latex reclaim in virgin elastomers, efforts to modify the material also are reported[121]. The chlorination of latex reclaim to produce chlorinated natural rubber with similar properties to that of commercial chlorinated rubber is carried out by Mary et al.[121]. They carried out the reaction by passing chlorine through a solution of latex reclaim in carbon tetrachloride. A reduction in the particle size of latex reclaim is observed after the chlorination process. The FTIR spectrum as well as the thermogravimetric plots of the chlorinated latex reclaim and commercial chlorinated natural rubber are found to be similar.

The conversion of latex foam and microcellular solid waste (natural rubber / high styrene resins & NBR/PVC) to a processable form and their reuse in corresponding microcellular soles is reported by Stilathakutty et al.[122] As observed in earlier studies [118-120], the addition of latex foam waste reduced the optimum cure time and scorch time. A marginal increase in relative density is also noted with the addition of latex foam waste. This increased the hardness of the microcellular sheets. The presence of crosslinked latex foam is found to be effective in reducing the expansion of microcellular sheets which caused reduction in compression set, heat shrinkage, water absorption and abrasion loss. Upto the addition of 15 phr of latex foam waste, split tear strength increased. The reduction observed with further loading of latex foam waste is found due to its poor dispersion at higher loadings. Addition of NR/HSR microcrumb in NR/HSR microcellular sole also produced similar results. Addition of modified NR/HSR microcrumb [using ZMBT (zinc salt of mercaptobenzothiazole) and parafinic oil] increased the expansion of microcellular sheets compared to the addition of unmodified crumb. Compression set is found to be only marginally affected with the addition of modified and autoclaved microcrumb. Addition of NBR/PVC microcrumb into NBR/PVC microcellular soles increased the relative density and hardness while it decreased the expansion ratio, heat shrinkage, compression set and water absorption of the microcellular soles. Split tear strength showed an increasing trend even upto the addition of 100% crumb.

The development of blends based on modified latex waste (thread and glove wastes) and polyethylene (LDPE) is carried out by Rajalekshmi et al. [123]. The tensile strength, tear strength, hardness and Young's modulus of the developed blends are found

to be comparable to that of LDPE/rubber blends. In these novel blends, the elastomer phase remained as dispersed and less deformed particles. Lower elongation at break is observed for LDPE/ thread and glove waste compositions compared to LDPE/virgin rubber. Impact strength values of more than 1 kJ/m are obtained for these recycled blends because of the effective absorption of energy by the soft and flexible rubber particles. Partial devulcanisation and molecular breakdown occurred during the processing of the waste material caused lower viscosity of the blends. At lower shear rate, the surface of the extrudates appeared smooth but at high shear rate, the difference in the rate of flow of rubber and plastic phases produced a rough surface.

1.6. Present work

From the forgoing discussions it is clear that a number of works have been carried out in the use of latex waste such thread waste, gloves waste and other microcellular wastes. Even though tire rejects, gloves waste, thread waste, microcellular sheet waste etc. and condom rejects are basically elastomers, condom rejects contains very high quality rubber hydrocarbon which is only lightly crosslinked. Therefore, its performance, when added as filler, on the properties of other elastomers and plastics cannot be predicted from the earlier results reported so far for tire rejects as well as latex reclaim. This means that there is a gap in the knowledge regarding the performance of powdered latex rejects in other elastomers and plastics. This study is aimed to fill this gap noted in the field of polymer recycling. Therefore, it is clear that a systematic study based on the efficient utilisation of waste condom rejects, as filler in elastomers and plastics deserves much importance. The results of such a study can open up new areas of research in polymer science and potential markets for waste condom rejects.

This thesis work of ten chapters, works on the main aspects of using mechanically ground prophylactics rejects as filler in synthetic elastomers and plastics. The first chapter is the introduction chapter discussing the concepts and metamorphosis of recycling in a very detailed manner providing the necessary information to a follower in this field. The second chapter gives the details of the materials used for the present study and the methodology as well as the theoretical backgrounds. The third chapter describes the rheometric processing, curing, mechanical and swelling behaviour of increasing loading

and particle size of prophylactics filler in an amorphous elastomer, styrene butadiene rubber (SBR). The fourth chapter discusses the rheological aspects of prophylactics filled styrene butadiene rubber compounds in the presence and absence of particulate fillers. In the fifth chapter, the works focuses on a strain crystallising elastomer of relatively recent origin, epoxidised natural rubber (ENR-25) describing the influence of both particle size and loading on the various properties of ENR. An emphasis to theoretical prediction of modulus of the samples with varying loading of the prophylactics filler is discussed. The work in chapter 6 moves to epoxidised natural rubber of higher epoxy content (ENR-50) giving emphasis to the processing and mechanical aspects of the prophylactics filled ENR-50 vulcanisates and use of dynamic mechanical aspects as a tool for the determination of distribution of particulate filler among the phases. In chapter 7, the influence of prophylactics filler loading on the curing, mechanical and swelling resistance of ethylene propylene diene rubber (EPDM) is investigated, giving emphasis to the effect of temperature. In chapter 8, the effectiveness of the prophylactics filler in the impact modification and dynamic mechanical properties of an amorphous plastic, polystyrene is analysed. In the chapter 9, the use of reclaimed and chemically modified prophylactics filler for the development of polypropylene composites is investigated. The tenth chapter is a conclusion of the results in the thesis for a quick reference.

1.7. REFERENCES

1. V.F.Drozdovskii., Kauchuk i. Rezina, 4, 23(1992).,Also Int.Polym.Sci. Technol, 19(11) 57 (1992)
2. Mod. Plast., March, 44-47 (1987).
3. J.R.Gunnigle., Proc.Conf. Rubber Div., Amer. Chem. Soc., Pittsburgh, PA, paper #68,Oct.11-14, 1994.
4. J. Schmitt-Tegge, Waste Management Forum, Saarbrucken, Germany, April 1994.
5. D. Burkle, Int. Recycling Congress R'93, Geneva, January 1993.
6. C.P. Rader and R.F.Stockel., Plastics, Rubber and Paper Recycling., ACS Symposium Series 609, Am.Chem.Soc., Washington DC, Ch 1, p.2, 1995.
7. J. Milgrom., Reuse-Recycle, 27,3 (1997).
8. U.S.Patent 5, 022, 985, to Plastic Recovery Systems, Inc., Toledo, OH, USA.
9. G. Fahrbach and H.R. Schnettler., 'New Dry Preparation Techniques to Prepare Used Packaging Plastics for Feedstock Recycling' Proc. Globec'96, Davos, Switzerland, paper 17-4.1,1996.
10. K.H. Unkelbach., 'High Duty Plastics Recycling with Centrifugal Force'(document available from KHD Humboldt Wedag AG, Koln, Germany)
11. M.S.Super, R.M.Enick and E.J.Beckman., ANTEC'91 (37) 2130 (1991)
12. M.S.Super, R.M.Enick and E.J.Beckman., Resources, Conservation and Recycling,9,75 (1993).
13. B.L.Altland, D.Cox, R.M.Enick and E.J.Beckman, Resources, Conservation and Recycling, 15,203(1995).
14. G.A.Serad and T.S.Thornburg., U.S.Patent#5,462,973,Separation of PET and PVC Using Supercritical CO_2 (to Hoechst Celanese Corp)(1995).
15. R.W.Kobler., U.S.Patent, 5,234,110(1993).
16. J.H. Schut, Plastic World, p.33, Nov 1994.
17. C.Gray., "Recent Development in Plastic Flake Sorting", Proc. SPE 3rd Ann. Recycling Conf., Chicago, IL, Nov 7-8th, , p 291, 1996.
18. G.Zachmann, J.Molecular Structure,348,453 (1995)
19. J.Graham., P.J.Hendra and P.Mucci., Plast Rubb. Compos.Process.Appln.,

24,55(1995).

20. N.Eisenreich and TH.Rohe., Kunststoffe, Feb, p.31, 1996.
21. T.Amano., Proc Recycle'95, Davos, Switzerland, Paper 18-3.1, 1995.
22. B.K. Mikofalvy and H.K. Boo., 'Technical Aspects of Vinyl Recycling' in Emerging Technologies in Plastic Recycling (ed.G.D.Andrews and P.M. Subramanian. ACS Symposium Series 513, Ch 23, p 296, 1992.
23. D.Vaughan and G.R.Kenny., New Challenges in Plastic Sorting' Proc.SPE, 3 rd Annual Recycling Conf, Chicago, IL, Nov, p 311, 1996.
24. P.E.Mucci, British Patent PCT/GB94/00101(1994).
25. K.Eichas., Triboelektrische Sortierung im Feinkornbereich, Cuvillier Verlag, Gottingen, 1993.
26. H. Schubert., Aufbereitung fester Stoffe, 4., Auflage Verlag fur Grundstoffindustrie, StutTgart (1996)
27. H.Hoberg and T.Schultz., Elektrstatische Trennung von Kunststoffen Nach Vorbehandlungihrer Oberflachen, Berg-und Huttenmannischer Tag, Freiberg, (1995)
28. P.A.Toesmaier, Modern Plastics, June, p.15 (1990)
29. E.B. Nauman, J.C.Lynch and S. Norwalk., 'Overcoming Challenges in Recycling High Value Plastics from Durable Goods' Presented at the University of North Carolina at Charlotte Symposium on Plastics Recycling, September, 1996.
30. E.B.Nauman and J.C.Lynch., 'Polymer Recycling by Selective Dissolution', US, Patent 5, 278, 282 (1994).
31. C.Spankuch and M.Fass., Kunststoffe, 84,8 (1994).
32. M.M.Fisher., ' Developing Technologies for the Recovery of Plastics from End-of-Life Durables-APC Initiatives', Proc. Globec.'96, Davos, Switzerland, p 12-3.1,1996.
33. C.Muther., 'Separation of Laminates Using Result Technology' Proc. SPE 3 rd Ann, Recycling Conf, Chicago, IL, Nov 7-8, p 37, 1996.
34. S.Hemel., Proc. SPE 3rd Ann, Recycling Conf, Chicago, IL, Nov 7-8, p 395. 1996.
35. J.A.Horrocks., 'Recycling of Plastic Fiber and Packaging Waste',

Proc.Ecotextile'95 Conf., 11-12 April 1995.

36. J.Ogando., Plastics Technol., June, p.37 (1994)
37. A.Riahi, J.L.H.Arastoopour, G.Ivanov and F.Shutov., Proc.ANTEC'93, 891(1993).
38. K.Khait., Proc.ANTEC'94, 3006 (1994)
39. K.Khait, Proc. GLOBEC'96, Davos, Switzerland, March 18-22, paper 18-3.1,1996.
40. Gneuss document,'Filteration of Plastics Melt',ed. Detlef Gneuss, 1988, [available from Gneuss Kunststofftechnik GmbH, 4970 Bad Oeynhausen, Germany]
41. W. Michaeli and K. Breyer, Macromol.Symp., 135, 83 (1998).
42. G. Patuska, W.Lutzow, Testing of Plastics for Long Term Properties After Repeated Work-Up. In:Entsorgung von Kunststoffabfallen Durch Verwertung, Expert-Verlag, Grafenau (Wuert), 1982.
43. H. Saechtling, Kunststoff Taschenbuch, Hanser, Munchen-Wien, 1986.
44. J. Herrler, Is an Environmentally Tolerable Recycling of House Hold Plastics Possible? In: K.J.Thome-Kozmiensky, H. Kaufer, Recycling von Kunststoffen 1, EF-Verlag fur Energie und Umwelt, Berlin, 1987.
45. R. Gachter and H.Muller, Taschenbuch der Kunststoff –Additive, Hanser, Munchen, 1989.
46. R. Pfaender, H. Herbst and K. Hoffmann, Macromol. Symp., 135, p. 97, 1998.
47. H.Herbst, K.Hoffmann and R.Pfaender, Durable Goods from Recyclate from Out Door Applications- the Role of Light Stabilisers, Presented at R'97 Congress, February 4-7, p. 1116-1121,1997, Geneva, Switzerland.
48. R.Pfaender, Perspektiven zum werkstofflichen Kunststoff-Recycling-Mit Additiven die Marktchancen von Recyclaten verbessern, presented at Colloquium Werkstoffliche VerwertungThermoplastischer Kunststoffe, Aachen, p. 8.1-8.31, February 4, 1997.
49. H.Hoberg, H.Hocker, W. Michaeli, K.W. Pleβmann, K.Breyer, P. Laufens, T. Schultz, P. Schwarz and C. Zurbig, Material recycling of thermoplastics, Proc. 22 nd Int. Mineral Processing Congress, Aachen, 1997.

50. O.Appel, M. Bittner, J. Dassow, K. Kerres, V. Lackner and B. Lewen, Recycling von Kunststoffen, Proc. 16 th Plastics-Technological Colloquium, Inst. Plast.Process., Aachen, 1992.

51. K. Niemann: "Utilisation of Waste Plastics by Hydrogenation", in DGMK-Tagungsbericht 9603, p. 35, 1996.

52. H. Loffler, Thermal Treatment of Residues in Vienna, Austria, Madrid, October 1996.

53. C. Ammundsen, Waste Meeting, Copenhagen, March 1995.

54. A.Cabanes, Conference of Association de Mairies Operant un Reseau de Chaleur et d'Electricite (AMORCE), Pollutec Lyon, France, October 1996.

55. P. Straka, J. Buchtele and J. Kovarova, Macromol. Symp., 135, 19-23 (1998).

56. P. Straka and J. Buchtele: Proc. 2 nd Int. Conf. on Energy and Environment: Transitions in East Central Europe, pp. 471-475, 1-5 November, Praha, 1994,

57. M.S.O.: Burdova, Thesis, Prague Institute of Chemical Technology, 1996.

58. H. Bockhorn, A. Hornung and U. Hornung., Macromol. Symp, 135, 35-41 (1998)

59. W. C. Mc Caffrey, D.G. Cooper and M.R. Kamal., Polym. Degrad. Stabil., 62, 513 (1998).

60. W.E. Stafford and R.A.Wright., 'The Applied Science of Rubber', W.J.S. Naunton, Edward Arnold (Publishers) Ltd., Ch IV, Part 1, p. 253, 1961.

61. F. G. Smith, 'Reclaimed Rubber', Ch 5, TheVanderbilt Rubber handbook, Corporate Office and Laboratories, 30 Winfield Street, Norwalk, Connecticut 06855 (203) 0 853-1400, TWX 710-486-2940, 1978.

62. J.M. Ball, 'Reclaimed Rubber', Ch. 1, Rubber Reclaimers Assoc., New York, 1947.

63. N.Hader and D.S. Le Beau., Ind.Eng.Chem., 43, 250 (1951).

64. W.E.Stafford and R.A. Wright., Proc. Inst.Rubber Ind., I, 40 (1954)

65. P. Alexander, Proc.Rubber.Tech.Conf., London, paper 55, 1938.

66. A.H. Marks., USP, 635, 141 (1899)

67. D.A.Cutler., USP, 673,057(1913)

68. C.S.Whitby, Synthetic Rubbers (New York).

69. I.Drogin, India Rubb. World, 128, 772; 129,63 (1953).

70. H.L.Hall., USP, 22,217 (1858).

71. N.C. Mitchell, USP, 249, 970(1881).

72. J.M.Ball, Reclaimed Rubber, Ch. 2, Rubber Reclaimers Assoc., New York, 1947.

73. Rubb. Age, NY. 75, 548 (1954).

74. E. Bemelmans., BP, 435, 890 (1935).

75. F.H.Cotton and P.A.Gibbons., BP, 577, 829 (1946).

76. P.J Dasher, B.F.Goodrich Co., inv. USP, 2, 498, 398(1950)

77. F.L.Kilbourne and G.W. Miller, Ind. Eng. Chem., 22, 69 (1930).

78. H.A.Winkelmann., Rubb. Age, NY 65,57 (1949).

79. F. Kirchoff., Kautsch.u.Gummi, 2, 151 (1949).

80. B.S. 903:73 (1950).

81. ASTM, p.146 (1950)

82. D.S. Le Beau., Anal. Chem., 20,355 (1948)

83. H.J.Stern, Rubber-Natural and Synthetic (London:Mac Laren), 478,1954.

84. J.M.Ball, Reclaimed Rubber, Ch. 8, Rubber Reclaimers Assoc., New York, 1947.

85. F.L.Kilbourne, J.E.Misner and R.W. Fairchild., Rubb. Age, NY 66,423(1950).

86. T.Baader., Rubber Chem.Technol., 28,588 (1955).

87. H.Winkelmann., Ind. Eng. Chem., 18,1163 (1926).

88. E.H.Wallace, India Rubb.J., 103, 633 (1942).

89. F.L.Kilbourne. Rubb. Age., NY 62,541 (1948).

90. R.M. Randall and J.M. Ball., India Rubb. World, 130, 795 (1954).

91. G. Shaboyashi., J. Soc.Rubb.Ind. Japan., 15,514 (1942).

92. Compounding Ingredients for Rubber, (New York: India Rubb. World) 569, 1947.

93. H.F.Palmer and R.H.Crossley., IRI Trans., 17, 261 (1941/42).

94. B.F. Goodrich Co., Reclaimed Rubber-Industrial Products.

95. M.Schade., Rubb.Age, NY, 63,498 (1948).

96. Vanderbilt News, 16(4), (1950).

97. S.T.I.K. Polymers (India) Pvt. Ltd, Technical Bulletin, DLB.1, International Seminar and workshop on devulcanisation using De Link process, Brickendonbury,

Hertford, UK. April, 1995.

98. S. Isshiki, T. Shimorizu and M. Kuroda, Eur.Pat. Appl., DE 2216594 .

99. A. Casale and R.S.Porter, "Polymer Stress Reactions" Academic press, NY, 1977.

100. A. Tukachinsky,., D. Schworm and A.I. Isayev, Rubber Chem. Technol., 69, 92 (1996).

101. V.Yu.Levin, S. H.Kim, A. I. Isayev, J. Massey and E. von. Meerwall, Rubber Chem. Technol., 69, 104 (1996).

102. A. I. Isayev, J. Chen and A. Tukachinsky., Rubber Chem. Technol., 68, 267 (1995).

103. A. I. Isayev, S. P. Yushanov and J. Chen., J. Appl. Polym. Sci., 59, 803(1996).

104. P.Kennedy, "Tire Pile Improvement and Remediation Effectiveness Act, "United States Congress Bill, H.R. 1041, 105th Congress, 1997.

105. N. Gebhardt., Rubber Asia, p. 54, Jan-Feb 1996.

106. I. Gawel, L. Slusarski, Progress in Rubber and Plastics Technology, 15 (4) (1999).

107. Y.K. Park, J.T. Reaves, C.W. Curtis and C.B. Roberts, J. Elast. Plast., 31,162 (1999).

108. I. Funazukuri, S. Ogasasawara and N. Wakao and J.M.Smith, J. Chem. Eng., Japan 18(5) 455 (1985).

109. I. Funazukuri, T. Takahashi and N. Wakao., J. Chem. Eng., Japan 20(1) 23 (1987).

110. D.S. Le Beau, Rubber Chem. Technol., 40, 217 (1967).

111. V.N. Kalinichenko, G.A. Blokh, A. Ya. Vasker Sulyaeva, Int.Polym. Sci.Technol., 11, T/87 (1984).

112. R.P.Burford and M.Pittolo, Rubber Chem Technol., 55, 1233 (1982).

113. R.H. Wolk, Rubber Age., 104, 103 (1972).

114. N. Kawabata, T. Murkami, S. Yamashita, Int.Polym.Sci.Technol., 7, 29 (1979).

115. N.M. Claramma, B. Kuriakose, E.V. Thomas, paper presented at the International Conference on Rubber and Rubber-like Materials 6-8 Nov.1986, Jamshedpur, India.

116. Y. Aziz, "High Quality Reclaimed Rubber from Latex Waste", paper presented at

the Plastics Rubber Institute Seminar, Kuala Lumpur, Malaysia, 4th August 1990.

117. Y. Aziz, "Utilisation of Reclaimed Rubber from Latex Glove Factory Rejects", paper presented at Polymer 90. Kuala Lumpur, Malaysia, 23 September 1990.

118. S.G. Reena and J. Rani, Die Angew. Makromol. Chemie., 215 (3711), 25 (1994).

119. S.G. Reena and J. Rani, Iran. Polym. J., 5(3), 199 (1996).

120. S.G. Reena, J. Rani, K.E. George and D.J. Francis., J. Elast.Plast., 27, 138 (1995).

121. J. Mary, R.Joseph and K.E.George, "Production of Chlorinated Rubber from Latex Waste", paper presented at 7th Kerala Sci. Congress.27-29 Jan, 1995, Palakkad, Proceedings Paper no 02-01, p. 60-62.

122. R. Stilathakutty, J. Rani and K.E.George., Polym. Recycl., 3(4), 303 (1997).

123. S. Rajalekshmi and J. Rani., Polym. Recycl., 6 (2/3), 99 (2001).

Chapter 2

CHAPTER 2

MATERIALS AND EXPERIMENTAL DETAILS

ABSTRACT

This chapter gives information regarding the basic materials and methodology used in the thesis. The source and basic characteristics/properties of the various raw materials used for the experiments are discussed. Discussions give emphasis to the basic formulations, conditions and procedure used for the preparation of the samples, giving their codes also.

The details of various instruments used for the characterisation of the samples, the relevant ASTM test methods and the mathematical equations used for the determination of different parameters etc. are also provided. In the case of some special experiments which are not very common, sketches or figures to clarify the experiments have been included.

CHAPTER 2

MATERIALS AND EXPERIMENTAL DETAILS

2.1 Materials

2.1.1. Styrene butadiene rubber (SBR)

Styrene butadiene rubber (Synaprene 1502) is a copolymer of styrene and butadiene produced by emulsion polymerisation using free radical catalysts. It was obtained from Synthetics and Chemicals Ltd.,Bareilly,U.P., India. The basic characteristics of SBR are given in **Table 2.1**.

Table 2.1.Basic characteristics of SBR used

Ingredients	Percentage
Styrene	21.5-25.5
Volatile matter (max)	0.75
Soap (max)	0.7
Ash (max)	0.5
Antioxidant	0.5-1.5
Cis-1,4	18
Trans-1,4	65
1,2(vinyl)	17

2.1.2. Natural rubber prophylactics filler

Natural rubber prophylactics filler was prepared from condom rejects which was obtained from Hindustan Latex Ltd., Thiruvananthapuram, Kerala, India. The basic characteristics of prophylactics filler are given in **Table 2.2.**

Table 2.2.Basic characteristics of prophylactics waste material

Property	Value
Colour	Light pink / yellow
Glass transition temperature, ^{0}C	-63

Preparation of NR prophylactics filler

The ground vulcanisate preparation was done in a fast rotating toothed wheel mill. The advantage of this technique was the ability to obtain a fine elastic rubber powder, unlike cryoground rubber (CGR) which is stiff[1]. Therefore CGR will not permit easy diffusion of curatives into it. The powder rubber was found to be polydispersed in particle size. It was then sieved into four different particle sizes, ranging from 0.3-0.5 mm (size 1 or S1), 0.6 - 0.9 mm (size 2 or S2), 1.7 - 2.5 mm (size 3 or S3) and 9-11 mm (size 4 or S4). A mill-sheeted form (M) of the latex rejects also was prepared by the repeated passing of the rejects through a hot two-roll mill at tight nip.

2.1.3. Natural rubber (NR)

Natural rubber (ISNR 5) was supplied by the Rubber Research Institute of India, Kottayam, Kerala, India. Approximate composition and basic characteristics of ISNR-5 are given in **Table 2.3** and **2.4**.

Table 2.3. Approximate composition of ISNR-5 used

ISNR-5	% / mass
Dirt Content (max)	0.04
Volatile Matter (max)	0.3
Nitrogen (max)	0.3
Ash (max)	0.4
Initial Plasticity (P_0) (min)	45
Plasticity Retention Index (PRI) (min)	75

Table 2.4. Basic characteristics of ISNR-5

Properties	ISNR-5
Specific gravity, gm/cc	0.93
Glass transition temperature, ^{0} C	-75
Solubility parameter, $cal^{1/2} / cm^{3/2}$	8.25
Resilience, at 20^0 C	4
at 100^0 C	4
Tensile strength, gum	3
reinforced	4
Dielectric properties	3
Bonding to substrates	3
Resistance to gas permeation	2
Tear resistance	3
Resistance to cutting and cut growth	3
Resistance to flexing and fatigue	3
Heat resistance	2-3
Flame resistance	2
Ozone resistance	1
Environmental resistance	2-3
Resistance to acids	2
aqueous	3
aliphatic	1
aromatic	1
animal and vegetable oils	1
oxygenated organics	2-3

1 – poor 2- moderate 3- good 4- outstanding

2.1.4. Epoxidised natural rubber (ENR)

The epoxidised natural rubber samples used were ENR-25 and ENR-50, supplied by Malaysian Rubber Research Bureau, Malaysia. A comparison of their general properties is given in **Table 2.5**.

Table 2.5. General properties of ENR used

Property	ENR-25	ENR-50
Epoxide level, mole %	25+-2	50+-2
Glass transition temperature ^{0}C	-47	-24
Density, gm /cc	0.97	1.02
Solubility parameter, $(J\ m^{-3})^{0.5}$	17.4	18.2
Lovibond colour	4.5	3.5
Protein level, [a] mg/g rubber	0.0008	0.0008
Latex protein activity,[b] Normalised unit	2-4	2-4

a. Lowry method used.
b. RAST method.

2.1.5. Ethylene propylene diene rubber (EPDM)

Ethylene propylene diene rubber (Roylene® 521) was manufactured and supplied by Uniroyal, USA. The characteristic properties are given in **Table 2.6**.

Table 2.6. General characteristics of EPDM rubber used

Properties	EPDM
Specific gravity, gm/cc	0.86
Glass transition temperature, ^{0} C	-58
Solubility parameter, $cal^{1/2} / cm^{3/2}$	8
Resilience, at 20^0 C	3
at 100^0 C	3
Tensile strength, gum	1
reinforced	3
Dielectric properties	3
Bonding to substrates	2
Resistance to gas permeation	2
Tear resistance	2
Resistance to cutting and cut growth	2
Resistance to flexing and fatigue	3
Heat resistance	3
Flame resistance	2
Ozone resistance	4
Environmental resistance	4
Resistance to acids	3
aqueous	3
aliphatic	1
aromatic	1
animal and vegetable oils	3
oxygenated organics	3

1 – poor 2- moderate 3- good 4- outstanding

2.1.6. Polystyrene (PS)

Polystyrene used for the present study was Polystron 678 SF-1, (crystal grade) and was manufactured and supplied by Polychem Ltd, India. The characteristic properties are given in **Table 2.7.**

Table 2.7. General characteristics of Polystyrene used

Property	Value
MFI (g/10 min)	15
Density, g/cm^3	1.05
Softening point, ^{0} C	100
Elongation at break, %	9
Tensile strength, MPa	34
Youngs's modulus, MPa	390

2.1.7. Polypropylene (PP)

Polypropylene used for the present study was Stamylan P 13 E 10 and was manufactured and supplied by DSM, USA. The characteristic properties are given in **Table 2.8.**

Table 2.8. General characteristics of Polypropylene used

Property	Value
MFI (g/10 min)	6
Density, g/cm^3	0.91

2.1.8. Solvents

Toluene, chloroform etc were of reagent grade and supplied by Merck India Ltd., Mumbai, India.

2.1.9. Chemicals and fillers

All the chemicals used for the preparation of rubber compounds were of industrial purity. Cetyl trimethyl ammonium bromide (CTAB), sodium hydroxide, dicumyl peroxide (40% active) (DCP), zinc oxide, stearic acid, N-cyclohexyl-2-benzothiazyl sulphenamide (CBS), mercaptobenzthiazyl sulphenamide (MBTS), 2,2,4-trimethyl -1,2-dihydroquinoline

(TDQ), maleic anhydride, dimethylol phenol, processing aid (aromatic oil), stannous chloride and sulphur were of commercial grade. De Link used for reclamation was obtained from STI-K polymers (India) Pvt. Ltd, Mumbai, India.

The fillers such as carbon black [high abrasion furnace (HAF)], precipitated silica and marble powder also were of commercial grade.

2.2. Methods

2.2.1. Preparation of polymer blends

The mixing of matrix polymer with the compounding ingredients as well as polymeric inclusions was carried out at room temperature on a laboratory size two roll mixing mill (15 cm x 30 cm) at a friction ratio of 1:1.5 as per ASTM D-3182-74 by carefully controlling the temperature, nip gap, time of mixing, and uniformity of cutting operations[2]. Basic formulation used for each work is given in the respective chapters. The temperature of the mill was maintained at room temperature by the circulation of cold water through the rolls.

2.2.2. Preparation of surface epoxidised NR prophylactics filler

The surface epoxidation[3] of prophylactics filler at room temperature was carried out by using performic acid formed from a mixture of formic acid and hydrogen peroxide of varying concentrations **(Table 2.9)**. The reaction mixture was stirred, washed with distilled water and finally dried in vacuum oven. The progress of the reaction was monitored by determining the epoxy value of the samples withdrawn from the reaction mixture at different intervals of time. The reaction can be represented as given below.

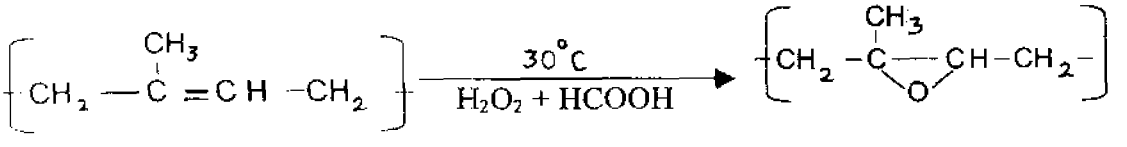

Scheme 2.1 Epoxidation reaction

Table 2.9. Details of epoxidation

Concentration of epoxidation reagent (H_2O_2 + HCOOH)	Time of reaction
Variable	Variable
10-30 %	0-144 h
i.e.,	i.e.,
10 % solution, 20 % solution and	0, 0.5, 1, 2,
30 % solution	6, 24 and 144 hrs

2.2.3. Preparation of surface dichlorocarbene modified prophylactics filler

The dichlorocarbene modification was done according to the method by Makosza and Wawrzyniewics[4] and later developed by Joshi et.al.[5] A slurry of prophylactics filler in toluene was stirred in the presence of chloroform and alkali (50%) in the presence of a phase transfer catalyst CTAB at room temperature. Finally, the mixture was washed with slightly warm distilled water until it is free of chlorine. Then the prophylactics filler was dried in vacuum oven. The modification was monitored **(Table 2.10)** by withdrawing a certain amount of reaction mixture at different intervals of time and analysing it for chlorine content.

The reaction can be represented as given below.

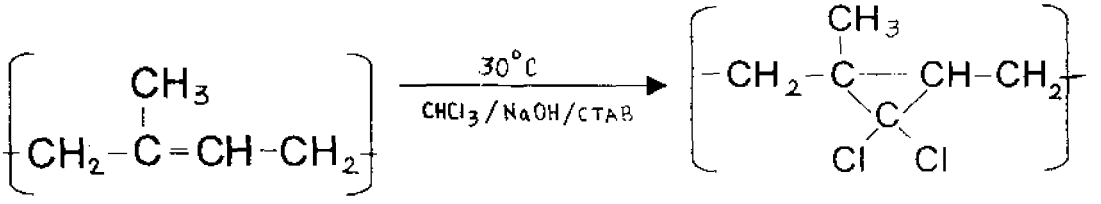

Scheme 2.2. Dichlorocarbene modification

Table 2.10. Sample codes of dichlorocarbene modification

Time of reaction, h	Code
0	C0
2	C1
4	C2
8	C3
24	C4
48	C5
72	C6

2.2.4. Reclamation

The reclamation was done by the De Link process. De Link is a specially made reclaiming agent whose composition is a trade secret and subject of a number of worldwide patents. It is a mixture of highly active chemicals which can sever sulphur crosslinks at ambient temperature, without the assistance of pressure. The process can be carried out using simple standard rubber mixing machines which provide the necessary mechanical shearing action. The final reclaimed material obtained from De Link reclamation is called De Vulk which can be revulcanised easily without even adding any sulphur. The recommended recipe for De Link reclamation is given in **Table 2.11** and the reaction can be represented as shown in **Scheme 2.3**.

Table. 2.11. Reclamation recipe

Material	Control, phr
NR Prophylactics	100
De Link	6
Processing Aid	2
Premasticated NR	6
Total (De Vulk)	114

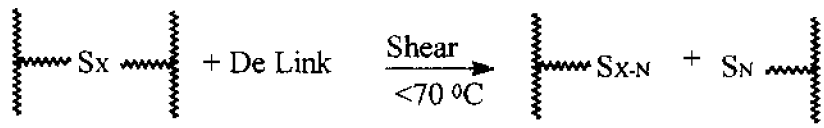

crosslinked prophylactics rejects

delinked prophylactics rejects

[If X is the total number of sulphur crosslinks, N specifies the number of crosslinks broken due to reclamation]

Scheme 2.3. Reclamation Process

2.2.5. Preparation of maleic anhydride modified polypropylene (MA-PP)

This was carried out using a two roll mixing mill (tight nip) according to the recipe given in **Table 2.12**. The temperature used was around 170^0 C in order to ensure the softening / melting of polypropylene. This was done in special two roll mixing mill with the facility for oil heating. This is presented in **Scheme 2.4.**

Table 2.12. Recipe for maleic anhydride modification

Material	Control, php
Polypropylene	100
Maleic anhydride	5
Antioxidant (TDQ)	1
Dicumyl peroxide	3

[php-parts per hundred plastic]

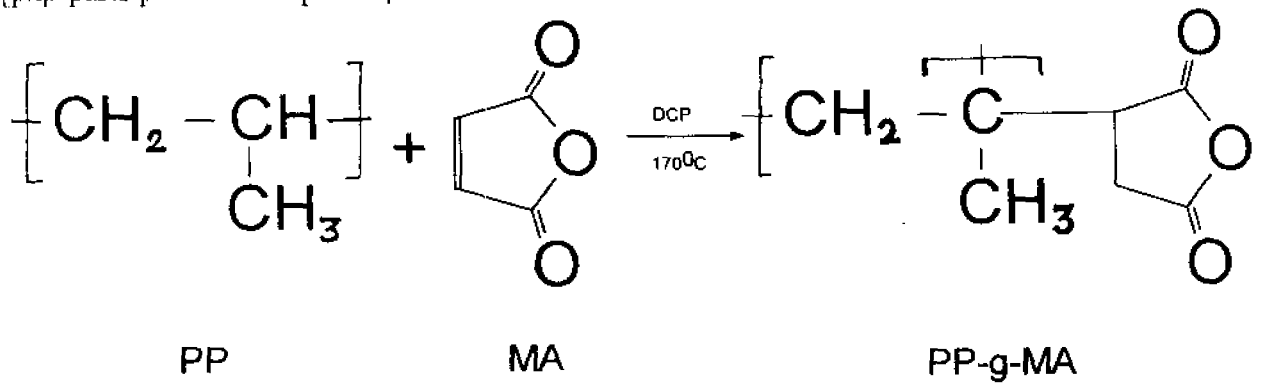

Scheme 2.4. Maleic anhydride modification of polypropylene

2.2.6. Preparation of dimethylol phenol modified polypropylene (Ph-PP)

This also was carried out as in the earlier case according to the recipe given in **Table 2.13**. This is presented in **Scheme 2.5.**

Table 2.13. Recipe for dimethylol phenol modification

Material	Control, php
Polypropylene	100
Dimethylol phenol	4
Stannous chloride	1

[php-parts per hundred plastic]

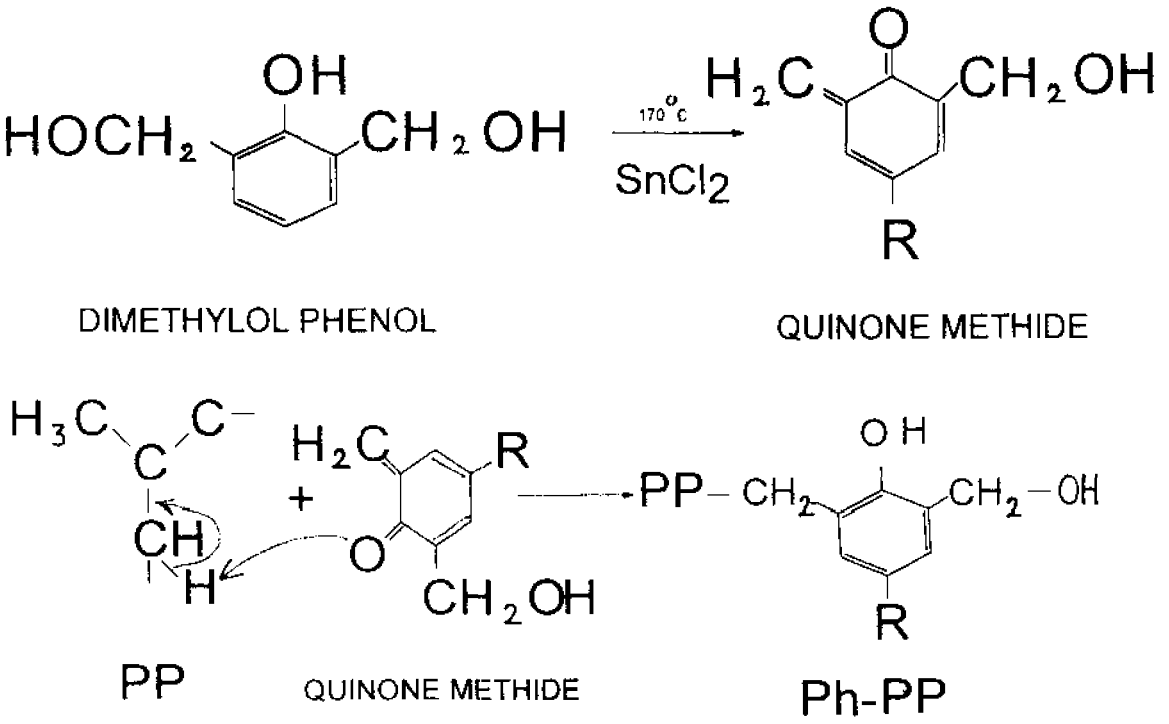

Scheme 2.5. Phenolic modification of polypropylene

2.3. Characterisations

2.3.1. Processing and curing characteristics

The rheometric processing characteristics include the minimum and maximum torque in rheographs at 150°C. The minimum torque (M_n) in rheograph was taken as the minimum viscosity or torque. The maximum torque (M_h) in rheographs was presented as the maximum viscosity or torque and is a direct measure of the crosslink density in the cured sample. These were measured using a Monsanto Rheometer model R-100 at 150^0 C.

The cure characteristics also were determined using a Monsanto Rheometer model R-100. Optimum cure time (t_{90}) is the time corresponding to the development of 90% of maximum torque. It was calculated using the equation,

$$t_{90} = \frac{(M_h - M_t)\ 90}{100} + M_n \qquad (2.1)$$

where M_h and M_n are the maximum and minimum rheometric torque respectively.

Rheometric scorch time (t_2) is the time required for the torque value to increase by two units above the minimum torque at 150^{0}C. It is a measure of the scorch safety of the rubber compound. Rheometric induction time (t_1) is the time required for the torque value to increase by one unit above the minimum torque at 150^{0}C.

Cure reaction kinetics

The fastness of the curing reaction was analysed by measuring two parameters, cure rate index (CRI) and cure reaction rate constant.

$$CRI = \frac{100}{t_{90} - t_2} \qquad (2.2)$$

The kinetics of vulcanisation was studied from these rheographs by the method[6] given below.

The general equation for the kinetics of a first order chemical reaction is

$$\ln (a-x) = -kt + \ln a \qquad (2.3)$$

where a = initial reactant concentration

x = reacted quantity of reactant at time t

k = first order rate constant

For the vulcanisation of rubber, the rate of crosslink formation is monitored by measuring the torque developed during vulcanisation. The torque so obtained is proportional to the modulus of rubber. So following substitutions can be made

$$(a-x) = M_h - M_t, \qquad (2.4)$$

$$a = M_h - M_n \qquad (2.5)$$

M_h = Maximum rheometric toque

M_n = Minimum rheometric torque

M_t = Rheometric torque at time t

So the equation is

$$\ln (M_h - M_t) = -kt + \ln (M_h - M_n) \quad (2.6)$$

This equation is of the general form of a straight line. Therefore, if a plot of $\ln (M_h - M_t)$ verses time t is a straight-line graph, it means that the cure reaction follows first order kinetics. The cure reaction rate constant (k) can be directly obtained from the slope of the respective straight lines.

The energy of activation E_{act} of curing can be determined using the Arrhenius equation given below.

$$k = A \exp(-E_{act} / RT) \quad (2.7)$$

$$\log k = \log A - \frac{E_{act}}{2.303\, RT} \quad (2.8)$$

where A is the Arrhenius constant, E_{act}, the activation energy, R, universal gas constant and T, the absolute temperature.

2.3.2. Vulcanisation

Vulcanization to optimum cure was carried out in a hydraulic press at 150^{0}C and at a pressure of 45 Kg / cm^2 on the mold.

2.3.3. Mechanical property characterisation

Stress-strain data of the vulcanisates were determined using an Instron Universal Testing Machine, with dumb-bell shaped test pieces[7]. Test pieces were punched out from the compression molded sheets using a die, along the mill grain direction. Five specimens were tested for each composition at a crosshead speed of 500 mm/min and the results were averaged. The stress-strain data thus obtained was also used to calculate ν_{phys}, the physical crosslinks.

Young's modulus, secant modulus, tensile strength and elongation at break

The slope of the initial linear portion of the stress-strain curve was taken as the Young's modulus. Secant modulus was taken as the force for a particular elongation. Tensile strength and elongation at break were determined according to ASTM D412-92. Young's modulus, secant modulus and tensile strength were reported in MPa and elongation at break, in percentage.

Tear resistance

Tear resistance[8] of the samples was tested as per ASTM-D-624-81, using unnicked 90° angle test specimens punched out from molded sheets, along the mill grain direction. This test also was carried out on an Instron Universal Testing Machine, at a crosshead speed of 500 mm per minute. The tear strength is reported in kN/m.

Hardness

Hardness[9] of the samples was measured according to ASTM D-2240-81 using an IRHD hardness tester.

Impact strength determination

Impact strength of the samples were determined on a Ceast Impact Tester (Model 6545/000) using rectangular pieces of diamension 5 x 0.5 x 0.5 cm^3.

Dynamic mechanical properties

The dynamic mechanical properties of the blends were measured using a dynamic mechanical analyzer, DMTA, MK II (Polymer Laboratories, Laboratory of Macromolecular Structural Chemistry, Heverlee, Belgium) consisting of a temperature programmer and a controller. Samples of dimension 5 x 0.5 x 0.5 cm^3 were prepared for testing. At least two molded bars of the same sample were measured to get the average of one data point. It measured the dynamic moduli (both storage and loss) and damping of the specimen under oscillatory load as a function of temperature. The experiment was conducted at a dynamic strain of 4 % at frequencies 0.1 to 100 Hz. Liquid nitrogen was used to achieve sub ambient temperature and a programmed temperature range of – 80 to + 30 ^0C starting from the lower temperature to the higher one on a given sample. Mechanical loss factor tan δ and the dynamic moduli (E′ and E″) were calculated with a microcomputer. Glass transition temperature of the samples also were obtained in this work from E''-temperature plots.

The activation energy E_{act} for the glass transition of the samples can be calculated using the Arrhenius equation given below.

$$f = f_0 \exp(-E_{act} / RT) \qquad (2.9)$$

where f is the experimental frequency, f_0 is the frequency at T tends to infinity, and T is the temperature corresponding to the maximum of the E''-temperature curve (since glass transition values were taken from these plots in this work)

2.3.4. Chemical analysis

Epoxy content determination

Accurately 0.7 - 1.5 gms (W) of the epoxidised material was weighed into a 250 ml iodine flask, which was followed by the addition of 80 ml of acetic acid. This was titrated against HBr solution in a 50 ml burette (Normality N) with crystal violet indicator until the end point of green colour appears. From the volume of HBr used (V), the epoxy value was calculated as

$$\text{Epoxy value} = \frac{V \times N \times 0.1}{2 \times W} \qquad (2.10)$$

Estimation of chlorine content

This analysis was carried out in the elemental analysis lab of Department of Chemistry, National University of Singapore, Singapore.

2.3.5. Spectroscopic studies

Fourier Transform Infrared Analysis

IR spectra of samples were recorded with a Shimadzu–8101 M Fourier transform infrared spectrophotometer, using KBr pellet method. The light source (an electrically heated solid, e.g., a nichrome wire) produced a beam of infrared radiation which was divided (by a system of mirrors) into two parallel beams of equal intensity radiation. The sample was in the path of one beam. A slowly rotating diffraction grating or prism varied the wavelength of radiation reaching the sample and then the detector. The detector recorded the difference in intensity between the two beams on a recorder chart as percentage transmittance. Maximum transmittance was at the top of the vertical scale, so absorbance was observed as a minimum on the chart even though it was called a peak.

2.3.6. Thermal analysis

Thermal analysis was carried out using a differential scanning calorimeter (DSC) and a thermogravimetric analyser with simultaneous difference temperature (TGA-SDT).

Differential scanning calorimeter

Direct calorimetric measurements, characterisation and analysis of thermal properties of the sample were made using a DSC instrument DSC 2920 series differential scanning calorimeter manufactured by TA instruments. Sub-ambient operation was carried out by cooling the specimen and the specimen holder with liquid nitrogen. Exactly weighed (about 5 mg) sample was used for the studies. Samples were encapsulated in standard aluminium pans with holes and covers and sealed by crimping. For purging the sample holders pure air was used. The inlet gas pressure was adjusted at 2 kg/cm^2 to attain a flow rate of about 25 ml/min. Scanning rate was 20°C/min.

Thermogravimetry

A thermogravimetric analyser with facility for simultaneous difference temperature (SDT) measurement SDT 2960 was used for the studies. It was a computer controlled instrument that permitted the measurement of weight changes as well as difference in temperature between sample and reference pans (SDT) as a function of temperature or time. It was programmed from an initial to final temperature and measured the weight change resulting from chemical reaction, decomposition, solvent and water evolution, curie point transitions and oxidation of the sample. The temperature was scanned at a linear rate. The instrument supplied by TA instrument had two components, an ultra sensitive microbalance and a furnace element with a special device for SDT measurement. The balance was sensitive to 0.1 microgram and the furnace could be heated from ambient to 1000°C at rates of 0.1 to 200°C per min. For purging the sample holder, gases commonly used were oxygen, air (a mixture of 80% nitrogen and 20% oxygen) or nitrogen so as to study the oxidation, burning and thermal stability of the materials. The purge gas flowed directly over the sample. The recommended flow rate of the sample purge was kept less than the flow rate of the balance purge at all times.

2.3.7. Contact angle analysis

Contact angles of the materials were determined using a goniometer SCV 3568 (Chiu Technical Corporation, Singapore) with water as the liquid (sessile drop method-**Figure 2.1**). The measurements were made after conditioning the samples in a humidity chamber for 24 hrs.

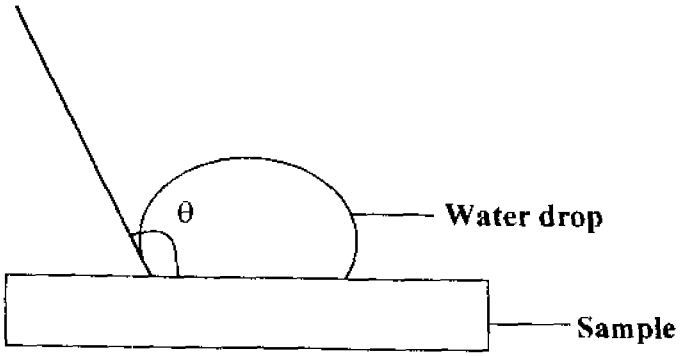

Figure 2.1. Determination of contact angle by sessile drop method

2.3.8. Ageing studies

In order to analyze the aging resistance of the samples, dumbbells were kept in an air oven at 100°C for 72 h. The stress-strain behavior and tensile strength of these aged samples were tested under similar conditions given earlier.

2.3.9. Scanning electron microscopy

The scanning electron microscopy (SEM) photomicrographs given in this work were obtained using JEOL JSM 35C model scanning electron microscope. The fracture surfaces were carefully cut from the failed test specimens without touching the surface and are sputter-coated with gold within 24 h. of testing. The SEM observations were made within 24 h of gold coating. The fractured specimens and the gold coated samples were stored in desiccators till the SEM observations were made. There should not be any change in the fracture pattern when the SEM observations were made one month after gold coating[10].

2.3.10. Swelling studies

Equilibrium swelling[11] studies were carried out in toluene to analyze the swelling resistance of the gum and filled samples. Circular samples of 2 cm diameter were allowed to swell in toluene at 28°C until equilibrium was reached. In order to analyze the extent of swelling, of gum and filled elastomer vulcanisates, swelling index and swelling coefficient[12] (α) values were calculated, using equations given below.

$$\text{Swelling index (\%)} = \frac{(w_2 - w_1)}{w_1} \times 100 \qquad (2.11)$$

where w_1 = Initial weight of the sample

w_2 = Final or swollen weight of the sample.

$$\text{Swelling coefficient } \alpha = \frac{A_s}{m} \times \frac{1}{s} \qquad (2.12)$$

where A_s = Amount of solvent absorbed

m = Initial weight of the sample

s = Density of the solvent used.

The more these values, the more will be the extent of swelling and less will be the filler-matrix adhesion.

The volume fraction of rubber in the solvent swollen sample was calculated by the method reported by Ellis and Welding[13] as;

$$V_{rf} = \frac{(d - fw)\,\rho_r^{-1}}{(d-fw)\,\rho_r^{-1} + A_s\,\rho_s^{-1}} \qquad (2.13)$$

A_s = Solvent uptake of the sample

ρr = Density of rubber

ρs = Density of solvent (toluene)

w = Initial weight of the sample

d = Deswollen weight of the sample

f = Volume fraction of filler in rubber.

Diffusion, sorption and permeation coefficients

The mol % uptake was calculated using the equation;

$$Q_t = \frac{M_e\,(m)/M_r\,(m) \times 100}{M_i\,(s)} \qquad (2.14)$$

where M_e (m) is the mass of solvent at a given time.

M_r (m) is the molecular weight of the solvent

M_i (s) is the initial weight of the specimen.

At equilibrium swelling, Q_t was taken as Q_α the mol % uptake at infinite time.

The mechanism of penetrant transport into the elastomer network was analysed in terms of the empirical relation[14]

$$\log \frac{Q_t}{Q_\alpha} = \log k + n \log t \qquad (2.15)$$

where Q_t is the mol % uptake at time t, and Q_α is the equilibrium mol % uptake. The factor k is a constant depending on the structural characteristics of the filler and polymer/ solvent interaction. The parameter n determines the mode of sorption mechanism. If the value of n is 0.5, it means that the rate of diffusion of penetrant molecules is much less than the rate of relaxation of polymer chains. This mode of transport is termed as Fickian. On the other hand, if the value of n is unity, the mode of diffusion is termed as non Fickian when the rate of diffusion of penetrant molecules is much faster than polymer relaxation. When the rates of both processes are similar, value of n will fall between 0.5 and 1, presenting an anomalous behavior. The computation of n and k was done by constructing the plots of log Q_t vs. log t and linear regression considering only the data upto 50%. sorption.

The effective diffusivity[15], D of the elastomer-solvent system was calculated from the initial linear portion of the sorption curves using the equation given below.

$$D = \pi \left[\frac{h\theta^2}{4 Q_\alpha} \right] \qquad (2.16)$$

where θ is the slope of the initial linear portion of the sorption curve

h, the thickness of the polymer sample

Q_α, the equilibrium mol % uptake.

If there is extensive swelling for the samples, correction to diffusion coefficients are necessary by calculating the intrinsic diffusion coefficients[16], D* which is given by;

$$D^* = \frac{D}{\phi^{7/3}} \qquad (2.17)$$

Another parameter called sorption coefficient[17] which was calculated from the equilibrium swelling using the relation

$$S = \frac{M_\alpha}{M_0} \qquad (2.18)$$

'S' can better describe both the initial penetration and dispersal of penetrant molecules into the elastomer network. Here M_∞ is the mass of the penetrant sorbed at infinite time and Mo, the initial weight of the polymer sample.

The permeation coefficient which is a characteristic parameter reflecting the collective processes of diffusion and sorption was calculated using the equation;

$$P = D\,S \qquad (2.19)$$

The molar equilibrium sorption constant Ks, which is defined by Hung[18] as

$$Ks = \frac{\text{No. of moles of solvent sorbed at equilibrium}}{\text{Mass of polymer sample}} \qquad (2.20)$$

also can be calculated.

Sorption kinetics

In the case of a polymeric network, extensively being swollen by a penetrant, the diffusion process is characterized by linear kinetics. According to Thomas and Windle[19], a thermodynamic swelling stress is exerted by the penetrant on the polymer network which therefore undergoes time dependant mechanical deformation. But in the early stages of swelling this deformation is prevented[20] to some extent by the undeformed and unswollen polymer layers below. This factor extends the stress to two dimensions. But with the progress of swelling process, the magnitude of the stress is reduced and the equilibrium swelling of the surface layer occurs. Since the rate determining step of the process is the above said time dependent mechanical deformation, it can be confirmed that rate of sorption will be proportional to the difference in osmotic pressure inside and outside the polymeric materials.[21] Consequently, since this can be related to the concentration of the penetrant in the polymer, the first order kinetic equations given below can be used.

$$\frac{dc}{dt} = k_1(C_\infty - C_t) \qquad (2.21)$$

$$k_1 t = 2.303 \log \frac{C_\infty}{C_\infty - C_t} \qquad (2.22)$$

First order rate constant values (k_1) obtained from a plot of log ($C_\infty - C_t$) verses time t will be a measure of the speed with which the polymer chain segments and penetrant molecules exchange their positions.

2.3.11. Assessment of filler-matrix adhesion

Filler/matrix adhesion was analysed by using three previously established equations called Kraus[22], Cunneen- Russell[23] and Lorenz-park[24].

Kraus equation is given by;

$$\frac{V_{r0}}{V_{rf}} = 1 - m\left[\frac{f}{1-f}\right] \qquad (2.23)$$

where V_{r0} = volume of rubber in solvent swollen unfilled sample

V_{rf} = Volume fraction of rubber in solvent swollen filled sample

f = volume fraction of filler.

This equation is of the general form of a straight line.

So a plot of Vr_0/V_{rf} as a function of f/1-f will be a straight line, whose slope, m will be directly proportional to the filler-matrix adhesion. A constant 'C' which wais characteristic of the filler also was determined from the slope using the relation;

$$C = m - V_{ro} + 1/3(1 - V_{ro}^{1/3}) \qquad (2.24)$$

Filler/matrix adhesion was also analysed by Cunneen – Russell[23] equation. The equation is given by;

$$V_{ro}/ V_{rf} = ae^{-z} + b \qquad (2.25)$$

where V_{ro}, V_{rf} are same as explained earlier, z is the weight fraction of the filler, 'a' and 'b' are constants which depends on filler activity. High values of 'a' and 'b' indicate strong polymer/filler adhesion.

The Lorenz-Park equation[24] is

$$Q_f / Q_g = ae^{-z} + b \qquad (2.26)$$

where Q is defined as the amount of solvent absorbed / gm of rubber and is given by

$$Q = \frac{\text{Swollen weight - dried weight}}{\text{Original weight x 100 / formula weight}} \qquad (2.27)$$

The subscript f and g refer to filled and gum vulcanisates respectively; z is the weight fraction of the filler. As described earlier, a plot of Q_f / Q_g versus e^{-z} must give a straight line with slope 'a' and y intercept 'b', which can indicate the polymer-filler interaction.

2.3.12. Crosslink density determination

(a). From mechanical property measurements

The extent of physical crosslinks in an elastomer vulcanisate was detrmined by the use of Mooney-Rivlin equation[25].

$$F = 2 A_0 (\lambda-\lambda^{-1}) (C_1 + \lambda^{-2} C_2) \qquad (2.28)$$

where F is the extension force required to stretch a piece of rubber vulcanisate of cross-section area A_0, to an extension ratio λ. A plot of $F/2A_0 (\lambda-\lambda^{-1})$ versus λ^{-1} gives a straight line whose λ intercept C_1, was directly related to the physically effective crosslink density (∂_{phys}) by the equation,

$$C_1 = \rho_r RT \, \partial_{phys} \qquad (2.29)$$

(b). From swelling measurement

The crosslink density of the samples was determined by the swelling method. The samples were allowed to swell in toluene and the equilibrium uptake was noted. The molecular weight between the crosslink M_c was calculated using the following equation.

$$M_c = \frac{- \rho_r V_s (V_{rf})^{1/3}}{\ln (1-V_{rf}) + V_{rf} + \chi V_{rf}^2} \qquad (2.30)$$

where M_c = molecular weight of polymer between two crosslinks

ρ_r = density of polymer, V_s = molar volume of solvent

V_r = volume fraction of polymer in swollen mass was calculated by the method of Ellis and Welding[13] given earlier.

From molecular weight between crosslinks M_c, the crosslink density ∂ was calculated using the following equation.

$$\partial = 1 / 2 M_c \qquad (2.31)$$

(c). From dynamic mechanical analysis

Since the storage modulus in dynamic mechanical analysis (DMA) measurements is

a direct measure of the crosslink density, enhanced modulus can be attributed to the higher crosslink density of the matrix in the presence of inclusions.

According to the statistical theory of rubber elasticity[26], the crosslink density $n_{E'_r}$ for a tetrafunctional network can be calculated according to the equation.

$$n_{E'_r} = Er' / 6RT \qquad (2.32)$$

where Er' is the dynamic storage modulus of the rubber measured from the rubbery plateau region, R is the universal gas constant and T, the temperature in Kelvin.

2.3.13. Sulfur migration studies

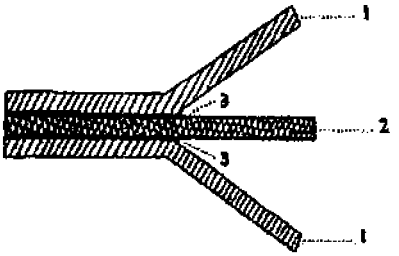

THREE LAYER MODEL

1. GUM MATRIX
2. NR LATEX WASTE
3. ALUMINIUM FOIL

DIMENSIONS OF THE SAMPLE

	LENGTH (cm)	BREADTH (cm)	THICKNESS (cm)
1. GUM MIX	16	8	0.2
2. NR LATEX WASTE	16	8	0.2
3. ALUMINIUM FOIL	8	8	0.004

Figure 2.2. Three layer model specimen

The sulfur migration phenomena which occured between the matrix and the filler phase was studied using a three layer model[27] **(Figure 2.2)** system. It consisted of three layers, one layer of NR latex waste (all sizes1, 2, 3, 4 and M were tried) was sandwiched between two layers of gum elastomer matrix compounds. In one half of the specimen, the outer gum matrix layers were separated from the inner latex waste layer by using aluminum foils (non contact surface, NCS) and in the other half, aluminum foil was

omitted (contact surface, CS). The system was then subjected to vulcanisation at low pressure. Then the middle latex waste layer was separated. The crosslink densities of this layer as well as outer layers were determined by swelling the samples taken from the contact and non-contact regions. If sulfur migration occurs from outer gum elastomer layers to middle NR prophylactics waste layer, the crosslink density at the contact surface will be increased at the expense of the outer layers.

2.3.1.4. Melt Rheological Analysis

Rheological studies were carried out using a capillary rheometer attached to a Zwick Universal testing Machine, model 1474. The extrusion assembly consists of a hardened steel barrel underneath the moving crosshead of the machine. A hardened steel plunger was held to the load cell by a latch assembly. The barrel was thermally insulated from the other parts of the machine. The capillary used was made of tungsten carbide and has an l_c / d_c ratio of 40 with an angle of entry 180^0. The measurements were carried out at 120, 150, 160 and 170^0 C with an accuracy of $\pm$ 1 ^{0} C. The barrel was electrically heated and the crosshead speed could be varied in the range of 0.06 – 20 cm min^{-1}. About 8-10 gms of the test sample was put in to the barrel of the capillary rheometer and forced down to the capillary by the plunger. After a warming up period of 5 min, the sample was extruded through the capillary at different speeds given above. Forces corresponding to each plunger speed was measured by the pressure transducer attached to the plunger and were recorded using a strip chart recorder assembly.

The force and crosshead speed were converted to apparent shear stress ($\Im_w$) and shear rate (γ_w) at the wall respectively using the equations given below, which involves geometry of the capillary and plunger.

$$\Im_w = \frac{F}{4 A_p \ (l_c / d_c)} \qquad (2.33)$$

$$\gamma_w = \frac{3n' + 1}{4n'} \ \frac{32 Q}{\pi d_c^3} \qquad (2.34)$$

where F is the force applied at a particular shear rate, A_p is the cross-sectional area of the plunger, l_c is the length of the capillary, d_c is the diameter of the capillary, Q is the volumetric flow rate (calculated from the velocity of the crosshead and the diameter of the plunger) and n', the flow behavior index defined as,

$$n' = \frac{d (\log \Im_w)}{d (\log \gamma_{wa})} \qquad (2.35)$$

where γ_{wa} is the apparent shear rate at the wall calculated from the equation

$$\gamma_{wa} = \frac{32\ Q}{\pi\ d_c^3} \qquad (2.36)$$

The shear viscosity was calculated as

$$\eta = \frac{\Im_w}{\gamma_w} \qquad (2.37)$$

3n' +1 / 4n' is the Rabinowitch correction applied to calculate the true shear rate at the wall from apparent Newtonian shear rate at the wall.

2.3.1.5. X-ray Diffraction Studies

X-ray diffraction studies of the samples were carried out using a Siemens D 5005 X-ray diffractometer with Cu-Kα radiation (40 kV, 40 mA).

2.4. REFERENCES

1. Z. I.Grebenkina, , N. D.Zakharov, and E. G.Volkova, Int. Polym. Sci. Technol. 5(11), 2 (1978).
2. Annual Book of ASTM Standards, D 3182 -1989.
3. S.-C. Ng and L.H.Gan., Eur.Polym. J., 17,1073 (1981).
4. M. Makosza and M. Wawrzyniewics, Tetrahedron Lett., 53, 4659 (1969).
5. G. C. Joshi, L. M. Pande, A. K. Mukherjee, K. K. Ganguli, P. K. Tiwari and S. C. Raman, Proc. Symp. High Polymers, Kanpur, India, 1972.
6. K. Fujimoto, T. Nishi and T. Okamoto, Int. Polym. Sci. Technol., 8(8), T/30 (1981).
7. Annual Book of ASTM Standards, D 412, 1992.
8. Annual Book of ASTM Standards, D 624, 1981.
9. Annual Book of ASTM Standards, D 2240, 1981.
10. S.K.De and B.K.Dhindaw., J.Scanning Electron Micros., 3, 973, (1982).
11. A.D.T. Gorton and T.D.Pendle, NR.Technology., 7(4), 77 (1976).
12. U.S.Aithal and T.M.Aminabhavi., J.Chem. Edn., 67, 82 (1990).
13. B.Ellis and G.N.Welding., Techniques of Polymer Sciences., Soc. Chem.Ind., London, p.46, (1964).
14. L. M. Lucht and N. A. Peppas., J. Appl. Polym. Sci., 33, 1557 (1987).
15. T. M. Aminabhavi, and R. S. Khinnavar, Res.Polym., 34(5), 1006 (1993).
16. T. M. Aminabhavi, and R.S. Khinnavar, J.Chem Edn., 68, 343 (1994).
17. S. B. Harogoppad and T. M. Aminabhavi, Macromolecules, 24, 2595 (1991).
18. G. W. C. Hung, Microchem J., 19,130 (1974).
19. N. L. Thomas, and A. H. Windle, Polymer., 18, 1195 (1977).
20. E. Southern, and A.G. Thomas, J. Polym. Sci. (A), 3, 641 (1965).
21. J. D. Cosgrove, T. G. Hurdley. and T. J. Lewis, Polymer, 23, 144 (1982).
22. G.Kraus., J.Appl.Polym.Sci., 7,861 (1963).
23. J.I.Cunneen and R.M.Russell., Rubber Chem.Technol., 43,1215 (1970).
24. O.Lorenz and C.R.Parks., Rubber Chem.Technol., 50,299 (1961).
25. L. R. G. Treloar, The Physics of Rubber Elasticity, 3rd edn., Clarendon Press, Oxford, (1976).
26. J.J.Aklonis and W.J.Mac Knight, "Introduction to Viscoelasticity", John Wiley and Sons, (1983).
27. L. N. Sharapova, A. A. Chekanova, N. D. Zakharov and E.Yu.Borisova., Int.Polym.Sci.Technol., 10, 4 (1983).

Chapter 3

CHAPTER 3

USE OF NATURAL RUBBER PROPHYLATICS WASTE AS A FILLER IN STYRENE BUTADIENE RUBBER COMPOUNDS

ABSTRACT

This chapter deals with the use of natural rubber prophylactics waste as filler in styrene butadiene rubber compounds. Natural rubber prophylactics waste has been ground in a toothed wheel mill to get a rubber powder polydispersed in size. This has been sieved and separated into four different fractions. A mill-sheeted form of natural rubber prophylactics has also been prepared using a two-roll mill. All the fractions from size 1 to 4 have been characterised by scanning electron microscopy, average particle size, most frequent size range, number and weight average diameters and by particle size distribution curves. Each fraction has been added to styrene butadiene rubber (SBR) at different loadings of 0,10,20,30 and 40 phr. The vulcanisation of styrene butadiene rubber compounds has been carried out using a conventional vulcanisation system. Curing characteristics of the styrene butadiene rubber compounds such as optimum cure time, scorch time and induction time have been found to be decreasing with the addition of natural rubber prophylactics filler, with a corresponding decrease in cure reaction rate constant. The presence of unreacted accelerator in natural rubber prophylactics rejects causing such an observation has been identified. Good improvement in the tensile as well as tear strengths of the vulcanisates has been noted with increasing concentration of prophylactics filler, the effect being greater in the case of large sized fillers for tensile strength and smaller fillers for tear strength. The comparatively better performance of large sized fillers and mill-sheeted form of the prophylactics filler has been supported by swelling index, cross-link density values, Kraus, Cunneem-Russell equations as well as scanning electron fractography. As in the case of particulate filled elastomers, natural rubber prophylactics filler particles have been observed as phase separated entities.

CHAPTER 3

USE OF NATURAL RUBBER PROPHYLACTICS WASTE AS A FILLER IN STYRENE BUTADIENE RUBBER COMPOUNDS

Results of this chapter have been published in

J. Appl.Polym.Sci., 61, 2035, 1996

In recent years, there has been a great deal of interest in polymer industry about the development of cost effective techniques to convert waste and used rubber into a processable form[1-3]. Even though the use of reclaimed rubber claims economic advantages, it constitutes only a small percentage of the raw rubber consumption because of its inferior physical properties. Compared to reclaimed rubber, scrap NR prophylactics rejects have recently become a focus of attention because of the lightly crosslinked and high quality nature of the rubber hydrocarbon.

Scientists have conducted several experiments on

(1) various recycling techniques [1-4]

(2) characterisation of rubber crumbs [5,6]

The interface of rubber crumbs/polymer matrix has been extensively studied by Fujimoto et al.[7,8] In addition to these, Acetta and Vergnaud [9,10] tried to upgrade scrap rubber powder by vulcanisation without new rubber. Phadke et al [11,12] studied the mechanical properties and rheological behaviour of cryoground rubber-natural rubber blends. Similarly, the recycling of cheap packaging waste has been done by Karlsson and Albertsson.[13] The chemical recycling of waste saturated polyesters and urethane polymers to get raw materials for the production of polyurethanes has been carried out by Kacperski and Spychaj.[14]The conversion of tire waste using subcritical and supercritical water oxidation has been performed by Park et al.[15] Slightly differing from this approach, Kawser and Farid[16] conducted the thermochemical processing of rubber waste to liquid fuel. Catalytic degradation of different polymers[17] and copyrolysis of waste polymers with coal[18] also has been reported in the literature. Even though a large number of studies have

been done in the field of polymer recycling, studies on the use crosslinked prophylactics rejects, as filler has not been addressed so far.

In this chapter we report on an economic method to convert NR prophylactics rejects into a processable form and to reuse them as filler in styrene butadiene rubber (SBR). Emphasis was given to understand the influence of both particle size and loading of NR prophylactics filler on the cure characteristics and mechanical performance of the vulcanisates. Swelling studies were carried out to understand the interaction of NR prophylactics waste filler with the SBR matrix. Sulphur diffusion in these compounds was analysed by the help of a three layer model. Particle morphology, filler distribution and filler–matrix interface adhesion were analysed using scanning electron microscopy (SEM).

3.1 Results and discussions

The compounding recipe used for the study is given in **Table 3.1**.

Table 3.1.Basic formulation

Material	Control, phr
SBR	100
Zinc oxide	5
Stearic acid	2
CBS	1
TDQ	1
Sulphur	2.2
Prophylactics filler	Variable (0, 10,20,30 and 40)

3.1.1. Physical Characteristics of Ground NR Prophylactics Waste

(a) Particle Morphology

Figure 3.1 represents the SEM photograph of the NR prophylactics filler particles (size1) used in the present work. The particles are with rough surface.

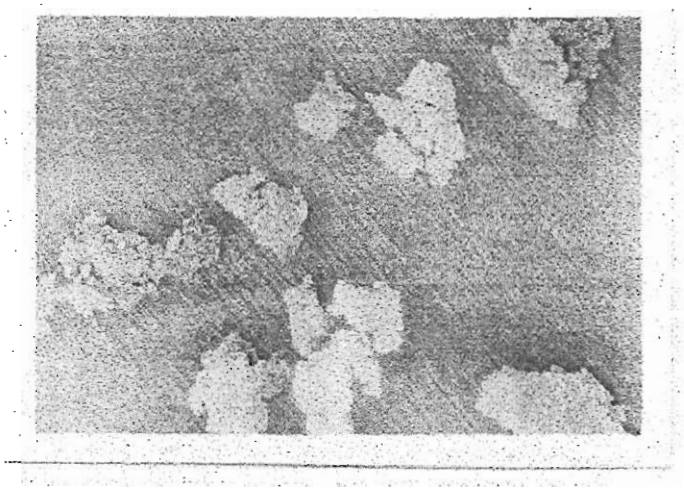

Figure 3.1. SEM photograph of NR prophylactics waste particles (size 1; Magnification X 60)

(b) Particle size distribution

The photograph of the NR prophylactics waste filler of different particle sizes and the mill-sheeted form used in this study is presented in **Figure 3.2**.

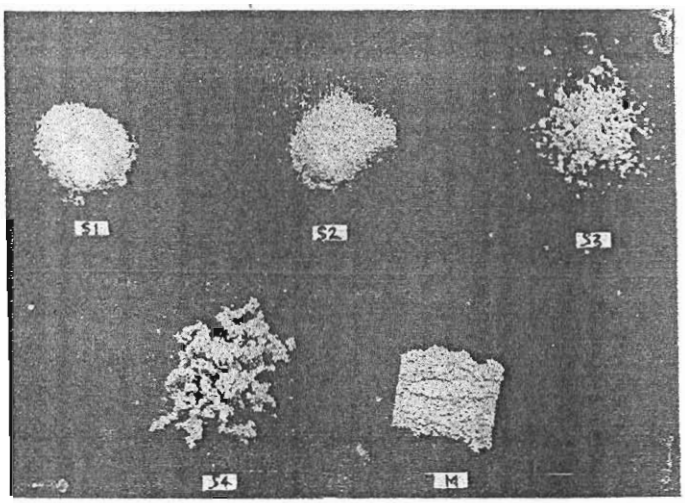

Figure 3. 2. Photograph of various particles sizes and the mill sheeted form of prophylactics filler

[from left top to right - size 1, size 2, and size 3]

[from left bottom to right - size 4 and mill sheeted form]

It is clear from the photograph that as we move from size 1 to size 4, particle size increased. Since it is possible for particles of somewhat larger diameter also to penetrate the meshes due to their elasticity, it is better to represent them by size distribution curves, as given in **Figure 3.3**. Size 4 shows the broadest distribution. Sizes 1 and 2 have narrow distribution, while size 3 takes the intermediate position. The average particle sizes, most frequent size range, number and weight average diameters of prophylactics filler are presented in **Table 3.2**. All these values exhibit an increase as we move from size 1 to size 4. The shape factor (p) is the quotient of the length and breadth of the particles. Its role comes when the shape of the inclusion influences the mechanical properties of the vulcanisates[19]. According to the theoretical treatment by Wu[20], disc shaped particles can reinforce better than spherical or needle shaped particles. Such a treatment brings anisotropy in properties, which leads to the transverse and longitudinal moduli.[21] It can be seen that generally 'p' decreases from size 1 to 4 eventhough the value for size 3 is slightly higher than that of size 2. The specific gravity of the NR prophylactics waste filler is 1.1529.

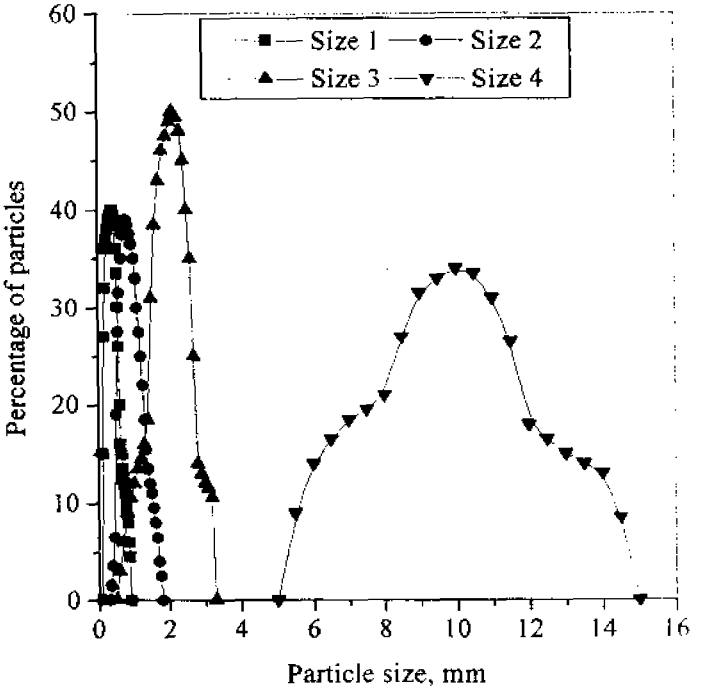

Figure 3.3. Particle size distribution curves

Table 3.2. Particle size data

Particle size	Average size mm	Most frequent size range, mm	Number average diameter $\overline{Ln}$	Weight average diameter $\overline{Lw}$	Shape factor P
Size 1	0.5	0.3-0.5	0.401	0.489	2.2951
Size 2	1.05	0.6-0.9	0.961	1.083	2.0067
Size 3	1.9	1.7-2.5	2.11	2.34	2.1667
Size 4	10	9-11	10.09	10.72	1.6513

3.1.2 Processing Characteristics

The processing characteristics of the compounds are shown in **Figures 3.4** to **3.8**. The variation of optimum cure time (time for attaining 90% of maximum torque), scorch time (premature vulcanisation time) and induction time (time for the start of vulcanisation process) are presented in **Figures 3.4, 3.5** and **3.6** respectively.

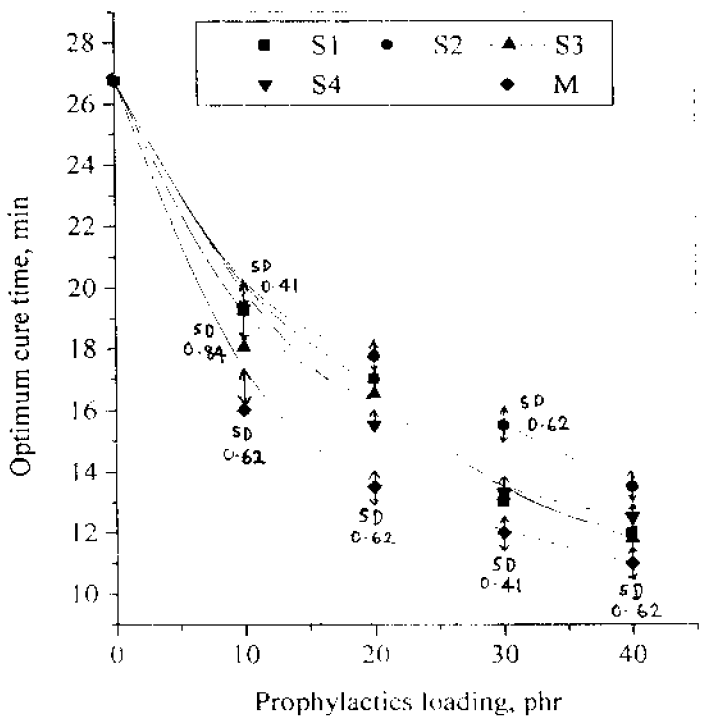

Figures 3.4. Variation of optimum cure time of SBR compounds with particle size and loading of filler.

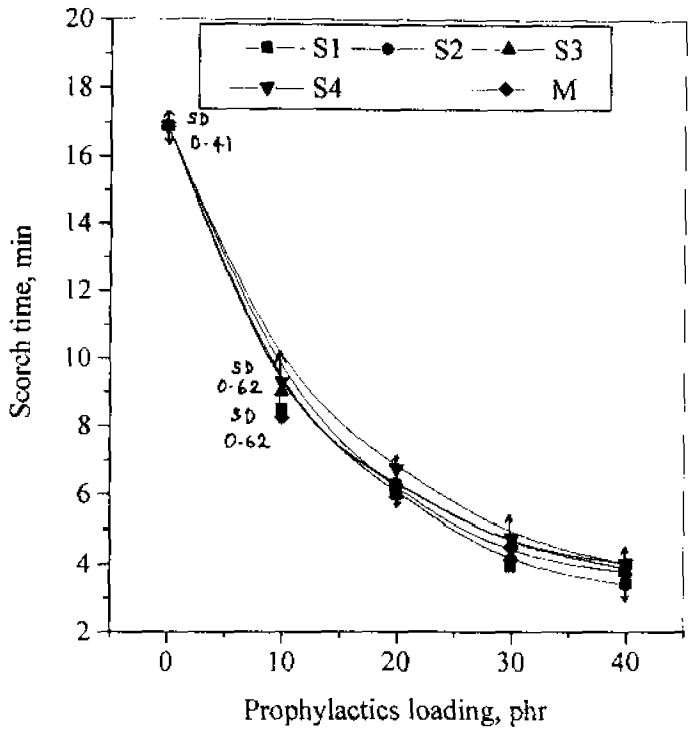

Figures 3.5. Variation of scorch time of SBR compounds with particle size and loading of filler

A considerable decrease in all these parameters is noted with increasing loading of filler in SBR. This is due to the presence of unreacted curatives in the NR prophylactics rejects. The latex products such as condoms and gloves are manufactured by a dipping process which involves a very fast accelerator. The accelerator used normally is ZDEC, i.e., zinc diethyldithiocarbamate having the structure given below.

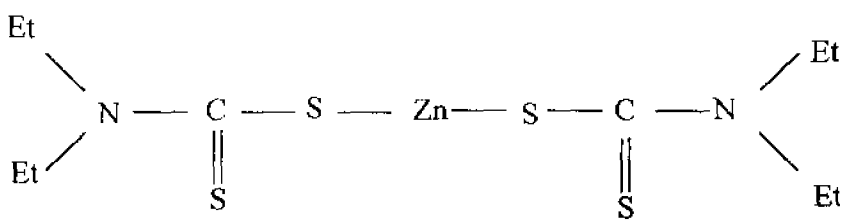

Some of this accelerator will remain unreacted after the curing process. This was extracted using spectroscopic grade acetone and the spectrum of the sample is given in **Figure 3.7**. The peak at 790 – 770 cm^{-1} indicates the presence of ethyl chain (- CH2-CH3) and that at 700- 600 cm^{-1} is due to C-S stretch. The C= S stretch is clearly visible at 1250-1020 cm^{-1}

range and the peak at 2820-2760 cm^{-1} confirms the presence of N-CH2 group in the compound.

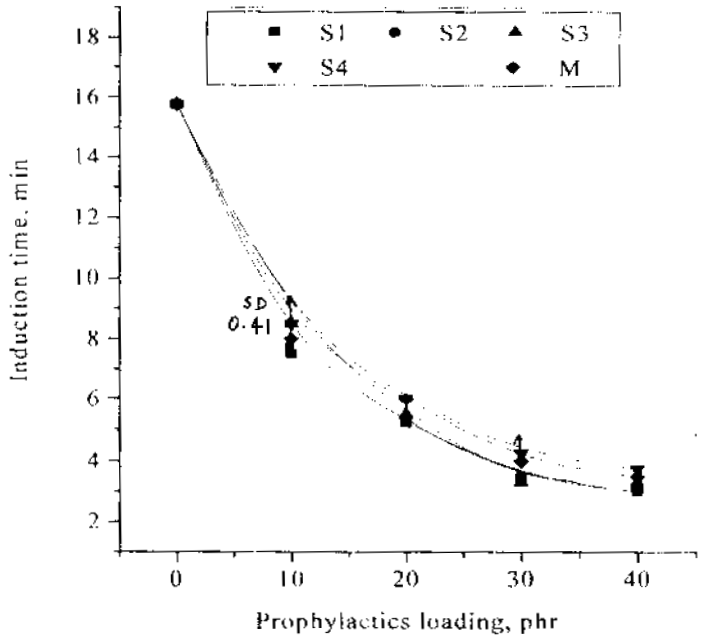

Figures 3.6. Variation of induction time of SBR compounds with particle size and loading of filler

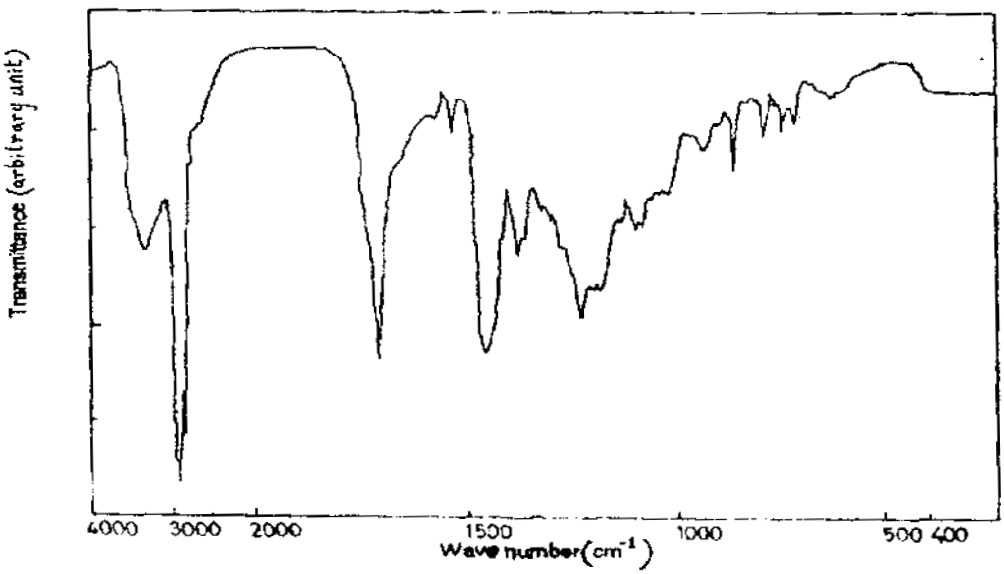

Figure 3.7.IR spectrum of unreacted accelerator

These observations indicate the presence of unreacted accelerator in NR prophylactics. As the loading of NR prophylactics increases, the availability of the unreacted accelerator also increases, which results in further reduction in these curing characteristics such as optimum cure time, scorch time and induction time. The decrease in optimum cure time is minimum for SBR filled with size 2 filler and maximum for SBR filled with size mill sheeted form. The reduction in scorch time as well as induction time **(Figures 3.5 and 3.6)** is maximum for SBR filled with size 1 filler and minimum for that with size 4 filler.

In order to study the kinetics of the curing reaction, ln (M_h-M_t) is plotted against t, to get a straight line graph as shown in **Figure 3.8**, which proves that the cure reaction follows first order kinetics. The cure reaction rate constant (k) values are obtained from the slope of the respective straight lines. These values are presented in **Table 3.3**. The rate constant values generally increase with increasing filler loading. The higher the amount of filler loading, greater the amount of curatives available. This indicates an increase in the rate of crosslinking. This increase of rate constant is most noted for SBR loaded with mill-sheeted form of the filler. Some unexpectedly low values of k also are noted in **Table 3.3.**

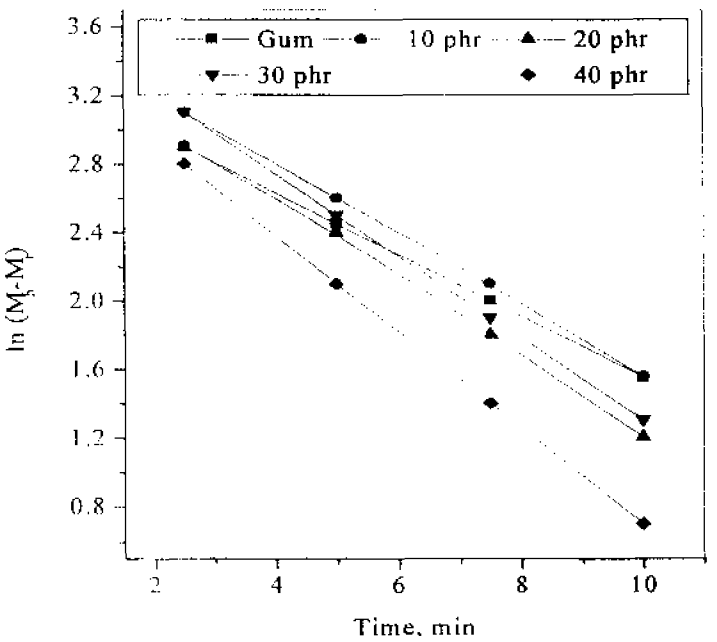

Figure 3.8. Plots of ln (M_h-M_t) Vs. time (min) of gum and filled (size 1) SBR compounds

Table 3.3. Rate constant and modulus values

SBR compound	Cure reaction rate constant, k min^{-1}	Young's modulus MPa	Modulus at 300 % elongation MPa
Gum SBR	0.18 SD 0.01	1 SD 0.13	0.92 SD 0.02
Size 1 filler			
10 phr	0.21	1	0.91
20 phr	0.22	1	0.88
30 phr	0.24	1	0.90 SD 0.01
40 phr	0.28	0.77 SD 0.16	0.97
Size 2 filler			
10 phr	0.23	1	0.92
20 phr	0.29 SD 0.02	1	0.79
30 phr	0.24	1	0.79
40 phr	0.25	1	0.86 SD 0.02
Size 3 filler			
10 phr	0.24	1	0.91
20 phr	0.25 SD 0.01	1	0.88
30 phr	0.24	1	0.86
40 phr	0.34	0.85	0.95 SD 0.05
Size 4 filler			
10 phr	0.20	1	0.79
20 phr	0.26 SD 0.01	0.80	0.78
30 phr	0.23 SD 0.01	0.80	0.86 SD 0.05
40 phr	0.30	0.70	0.70
Mill sheeted form			
10 phr	0.36	1	0.94
20 phr	0.37	0.85	0.92
30 phr	0.33 SD 0.02	0.80	0.87
40 phr	0.42	0.80	0.95 SD 0.05

3.1.3. Mechanical properties

Figure 3.9 represents the stress-strain curves of the gum and filled (size 1 filler) SBR compounds. The stress-strain behaviour of filled SBR vulcanisate is controlled by the characteristics of the filler and the matrix. The deformation behaviour seen from the curves is almost similar for gum and filled samples. At higher strains, the stress value is found to be increasing slowly, rather than exhibiting yielding behaviour. This behaviour is typical of vulcanised low strength materials.

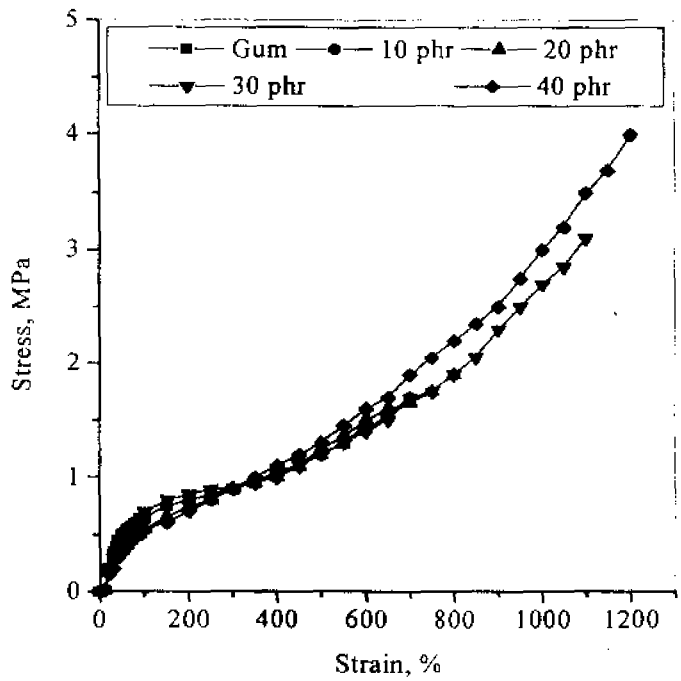

Figure 3.9. Stress – strain curves of the gum and filled (size 1) SBR vulcanisates

The Young's modulus values are shown in **Table 3.3**. They are found to be unaffected at lower loadings of the filler, while a slight decrease is observed at higher loadings for most of the cases. The modulus at 300 % elongation presented in **Table 3.3**, decreases upto 30 phr and then increases slightly for 40 phr filler loading. Some unexpectedly low values of secant modulus also are noted in **Table 3.3.**

A remarkable increase in tensile strength is observed with increasing filler loading as shown in **Figure 3.10**. This points out the fact that NR prophylactics waste filler has

some reinforcing effect in SBR matrix. This reinforcing effect observed with increasing loadings of NR prophylactics is due to the strain crystallisation behaviour of crosslinked NR prophylactics filler. In a weak matrix like SBR, NR prophylactics filler is found to retain its strain crystallising nature even if it is in the form of a fine filler.

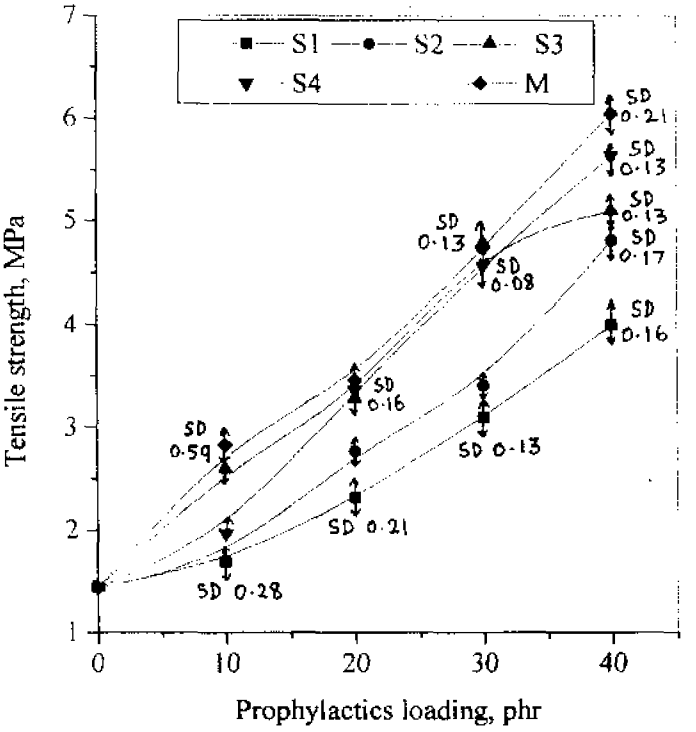

Figure 3.10. Effect of the size and loading of filler on the tensile strength of SBR vulcanisates

But contrary to the usual behaviour of fine filler being more reinforcing, here the largest size (size 4) and mill sheeted form show relatively good tensile properties. This is due to the sulphur diffusion phenomena noted here and reported earlier in similar systems[22]. For the fine filler (size1), the contact surface area with SBR matrix is more. This can lead to an increase in sulphur migration from matrix to filler phase. Enhanced sulphur migration weakens crosslinks in the matrix and therefore the tensile properties which were expected to be superior for size 1 filler actually becomes inferior. The extent of sulphur migration is controlled not only by the particle size of the filler but also by the degree of polysulphidic linkages in the filler. The degree of polysulphidic linkages in the filler has a direct relation

with the extent of sulphur migration [8]. Mill sheeted form of the NR prophylactics waste filler is prepared by the repeated passing of the waste through a two-roll mill. This leads to substantial breakdown of polysulphidic linkages in the filler resulting in a low degree of polysulphidity for mill-sheeted form [8]. It is obvious that mill sheeted form also undergoes size reduction during the mixing procedure. Still the extent of sulphur diffusion is least in SBR compounds filled with mill-sheeted form. Owing to this, they show better values of tensile strength over others.

The tear strength of SBR vulcanisates **(Figure 3.11)** also shows an increase with increasing loading of filler. Among the filler sizes used, smaller sizes size1, size 2, and size 3 show the maximum tear strength at 40 phr loading. Size 4 filler is inferior to these, both at low and high filler loading. This is due to the more uniform particle size distribution of smaller size of prophylactics filler (size 1, 2 etc.) compared with larger sizes.

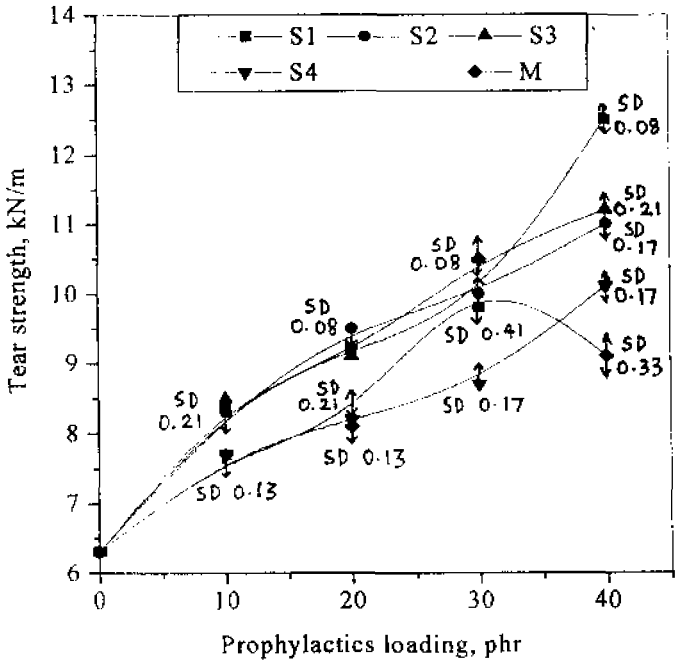

Figure 3.11. Effect of the size and loading of filler on the tear strength of SBR vulcanisates

The effect of filler loading on IRHD hardness is shown in **Figure 3.12**. The observed decrease in IRHD hardness with increasing filler loading is due to the decrease in crosslink density. The most intense reduction in IRHD is observed for the SBR vulcanisates filled with size 3 prophylactics filler. In the case of SBR vulcanisate with size 1 filler, there is a leveling off in IRHD after 10 phr prophylactics loading.

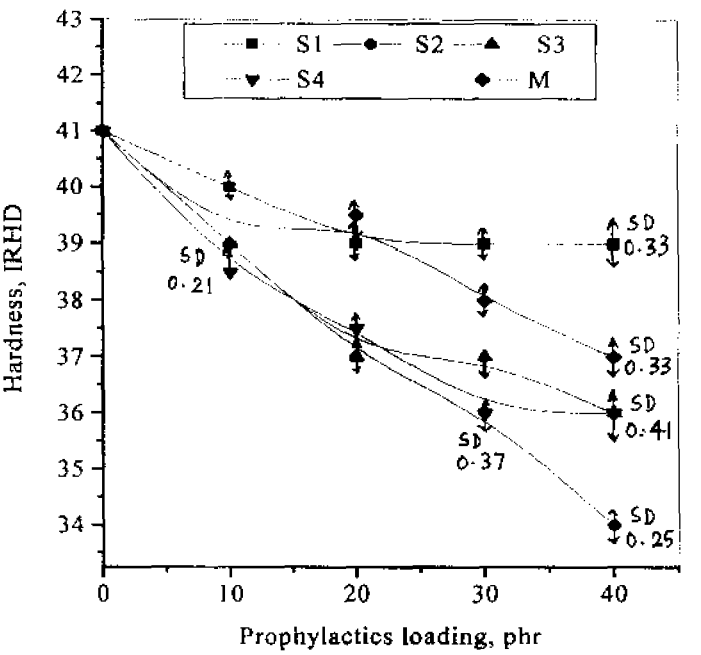

Figure 3.12. Effect of the size and loading of filler on the hardness (IRHD) of SBR vulcanisates

3.1.4. Swelling index and crosslink density determination

Swelling index values represent the swelling resistance of the rubber vulcanisate. The swelling index values are shown in **Table 3.4**. The value obtained for gum SBR compound is lower than that of any other filled system. This indicates that the gum compound has more resistance to swelling than the filled SBR compounds. This observation points to the decrease in crosslink density in filled compounds. With increasing filler loading, swelling index values are found to be increasing, but the increase is not always uniform. For a fixed filler loading, the value is minimum for SBR compound filled with mill-sheeted form of the filler.

Table 3.4. Effect of the size and loading of prophylactics filler on the swelling index values of SBR compounds

Sample	Swelling index values, %				
	Filler loading, phr				
	0 phr	10 phr	20 phr	30 phr	40 phr
Gum SBR	427 SD 2.45				
Size 1		439 SD 3.27	469 SD 4.1	503 SD 2.45	463 SD 1.63
Size 2		447 SD 2.45	489 SD 2.45	520 SD 1.63	526 SD 1.63
Size 3		461 SD 1.63	497 SD 3.27	485 SD 3.26	497 SD 2.45
Size 4		462 SD 1.63	476 SD 1.63	477 SD 4.1	468 SD 2.26
M		431 SD 3.27	428 SD 2.45	449 SD 3.27	449 SD 3.27

This indicates comparatively better reinforcement in SBR vulcanisates loaded with mill-sheeted form of the filler. The crosslink density (1/2Mc) is determined using the Flory-Rehner equation given in chapter 2 (equations 2.30, 2.31).

The variation in crosslink density as a function of increasing filler loading is given in **Figure 3.13**. It can be seen that the crosslink density of the samples decreases as the loading of prophylactics filler increases. This means a decrease in swelling resistance of filled systems. This crosslink density decrease is minimum for SBR vulcanisates containing mill-sheeted form of the filler. The above observation on the swelling shows that as the content of NR prophylactics filler increases, swelling increases and reaches a maximum. When sulphur migrates to the NR prophylactics phase, the crosslink density of this phase should increase which intern should reduce swelling. Hence a combined effect may be the reason for the present observations.

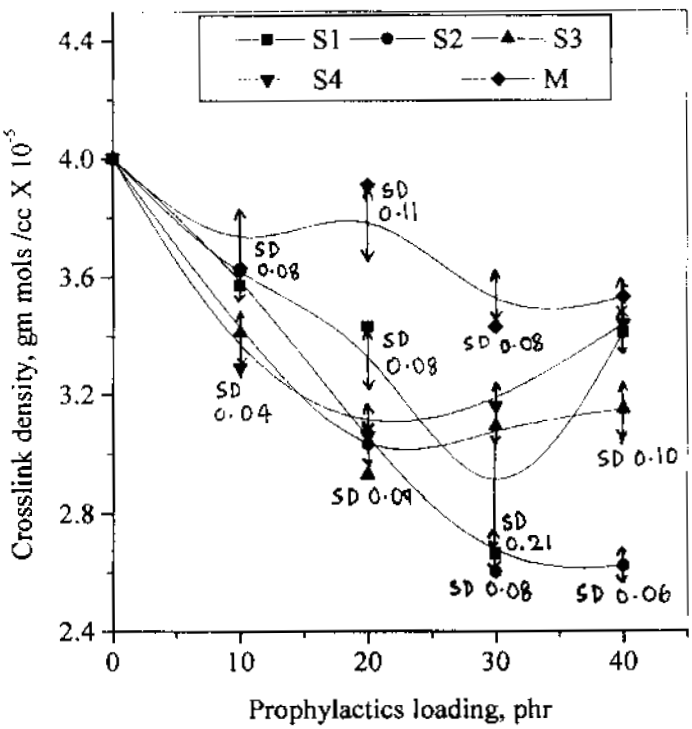

Figure 3.13. Variation of crosslink density SBR vulcanisates with particle size and loading of filler.

3.1.5. Extent of reinforcement

The extent of reinforcement is assessed by using Krause[23] and Cunneen–Russell[24] equations given in chapter 2 (equations 2.23 and 2.25). Since Kraus equation has the general form of an equation for a straight line, a plot of V_{r0} / V_{rf} as a function of $f / 1 - f$ should give a straight line, whose slope 'm' will be a direct measure of the reinforcing ability of the filler used. The more the reinforcing ability of the filler, the more will be the swelling resistance caused by that filler. The plots of Kraus equation for various particle sizes of fillers are shown on **Figure 3.14**. and the values of slopes and 'C' are presented in **Table 3.5**.

According to the theory developed by Kraus[23], for highly reinforcing carbon black, negative-higher slope values indicate a better reinforcing effect. In the present study, we observed that as the filler loading increases, the amount of solvent absorbed 'A_s' also increases considerably. This increase will cause a reduction in the V_{rf} values. Since V_{r0}

remains unaffected with filler loading, the ratio V_{r0} / V_{rf} increases considerably with increasing loading of filler which gives rise to a positive slope.

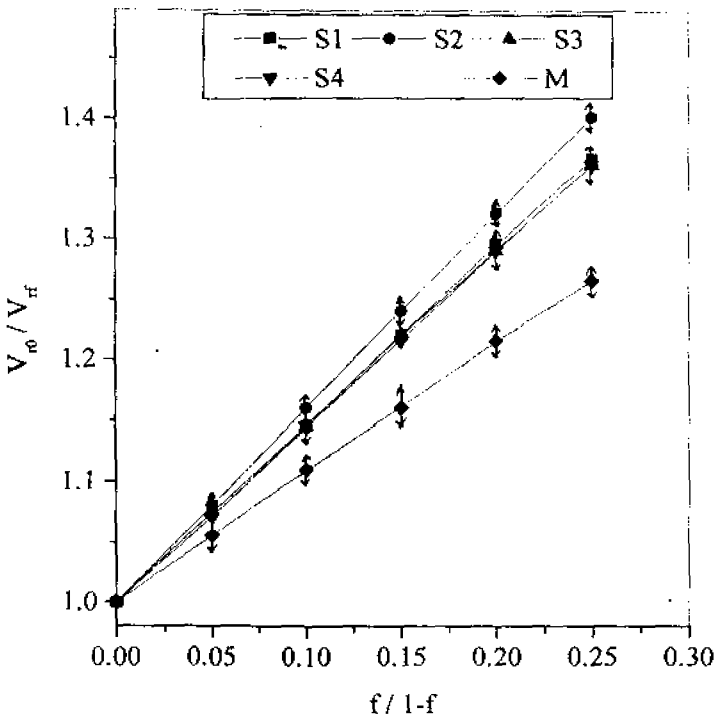

Figure 3.14. Kraus plots

It is clear from **Figure 3.14** that the slopes are positive and are higher for SBR loaded with smaller sized fillers. The slope is found to be the lowest for SBR filled with mill sheeted form. So it is clear that SBR vulcanisate containing mill-sheeted form of the filler absorbs a minimum amount of solvent. Therefore the decrease in V_{rf} is comparatively less; hence the ratio V_{r0} / V_{rf} is least at a particular loading. This compound therefore presents a lower positive slope compared to others. This suggests that as far as the extent of reinforcement is concerned, the mill-sheeted form is superior to other fillers.

The Cunneen – Russell equation[24] is given in chapter 2 (equation 2.25). A plot of V_{r0} / V_{rf} versus e^{-z} should give a straight line whose slope, '*a*' will be directly proportional to the reinforcing ability of the filler. The plots of the Cunneen and Russell equation are shown in **Figure 3.15**. and slope 'a' values are presented in **Table 3.5**.

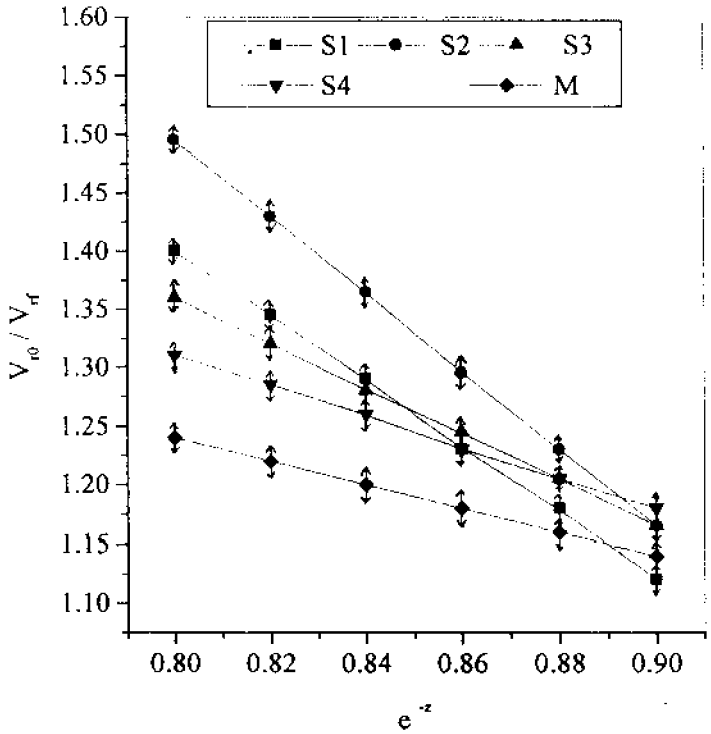

Figure 3.15. Cunneen - Russell plots

Table 3.5. Values of slope 'm' and 'C'

Particle size	Cunneen-Russell equation	Kraus equation	
	a	m	C
Size 1	2.8	1.46	1.67
Size 2	3.3	1.6	1.77
Size 3	1.9	1.43	1.64
Size 4	1.3	1.43	1.64
M	1	1.1	1.41

In this case V_{r0}/ V_{rf} also increases with increasing filler loading, and this increase is most noted for fillers of small particle sizes. Comparatively higher reinforcing mill-sheeted form of the filler absorbs minimum amount of solvent. Therefore SBR vulcanisate loaded with mill-sheeted form of the filler shows the lowest V_{r0} / V_{rf} value at a particular loading and

presents a smaller positive slope. Both Kraus and Cunneen–Russell equations point out the comparatively higher reinforcing nature of the SBR vulcanisates containing the mill sheeted form of the filler. Even though the theories of Kraus as well as Cunneen-Russell equations were developed originally for polymer systems containing particulate fillers, results on the use of these equations for SBR containing nonadhering fillers such as glass beads[25] and elastomeric fillers[26] were reported.

3.1.6. Three layer model for sulphur diffusion experiment

The diffusion of sulphur from the SBR matrix to the filler phase is analysed by using a three layer model,[22] as shown in chapter 2 **(Figure 2.2)**. The crosslink density of the sample obtained from the contact surface area of the middle NR prophylactics waste layer is found to be higher than that of the sample obtained from the non-contact surface area. This is clear from **Table 3.6**. The results from three layer model support the sulphur migration from the matrix to the filler phase. This is because of the sulphur diffusion from the outer gum SBR layers to the middle latex waste layer. In addition to this, we have also determined the crosslink density of the outer gum SBR layers in contact and out of contact with the middle prophylactics waste layer. In the case of contact region, the crosslink density of the outer layer is found to be lower than that from noncontact region. This stands as a strong proof for the facts that the sulphur migration occurs from the outer gum SBR layers to the prophylactics layer and that the increase in crosslink density of the middle prophylactics layer is certainly at the expense of the crosslink density of outer gum SBR layer.

Table 3.6. Crosslink density values from sulphur diffusion experiment

Sample	**Crosslink density, gm mols /cc X 10^{-5}**
Middle prophylactics layer	
Contact area	2.43
Non contact area	1.81
Outer gum SBR layer	
Contact area	2.90
Non contact area	3.65

3.1.7. Morphology and fractography

The tensile as well as tear strengths of the polymers are related to the morphological features of the fractured surface. **Figures 3.16** to **3.20** represent the SEM pictures of tensile and tear fractured surfaces. The SEM of the failed tensile gum vulcanisate is presented in **Figure 3.16a**.

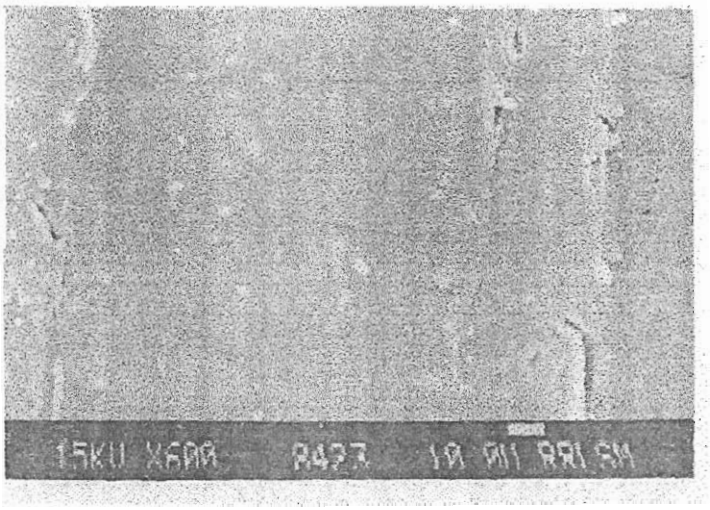

Figure 3.16(a)

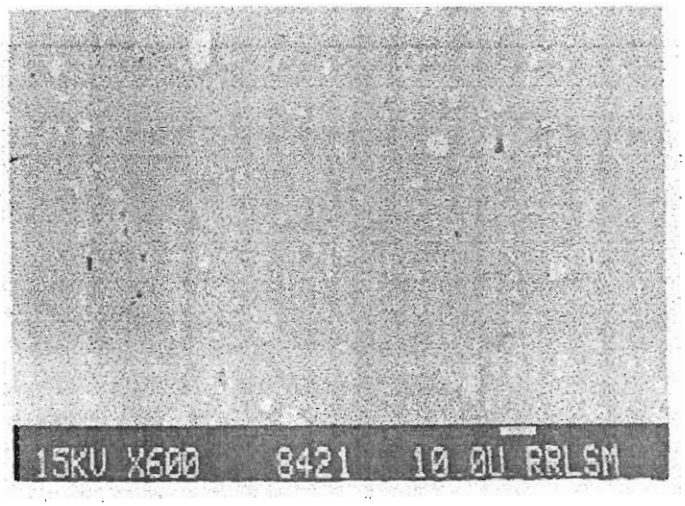

Figure 3.16(b)

Figure 3.16. SEM photographs of the tensile fractured surface of gum SBR vulcanisate (a) and the tear fractured surface of gum SBR vulcanisate (b)

Here, the fracture is smooth with out any deviation. This observation is in agreement with the low tensile strength of the gum SBR vulcanisates. The SEM of the failed tear gum vulcanisate shown in **Figure 3.16 b** also presents smooth torn areas. This indicates low

tear properties.

The tensile fractured surface of filled (40 phr of size 1) SBR vulcanisate are presented in **Figure 3.17a**. Here the fracture is not smooth as in the case of gum. As a result of enhanced sulphur migration, de-wetting is observed in this case as shown in **Figure 3.17b**.

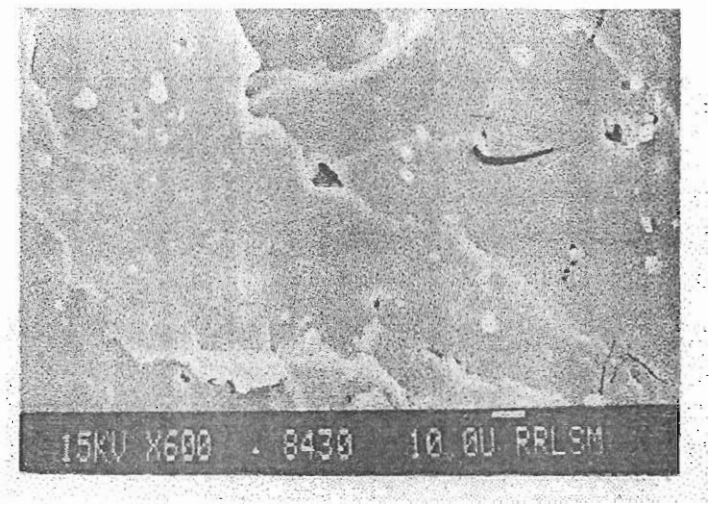

Figure 3.17(a)

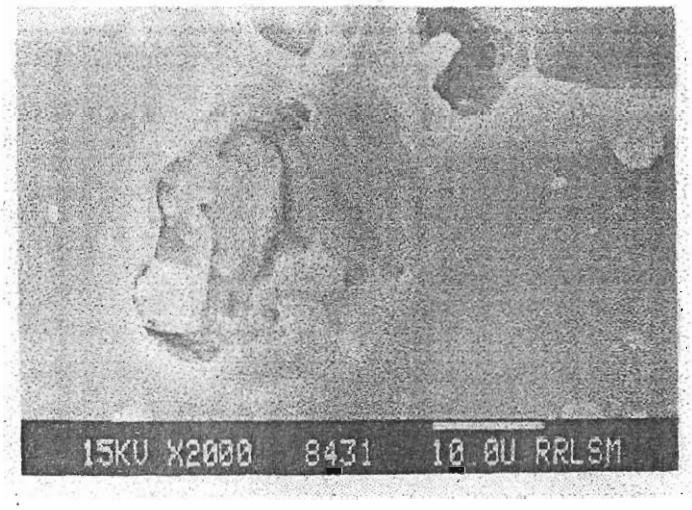

Figure 3.17(b)

Figure 3.17. SEM photographs (a) and (b) of the tensile fractured surface of filled (size 1) SBR vulcanisate

Figure 3.18a represents the torn surface of the SBR vulcanisate filled with 40 phr of size 1 filler. This figure shows crack deviation due to the restriction to crack propagation by filler particles. In this case also, de-wetting is observed, as can be seen

from **Figure 3.18b**. The observation of de-wetting is in agreement with the non-compatible behaviour of these filler systems discussed earlier.

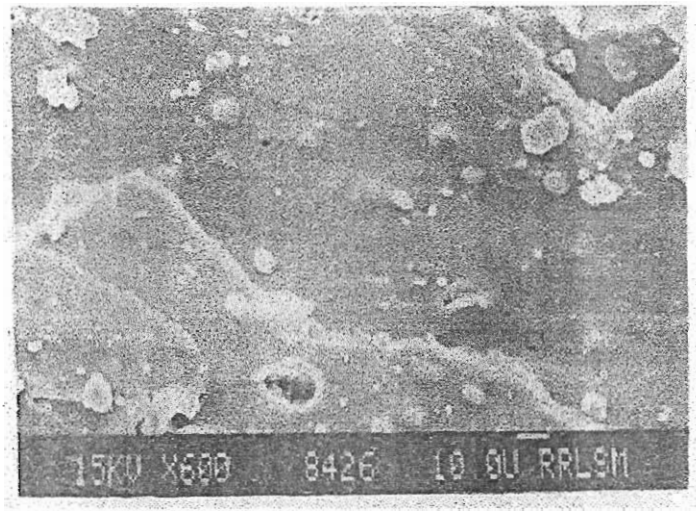

Figure 3.18(a)

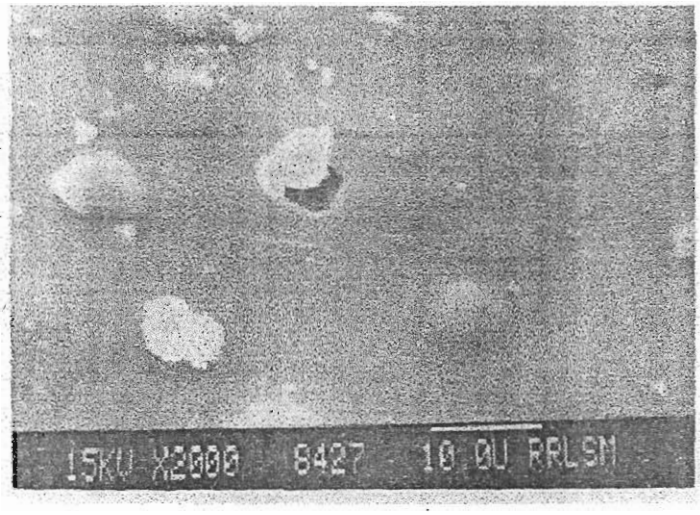

Figure 3.18(b)

Figure 3.18. SEM photographs (a) and (b) of the tear fractured surface of filled (size 1) SBR vulcanisate

The tensile and tear fractured surface of SBR vulcanisate loaded with 40 phr (size 4) filler is shown in **Figures 3.19 a** and **b**, respectively. In both cases, extensive crack deviation can be seen.

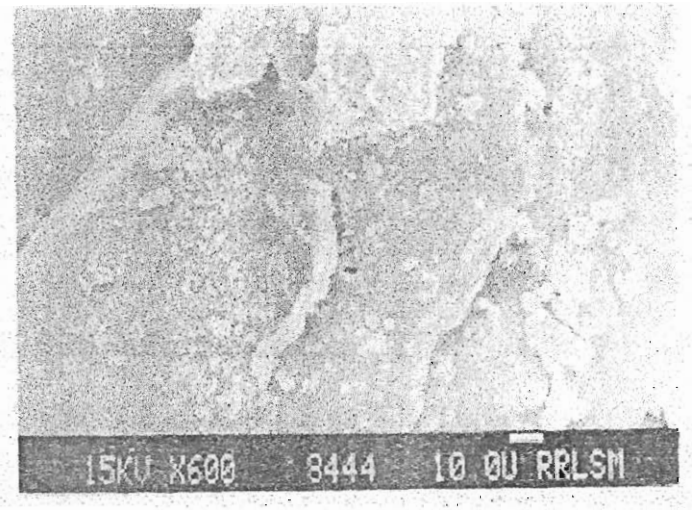

Figure 3.19 (a)

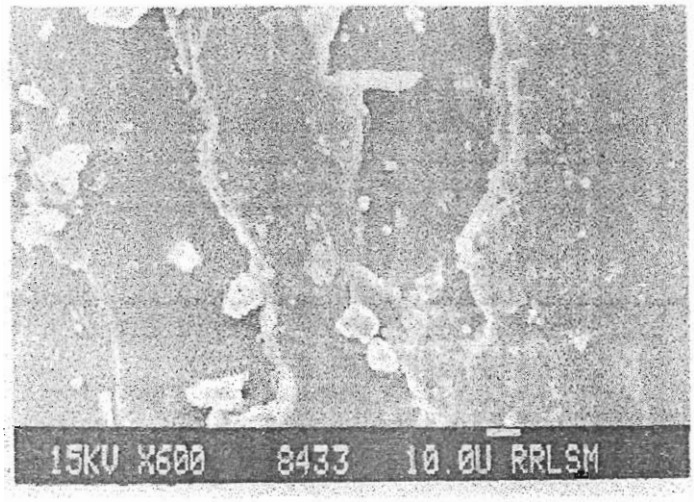

Figure 3.19 (b)

Figure 3.19. SEM photographs of the tensile fractured surface of filled (size 4) SBR vulcanisate (a) and the tear fractured surface of filled (size 4) SBR vulcanisate (b).

Figure 3.20 is the tensile fractured surface of the SBR vulcanisate filled with the 40 phr mill sheeted form of the filler. Since sulphur diffusion is minimum in this case, filler-matrix adhesion is fairly good, and hence de-wetting is less predominant. In this case also. filler particles obstruct the crack propagation and cause crack deviation. The torn surface of the SBR compound loaded with 40 phr of the mill-sheeted form is presented in **Figure 3.20 b**. Wavy pattern of fracture surface indicates a high tear resistant material.

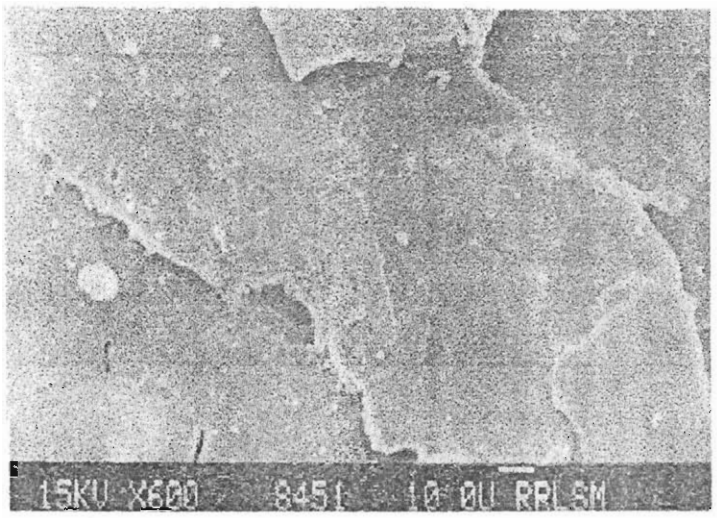

Figure 3.20 (a)

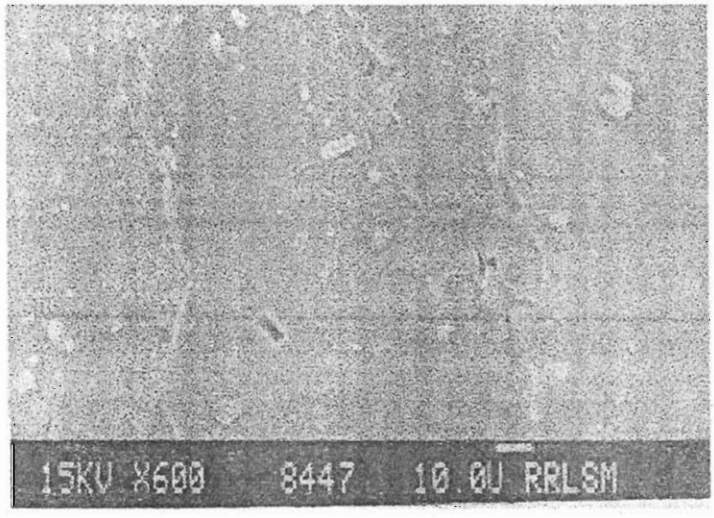

Figure 3.20 (b)

Figure 3.20. SEM photographs of the tensile fractured surface of (mill-sheeted form) SBR vulcanisate (a) and the torn surface of filled SBR vulcanisate (b).

In the case of all the filled vulcanisates, the torn surfaces show much crack deviation. These deviated tear lines result from the interaction of main fracture fronts with subsidiary fracture fronts and from the obstruction to tear propagation by filler particles. The SEM pictures also indicate that the NR prophylactics waste particles are not completely compatible with the SBR matrix. In all cases, the particles could be seen as phase separated entities.

3.2.REFERENCES

1. A.A. Harshaft, Environ. Sci. Technol., 6,412 (1972).
2. M.C.Kazarnowics, E.C.Osmundson, J.P.Boyle and R.W. Savage, paper presented at Rubber Division Meeting., Am.Chem.Soc., Cleveland, Ohio, Oct 4-7, 1977: Rubber Chem. Technol., (Abstr), 51, 386 (1978).
3. T.C.P. Lee and W. Millens, U.S.Patent, 4, 046, 834 (1977) (to Gould Inc.).
4. A. Ratcliffe, Chem. Eng., 79, 62 (1972).
5. R.P.Burford and M.Pittolo, Rubber Chem. Technol., 56, 1233 (1983).
6. L.Slusarski and R. Sandlewski, Int.Polym.Sci.Technol., 11,6 (1984).
7. K.Fujimoto and T.Nishi., Int.Polym.Sci.Technol., 8,25 (1981).
8. K.Fujimoto, T.Nishi and T. Okamoto., Int.Polym.Sci.Technol, 8,30 (1981).
9. A.Acetta and J.M. Vergnaud., Rubber Chem. Technol., 54, 302 (1981).
10. A.Acetta and J.M. Vergnaud., Rubber Chem. Technol, 55, 961 (1982).
11. A.A.Phadke, S.K.Chakraborty and S.K.De., Rubber Chem. Technol., 57, 19 (1984).
12. A.A.Phadke and B.Kuriakose., Kautsch Gummi. Kunstst., 38, 694 (1985).
13. S. Karlsson and A.C. Albertsson, Macromol. Symp., 135,1 (1998)
14. M. Kacperski and T. Spychaj., Prog. Rubb.Plast.Technol., 16(1), 61 (2000).
15. Y.K.Park, J.T.Reaves, C.W. Curtis and C.B. Roberts., J.Elast.Plast., 31,162 (1999).
16. Md. J.Kawser and N.A. Farid, Plast.Rubb.Compos., 29(2) (2000).
17. Y.Sakata., Macromol. Symp., 135,7 (1998).
18. P.Straka, J. Buchtele and J. Kovarova., Macromol. Symp., 135,19 (1998).
19. A.M. Bueche., J.Polym.Sci., 25,139 (1957).
20. T.T.Wu, Int.J.Solids.Struct., 2,1 (1966).
21. T.S. Chow, J.Polym.Sci, Polym.Phys.Edn., 16,959 (1978).
22. L.N.Sharapova, A.A.Chekanova, N.D. Zakharov and E.Yu. Borisova, Int.Polym.Sci.Technol.,10, 4 (1983).
23. G.Kraus, J.Appl.Polym.Sci., 7,861 (1963).
24. J.I.Cunneen and R.M. Russell., Rubber Chem. Technol., 43, 1215 (1970).

25. C.M.Blow and C.Hepburn, "Rubber Technology and Manufacture", 2nd edn., Butterworths, London, Ch.7, p. 301, 1987.

26. K.C. Baranwal, B.L. Lee and K.M. Schur., Proc. Int.Conf.Rubber and Rubber like Materials, Article 1.6, p.38, Jamshedpur, 6-8 Nov,1986.

Chapter 4

CHAPTER 4

MELT RHEOLOGICAL BEHAVIOUR OF SBR COMPOSITES FILLED WITH NR PROPHYLACTICS WASTE AND PARTICULATE FILLERS

ABSTRACT

Rheological properties of polymeric materials have paramount importance during their conversion to useful products. This chapter discusses the melt rheological behaviour of styrene butadiene rubber compounds filled with natural rubber prophylactics rejects and selected particulate fillers such as carbon black, silica, and marble powder. All the rubber compounds, irrespective of the composition, prophylactics particle size, mixing conditions and temperature, have showed pseudoplastic behaviour. An increase in the melt viscosity of styrene butadiene rubber compounds has been noted with the increasing loading of prophylactics filler. But this trend has been found to be dependent on the shear rate. The presence of particulate filler has been found to be increasing the viscosity of the rubber compounds only at the highest shear rate while at lower shear rates, a reverse trend has been observed. At the highest shear rate, among the particulate fillers used, the order of increasing the viscosity has been found to be marble powder<silica=black. The general inverse relation between particle size of the filler and viscosity in the case of particulate alone filled elastomer composites has not been observed for the present cases. The influence of particle size of prophylactics filler also has been found to be dependent on the shear rate. At low and intermediate shear rates and at a temperature of 150^0C, the compound mixed for 5 minute showed least viscosity but at highest shear rate the curves converge to a point due to 'spurt' or sudden combined flow. In the case of samples without particulate fillers, the influence of temperature has been found to have a notable effect on viscosity, only in the case of gum styrene butadiene rubber compounds. In these cases an inverse relation between temperature and viscosity has been observed with some abnormalities in the results at 160 and 170^0C. Such abnormalities have not been observed in the case of particulate filled samples at higher

shear rates. Flow behaviour index values have been found to be irregularly decreasing with the loading of prophylactics filler at 150 and 160^{0}C while at 170^{0}C a regular decrease has been observed. Except at 160^{0}C, all the samples filled with particulate fillers have been found to be less pseudoplastic than gum SBR and other prophylactics filled samples. Among the theoretical models studied, Eiler van Dyck equation has been found to be giving closely agreeing values of viscosity to that of experimental values. The variation of 'm' and 'C' which are characteristic rheological properties have been checked with the composition, particle size of prophylactics, mixing time and temperature of samples. A decrease in the extrudate distortion also has been observed with the addition of prophylactics and particulate fillers to styrene butadiene rubber compounds.

CHAPTER 4

MELT RHEOLOGICAL BEHAVIOUR OF SBR COMPOSITES FILLED WITH NR PROPHYLACTICS WASTE AND PARTICULATE FILLERS

Results of this chapter have been communicated to

Plast. Rubb. Compos. and Int. Polym. Process.

One of the objectives of polymer blending is the production of a better processing material. Processing of a rubber or elastomer blend involves all operations starting from the initial mastication to the formation of finished material. The knowledge of the rheological behavior of rubber compounds is important than any other properties[1-3]. In addition to these, careful control of manufacturing processes strongly depends on the appropriate classification of raw materials and their processability characteristics[4-6]. The complex rheological behaviour of polymer blends has been analysed by various researchers.[7,8] A number of publications focusing the rheology of various polymer blends are available in the literature. These include the rheological investigations on interacting blend solutions of poly (acrylic acid) with poly (vinyl pyrrolidone) or poly (vinyl alcohol)[9], polyphenylene sulphide/polyamide-66 blends[10], polypropylene/liquid crystal copolyester[11], ternary blends based on polypropylene/ethylene propylene rubber/polyethylene[12] and binary blends of LDPE/LLDPE[13] & HDPE/LLDPE.[14]

According to a review by Utracki et al.[15] three types of rheological behaviour are shown by polymer blends. These are the positive deviation behaviour where the blend viscosities are synergistic, the negative deviation behaviour where the blend viscosities are antagonistic, and finally the positive-negative deviation behaviour The actual behaviour shown by a polymer melt is in fact decided by the composition, morphology and processing conditions.

Rheological characteristics of single polymeric materials as well as polymer blends and especially that of rubber-rubber blends are greatly affected by the presence of fillers.

The filler loading used in most of these studies is in the range of 40 to 60%. The influence of fillers on the rheological behavior of 1,2 polybutadiene rubber has been studied by Bhagawan et al.[16] They observed that the highest viscosity is shown by silica filled samples, while the lowest by clay at all shear rates. Similar studies on silica filled silicone rubber has been studied by Aranguran et al[17] and also by Li et al.[18], taking zinc oxide and calcium carbonate in addition to black and silica. The greatest yield value and viscosity were observed with calcium carbonate and zinc oxide filled compounds. Recently, the influence of fillers on the compatibility of polymer blends also is reported in the literature[19]. Studies revealed that the compatibilising effect of the filler depends on the change in free energy of mixing between the two polymers.

In the field of recycling, the rheological behaviour of cryoground rubber-natural rubber blends has been observed by Phadke et al.[20] and that of polystyrene-SBR blends by Ciesielska et al.[21] Publication of Reena et al.[22] regarding the rheological and extrudate behaviour of natural rubber/latex reclaim blends also is noteworthy.

This chapter in two parts examines the rheological behavior of SBR/prophylactics systems by using a capillary rheometer. In the first part, the main parameters focused are the variation in viscosity and elastic effects, with respect to shear rate, shear stress, temperature & loading, particle size and mixing time of natural rubber prophylactics waste with SBR. In the second part, the influence of selected particulate fillers such as carbon black, silica and marble powder in SBR mixes with natural rubber prophylactics (size 2) is discussed.

4.1. Results and discussion

PART 1. Influence of Prophylactics Loading, Particle Size, Mixing Time and Temperature

The basic formulation used for the study is given in **Table 4.1**

4.1.1. Viscosity variation

(a). Influence of prophylactics loading

The variation of log melt viscosity with log shear stress of SBR compound with natural rubber prophylactics waste (S1) loading at different shear rates and at 150^0 C is presented in **Figure 4.1**. (The antilog values of viscosity (y-axis) are in Pa-s and that of

shear stress (x-axis) are in Pa).

Table 4.1. Basic formulation

Ingredients	Control (phr)											
	[a]Gum	[a]1	[a]2	[a]3	[a]4	[a]5	[a]6	[b]7	[c]8	[a]9	[a] 10	[a]11
SBR	100	100	100	100	100	100	100	100	100	100	100	100
Zinc oxide	5	5	5	5	5	5	5	5	5	5	5	5
Stearic acid	2	2	2	2	2	2	2	2	2	2	2	2
CBS	1	1	1	1	1	1	1	1	1	1	1	1
TDQ	1	1	1	1	1	1	1	1	1	1	1	1
Sulphur	2.2	2.2	2.2	2.2	2.2	2.2	2.2	2.2	2.2	2.2	2.2	2.2
Prophylactics Filler	0	10(S1)	20(S1)	40(S1)	20(S2)	20(S4)	20(M)	20(M)	20(M)	20(S2)	20(S2)	20(S2)
Carbon Black, HAF										10		
Silica											10	
Marble powder												10

[a] - mixing time 10 min, [b] – mixing time 5 min, [c] – mixing time 20 min

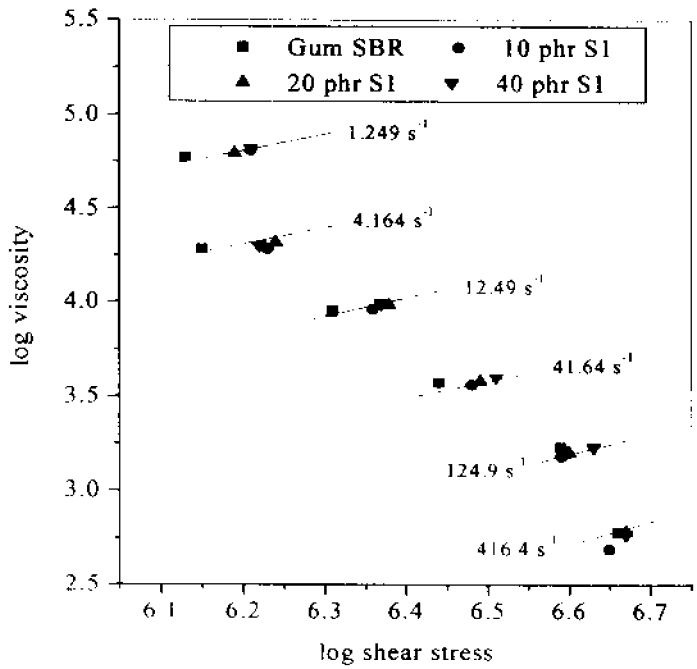

Figure 4.1. Variation of melt viscosity with shear stress for SBR samples with increasing prophylactics loading

The melt viscosity is found to be decreasing with shear stress and shear rate for all the mixes under study. This observation confirms the pseudoplastic behaviour of the mixes. At zero shear, the polymer chains are extensively entangled and randomly oriented. Under the application of shear, the chains get disentangled and become oriented. Pseudoplasticity results from this behaviour of the polymer chains. In the case of prophylactics filled cases also, pseudoplastic nature is observed. This is because of the orientation of the randomly oriented prophylactics particles under the action of shear with their major axis in the direction of shear. With increasing shearing force, this orientation also is facilitated. Therefore the viscosity drops considerably with increase in shear stress and shear rate. It is reported[23] that even in a molecular level, such orientation can help the smooth sliding of molecules over each other dissipating less energy than the randomly oriented and entangled molecules. Such a flow of gum SBR in layers is clearly visible from the scanning electron micrograph given in **Figure 4.2**.

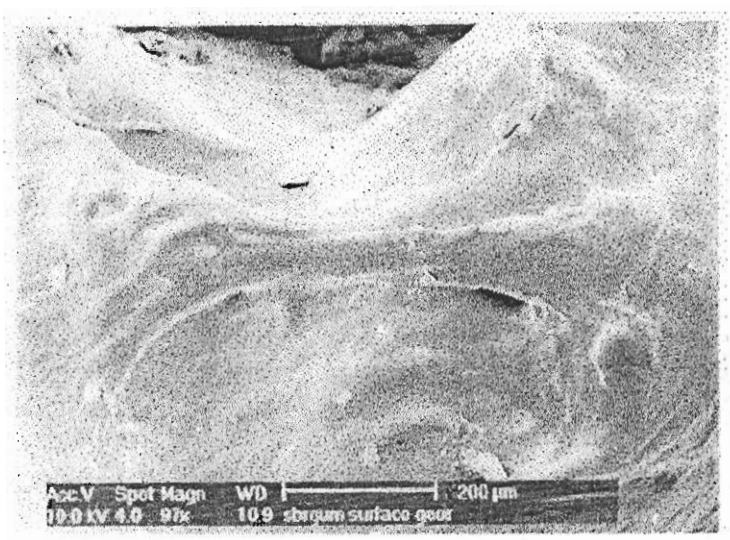

Figure 4. 2. SEM photo of gum SBR extrudate

Another observation is that the gum mix exhibits a lower viscosity at lower shear stress and a higher viscosity at higher shear stress. At lowest shear rate of 1.249 s^{-1}, as the concentration of waste prophylactics increases, the melt viscosity increases slightly, which becomes maximum for the mix with 40 phr prophylactics. When the shear rate increases the value of gum becomes comparable to that of prophylactics filled mixes and at higher shear rates, gum remains as one among those with higher viscosities. At the highest shear

rate, instead of gum SBR, the mix with 10 phr prophylactics exhibits the minimum melt viscosity. The slightly increasing trend in the melt viscosity with the addition of prophylactics is expected from the presence of crosslinked particles in an elastomer matrix[24]. The increase in viscosity with the addition of prophylactics at low shear rate indicates the restriction to the flow of the material induced by prophylactics particles. This results from the inability of prophylactics particles to get oriented at low shear rate. The structural build up, as reported earlier by Munstedt[25], is a possible reason for this. At high shear rates this will be less predominant and therefore such an increasing viscosity behaviour with the addition of prophylactics particles is absent. **Figure 4.3** clearly indicates the presence of a structural build up in the composite sample.

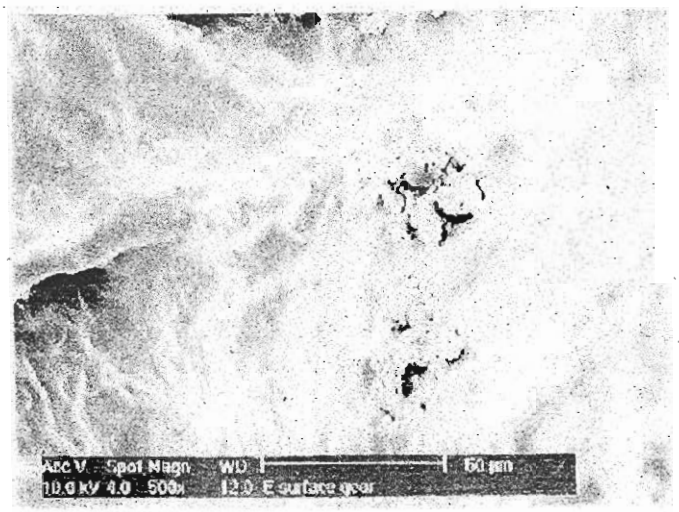

Figure 4.3. SEM photo of SBR extrudate with 10 phr prophylactics

The low melt viscosity of SBR compound with 10 phr prophylactics filler at higher shear rates indicates the better mould flow for these samples in a molding process. In such cases, the additional energy consumption for molding will be much less[26]. Such a behavior is due to the difference in the size of the flow units initially suggested by Mooney and Wolstenholme[27] and later developed by the theory of Nakajima and Collins[28]. At low shear rate, the size of the flow unit must be smaller than the size of the prophylactics particles. In such a case, the prophylactics particles act as flaws and therefore viscosity increases with prophylactics loading at low shear rates. But at high shear rates, the combined flow occurs in which the size of the flow units increases over the size of prophylactics particles. Therefore, no significant effect on the viscosity can be observed with the presence of

prophylactics particles.

It is interesting to note in **Figure 4.1**, that the melt viscosity verses shear stress curves present a change in the slope at an earlier shear rate of 4.164 s^{-1} and later at 124.9 s^{-1}. The slope is higher at both low and high shear rates while it is less at intermediate shear rates. It is interesting to see that most of the curves converge at the higher shear rate. Similar slope changes as noted in **Figure 4.1** are reported in the case of natural rubber –cryoground rubber systems also[29] at $30s^{-1}$. The convergence of the curves at higher shear rates is due to a phenomenon called 'spurt'[30,31] which is a sudden combined flow.

(b). Influence of prophylactics particle size

The effect of particle size of waste prophylactics filler (20 phr loading) on the log viscosity-log shear stress plots at 150^0 C is presented in **Figure 4.4.**

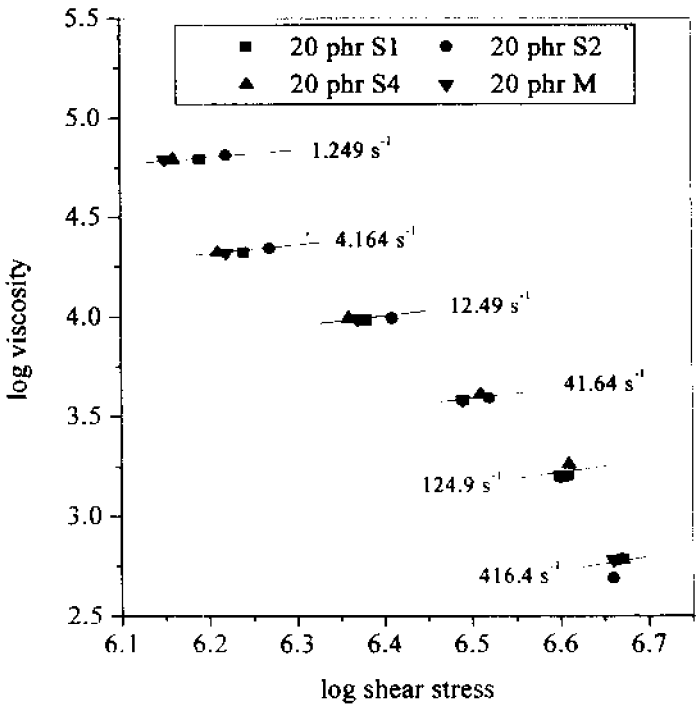

Figure 4.4. Variation of melt viscosity with shear stress for SBR samples with increasing prophylactics particle size

For all the particle sizes under study, pseudoplasticity is observed. At the lower shear rate, comparatively higher viscosity is shown by size 2 prophylactics filled samples

while at intermediate shear rates, values become comparable. At the highest shear rate, large size fillers such as size 4, M and gum compound exhibit highest viscosity while size 2 shows the lowest. Normally, in the case of elastomers filled with particulate fillers, the viscosity is reported to be increasing for smaller particles with larger surface area than larger particles with smaller surface area[32]. But here, such a trend cannot be observed.

(c). Influence of mixing time

SBR mix containing mill-sheeted form of the prophylactics is selected to study the effect of mixing time. The mixing time of the SBR compound containing 20 phr of mill sheeted is varied as 5, 10 and 20 minutes **(Figure 4.5)**.

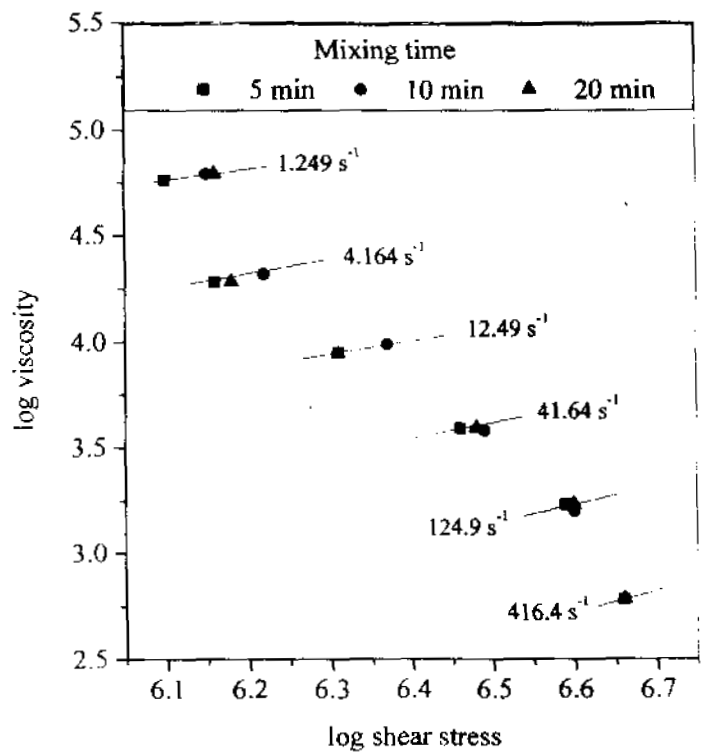

Figure 4.5. Variation of melt viscosity with shear stress for SBR samples with increasing mixing time

At low and intermediate shear rates, the compound mixed for 5 min shows the lowest viscosity (at 150° C) while the maximum viscosity is exhibited by the sample when the mixing time is 10 minutes. An intermediate viscosity is shown by the sample mixed for 20 minutes. At the highest shear rate, it is found that the curves converge at a point

proving the non-dependence of mixing time on the viscosity of the mixes. In these cases also, the variation in viscosity is marginal. Here it should be noted that the viscosity of a rubber matrix filled with crosslinked rubber particles depends on many phenomena such as size distribution of particles and their agglomeration effects in the matrix. The convergence of viscosity values at the highest shear rate to a point can be due to 'spurt' or combined flow observed in flowing polymer melts.

(d). Influence of temperature on melt viscosity

The effect of temperature on the melt viscosity of SBR gum compound is presented in **Figure 4.6**. It is a general observation that as the temperature increases, the melt viscosity decreases at all shear rates. However, some abnormality exists between the mixes at 160 and 170 ^{0} C.

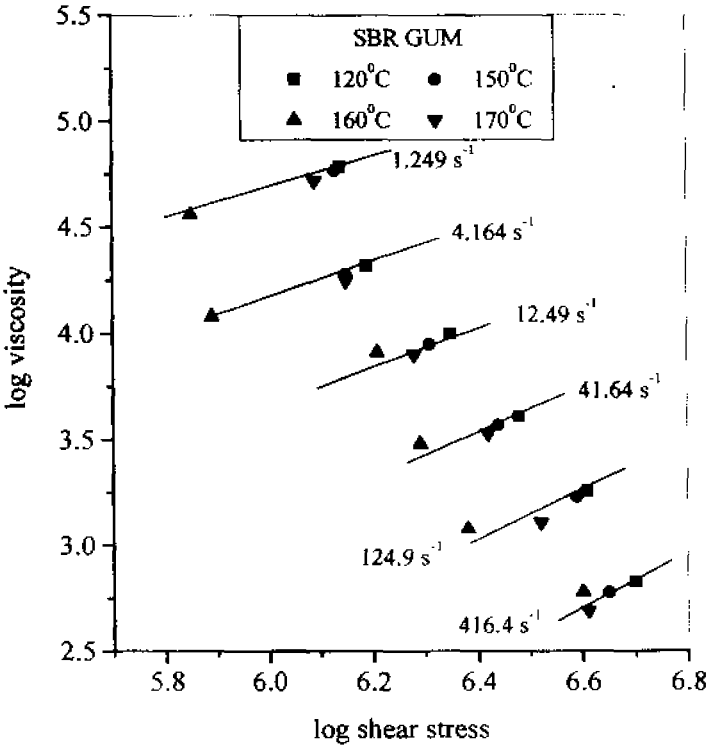

Figure 4.6. Variation of melt viscosity with shear stress for gum SBR samples at different temperatures

The influence of temperature in SBR compound containing 20 phr size 1 prophylactics filler is shown in **Figure 4.7**.

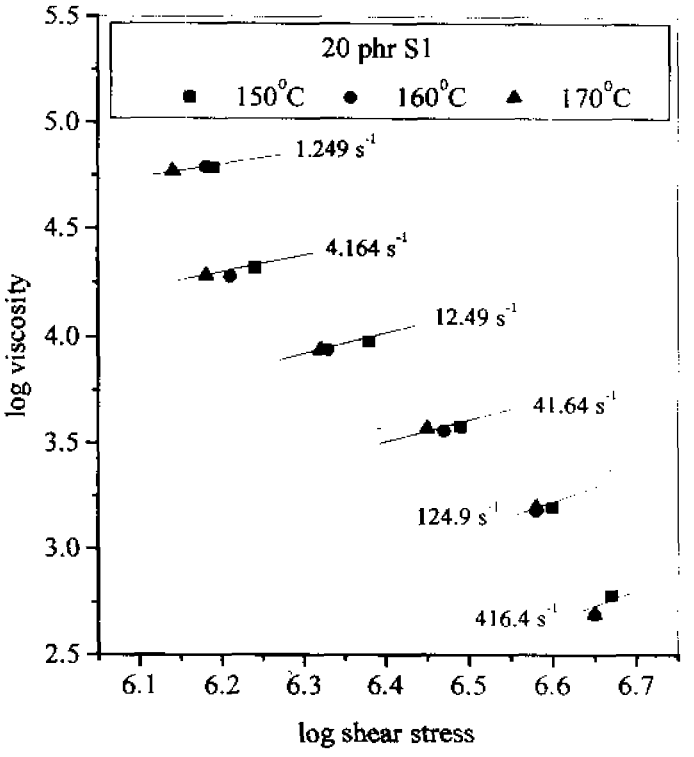

Figure 4.7. Variation of melt viscosity with shear stress for SBR with 20 phr size 1 prophylactics at different temperatures

The melt viscosity is found to be almost unaffected with temperature at most of the shear rates. But at the highest shear rate of 416.4 s^{-1}, similar values are shown by the sample at 160 and 170 ^{0}C while higher value is observed at 150^0 C. In the case of SBR sample filled with 40 phr size 1 prophylactics filler **(Figure 4.8)**, comparable values are observed at various temperatures given.

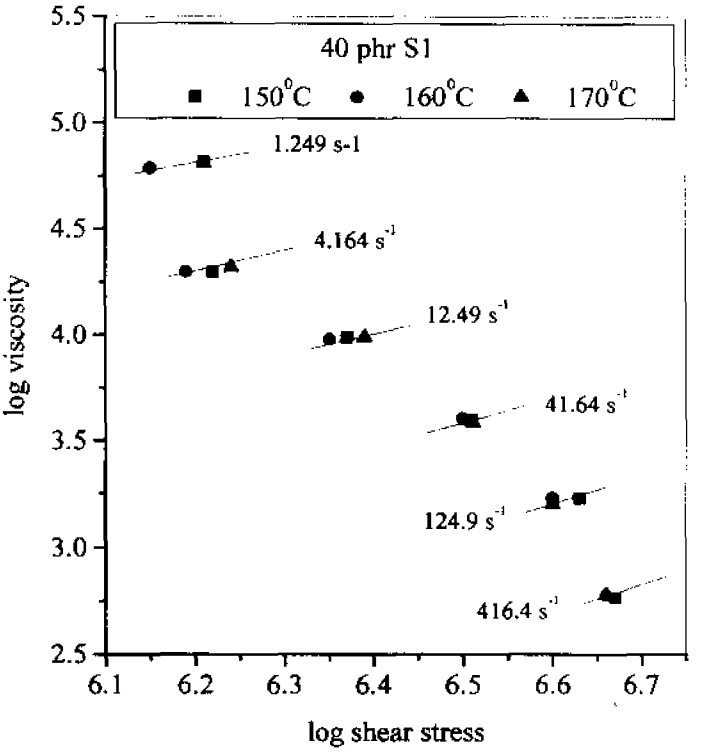

Figure 4.8. Variation of melt viscosity with shear stress for SBR with 40 phr size 1 prophylactics at different temperatures

4.1.2. Flow behaviour index

The flow behaviour index (n'), which is a measure of the pseudoplasticity, is presented in **Table 4.2**. As per the theory, the more the value of n', lesser is the non-Newtonian behaviour(or higher the Newtonian behaviour), the lower the pseudoplasticity.

(a). Influence of prophylactics loading

At 150 ^{0} C and for a mixing time of 10 min, it can be seen that the presence of prophylactics filler decreases the n' values in an irregular manner, i.e., as the loading of prophylactics filler in SBR increases, the value first decreases at 10 phr and then increases for further loading. So SBR mix with 10 phr prophylactics loading shows the maximum pseudoplasticity **(Table 4.2)**. At 160^{0}C also, the same trend is observable while at 170^{0}C, a regular drop in n' value can be observed with the temperatures studied.

Table 4.2. Flow behaviour index (n') values

Mix	Temperature (^{0}C)			
	120	**150**	**160**	**170**
Gum	0.2373	0.2300	0.3009	0.2203
10 phr S1[a]	ND	0.1943	ND	ND
20 phr S1[a]	ND	0.2031	0.2033	0.2191
40 phr S1[a]	ND	0.2111	0.2260	0.1999
20 phr S2[a]	ND	0.1928	0.2047	0.2206
20 phr S4[a]	ND	0.2219	ND	ND
20 phr M[a]	ND	0.2169	0.1958	0.2094
20 phr M[b]	ND	0.2397	ND	ND
20 phr M[c]	ND	0.2234	ND	ND
20 phr S2+10 black[a]	ND	0.2607	0.2569	0.2375
20 phr S2+10 silica[a]	0.2833	0.2568	0.2106	0.2457
20 phr S2+10 marble powder[a]	0.1724	0.2425	ND	ND

[a] - mixing time 10 min, [b] – mixing time 5 min, [c] – mixing time 20 min

ND- Not determined

(b). Influence of prophylactics particle size

In the case of n' values of SBR mixes at 150 ^{0} C with different particle sizes **(Table 4.2)**, the lowest value is obtained for 20 phr size 2 prophylactics filled system which agrees with the its low viscosity value only at highest shear rate 416.4 s^{-1} **(Figure 4.6)**. The highest n' value is observed for SBR mix with size 4 prophylactics system.

(c). Influence of mixing time

The effect of mixing time on n' value can also be seen from **Table 4.2**. The n' value for the SBR compound with 20 phr M prophylactics filler is lower for samples with mixing time 10 and 20 min compared to that with a mixing time of 5 min.

(d). Influence of temperature

In the case of gum SBR compound, n' values decrease with increase of temperature from 120 to 170^0 C, except at 160^0 C. Similar reduction in n' value with temperature is reported in the literature[33]. Different mixes show highest n' value at different temperatures. In the case of gum SBR and the mix with 40 phr S1, the highest n' value is obtained at 160^0 C, in the case of the mix with 20 phr s1, at 170^{0}C, and in the case

of the mix with 20 phr M, the highest value is at 150°C. Similarly SBR gum and the mix show the minimum value with 40 phr s1 at 170° C, 20 phr s1 at 150° C, and for the mix with 20 phr M, at 160° C. Generally it can be understood that the n' value showed a decreasing trend with temperature except a few cases.

4.1.3. log ℑ Vs. log γ plots and 'm' & 'C' values

It is interesting to check the application of certain mathematical relations in the present cases. The flow rate depends on the nature of the compound being processed and its viscosity, which is shear rate –shear stress dependent. The extrusion rate depends upon changes in viscosity, which may result from changes in shear rates during the extrusion process, and so the slope 'm' and 'y' intercept 'C' of the plots are critical rheological properties. The proposed relation is

$$\log \Im = \log \gamma^{m} + C \qquad (4.1)$$

A typical plot is given in **Figure 4.9**

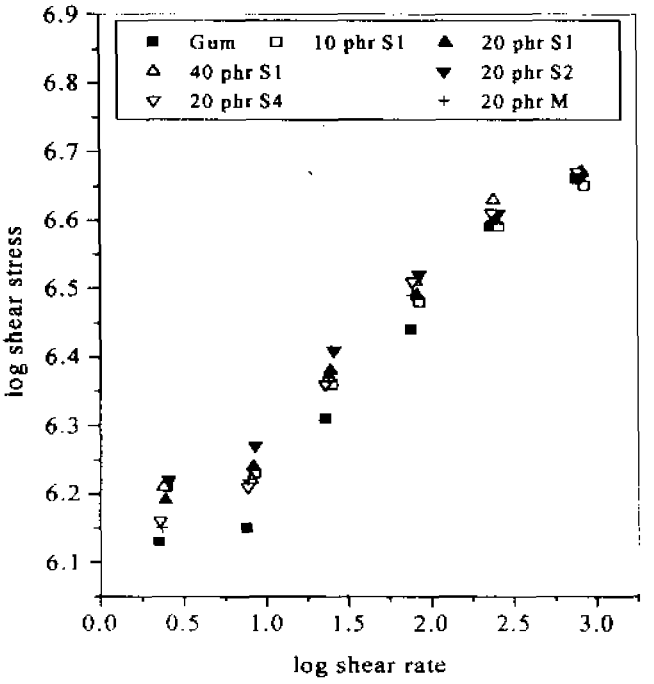

Figure 4.9. Variation of log ℑ verses log γ for SBR compounds with increasing prophylactics loading

[Antilog values of shear stress (y axis) are in Pa and that of shear rate (x axis) are in s^{-1}]

Values of 'm' and 'C' are given in **Tables 4.3** and **4.4**.

Table 4.3. Effect of composition of 'm' and 'C' values

Mix	m	C
Gum	0.2285	6.0119
10 phr S1[a]	0.1927	6.0989
20 phr S1[a]	0.2038	6.0911
40 phr S1[a]	0.2082	6.0926
20 phr S2[a]	0.1912	6.1299
20 phr S4[a]	0.2211	6.0604
20 phr M[a]	0.2166	6.0612
20 phr M[b]	0.2405	5.9932
20 phr M[c]	0.2231	6.0358
20 phr S2+10 black	0.2604	5.9664
20 phr S2+10 silica	0.2611	6.0317
20 phr S2+10 marble powder	0.2447	6.0027

[a] - mixing time 10 min, [b] – mixing time 5 min, [c] – mixing time 20 min

Table 4.4. Effect of temperature on 'm' and 'C' values

Mix	Temperature (°C)							
	120		150		160		170	
	m	C	m	C	m	C	m	C
Gum	0.2384	6.0279	0.2285	6.0119	0.3007	5.7367	0.2191	5.9878
20 phr S1	ND	ND	0.2038	6.0911	0.2041	6.0658	0.2207	6.0269
40 phr S1	ND	ND	0.2082	6.0926	0.2236	6.0461	0.1958	6.1109
20 phr M	ND	ND	0.2166	6.0612	0.2002	6.1073	0.2066	6.0701
20 phr S2	ND	ND	0.1912	6.1299	0.2041	6.0658	0.2207	6.0269
20 phr S2+ 10 black	ND	ND	0.2604	5.9664	0.2557	5.9600	0.2422	5.9929
20 phr S2 +10 silica	0.2799	6.0072	0.2611	6.0317	0.2140	6.1296	0.2109	6.1434
20 phr S2 + 10 marble powder	0.1723	6.2333	0.2447	6.0027	ND	ND	ND	ND

It can be seen that except in the case of the sample with 5 min mixing time, the presence of prophylactics in gum SBR mix decreases the 'm' values while 'C' values increase slightly. Similarly, as the particle size of the prophylactics increases from size 1 to 4 and M (at same loading of 20 phr), 'm' values increase (only one exception is the value of S2 which

is less) while the 'C' values decrease slightly. In the case of SBR with 20 phr mill sheeted form, as the mixing time increases from 5 to 10 min, 'm' value decreases considerably and for the sample with mixing time 20 min, it slightly increases compared to 10 min sample, but still it is much less than that of the sample mixed for 5 min. 'C' value first increases for 10 min sample and then decreases for 20 min sample. It can be suggested here that the interactive effect of SBR with the inclusion can be characterised by changes in 'C' while it is more related to particle size of the prophylactics filler.

Table 4.4 gives the effect of temperature on 'm' and 'C' values. In the case of gum SBR, as the temperature increases, 'm' value first shows a decrease at 150^0C, an increase at 160^0C and finally a drop at 170^0C while 'C' values show a regular drop upto 160^0C and finally a slight increase at 170^0C. For SBR mix containing 20 phr S1 prophylactics, value of 'm' goes on increasing and that of 'C', decreasing with temperature. At a loading of 40 phr S1 prophylactics filler to SBR, the highest 'm' value is obtained at 160^0C while 'C' value is lowest at that temperature. For SBR filled with 20 phr M case also, lowest 'm' value is at 160^0C while lowest 'C' value at 150^0C.

4.1.4. Theoretical modeling of viscosity

The variation in the melt viscosity of SBR with NR prophylactics loading at different shear rates is compared with different previously established mathematical models. These are Einstein, Mooney, Guth, Kerner, Sato-Furukawa, Eiler van Dyck, Bills, Brinkman and Narkis models. The terms used in this section are the following. η- viscosity, V_f- volume fraction of filler, S- crowding factor, ν- Poisons ratio, suffixes c and m denote composite and gum matrix. The equations are given below.

1. **Einstein equation**

Einstein[34] has proposed an equation for the viscosity of the composite assuming perfect bonding between the phases.

$$\eta_c = \eta_m(1+ 2.5\ V_f) \qquad (4.2)$$

2. **Mooney equation**

This equation[35] considers the interaction of strain fields around particles while it agrees with Einstein's equation at low volume fraction of the filler, it can represent the data at higher volume fractions as well.

$$\eta_c = \eta_m \exp\left[\frac{2.5\, V_f}{1 - S\, V_f}\right] \qquad (4.3)$$

3. Guth equation

Guth[36] modified Einstein equation by considering the particle interactions also.

$$\eta_c = \eta_m (1 + 2.5\, V_f + 14.1\, V_f^{\,2}) \qquad (4.4)$$

4. Kerner equation

The equation derived by Kerner[37] assumes spherical particles.

$$\eta_c = \eta_m \left\{1 + \frac{V_f}{V_m}\left[\frac{15\,(1-\nu_m)}{8 - 10\,\nu_m}\right]\right\} \qquad (4.5)$$

5. Sato-Furukawa equation

The weak adhesion between matrix and filler is best represented in the literature[38] by Sato-Furukawa equation

$$\eta_c = \eta_m \left[\left\{1 + \frac{y^2}{2(1-y)}\right\}\left\{1 - \frac{y^3 T}{3}\left[\frac{1+y-y^2}{1-y+y^2}\right]\right\} - \left\{\frac{y^2 T}{3\,(1-y)}\right\}\left\{\frac{1+y-y^2}{1-y+y^2}\right\}\right] \qquad (4.6)$$

where y is a filler concentration variable equal to $V_f^{\,1/3}$ and T is a constant characterising the filler-matrix adhesion. If the adhesion is perfect T=0, and if it is weak, T=1.

6. Eiler van Dyck equation[39]

$$\eta_c = \eta_m \left[1 + \frac{k\, V_f}{1 - S'\, V_f}\right] \qquad (4.7)$$

where k = 1.25 and S'= 1.20

7. **Bills equation[40]**

$$\eta_c = \eta_m \exp\left[\frac{A\, V_f}{1 - B\, V_f}\right] \qquad (4.8)$$

where A = 2.5 and B = - 6.4 X 10^{-3} T + 2.51 where T is the test temperature.

8. **Brinkman equation**[41]

$$\eta_c = \eta_m (1 - V_f)^{5/2} \qquad (4.9)$$

9. **Narkis**[42]

$$\eta_c = \eta_m \left[\frac{1}{K(1 - V_f^{1/3})} \right] \qquad (4.10)$$

where K is the stress concentration factor whose value ranges from 1.4 to 1.7.

Figure 4.10 represents the comparison of experimental viscosity values with the theoretical values at a shear rate 1.249 s^{-1}. It can be seen from the figure that at 10 phr prophylactics loading, the best agreement is shown by Eiler van Dyck equation and this agreement exits at all the loadings.

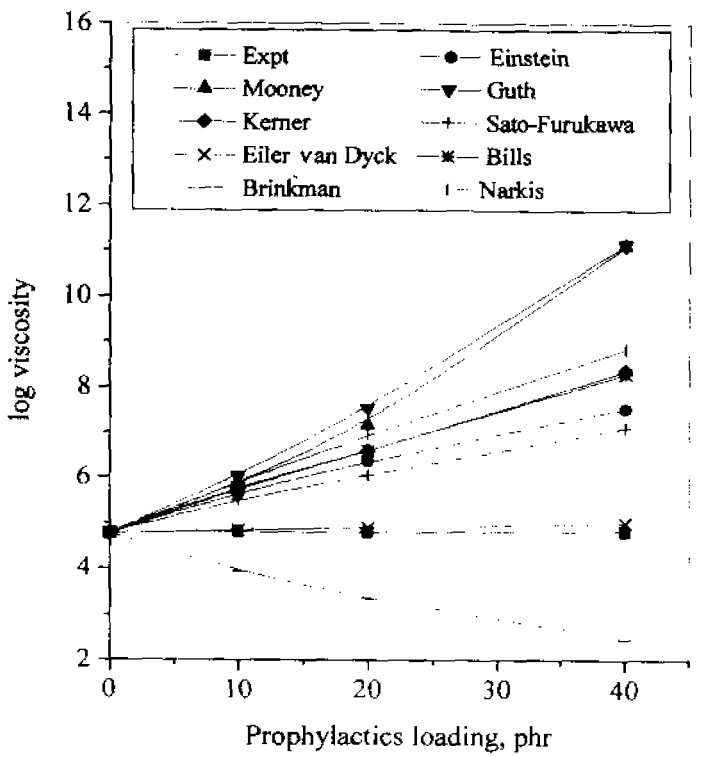

Figure 4.10. Experimental and theoretical plots for the melt viscosity of SBR compounds at a shear rate of 1.249 s^{-1}

When Brinkman equation shows negatively deviated values, all other equations give positively deviated values. Among the equations showing positive deviation, better agreement is shown by Sato-Furukawa and then by Einstein equation. The least agreement is shown by Guth equation while all other equations show intermediate values. The same trend is repeated at 20 phr loading of prophylactics also. At 40 phr loading, the only difference noted is that the values given by Guth and Mooney equation are very close. At higher shear rates also, the best agreement between experimental and theoretical values is obtained in the case of Eiler van Dyck model.

4.1.5. Extrudate distortion

Most of the extrudates from capillary rheometer showed visual evidence of surface imperfections. The extrudate appearance can be used to assess the quality of the flow behavior, rupture behavior and to find the shear rate at which flow instability commences. The extrudate distortion shown by gum SBR is the highest **(Figure 4.11)**. In this case, the extrudates appeared like a twisted rope. The extrudate distortion at 120^0 C becomes high as the shear rate increases. This is clear from **Figure 4.11 a-c**. Also as the temperature increases, the extrudate distortion is found to be increasing **(Figure 4.11 a, d-f)**. The extrudate distortion is visible in the prophylactics filled sample (10 phr S1) also but to a lesser extent **(Figure 4.11 g)**. This means that the prophylactics particles suppress the distortion and thus they give more uniform extrudates and that the extrudate dimension is less sensitive to shear rate. As the loading of prophylactics increases **(Figure 4.11 g-i)**, still, extrudate distortion is present but it is less predominant. With the increase in the size of prophylactics, no notable change in the extrudate distortion can be observed **(Figure 4.11 h, j, k, l)**. In the case of SBR mix with 20phr M also, extrudate distortion is observable to some extent at 160 and 170^0 C **(Figure 4.11 l, n, o)**. A low extrudate distortion was noted at the lowest shear rate and at lowest temperature of 150^0C **(Figure 4.11 l)**. It is also found that as the mixing time increases in the case of the SBR mix with 20 phr M, extrudate distortion decreases as can be seen from **Figure 4.11 p, l, m**. The highest extrudate distortion shown by gum SBR is because of its low viscosity compared to the prophylactics particles. The low extrudate distortion in the presence of

prophylactics filler means that there is reasonably good bonding between prophylactics filler particles and SBR.

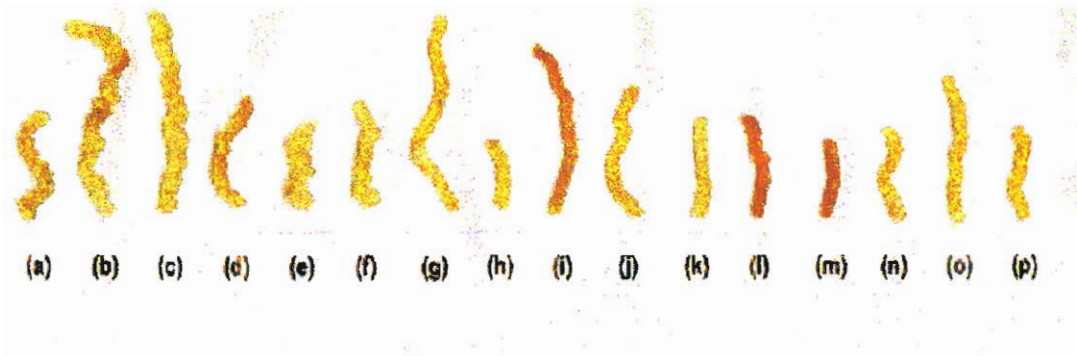

(a) SBR gum – 4.164 s^{-1} – 120^{0}C

(b) SBR gum – 41.64 s^{-1} – 120^{0}C

(c) SBR gum – 416.4 s^{-1} – 120^{0}C

(d) SBR gum – 4.164 s^{-1} – 150^{0}C

(e) SBR gum – 4.164 s^{-1} – 160^{0}C

(f) SBR gum – 4.164 s^{-1} – 170^{0}C

(g) SBR + 10 phr S1 – 4.164 s^{-1} – 150^{0}C

(h) SBR + 20 phr S1 – 4.164 s^{-1} – 150^{0}C

(i) SBR + 40 phr S1 – 4.164 s^{-1} – 150^{0}C

(j) SBR + 20 phr S2 – 4.164 s^{-1} – 150^{0}C

(k) SBR + 20 phr S4– 4.164 s^{-1} – 150^{0}C

(l) SBR + 20 phr M (10 min) – 4.164 s^{-1} – 150^{0}C

(m) SBR + 20 phr M (20 min) – 4.164 s^{-1} – 150^{0}C

(n) SBR + 20 phr M– 4.164 s^{-1} – 160^{0}C

(o) SBR + 20 phr M– 4.164 s^{-1} – 170^{0}C

(p) SBR + 20 phr M (5 min) – 4.164 s^{-1} – 150^{0}C

Figure 4.11. Extrudates of gum and prophylactics filled SBR compounds

Turner and Bickley[43] suggested that the low viscous phase (SBR) in the mix migrates to the surface through a roll mechanism, i.e., a radical flow in addition to longitudinal flow, which gives the extrudates a screw thread appearance. The reduced extrudate distortion also points out the decrease in the melt elasticity with the addition of

prophylactics filler. The presence of crosslinked particles decreases the deformation tendency of the SBR mix and fastens the recovery. The superior efficiency of sulphur crosslinked networks for this is reported in the literature[33]. The less sensitivity of extrudate distortion to temperature shown by the prophylactics filled mix (40 phr S1) is important in the dimensional stability of extruded profiles because during extrusion neither shear rate /stress nor temperature is constant across the profile.

PART 2. INFLUENCE OF PARTICULATE FILLERS

The recipe used is the same as **Table 4.1**.

4.1.6. Viscosity variation

The influence of particulate fillers on the rheological properties of molten polymers is both of great scientific and industrial importance. Such fillers are added primarily to strengthen the product and to reduce the cost. Normally, particulate fillers increase the level of viscosity[44,45] but the extent seems to vary from system to system and decrease with increasing shear rate[44]. The variation of melt viscosity with shear stress and shear rate for gum SBR and SBR mix with 20 phr size 2 prophylactics filler with and without particulate fillers at 150^0 C is presented in **Figure 4.12** (The antilog values of viscosity (y axis) are in Pa-s and that of shear stress (x axis) are in Pa). The melt viscosity is found to be decreasing with shear stress and shear rate for all the mixes.

At lower shear rate, an increase in the viscosity can be noted with the addition of prophylactics filler to SBR. The black and marble powder filled mixes exhibit the lower viscosity compared to other samples, and among them, marble powder filled mix presents slightly higher viscosity compared to carbon black. Silica filled samples give higher viscosities at most of the shear rates but at lower shear rates the values are comparable to that of other mixes without particulate fillers. However at the highest shear stress, the behavior becomes more normal, i.e., the SBR/prophylactics mix without particulate filler shows the lowest viscosity, the next higher value by marble powder, which is followed by comparable viscosity values by silica and black.

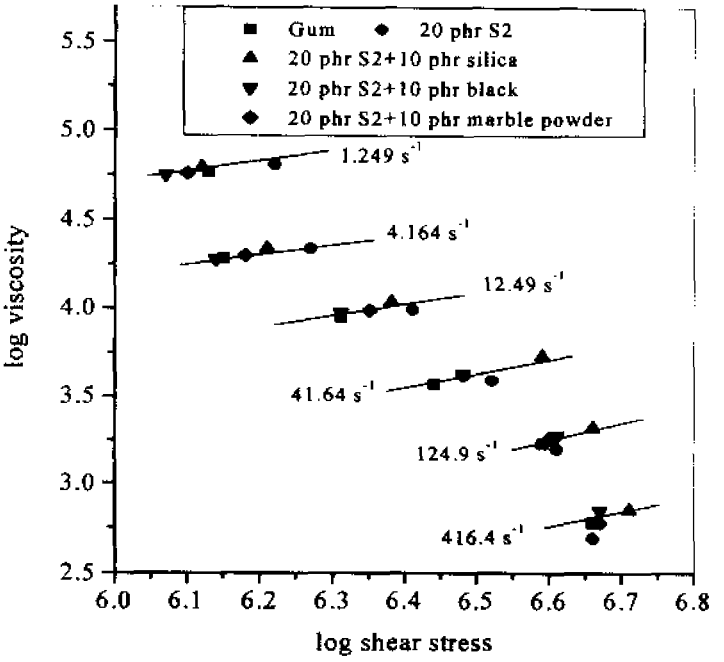

Figure 4.12. Variation of melt viscosity with shear stress for SBR samples filled with prophylactics and particulate fillers

Figure 4.12 reveals that at the highest shear rate, the silica filled samples show the highest viscosity values and that the drop in viscosity is fast at low and high shear rates. The slope of the plots is higher at both low and high shear rates while it is less at intermediate shear rates. It can be seen that the values tend to converge at a point at higher shear rate. The low viscosity of particulate filled samples compared to prophylactics alone filled samples at low shear rate is in agreement with the observation by Clarke[46]. It is also noticed by Shaheen[47] that addition of a little amount of small particles act as a lubricant to facilitate the rotation of larger particles, leading to a reduction in viscosity. However, at higher shear rates, the relative flow of different layers is checked to a great extent by the filler particles through the formation of adsorbed layers and so the viscosity rises for the particulate filled samples compared to prophylactics alone filled sample.

The observation of lowest viscosity shown by the SBR mix without particulate filler and the increase in viscosity with the addition of particulate fillers at the highest shear rate indicates that at highest shear rates, the particles in the SBR matrix are aligned in the

flow direction subject to the restriction for this imposed by the particulate fillers. Therefore, it is clear from these results that the ability of a filler to contribute to the viscosity depends very much also on the nature and components of the main matrix. The superior reinforcing nature of black in a single elastomer matrix[48] and the comparable behavior shown by black and silica in the case of ENR / NR blends[49] are important to mention here. The highest viscosity values shown by the silica filled mixes can be due to its equal distribution among the SBR and prophylactics phases. This can increase the interfacial thickness, reduce the interlayer slip, which in turn causes an increase in viscosity. This phenomenon shown by silica may also be due to its low density and high absorptive capacity, which causes similar effects of viscosity in filled polybutadiene samples[46].

Influence of temperature on melt viscosity

The influence of temperature on the viscosity of SBR filled with prophylactics filler in the presence of particulate fillers is presented in **Figure 4.13-4.15**.

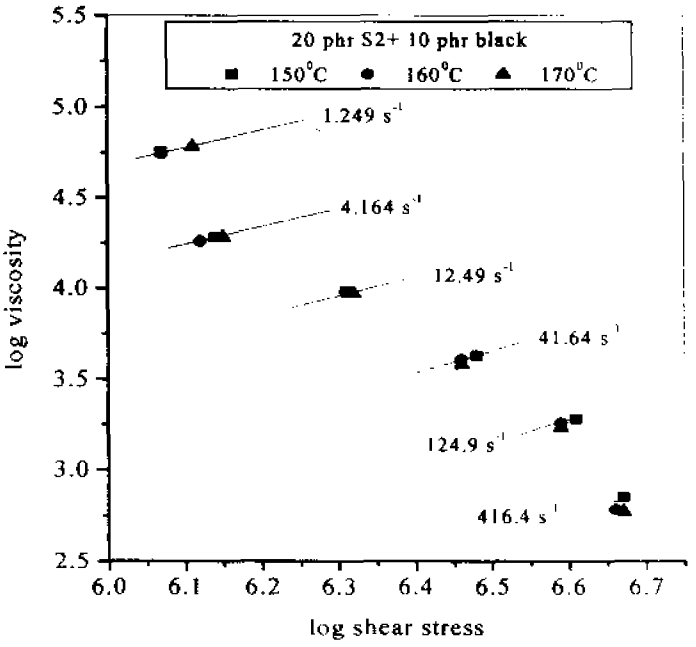

Figure 4.13. Variation of melt viscosity with shear stress for SBR samples filled with carbon black at different temperatures

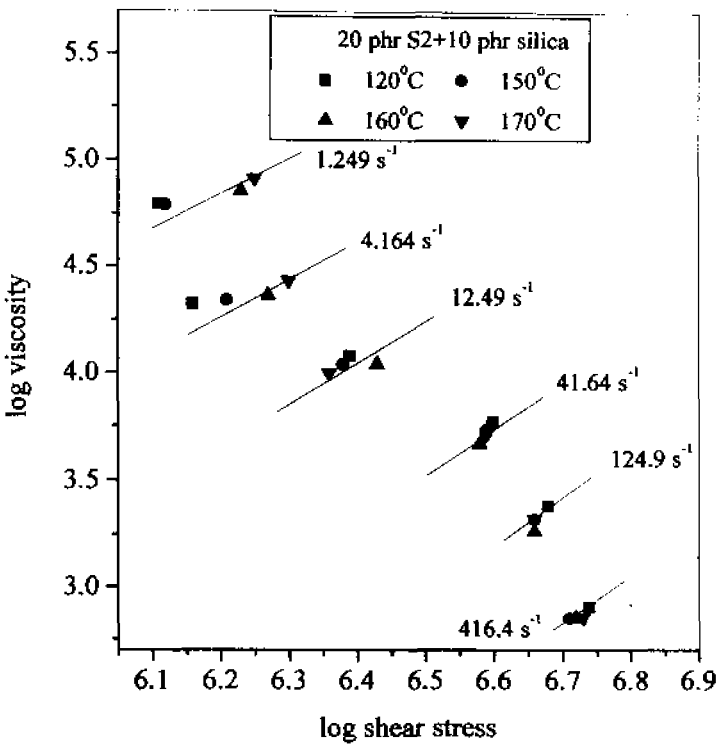

Figure 4.14. Variation of melt viscosity with shear stress for SBR samples filled with silica at different temperatures

In the case of black filled samples **(Figure 4.13)** at lower shear rate, the trend is a bit abnormal while at higher shear rate, the trend is as expected according to the already established viscosity-temperature relations. **Figure 4.14** represents the silica filled systems. Upto a shear rate of 4.16 s^{-1}, it is found that the viscosity increases with increase in temperature. But from a shear rate of 12.49 s-1 onwards the trend becomes somewhat similar to that expected from the influence of temperature. Similar inverse relation between viscosity and temperature is shown by marble powder filled samples also **(Figure 4.15)**.

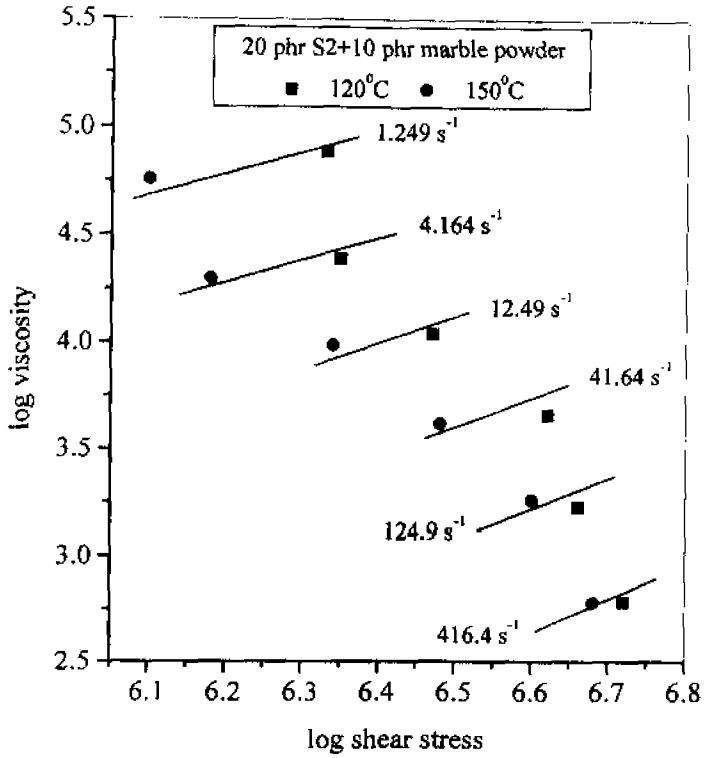

Figure 4.15. Variation of melt viscosity with shear stress for SBR samples filled with marble powder at different temperatures

4.1.7. Flow behavior index

The flow behavior index or n' values of the SBR compounds are presented in **Table 4.2.** It can be seen that except at 160^0 C, the n' values of mixes filled with particulate fillers are slightly higher than that of gum SBR mix and that with prophylactics filler alone. At 150^0 C, black filled sample presents highest n' values among the set. But it fails to give a direct relation with the viscosity data at lower shear rates given in **Figure 4.12.** It can be seen that a direct correlation between n' and viscosity exists at higher shear rates 124.9 $s^{-1}$and 416.4 s^{-1}. At 160 ^{0} C, the n' of gum SBR mix is found to be decreasing with the addition of prophylactics as well as particulate fillers black and silica. In earlier publications the higher pseudoplasticity of black filled polymer samples was reported compared to other particulate fillers[33]. But here in the presence of prophylactics, a reverse trend is observed. The black filled samples show the least pseudoplasticity among the fillers at 150^0 C. The higher n' values is due to the enhanced difficulty for chains to orient

and show pseudoplasticity. This results from the less freedom available to the chains.

4.1.8. log ℑ Vs. log γ plots and 'm' & 'C' values

Plots log ℑ verses log γ^{m} of then samples (at 150^{0} C) are given in **Figure 4.16** [Antilog values of shear stress (y axis) are in Pa and that of shear rate (x axis) are in s^{-1}] and the values of 'm' and 'C' are given in **Table 4.4.**

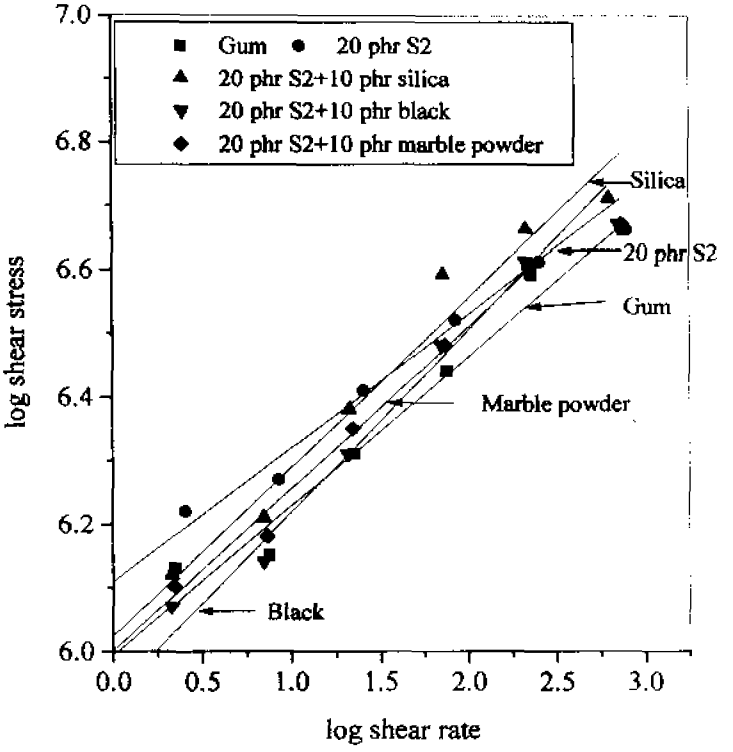

Figure 4.16. Variation of log ℑ verses log γ for gum and filled SBR compounds

A decrease in 'm' and an increase in 'C' are observed with the addition of prophylactics filler in gum SBR. Also, with the addition of particulate fillers, an increase in 'm' and a decrease in 'C' are again observed. But the variations observed are only marginal. The low 'm' and high 'C' values shown by silica compared to black at 160 and 170^{0} C, may be due to its uniform distribution among the components of the system. It can be seen that the presence of silica which gives maximum reinforcement in viscosity data fails to give low 'm' value but it succeed to present a slightly higher 'C' value among the set proving its reinforcing nature.

Table 4.4 gives the effect of temperature on 'm' and 'C' values. Normally, as the temperature increases, the interface will become strong and so 'm' must show a decrease while 'C' must show an increase. But for the present case, abnormalities exist. As discussed earlier, even though silica fails to present its reinforcing behaviour in SBR / prophylactics mix at 150^0C, it gives a low 'm' and a high 'C' value compared to black at 160 and 170^0 C. Among the particulate fillers, silica which gives maximum reinforcement in viscosity data fails to give low 'm' value but it presents a slightly higher 'C' value among the set. In the case of particulate filler containing samples, 'm' values show a regular drop with temperature while 'C' values show a regular increase and this is in agreement with the theory. Similar agreement can be seen for black also, but marble powder fails to give such an agreement.

4.1.9. Extrudate distortion

Generally particulate fillers and especially, titanium dioxide[50] is reported to smoothen the surface of the extrudate and delay the extrudate distortion to higher extrusion rates. The influence of particulate fillers on the extrudate distortion can be seen from the **Figures 4.17**. As the discussions on samples without particulate fillers were already completed in section 4.1.5, discussions here are limited to particulate filled samples only. It is reported[2] that addition of black can reduce the severity of distortion but cannot eliminate it. It can be seen from **Figure 4.17 l-v** that black is not effective to a satisfactory extent in reducing the extrudate distortion even at low shear rate and low temperature compared to silica. Compared to the behaviour in a single elastomer system, here, black presents an entirely different behaviour. Slightly less extrudate distortion is shown by black filled samples at higher temperatures **(Figure 4.17 l, o, p)**. Silica reduces the extrudate distortion considerably **(Figure 4.17 l-v)**. Even though the increase in elastic distortion with shear rate is still present, the same effect with increasing temperature was only marginal upto 160^0 C. At 170^0 C, extrudate distortion is again visible **(Figure 4.17 q-v)**.

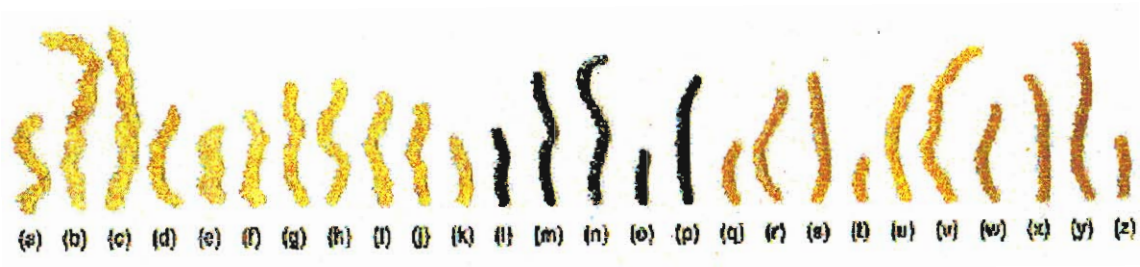

(a). SBR gum-4.164 s^{-1}- 120^0 C (b). 41.64 s^{-1} (c). 416.4 s^{-1} (d). 4.164s^{-1}-150^{0}C. (e) 160^{0}C (f). 170^{0}C

(g). SBR+20 phr S2-4.164 s^{-1}- 150^0 C (h). 41.64 s^{-1} (i). 416.4 s^{-1} (j). 4.164 s^{-1}-160^{0}C (k). 170^{0}C

(l). SBR+20 phr S2+10 phr black-4.164 s^{-1}- 150^0 C (m). 41.64 s^{-1} (n). 416.4 s^{-1} (o). 4.164 s^{-1}-160^{0}C (p). 170^{0}C

(q). SBR+20 phr S2+10 phr silica-4.164 s^{-1}- 120^0 C (r). 41.64 s^{-1} (s). 416.4 s^{-1} (t). 4.164 s^{-1}-150^{0}C (u). 160^{0}C (v). 170^{0}C

(w). SBR+20 phr S2+10 phr marble powder - 4.164 s^{-1}- 120^0 C (x). 41.64 s^{-1} (y). 416.4 s^{-1} (z). 4.164 s^{-1}-150^0 C

Figure 4.17. Extrudates of S2 prophylactics and particulates filled SBR compounds

The presence of marble powder at lower temperature and lower shear rate presents a lower extrudate distortion, as can be seen from **Figure 4.17 l-o**. The less sensitivity of dependence of elastic distortion on temperature is because of the interpenetration effect of silica in SBR/prophylactics system owing to its uniform distribution among the components. Han[50] and others[51-53] found that the black surface area and structure are responsible for the considerable extrudate distortion in polymer matrices. Since such a considerable reduction in the extrudate distortion could not be observed here (compared to silica), it means that in SBR/prophylactics system, black is unable to show its identity. Still, some reduction in extrudate distortion noted is due to the decrease in melt elasticity with the addition of black.

4.2. REFERENCES

1. R. Brezik, Int. Polym. Sci. Technol, 11(12), T / 76 (1984).
2. R.H. Norman and P.S.Johnson., Rubber Chem. Technol., 54(3), 493 (1981).
3. Yu. F. Shutilin, A.I. Omitrenkov, M.P. Parinova and V.S. Shein., Int.Polym. Sci. Technol., 15(9), T/24, (1988).
4. B.R. Gupta, Indian J. Nat. Rubber. Res, 2(2), 134 (1989).
5. Ibid, 2(1), 38 (1989).
6. K.Lakadawala and R. Salovey, Polym. Eng. Sci, 27(14), 1035 (1987).
7. B.K.Kim, H.M. Jeong and Y.H. Lee, J.Appl.Polym.Sci, 40, 1805 (1990).
8. K.T.Varughese, J.Appl.Polym.Sci, 39, 205 (1990).
9. R. Paladhi and R.P.Singh., Eur.Polym.J, 30(2),251 (1994).
10. H.Canshu, L.Jihong, W. Yinghan, C.Yongrong and W.Ling., Chinese.J.Polym.Sci, 14 (3), 225 (1996).
11. Y.Yongcheng, F.P.La Mantia, A.Valenza, V.Citta, U.Pedretti and A. Roggero., Eur.Polym.J., 27 (7), 723 (1991).
12. I.H.Do, L.K.Yoon, B.K.Kim and H.M. Jeong., Eur.Poly.J., 32 (12), 1387 (1996).
13. D. Abraham, K.E.George and D.J. Francis., Eur.Polym.J., 26 (2), 197 (1990)
14. P.Kurian, K.E.George and D.J. Francis., Eur.Polym.J., 28 (1), 113 (1992)
15. L.A. Utracki and M.R.Kamal., Polym.Eng.Sci., 26,96 (1982).
16. S.S.Bhagawan, D.K.Tripathy, S.K.De, S.K. Sharma and K.Ramamurthy., Polym.Eng.Sci., 28(10), 649 (1988).
17. M.I. Aranguren, E. Mora, C.W. Macosko and J. Saam, Rubber Chem. Technol., 67, 820 (1994).
18. L.L. Li and J.L.White, Rubber Chem. Technol., 69, 628 (1996).
19. A.E.Nesterov and Y.S. Lipatov., Polymer, 40,1347 (1999).
20. A.A.Phadke and B.Kuriakose., Kautsch Gummi. Kunstst, 38 (8), 694 (1985).
21. D.Ciesielska and P.Liu., Kautsch Gummi. Kunstst, 53 (5), 273 (2000).
22. S.G. Reena, R.Joseph, K.E.George and D.J. Francis, J.Elast.Plast, 27, 138 (1995)
23. W. Yong, W. Dacheng and L.I. Ruixia., Chinese J. Polym.Sci.,14(2), 99 (1996).

24. A. A.Phadke, S.K. Chakraborthy and S.K.De, Rubber Chem. Technol., 57, 19 (1984).

25. H. Munstedt, Polym.Eng. Sci, 5(21) 259 (1981).

26. M.J. Folkes , "Short Fibre Reinforced Thermoplastics", first edn., John Wiley, NY, Ch 6, 1982.

27. M.Mooney and W.E. Wolstenholme., J. Appl. Phys.25, 1098 (1954).

28. N.Nakajima and E.A.Collins, "Flow Behaviour of Raw Elastomers Containing Crosslinked Particles, J.Rheol., 22 (5) 547 (1978).

29. L.F.Ramos-De Valle and Aramburo., J.Rheol, 27, 295 (1983).

30. G.Angerer and D. Wolff, Rheol Acta., 15, 57 (1976).

31. G.Angerer., Rheol.Acta., 16, 444 (1977).

32. A.V.Shenoy., "Rheology of Filled Polymer Systems", Kluwer Academic Publishers, London, Ch.1, p.18, 1999.

33. B. Kuriakose and S.K.De., Polym.Eng. Sci, 25(10), 630 (1985).

34. A. Einstein, "Investigation on Theory of Brownian Motion", Dover, New York,1956 (English translation)

35. M. Mooney, J. Colloid. Sci., 6, 162 (1951).

36. E. Guth, J. Appl. Phys., 16, 20 (1945).

37. E.H. Kerner, Proc. Phys. Soc., 69B, 808 (1956).

38. L.E. Nielsen, J. Compos. Mater., 1, 100 (1967).

39. H. Eiler van Dyck, , Kolloid Z, 97, 313 (1941).

40. K.Bills, K. Sweeny and F. Salcedo, J.Appl.Polym.Sci, 12, 259 (1960).

41. N.Gambiroza, M. Hraste and J.M. Mencer, New Polym. Mater., 4(1), 13 (1993).

42. M. Narkis, Polym. Eng. Sci, 15, 316 (1975).

43. D.M.Turner and A.C. Bickley., Plast. Rubber.Process. Appln., 1(4), 357 (1981).

44. N. Minagawa and J.L.White., J.Appl.Polym.Sci., 20, 501 (1976).

45. J.L.White., Rubber Chem Technol., 50, 163 (1977).

46. B. Clarke., Trans.Instn. Chem.Engrs, 45, 251 (1967).

47. E.I.Shaheen.,Powder Tech., 5,245 (1971).

48. E.Sheng, I.Sutherland, R.H.Bradley and P.K. Freakley.,Eur.Polym.J.,32(1), 35 (1996)

49. C.S.L. Baker, I.R.Gelling, and R.Newell., Rubber Chem. Technol, 58, 67 (1985).

50. C.D.Han, J.Appl.Polym.Sci., 18, 821 (1974).

51. J.R.Hopper, Rubber Chem.Technol., 40, 463 (1967).

52. G.V. Vinogradov, A.Y.Malkin, E.P.Plotnikova, O.Y.Sabsai and N.E.Nikolayeva, Int.J.Polym.Mat., , 2,1 (1972).

53. J.L.White and Crowder., J.Appl.Polym.Sci, 18, 1013 (1974).

Chapter 5

CHAPTER 5

RECYCLING OF NATURAL RUBBER LATEX WASTE AND ITS INTERACTION IN EPOXIDISED NATURAL RUBBER

ABSTRACT

In this chapter, natural rubber prophylactics have been used as filler in a strain crystallising elastomer of relatively recent origin, ENR25. Discussions focus on the processing, mechanical and solvent swelling behaviour of gum and prophylactics filled epoxidised natural rubber compounds. Emphasis has been given to the loading of prophylactics filler of varying particle sizes, size 1, 2, 3, 4 and its mill-sheeted form. It has been observed that the rheometric processing characteristics such as minimum and maximum torque values generally increase with prophylactics loading in an irregular manner. The increase in the fastness of cure reaction with the loading of prophylactics has been found to be due to the presence of unreacted accelerator in the prophylactics rejects. Better tensile and tear properties have been exhibited by smaller size prophylactics fillers, especially size 1 at most of the loadings. Among the theoretical models used for the prediction of Young's modulus, Mooney and Guth equations have been found to be giving close values to that of experimentally observed values, mainly at higher loadings of 30 and 40 phr of prophylactics filler. Swelling studies, Kraus, Cunneem-Russell and Lorenz-Park equations and the scanning electron fractography of the samples have supported the comparatively better performance of size 1 prophylactics filler in epoxidised natural rubber vulcanisates. The appearance of prophylactics filler particles as phase separated entities classifies these filled systems as elastomer composites containing cross-linked rubber powder.

CHAPTER 5

RECYCLING OF NATURAL RUBBER LATEX WASTE AND ITS INTERACTION IN EPOXIDISED NATURAL RUBBER

Results of this chapter have been published in Polymer, 42, 2137, 2001.

The potential properties of an elastomer can be improved by the addition of certain fillers like silica, carbon black, mica[1,2] etc. As a result of severe energy crisis, and the need to reduce compound cost, the rubber product manufacturers are forced to increase the proportion of filler in the rubber compound. But this approach always resulted in a rubber compound with very high specific gravity[3]. In order to overcome this problem and also to make the rubber compound cheaper, new materials have been thought of to be used as fillers.

Just like waste plastic, waste rubber also is becoming a worldwide problem. The disposal/utilisation of tires, whose life span has ended, is a great economic and ecological problem. The earlier approach to this problem was to reclaim[4] (remove the crosslinks) the rubber rejects and then use it as a new rubber. But the use of reclaimed rubber was limited due to its inferior properties.

Now-a-days researchers pay more attention to scrap latex rejects compared to reclaimed rubber. This is because of the lightly crosslinked and high quality nature of the rubber obtainable from latex rejects. Moreover these rejects are available in huge quantities. The two main reasons for this surplus nature are the unstable nature of the latex and the strict specifications in the quality of latex products. So these scrap latex rejects are now considered as the best potential candidate for recycling. Many reviews regarding the disposal problem of rubber rejects and possible solutions are available from the literature[5-8]. The recycling of microcellular polyurethane elastomer waste,[9] the development of blends from recycled rubber and thermoplastics[10,11] and the thermochemical processing of rubber waste to liquid fuel[12] are some of the interesting works in connection with polymer recycling.

In this chapter, we evaluated the use of powdered NR prophylactics rejects as filler in ENR-25. The influence of filler loading on the curing characteristics is discussed. Also the effect of both particle size and loading of the filler on the mechanical properties, swelling and failure behaviour are compared and presented. The dependence of filler-ENR matrix adhesion on the particle size of the filler also is examined. Theoretical models were used to fit the experimental tensile modulus values. The filler particle morphology and and filler-matrix adhesion were analysed using scanning electron microscopy.

5.1. Results and discussions

The basic formulation used is given in **Table 5.1**.

Table 5.1. Basic formulation

Material	Control (phr)
ENR-25	100
Zinc oxide	5
Stearic acid	2
CBS	0.6
Sulfur	2.5
Calcium stearate	1
NR prophylactics filler	Variable (0,10,20,30,40)

5.1.1. Processing characteristics and cure kinetics

The rheometric processing and cure characteristics of the compounds **(Table 5.2)** can be studied from the rheographs **(Figure 5.1)**. The finest size filler (size 1) was selected for the determination of processing/curing characteristics. The minimum torque values denoted by M_n first register an increase with increasing filler content but later they decrease at 40 phr prophylactics loading **(Table 5.2)**. The initial increase is due to the presence of crosslinked prophylactics particles in epoxidised natural rubber and the decrease at 40 phr loading may be due to the higher extent of mastication during mixing. It is already found that the presence of particulate inclusions increases the maximum torque (M_h). But in our case, where the inclusion itself is a rubber, the variation may be due to

combined effects of crosslink density variation and presence of crosslinked particles. At 10 phr loading, presence of crosslinked particles increases M_h, but at later stages of loading, it decreases.

Table 5.2.Processing and curing characteristics

Loading (phr)	Minimum torque (M_l) (dN-m)	Maximum torque (M_h) (dN-m)	Cure rate index (CRI) (min^{-1})	Cure rate constant (k) (min^{-1})
0	3	35	12.5 SD 0.82	0.266 SD 0.003
10	4	44	33.3	0.631
20	4.5	44	33.3	0.675
30	6	43	36.4 SD 2.45	0.810 SD 0.02
40	4	42	32.1 SD 3.27	0.800 SD 0.02

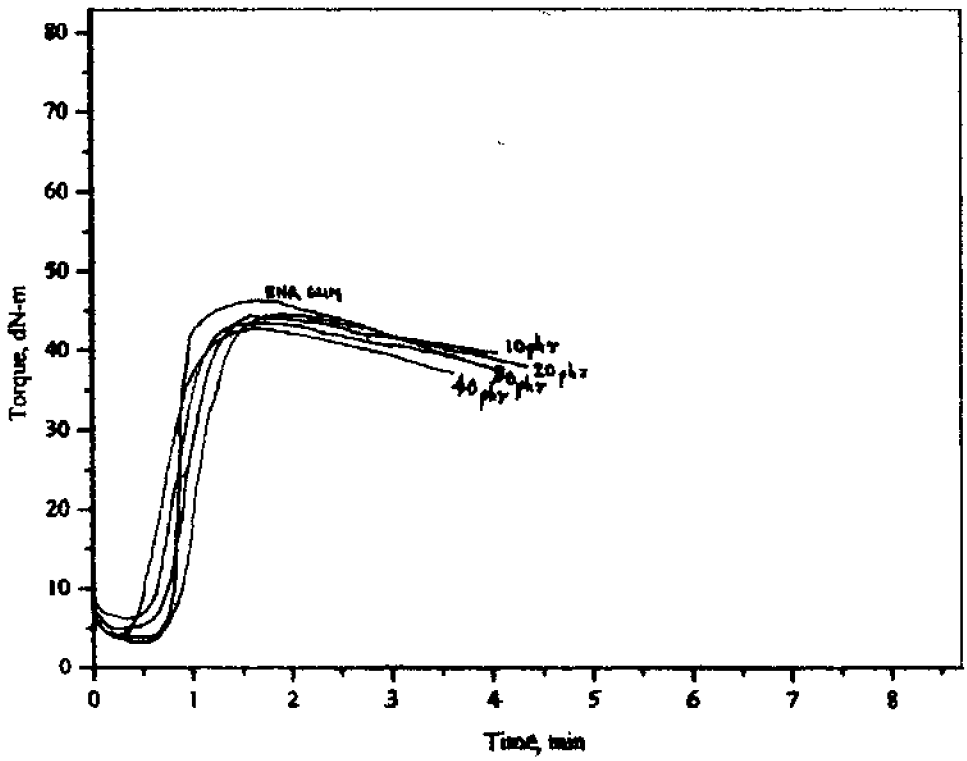

Figure 5.1. Rheographs of the ENR compounds

As the filler content increases, the optimum cure time, t_{90} (time needed for the formation of 90% crosslinks), scorch time t_2 (premature vulcanisation time) and induction time t_1 (time to start vulcanisation process) are found to be decreasing. These results are presented in **Figure 5.2**. This is due to the presence of unreacted accelerator in the prophylactics rejects. Its presence was confirmed by the studies given in chapter 3. The rubber compound contains the accelerator CBS (N-cyclohexyl benzthiazyl sulfenamide) added in the formulation **(Table 5.1)** and prophylactics rejects contain the unreacted accelerator, mainly ZDEC. As a result of the combined accelerating effect, the three parameters namely t_{90}, t_2 and t_1 decrease with loading of prophylactics filler.

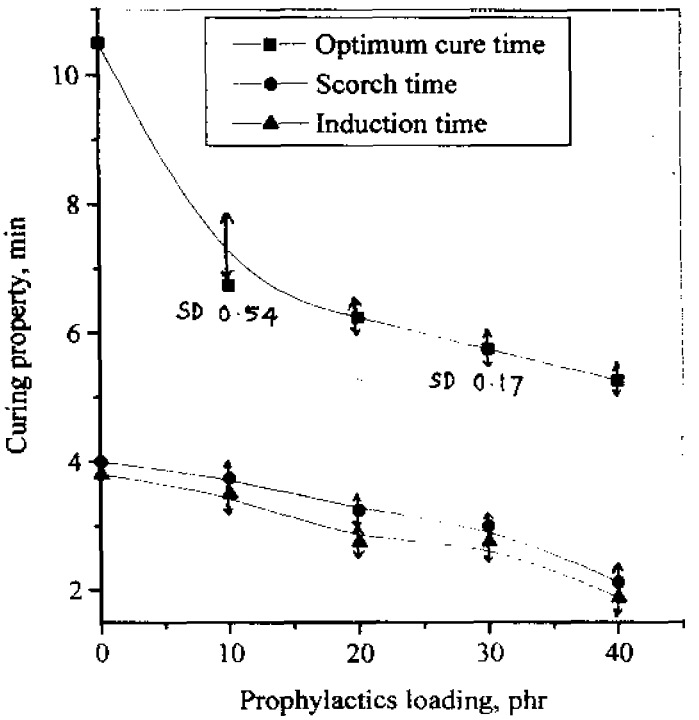

Figure 5.2. Effect of filler loading on curing characteristics

The increase in speed of the curing reaction with filler loading can be analysed systematically, by calculating two parameters namely, the cure rate index (CRI) and reaction rate constant (k). Their details are given in chapter 2 (equations 2.2 and 2.6).

The plots of ln (M_h-M_t) versus time 't' are presented in **Figure 5.3**.

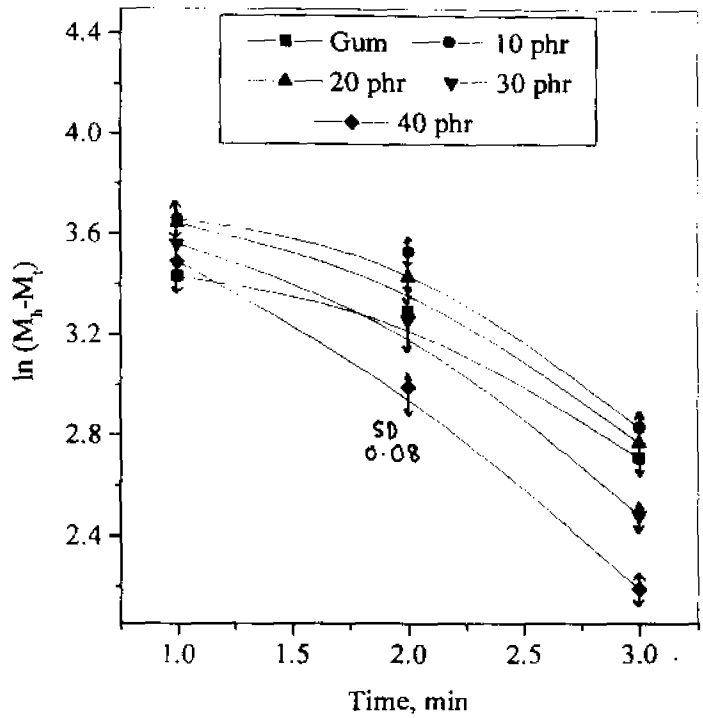

Figure 5.3. Plots of ln (M_h-Mt) vs. time t

Even though linearity is claimed for the plots theoretically, deviations from linearity are experimentally observed for certain points. The slope of the respective straight lines gives the cure reaction rate constant (k) and is presented in **Table 5.2**. It is clear from the **Table 5.2** that, both CRI and k values show an increase upto 30 phr prophylactics waste loading and later they decrease at 40 phr loading. The initial increase is again, due to the presence of unreacted accelerator in the prophylactics waste. This cure activating nature of prophylactics filler is an advantage, since a faster curing sample will have a high production rate. However this cure activation is found to be leveling off at higher loadings of prophylactics waste. Since the filled ENR compound in more stiff and non-tacky, the compound is easy to be handled for further processing. On the other hand, the unfilled ENR is very tacky which is difficult to handle.

5.1.2. Mechanical properties

The mechanical properties of elastomers filled with powdered rubber depend on many factors.

i) Strain crystallising nature of the filler

ii) Adhesion[13] of the filler with matrix

iii) Particle size of the filler

iv) Extent of sulfur migration[14] from matrix to filler phase which is controlled by many factors.

As the prophylactics filler content increases, the tensile strength **(Figure 5.4)** increases dramatically and reaches a maximum value at 30 phr loading.

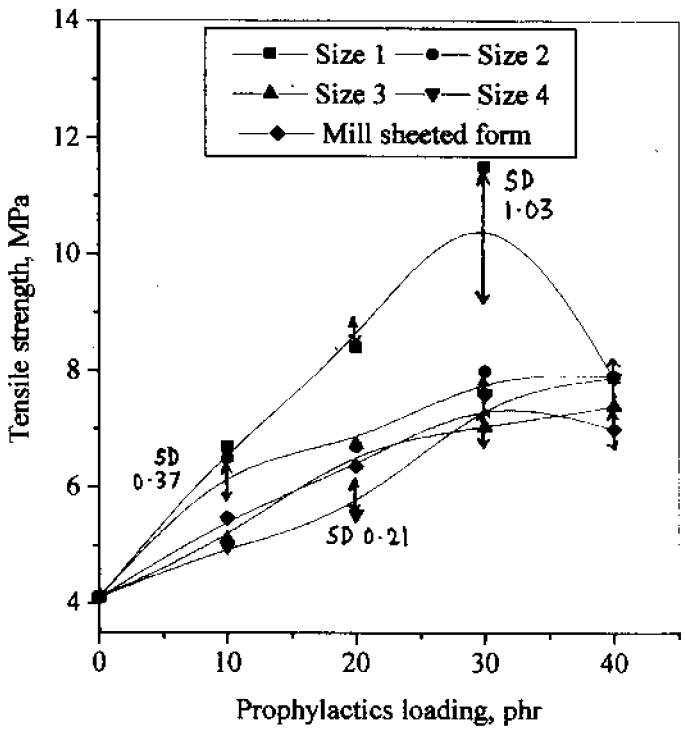

Figure 5.4. Effect of filler loading and size on the tensile strength of ENR

Beyond 30 phr loading, the tensile strength values show a decrease or leveling off behaviour. For size 1, the increase is about 300%. The increase in tensile strength is due to the strain crystallising nature of NR prophylactics filler particles. The threshold value of strain required for strain crystallisation of natural rubber (NR) is 250-300 percent. Since

the filler particle is very small, it will cover this value even at the initial stages of extension. The increase in tensile strength with loading confirms the fact that NR retains its strain crystallising nature, even if it is in the form of fine filler. Lewis and Nielsen[15] postulated that as the particle size of a particulate filler decreases, the contact surface area increases which provides a more efficient interfacial bond leading to better properties.

The tear strength of gum and filled ENR samples are presented in **Figure 5.5.** With increase in loading of the filler, there is slight improvement in the tear strength of the samples upto 30 phr loading. This increase is because of the restriction in the advancement of tear front. This restriction is caused by the elongation of filler particles in the tear path. The performance of size 1 filler is superior here. However at 40 phr loading, the value either drops or levels off for large filler sizes.

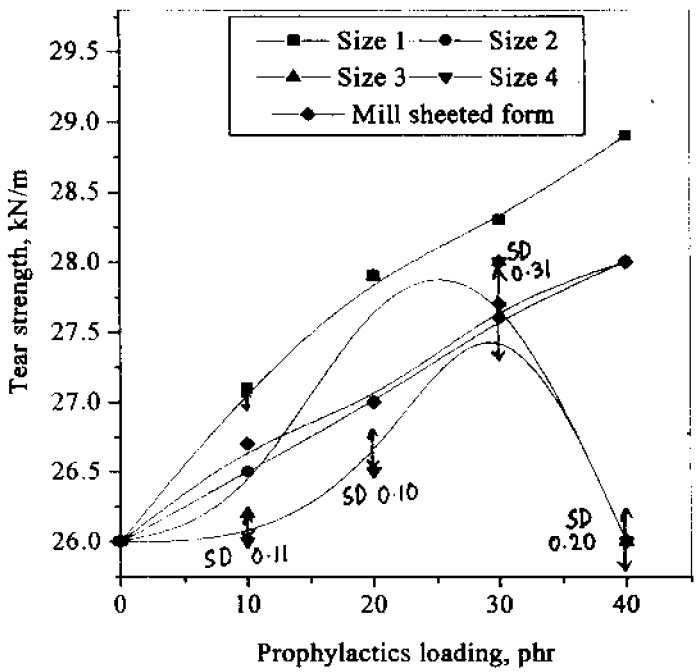

Figure 5.5. Effect of filler loading and size on the tear strength of ENR vulcanisates.

5.1.3. Theoretical modeling of Young's modulus

The Young's modulus of particulate filled composites can be predicted by using several theoretical models. Even though a large number of theoretical equations are generally available for composite materials, only few of them are specially formulated for composites with non-rigid matrices. These include Einstein, Mooney and Guth models.

Einstein equation and its modifications are usually applied to predict the modulus of the composites containing rigid fillers such as black and silica. Here these theories are applied to systems with nonrigid fillers such as prophylactics particles, which undergo strain crystallisation on stretching

The simplest theoretical equation for the reinforcement of a material due to a particulate filler is given by Einstein[16]. The equation is

$$M_c = M_m (1+2.5\ V_f) \qquad (5.1)$$

where

M_c = Young's modulus of the composite,

M_m = Young's modulus of the matrix and

V_f = Volume fraction of the filler.

The Young's modulus values of all the four particle sizes and mill sheeted form of the prophylactics waste filler are correlated with Einstein model in **Figures 5.6.**

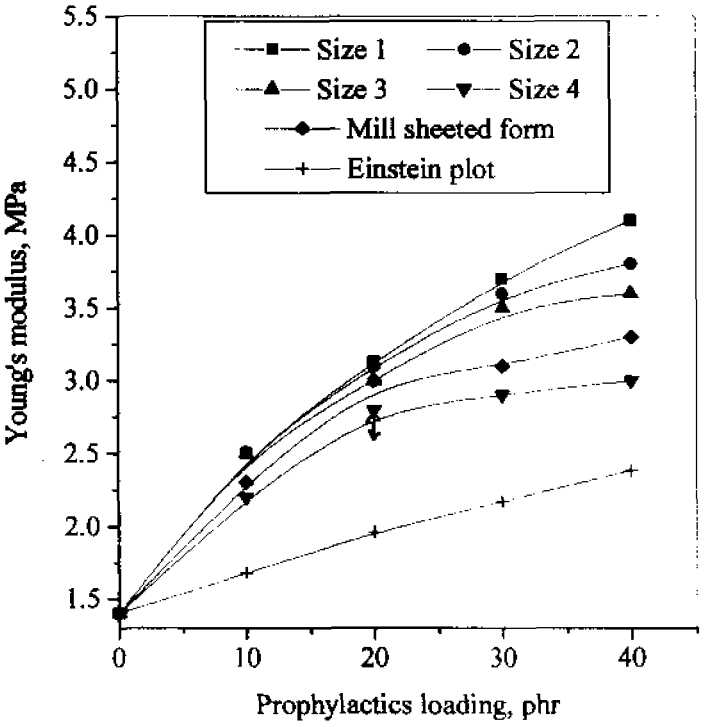

Figure 5.6. Comparison of the experimental data with Einstein's model

Figure 5.6 represents a system, where finest filler (size 1) is most reinforcing. Therefore it presents a plot which is far above that given by Einstein equation. It is a general observation from the figure that, only large size fillers such as size 3 and 4 are found to be giving close values to that of Einstein. With increasing loading of fillers, the deviation shown by finer size fillers such as size 1 and 2 goes on increasing, while that of large size fillers (size 3 and 4) decreases. The behaviour shown by mill sheeted form (M) is in between finer and large sized fillers.

The observed deviations from the model are due to the following reasons.

(1) Einstein model assumes that the stiffening action of a filler is independent of its size while it is already established by many workers[17] and also by our studies in chapter 3 that reinforcement of matrix by filler, changes with its particle size. Since this effect is not accounted by the model, the experimental values for different size grades deviate differently from the model.

(2) The model assumes that the filler particles are spherical in shape and there is perfect adhesion between the filler and matrix. It is clear from the SEM photos of filler particles given in chapter 3 that the filler particles have non-uniform size distributions and shape. Also we have noted from the scanning electron micrographs (see later) that the filler particles are not firmly bonded to the matrix. The presence of an air pocket over the filler particles has already been confirmed by the work of Phadke[18] et al. Therefore the imperfect adhesion between filler and matrix also contributes to the observed deviations from the model.

(3) It is stated by Mooney[19] that Einstein equation is valid only for low concentrations of filler. This is because at higher filler loading, the strain fields around filler particles can interact causing deviations from the model.

(4) The final and most important reason for the deviation may be the less rigidity of the filler compared to the normal particulate fillers such as carbon black or silica. Since it is assumed in Einstein model that the filler is much more rigid than the matrix, this factor may be causing a number of secondary reasons for deviations from the model. But it is already proved by Smallwood in the literature[20] that Einstein equation is more useful for predicting the elastic behaviour of rubbers

containing non or less reinforcing fillers. The correlation, even though less, between experimental and theoretical values observed in our case again proves this fact.

The Mooney equation[19] is given as;

$$M_c = M_m \exp \{ 2.5 V_f / 1 - S V_f \} \quad (5.2)$$

where M_c, M_m & V_f are the same, explained earlier

The term, 'S' is the crowding factor or relative sedimentation volume of the filler, which accounts for the agglomeration of filler particles. Agglomerates of filler particles tend to contain voids or air spaces so that their apparent volume will be higher than the true volume.

'S' is defined as the ratio of apparent volume occupied by the filler to true volume of the filler.

According to Mooney[19], the minimum possible value that 'S' can have is unity while its experimental value ranges from 1.2 to 2. However it has been reported[21] that upto V_f =0.5, a value of 1.4 (or1.35) can fit the best experimental values. For our system we have made our calculations using two values of 'S', 1.35 and 1.

Figure 5.7 is the Mooney model fitting curves of different size grades of prophylactics waste filler. When the value of S is 1.35, size 4 filler gives comparatively closer values with that given by equation at 10 & 20 phr loading. But as the loading increases to 30 phr, better value is shown by the mill-sheeted form while size 4 filler is below that of the model. All other filler sizes such as 1,2 and 3, deviate much from the model mainly at lower loadings. As the filler loading increases to 40 phr, the model plot shoots up and therefore closer values are shown by finer filler sizes1, 2 and 3. Size 4 and mill-sheeted forms lie much below that of the model at highest loading. When the value of 'S' is 1,the size 4 filler gives better agreement mainly at 30 phr loading and sizes 2 and 3, at 40 phr loading. Large size fillers size 3, 4 and mill-sheeted form are below that of Mooney model while finer sizes 1 and 2 are above. The general nature of Mooney equation, i.e., a modulus value which tends to infinity at higher filler loadings, which is previously reported[19-21], is observable here also. The above observed fitting of theoretical values, even though partial, may be due to the fulfilment of some of the assumptions connected

with Mooney model, such as Poisson's ratio of matrix must be 0.5 etc. This model also assumes that filler particles are uniformly distributed spheres with good adhesion to matrix and modulus of the filler is greater than that of matrix.

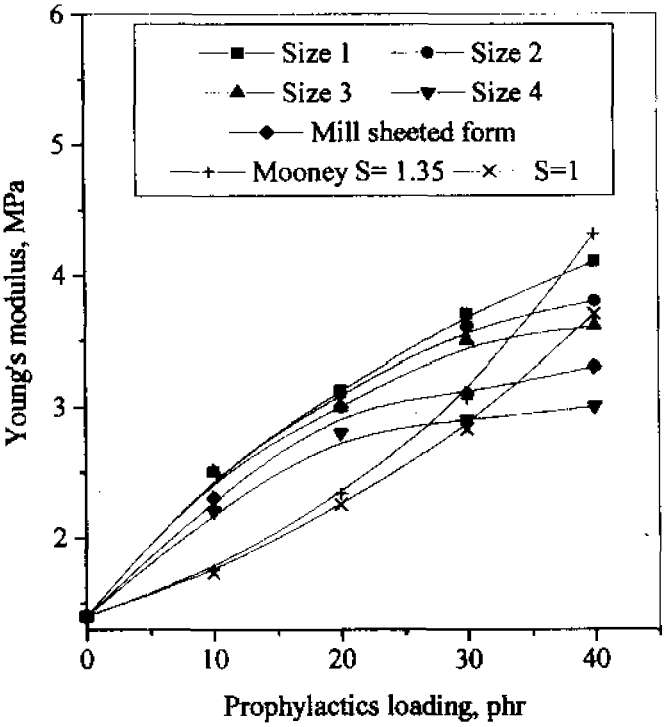

Figure 5.7. Comparison of the experimental data with Mooney model

Guth and Smallwood[22] equation can be written as;

$$M_c = M_m (1 + 2.5\ V_f + 14.1\ V_f^{\ 2}) \qquad (5.3)$$

where M_c , M_m & V_f are the same explained earlier

Guth model gives similar values as given by large size fillers (size 4) and mill sheeted form at 10 and 20 phr. This is clear from **Figure 5.8**. Size 1 and 2 plots, owing to their superior reinforcing behaviour, lie above the model at 30 phr loading. But at 40 phr filler content, modulus values slightly bend towards 'x' axis and lie equidistant from the model. Such a bending is observed for size 4 and mill sheeted form also. Since the model does not account for the agglomeration effects at higher loadings, the theoretical curve tends to infinite position, as in the case of Mooney equation.

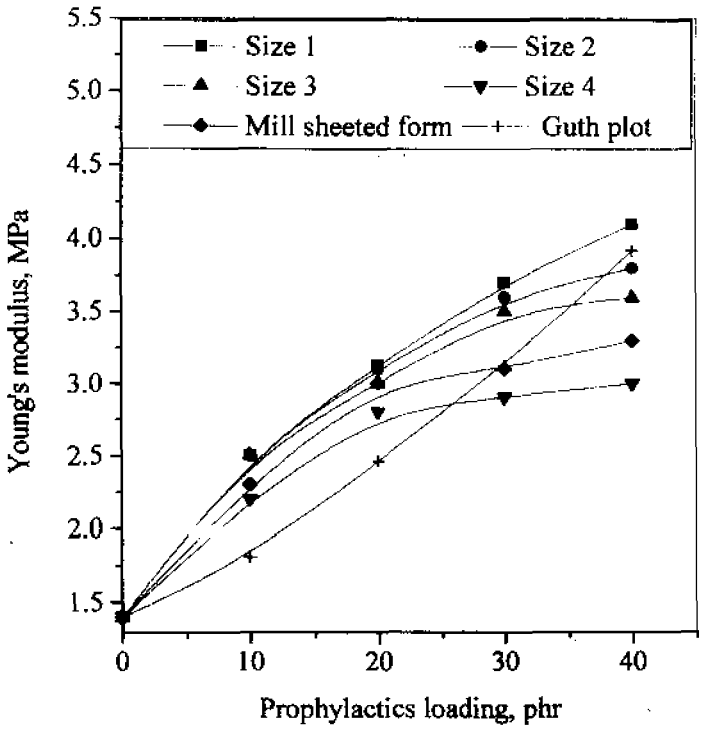

Figure 5.8. Comparison of the experimental data with Guth model

The model assumes that the change in elastic constant of the rubber by embedded spheres is entirely analogous to the theory of viscosity. For example, when a particulate filled suspension undergoes stretching, the suspended particles perturb the stresses and strains are set up in the body, which lead to an increase elastic energy and elastic constants. But for this to happen, filler particles must be spherical and rigid. Here, even though size 3 & 4 assumes somewhat spherical shape, their non-rigid nature violates the assumption. Therefore they deviate from the model.

5.1.4. Solvent transport studies and crosslink density determination

Swelling index value, which is a measure of the swelling resistance of the rubber vulcanisate is calculated as described in chapter 2. It is already reported in the literature[23,24] that in the case of various polymer solvent systems, differences in the solubility parameter (and hence interaction parameter) values can be used to characterise the sorption behaviour of the solvent. But our analysis proves that such a correlation is

ineffective since the diffusion behaviour of elastomer filled elastomer systems is more dependent on the compact nature of the sample. This fact is strongly supported by the literature[25]. Since the compact nature of the ENR sample decreases with the addition of prophylactics, the diffusion of the solvent through the sample also increases. It is also reported in the literature[26] that the diffusion mechanism in rubbery polymers is essentially connected with the ability of the polymer to continually provide opportunities for the solvent to progress in the form of randomly generated voids. Since ease for void generation in the sample increases with the addition of prophylactics, the uptake of the solvent also increases. Therefore as the filler content increases, the swelling index value increases for all size grades **(Table 5.3)**. This is due to the poor solvent resistance of prophylactics compared to ENR. The solvent absorption by the latex filler particles is found to be minimum for size 1 filler. This again confirms that in ENR matrix, size 1 filler shows good adhesion.

Table 5.3. Percentage swelling index values

Prophylactics Loading, phr	**Gum**	**Size 1**	**Size 2**	**Size 3**	**Size 4**	**M**
0	408 SD 1.43					
10		411	416	422	428	430
20		417	421	427	430	436
30		420	425	429	435	441
40		424	429	436	439	454

This behaviour is supported by the crosslinked density values **(Figure 5.9)**. As the filler content increases, the crosslink density values are found to decrease. It is to be noted that, the crosslink density decrease is minimum for finer filler size 1 and 2 which have comparatively more reinforcing action in ENR. So the crosslink density values presented here has good correlation with filler-matrix adhesion.

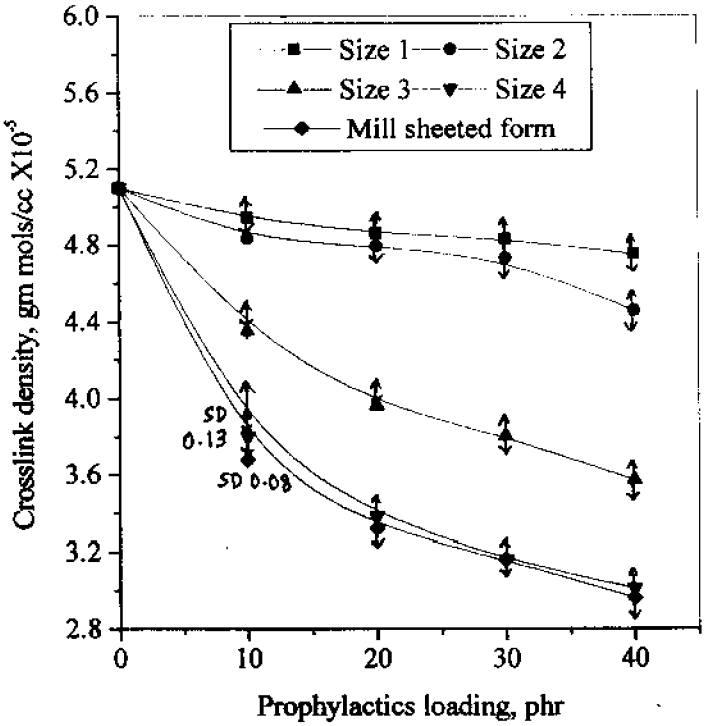

Figure 5.9. Effect of filler loading and size on the crosslink density of ENR vulcanisates

5.1.5. Extent of reinforcement

The extent of filler reinforcement can be analyzed by using Kraus[27], Cunneen and Russell[28] and Lorenz-Park[29] equations (chapter 2, equations 2.23, 2.25 and 2.26) The Kraus plots obtained are given in **Figure 5.10** and the slope values are presented in **Table 5.4**. According to the theory by Kraus, reinforcing filler such as carbon black will have a negative higher slope. For the present case, we observed that as the filler loading increases, the solvent uptake of the sample also increases. This will cause a reduction in V_{r_f} values, which will increase the ratio V_{r_0} / V_{r_f}, since V_{r_0} is constant. This behaviour leads to a positive slope in every case. Since size 1 filler exhibits minimum positive value of Kraus slope, it is clear that its solvent absorption is minimum thereby supporting its better adhesion with ENR matrix.

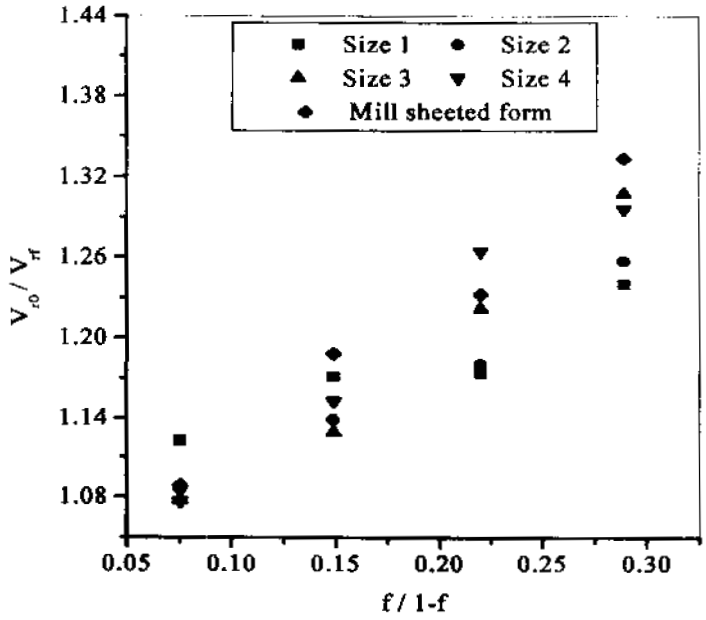

Figure 5.10. Variation of V_{ro} / V_{rf} as a function of filler loading (Kraus plots)

The Cunneen - Russell plots are given in **Figure 5.11.**

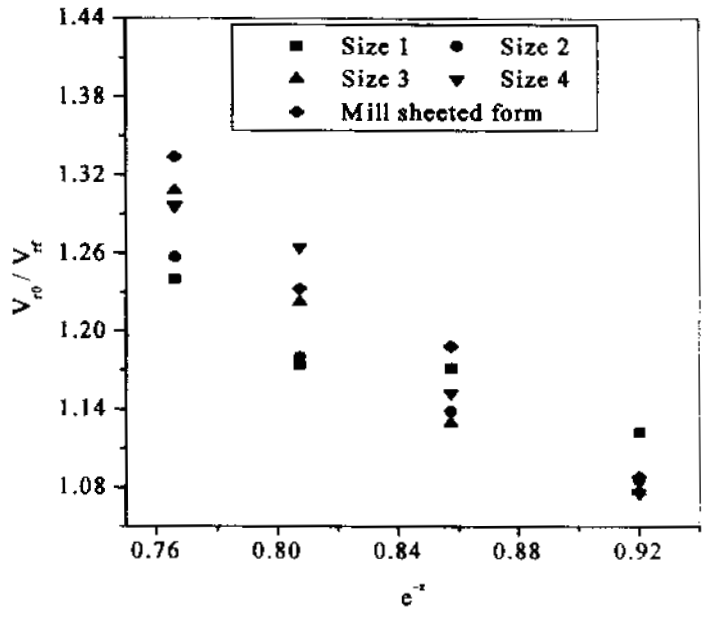

Figure 5.11. Variation of V_{ro}/V_{rf} as a function of filler loading (Cunneen-Russell plots)

V_{r_0}/V_{rf} is found to be increasing withincreasing filler loading. This increase is extensive in the case of large size fillers (size 4 & M). For finer fillers, size 1 and 2, which are comparatively highly reinforcing, the absorption of solvent is minimum, which results in a lower V_{r_0} / V_{rf} ratio and a smaller negative slope. The Lorenz-Park plots are given in **Figure 5.12**. As explained earlier, here also finer fillers (size 1 & 2) exhibit lower slope, proving their better adhesion with ENR.

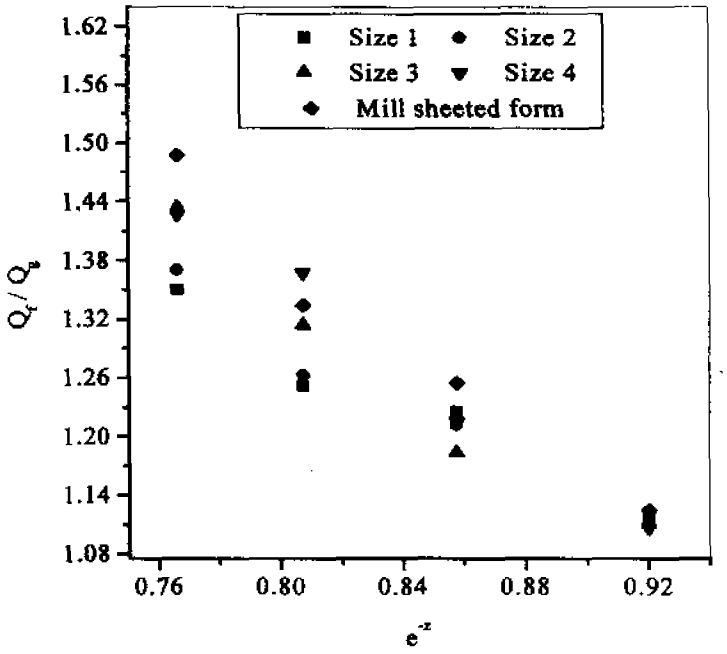

Figure 5.12. Variation of Q_f / Q_g as a function of filler loading (Lorenz - Park plots)

Above equations support the superior performance of size 1 filler.

Table 5.4. Values of slope

Particle Size	Kraus Equation	Cunneen-Russell Equation	Lorenz-Park equation
	Slope, 'm'	slope 'a'	slope 'a'
S1	0.4961	-0.6790	-1.3979
S2	0.7789	-1.0532	-1.5344
S3	1.0979	-1.5003	-2.1026
S4	1.0833	-1.5067	-2.1725
M	1.0956	-1.5107	-2.2144

5.1.6. Fractographic analysis

The improvement in tensile and tear performance with loading of filler is supported by the morphology of the fractured surfaces. These fractographs are presented in **Figures 5.13-5.17**. Since the presence of filler particles is clearly visible in all the filled cases, this latex filled ENR systems can be considered only as a composite material. All the composite samples exhibit a two-phase morphology.

In the case of ENR filled with 10 phr of size 1 filler, the tensile fractography reveals the presence of fine filler particles **(Figure 5.13a)**.

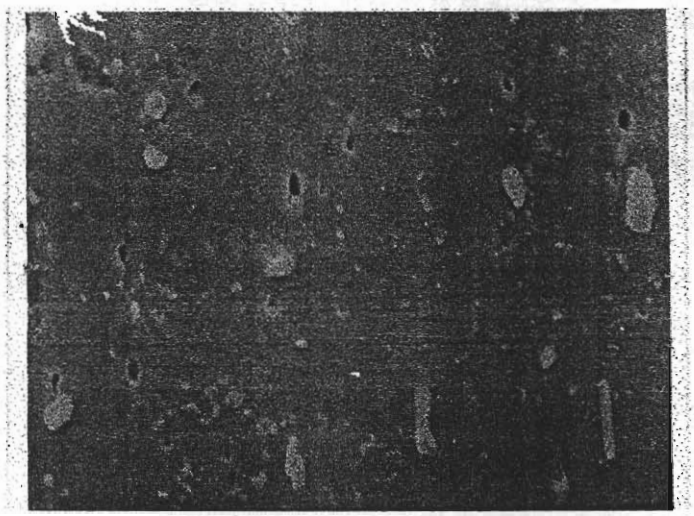

Figure 5.13a. SEM fractograph of tensile specimen filled with 10phr of size 1 filler, Mag X 2000

The presence of cigar shaped particles aligned in a particular direction also is observable. Moreover the fracture is found to be deviating only slightly **(Figure 5.13b)** presenting incomplete parabolic patterns. This confirms the comparatively low strength of the material. The presence of de-wetting also is visible in **Figure 5.13a**. **Figure 5.14** is the tensile fractured surface of ENR sample filled with 30 phr of size 1 filler. Here the cracks are extensive and much deviated.

Figure 5.13b. SEM fractograph of tensile specimen filled with 10phr of size 1 filler, Mag X 600

Such parabolic fractured surfaces support the high strength of the material. The role of filler particles in blocking the advancing crack also is observable.

Figure 5.14. SEM fractograph of tensile specimen filled with 30 phr of size 1 filler, Mag X 600

The torn surface of ENR filled with 40 phr size 1 filler is presented in **Figure 5.15a** and **b**. Here also crack deviation is extensive. The portions from which the filler particles are debonded are visible as holes in the figure. The filler particles elongate to high strains and

obstruct the tear **(Figure 5.15b)**. Thus, as explained above, the material filled with size 1 filler shows superior tear performance.

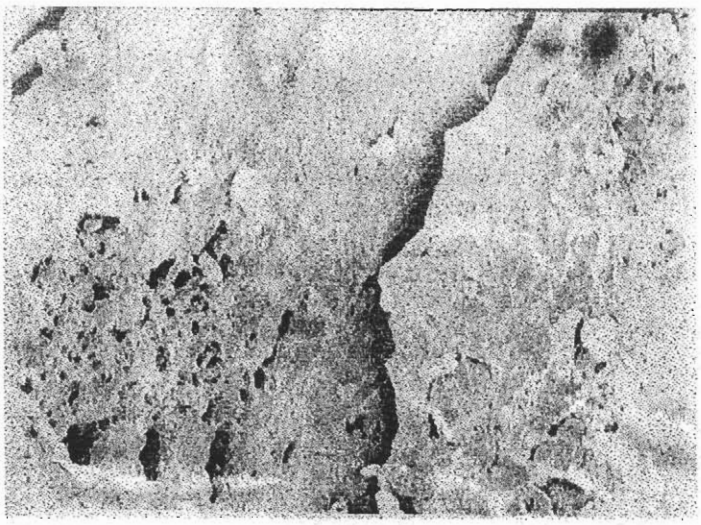

Figure 5.15a. SEM fractograph of tear specimen filled with 40phr size 1 filler, Mag X 200

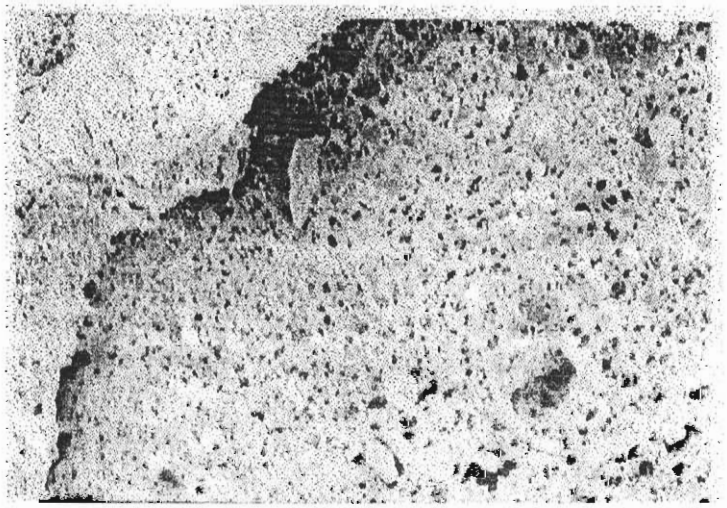

Figure 5.15b SEM fractograph of tear specimen filled with 40phr size 1 filler, Mag X 200

For fillers of higher sizes (size 4) at a loading of 10 phr, debonding is extensive. Also the

cracks are again becoming smooth. De-wetting is clear from the **Figures 5.16 a** and **b** and smooth fractures are visible in **Figures 5.16 b** and **c**. It can be seen from **Figure 5.16c** that the particle size of fillers is not uniform. This is because large size fillers undergo more size reduction during mixing.

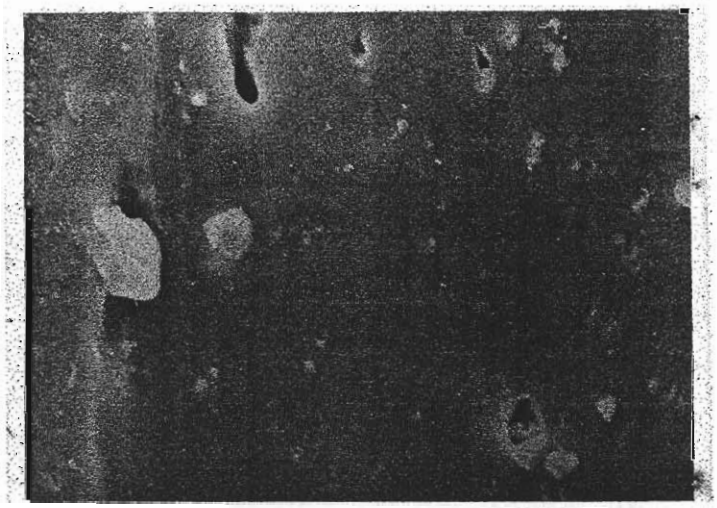

Figure 5.16a SEM fractograph of tensile specimen filled with 10phr size 4 filler, Mag X 600

Figure 5.16b SEM fractograph of tensile specimen filled with 10phr size 4 filler, Mag X 600

Figure 5.17 is the torn surface of ENR filled with 30 phr size 4 filler. The material shows cracks with slight deviations, which proves its good tear strength. The accumulation of filler particles on the crack path in an effort to prevent the advancing crack is visible in the figure. It is a general observation in **Figures 5.16c** and **Figure 5.17** that the larger size grade (size 4) filler particles are polydispersed in size due to their breakage during mixing.

Figure 5.16c SEM fractograph of tensile specimen filled with 10phr size4 filler, Mag X 600

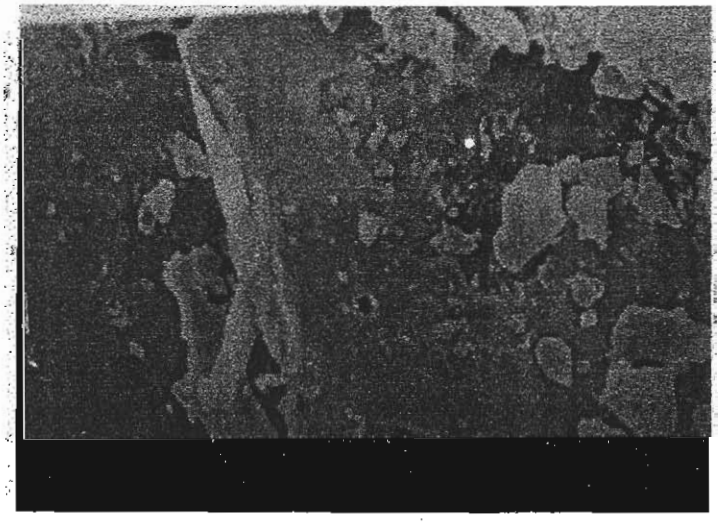

Figure 5.17 SEM fractograph of tear specimen filled with 30phr size 4 filler. , Mag X 600

For most of the filled cases, the fractured surfaces are much crack deviated and present a series of parabolic lines distributed all over the surfaces. Such a behaviour is due to the interaction of main fracture fronts with subsidiary fracture fronts and from the resistance in tear propagation by filler particles. Thus the superior mechanical performance of size 1 filler is strongly supported by the SEM fractographic studies.

5.2REFERENCES

1. S. Debnath, S. K. De and D. Khastgir,. J. Appl. Polym. Sci., 37, 1449 (1989).
2. S. Debnath, S. K. De, and D. Khastgir, J. Mater. Sci., 22, 4453 (1987).
3. R.A Swor, L.W. Jensen and M.Budzol, Rubber Chem. Technol, 53, 1215 (1980).
4. A.A. Phadke, A. K. Bhattacharya, S.K. Chakraborthy and S.K. De, Rubber Chem. Technol, 56, 726 (1983).
5. A.A. Phadke, S.K. Chakraborthy and S.K. De, Rubber Chem. Technol., 57, 19 (1984).
6. A. A. Phadke and B. Kuriakose, Kautsch. Gummi Kunstst., 38, 694 (1985).
7. N.M.Claramma, K.T. Thomas, and E. V. Thomas, Paper presented at the Rubber. Conf., Jamshedpur, Nov. 6-8, 1986.
8. Y. Aziz, Paper presented at Polymer 90, Kuala Lumpur, Malaysia, Sept. 23, 1990.
9. M.Modesti, F.Simioni and S.A.Rienzi., J.Elast.Plast, 24,288 (1992).
10. H.Michael, H. Scholz and G.Mennig., Kautsch Gummi.Kunstst, 52 (7-8), 510 (1999).
11. P.K.Pramanik and W.E.Baker., 27,253 (1995).
12. Md.J.Kawser and N.A.Farid, Plast.Rubb.Compos., 29(2), 100 (2000).
13. C. R. G.Furtado, R. C. R. Nunes and A. S. De Siqueira Filho., Eur. Polym. J., 30 (10), 1151 (1994).
14. K. Fujimoto, T. Nishi and T. Okamoto., Int. Polym. Sci. Technol., 8(8), T/30 (1981).
15. Lewis and L. E. Nielsen, J. Appl. Polym. Sci., 14, 1449 (1970).
16. A. Einstein, " Investigation on theory of Brownian motion " (Dover, New York, (1956) [English Translation]
17. D. C. Edwards, J. Mater. Sci., 25, 4175 (1990).
18. A. A. Phadke, A. K Bhowmick and S. K. De, Rubber Chem. Technol., 58, 4063 (1985).
19. M. Mooney, J.Colloid. Sci., 6, 162 (1951).
20. A.R. Payne, "Reinforcement of Elastomers", Krause, G. Ed., Wiley- Interscience, NY, 76, 1965.
21. L. E. Nielsen, J. Compos.Mater., 1, 100 (1967).
22. E. Guth, J. Appl. Phys., 16, 21 (1951).
23. T. Uragami, T. Morikawa and H. Okuno, Polymer., 30,1117 (1989)

24. H. Okuno, H. Nishimoto, T. Miyata and T.Uragami, Makromol Chem., 194, 927 (1993).

25. J.I.W. Rhim, S. Yoon, S.W. Kim, and K.H. Lee, J.Appl.Polym.Sci., 63, 521 (1997).

26. G.J.V. Amerongen, Rubber Chem.Technol., 37,1065 (1964).

27. G. Kraus, J. Appl. Polym. Sci., 7, 861 (1963).

28. J. I. Cunneen and R.M. Russell., Rubber Chem. Technol., 43, 1215 (1970).

29. O. Lorenz and C. R. Parks, Rubber Chem. Technol., 50, 299 (1961).

Chapter 6

CHAPTER 6

INTERACTION OF SELECTED PARTICULATE FILLERS WITH ENR-50 / NATURAL RUBBER PROPHYLACTICS WASTE SYSTEMS

ABSTRACT

The chapter discusses the processing aspects, mechanical and dynamic mechanical analysis of epoxidised natural rubber, ENR 50 containing prophylactics and particulate fillers. Size 2 fraction of prophylactics filler has been used for this study. Particulate fillers used are carbon black (HAF), silica and marble powder. It has been observed that the variation of minimum rheometric torque with the loading of prophylactics and particulate fillers is dependent on the composition of the system. Among the particulate fillers, only black has been found to be increasing the minimum torque in ENR/40 phr prophylactics system. When the presence of carbon black and silica increase the maximum rheometric torque values, marble powder shows a reduction. Reduction in the optimum cure time has been noted with the loading of prophylactics while the presence of particulate fillers further decrease the values. The speed of the vulcanisation reaction also has been increased with prophylactics and particulate fillers in most of the cases. Improvement in mechanical properties with the loading of prophylactics and particulate fillers has been evidenced by the increase in tensile and tear strengths. Addition of prophylactics filler to epoxidised natural rubber has been found to be increasing the glass transition temperature of epoxidised natural rubber while the presence of carbon black and silica increases it further. At highest frequency of 100 Hz, a reduction in the damping maximum of epoxidised natural rubber and natural rubber prophylactics with prophylactics and particulate filler loading has been noted. This indicates an improvement in the hysterisis of the system. Comparatively high concentration of particulate filler in the prophylactics phase has been noted from the analysis of filler distribution by damping maximum values. The crosslink densities obtained from dynamic mechanical data as well as swelling studies at room temperature are in agreement with

observed tensile strength values. The energy of activation for glass transition of the samples has been decreased with the addition of particulate fillers but the values show an increase with the loading of prophylactics filler in the presence of particulate filler.

CHAPTER 6

INTERACTION OF SELECTED PARTICULATE FILLERS WITH ENR-50 / NATURAL RUBBER PROPHYLACTICS WASTE SYSTEMS

Results of this chapter have been communicated to

1. J. Mater. Sci, 2. J. Polym. Recycl. and 3. Rubber Chem. Technol.

The solid waste management is becoming increasingly difficult as traditional landfills are becoming scarce. The ever-increasing volume of polymer waste is a severe problem deserving serious attention.[1-4] Of this polymer waste, only 8-12 % is plastic while the rest lion share is elastomer wastes.[5-7]

In addressing this issue, several scientists have carried out extensive investigation based on ground tire. Rajalingam et al.[8], focusing the effect of particle size, studied ground tire/thermoplastic composites and chemical modification[9] of the powdered tire rejects. Gibala and Hamed[10] investigated the influence of ground vulcanisates in styrene butadiene rubber (SBR) crosslinked with sulphur and dicumyl peroxide (DCP). They reported that for sulphur crosslinked system, the scorch time of SBR was affected while for peroxide crosslinked samples, scorch time remained unaffected. Gawel and Slusarski[11] analysed the use of recycled tire rubber for the modification of asphalt. They identified that the high initial costs of pavement made with asphalt-rubber binder can be compensated by their greater durability and the possibility of using thinner layers. Investigation on the development of natural rubber/cryoground polyurethane foam particles focusing the rheology[12] and the environmental effects in light-fill applications[13] also deserve much importance.

The present chapter deals with the interaction of selected particulate fillers such as carbon black, silica and marble powder in ENR-50/prophylactics waste systems. The influence of these fillers on the rheometric processing, curing, mechanical and dynamic mechanical analysis of the samples has been described.

6.1. Results and discussions

The basic formulation used for the study is given in **Table 6.1**.

Table 6.1. Basic formulation

Materials	Control (phr)								
	G1	G2	G3	G4	G5	G6	G7	G8	G9
ENR-50	100	100	100	100	100	100	100	100	100
ZnO	5	5	5	5	5	5	5	5	5
Stearic Acid	2	2	2	2	2	2	2	2	2
MBTS	2.4	2.4	2.4	2.4	2.4	2.4	2.4	2.4	2.4
TMTD	1.6	1.6	1.6	1.6	1.6	1.6	1.6	1.6	1.6
Sulphur	0.3	0.3	0.3	0.3	0.3	0.3	0.3	0.3	0.3
Sod.Carbonate	0.3	0.3	0.3	0.3	0.3	0.3	0.3	0.3	0.3
Aromatic oil	5	5	5	5	5	5	5	5	5
Prophylactics fillers	0	10	40	10	40	10	40	10	40
Carbon black	0			10	10				
Silica	0					10	10		
Marble powder	0							10	10

In every case, the particulate filler was first mixed with prophylactics filler which was then added to compounded ENR. For convenience, the discussion is carried out focusing the following;

1. Effect of increasing loading of prophylactics filler to gum ENR (samples G1, G2 and G3).
2. Effect of the presence of particulate filler (10 phr) in G2 and G3 (samples G4&G5 (black), G6&G7 (silica) and G8&G9 (marble powder).
3. Effect of increasing loading of prophylactics filler in the presence of particulate fillers (samples G4&G5 (black), G6&G7 (silica) and G8&G9 (marble powder).

6.1.1. Processing Aspects

The crosslinking process of the rubber compounds is characterised by the rheographs presented in **Figure 6.1** (G1-G9). It can be seen that all these are typical 'S' shaped[14] curves. The minimum (M_n) and maximum rheometric torque (M_h) values are presented in **Table 6.2**. Here, as the prophylactics filler also is a rubber with similar modulus values as the matrix, a notable increase in minimum torque is not observed.

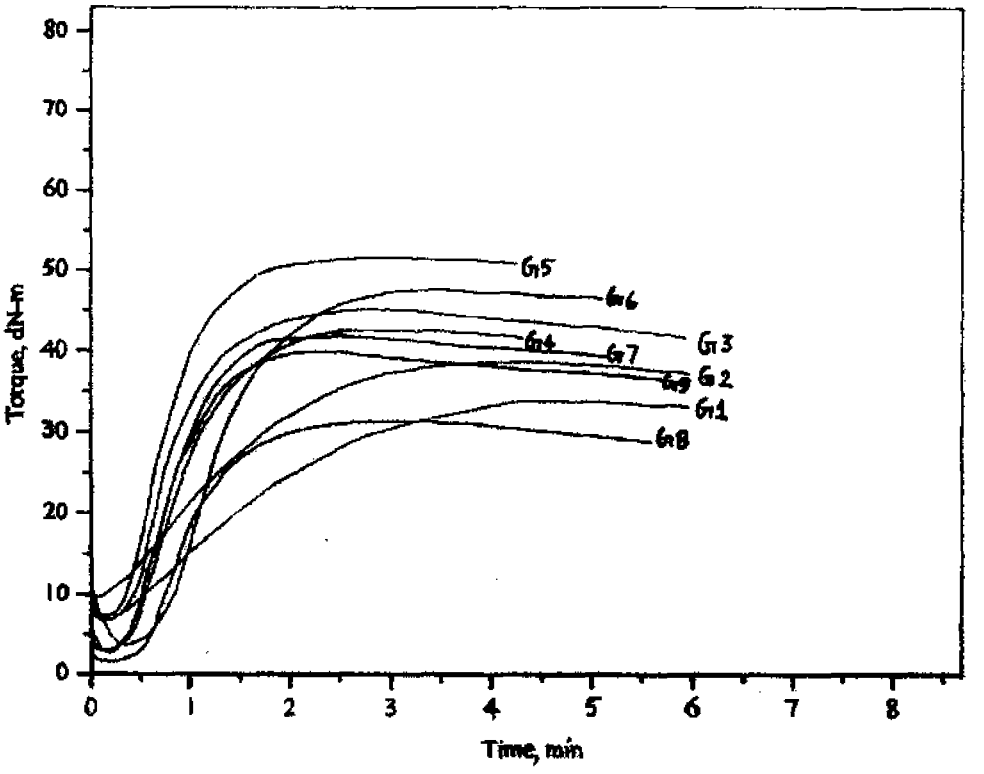

Figure 6.1. Rheographs of the ENR compounds

Table 6.2. Processing, vulcanization and mechanical data

Sample Code	M_n dN-m	M_h dN-m	CRI min^{-1}	k, min^{-1}	Young's Modulus MPa	Tensile Strength MPa	Tear Strength kN / m
G1	6.5	34.00	7.84	0.1670	0.85	1.44 $^{SD}_{0.08}$	8.3 $^{SD}_{0.49}$
G2	9	38.75	8.69	0.1990	1.05	1.73 $^{SD}_{0.16}$	9.7 $^{SD}_{0.49}$
G3	6	44.50	17.39	0.4407	1	2.19 $^{SD}_{0.16}$	10.5 $^{SD}_{0.41}$
G4	3	43	14.81	0.3800	1.5	6.6 $^{SD}_{0.33}$	11.55 $^{SD}_{0.40}$
G5	7	51.75	19.05	0.4320	1.7	7.46 $^{SD}_{0.32}$	12.38 $^{SD}_{0.25}$
G6	4	48	14.29	0.3440	1.56	6.8 $^{SD}_{0.25}$	12.8 $^{SD}_{0.57}$
G7	3	42	19.05	0.4840	1.28	8.5 $^{SD}_{0.24}$	14.5 $^{SD}_{0.32}$
G8	1.5	32.5	19.00	0.3728	1.3	5.49 $^{SD}_{0.24}$	10.8 $^{SD}_{0.61}$
G9	2.5	41.5	19.04	0.4593	1.45	6.12 $^{SD}_{0.29}$	11.5 $^{SD}_{0.25}$

It can be seen from **Table 6.2** that as the amount of natural rubber prophylactics in ENR-50 increases to 10 phr, the minimum torque increases, while at a loading of 40 phr, it

decreases. The increase in M_n at 10 phr loading of prophylactics is due to the lightly crosslinked nature of the prophylactics filler. Such an increase is already reported in the literature[15]. But the decrease observed at 40 phr may be due to the excessive mastication, which occurs to the elastomer compounds during the mixing process. The presence of 10-phr carbon black (G4) in the sample with 10 phr prophylactics (G2) decreases the minimum torque from 9 to 3, while in the case of the sample with 40 phr prophylactics (G3) a slight increase is observed (G5). The increase in the prophylactics loading from 10 to 40 phr in the presence of carbon black (G4 and G5) increases M_n. This is contrary to that noted earlier with the addition of prophylactics (G3) to ENR sample (G2). The presence of silica in both 10 and 40 phr prophylactics containing samples also is found to be decreasing the minimum torque of the samples.

The increase in the prophylactics loading from 10 to 40 phr in the presence of silica (G6 and G7) decreases the M_n. This is similar to that noted earlier with G3 compared to G2. The presence of 10-phr marble powder (G8) to the sample with 10 phr prophylactics (G2) decreases the minimum torque from 9 to 1.5, while in the case of the sample with 40 phr prophylactics (G3), the decrease is from 6 to 2.5 (G9). In this case, marble powder behaves similar to silica. The increase in the prophylactics loading from 10 to 40 phr in the presence of marble powder (G8 and G9) slightly increases M_n. This is contrary to that noted earlier with the addition of prophylactics (G3) to ENR sample (G2) but similar to the case of carbon black, in samples G4 and G5.

The observation of differences in the variation of M_n with the addition of different fillers to systems G2 and G3 and the addition of prophylactics in filled samples reveals that the M_n is very sensitive to many parameters such as mixing time, nature and number of components in the mix etc. Among the fillers tried, only black is found to be increasing M_n to a slight extent and that itself, in ENR/40 phr prophylactics systems (G5).

The maximum torque (M_h) is found to be regularly increasing with prophylactics loading (G1-G2-G3). The increase in M_h with the addition of prophylactics is due to the presence of crosslinked particles in ENR matrix. The presence of 10 phr carbon black in ENR / 10 phr (G2) and 40 phr (G3) prophylactics systems increases M_h to a considerable extent (G4 and G5). Similarly, with the increasing loading of prophylactics in the presence

of carbon black (G4 and G5), M_h increases. The presence of 10 phr silica in G2 to get G6 increases M_h considerably. But such an increase is not observed in the case of ENR/ 40 phr prophylactics system (G7) compared to G3. Similarly, when the content of prophylactics in silica containing ENR samples (G6 and G7) increases from 10 to 40 phr Mh decreases. Marble powder concentration of 10 phr in ENR/10 phr (G2) and 40 phr (G3) prophylactics systems decreases M_h. Similarly, as the concentration of prophylactics in G8 and G9 increases from 10 to 40 phr, M_h increases. The decreased values of M_h in the presence of marble powder indicate that marble powder is acting only as inert filler as far as maximum rheometric torque is concerned.

The variation of the rheometric curing properties such as optimum cure time (t_{90}), scorch time (t_2) and induction time (t_1) at 150^0 C are given in **Table 6.3**.

Table 6.3. Curing data

Sample Code	t_{90} min	t_2 min	t_1 min
G1	15	2.25	1.5
G2	13	1.5	1
G3	7.5	1.75	1.5
G4	8.5	1.75	1.5
G5	7	1.75	1.5
G6	10.5	3.5	2.5
G7	7	1.75	1.5
G8	8.25	3	2.5
G9	7.25	2	1.5

These values are calculated from the rheographs as given in chapter 2. It can be seen that, as the amount of prophylactics increases, optimum cure time, scorch time and induction time values decrease. The reduction in the curing properties with prophylactics loading is due to presence of unreacted accelerator in the prophylactics filler. With the addition of 10 phr carbon black (G4 and G5), the t_2 and t_1 values slightly increases in the case of ENR/10 phr prophylactics system while it levels off for ENR/40 phr prophylactics system. The addition of 10 phr silica to the samples G2 and G3 decreases the optimum cure time further (G6 and G7). Usually, a decrease in optimum cure time causes similar effects in scorch time and induction time values. But here, an increase in these parameters is noted with the addition of silica. With the addition of marble powder, the optimum cure time

decreases further in the case of ENR/10 phr prophylactics (G2 and G8) while it levels off in the case of ENR/40 phr prophylactics (G3 and G9). Scorch time and induction time increase with the addition of marble powder. As the amount of prophylactics filler increases in samples with particulate fillers, optimum cure time decreases. Except in the case of black, scorch time and induction time also show a decrease with the addition of prophylactics in samples with particulate fillers.

Normally, particulate fillers like clay, silica etc with hydroxyl groups on the surface adsorb the accelerator and thus increase the above curing parameters. Here, it should be thought that this is less predominant for the system of ENR / prophylactics due to the overcoming effect of cure activation by the prophylactics filler. The inability of particulate fillers to adsorb the unreacted accelerator fragments in prophylactics is clear from these results.

6.1.2. Vulcanisation Kinetics

The cure rate index (CRI) and the cure reaction rate constants are determined by the method given in chapter 2 (equations 2.2 and 2.6). The plot of ln (M_h-M_t) verses time t of the elastomer compounds at 150^0 C is shown in **Figure 6.2.**

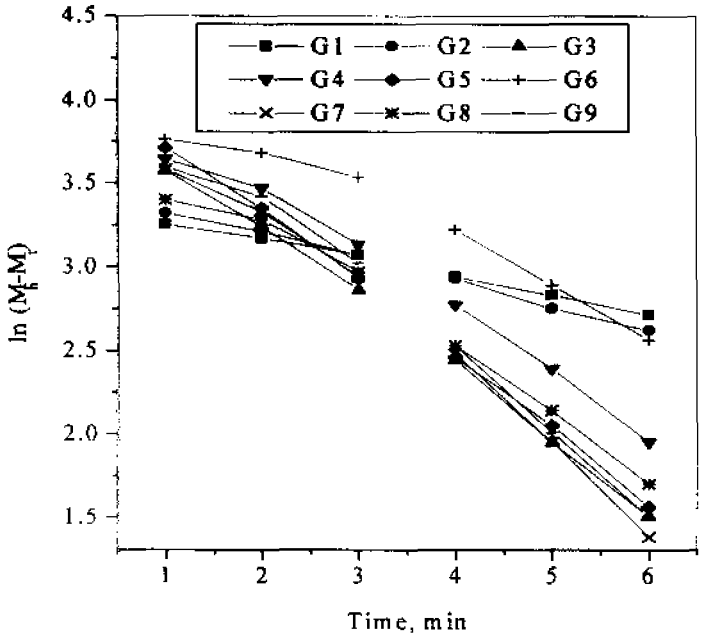

Figure 6.2. Kinetic plots

The plots are found be almost linear which proves that the cure reactions proceed according to first order kinetics. The cure reaction rate constants (k) are obtained from the slope of the respective linear equations. The cure rate index and cure rate constant values are presented in **Table 6.2**. Both CRI and k values show an increase with increasing prophylactics loading. This reveals the cure activation by the presence of unreacted accelerator fragments in the prophylactics filler. The presence of particulate fillers generally increases (except in the carbon black system, k of ENR/40 phr prophylactics which shows a slight decrease) these parameters. In samples filled with particulate fillers, the addition of prophylactics increases the CRI and k values.

The increased speed of cure reaction in particulate filled cases results from the combined effects of cure activation by the unreacted accelerator fragments in the prophylactics and inability of particulate fillers to adsorb these accelerator fragments. This ability of prophylactics as well as particulate fillers in the present system to activate the curing process is a great advantage since it can increase the production rate of the elastomer articles filled with it.

6.1.3. Technological properties

The stress-strain behaviour of a rubber network is mainly influenced by the presence of crosslinks and by constraints caused by the uncrossability of the network chains. The stress-strain curves of the gum and prophylactics filled ENR vulcanisates are presented in **Figure 6.3**. The curves are different from typical vulcanised low strength materials. This can be seen in the steeply rising stress value at higher strains while in the case of a low strength material such as SBR (chapter 3), the stress-strain plot will be bent a bit to the strain axis at higher strains. The observation of steeply rising stress value is due to the tendency of ENR for strain crystallisation. The addition of prophylactics is found to be increasing the stress value at a particular strain value. The presence of particulate fillers causes notable variation in the nature of the stress-strain curves, mainly in the maximum value of strain. Silica increases the initial stress values, while the intermediate stress values are found to be slightly lower for this case. Other particulate fillers present values above these.

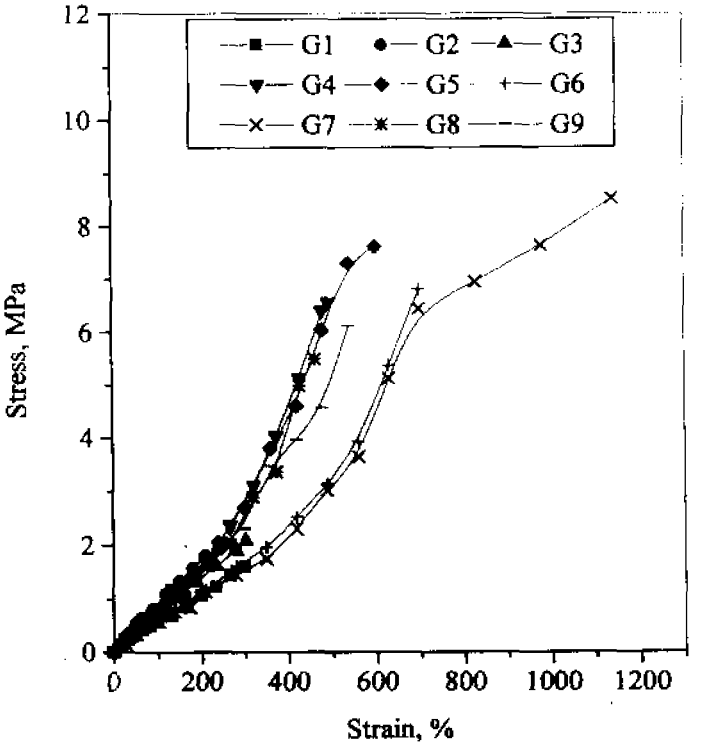

Figure 6.3. Stress-strain curves of the ENR samples

The slope of the initial linear region of the stress- strain curve, presented as the Young's modulus is given in **Table 6.2**. This value shows an initial slight increase with 10 phr loading of prophylactics, which is followed by a decrease. But, generally it can be understood that with the addition of prophylactics filler, the Young's modulus shows a slight increase. The addition of carbon black, silica and marble powder increases the Young's modulus of these systems. The greatest increase is shown by black for the ENR/40 phr prophylactics system while silica gets the credit for the ENR/10 phr prophylactics system. The addition of prophylactics in particulate containing systems increases the Young's modulus except in the case of silica. The slight increase in Young's modulus results from the strain induced crystallisation of ENR as well as prophylactics during the stretching of the specimen. Since, particulate filler reinforces the system, Young's modulus increases further for the filled samples.

The variation of tensile strength with the loading of prophylactics filler is given in **Table 6.2**. Tensile strength also shows an increase at 10 and 40 phr prophylactics loading. This clearly indicates the reinforcing phenomenon and strain induced crystallisation of prophylactics filler in ENR-50 matrix. The presence of carbon black, silica as well as marble powder in ENR/prophylactics system and also the increasing concentration of prophylactics in particulate filled samples increase the tensile strength of the samples. The highest increase is observed for the silica filled samples while the lowest for marble powder in the case of both ENR/10 and 40 phr prophylactics systems. These results clearly indicate the better interaction of silica in these present systems.

The behaviour noted for tear strength **(Table 6.2)** also is the same. The enhanced tear strength with the addition of prophylactics filler is due to the ability of prophylactics particles for higher elongation and thus obstruct the advancing tear. The particulate filler particles increase the tear strength further.

6.1.4. Viscoelastic behaviour

The storage modulus E' of most of the rubber materials depends very strongly on the external applied strain. The variation of storage modulus (E') of ENR (G1) and ENR with 10 and 40 phr prophylactics (G2 and G3) as a function of temperature at a frequency of 0.1 Hz is presented in **Figure 6.4**. Here the temperature region from –70 to -10^0 C can be taken as the glassy region, that from –10 to +10 ^{0}C as the transition region and the last region beyond +10 ^{0}C as the rubbery region. It is also observable from **Figure 6.4** that the storage modulus of the samples decreases with increase in temperature. This is due to the loss in stiffness of the material with temperature.

In the case of other ENR samples G2 and G3 containing 10 and 40 phr prophylactics filler, two transitions are visible even though the first one from –58 to –50 ^{0}C range is not very prominent for G2. It is more clearly visible for the G3 sample with 40 phr prophylactics. The observation of two transitions for the sample G2 and G3 can be taken as a primary evidence for the heterogeneous nature of ENR prophylactics system. At the low and high temperature region, slightly lower modulus values are shown by the gum ENR vulcanisate (G1). As the concentration of prophylactics increases modulus value also increases. This behaviour can be expected from the presence of crosslinked

particles in elastomer matrices[15].

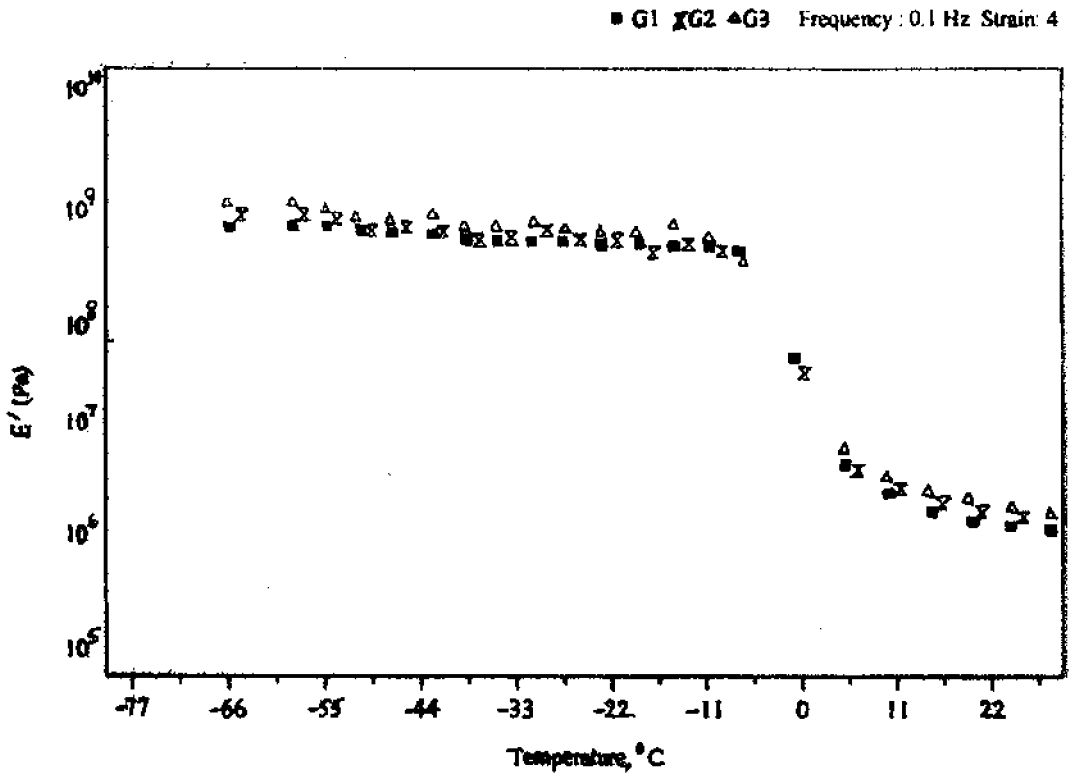

Figure 6.4. Variation of storage modulus of ENR/prophylactics samples with temperature

The samples with 10 and 40 phr prophylactics and similar compositions with particulate fillers are presented in **Figure 6.5**. For all these cases, only the main transition around -3^0 C is prominent and this transition does not undergo any shift to low or high temperatures with the addition of particulate fillers.

The loss in stiffness has been found to be less in the case of samples with carbon black filler. The presence of 10 phr particulate filler, carbon black, silica and marble powder increases the modulus value above that of ENR / prophylactics systems. In the case of carbon black and marble powder, this increase is found to be higher for the ENR/10 phr prophylactics sample while in the case of silica, the extent of increase in the modulus values in both ENR / 10 prophylactics and ENR / 40 phr prophylactics are the same. Increase in the concentration of prophylactics in black filled samples (G4 and G5) decreases the storage modulus values below the main transition while a slight increase is

observed above the transition. In the case of silica (G6 and G7), a slight increase is observed both below and above the main transition, while in the case of marble powder, a slight decrease is observed below the transition while a leveling off is observed above the transition.

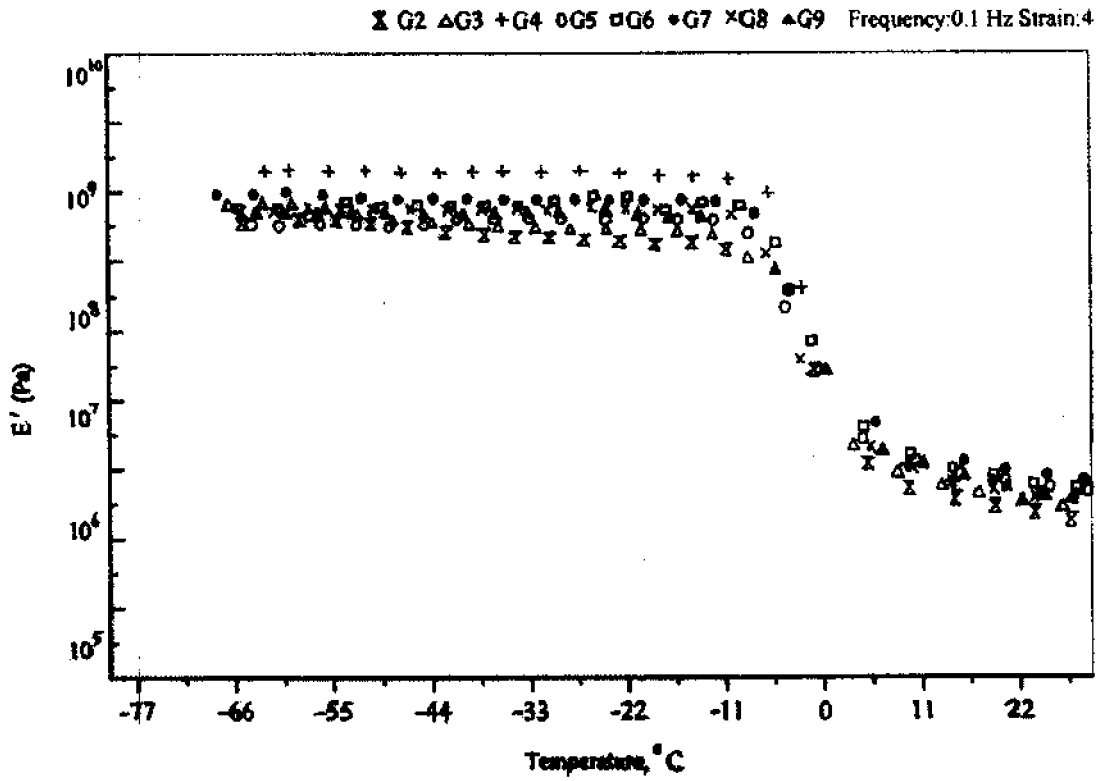

Figure 6.5. Variation of storage modulus of ENR / prophylactics / particulate filled samples with temperature

A typical plot showing the effect of frequency on the variation of storage modulus with temperature of gum ENR sample is presented in **Figure 6.6.** The storage modulus increases slightly with increasing frequency below the transition temperatures. But above this, there is a sharp increase with increasing frequency. It is also observable from **Figure 6.6** that the temperature corresponding to the beginning of transition is not changing with increase in frequency for the gum ENR.

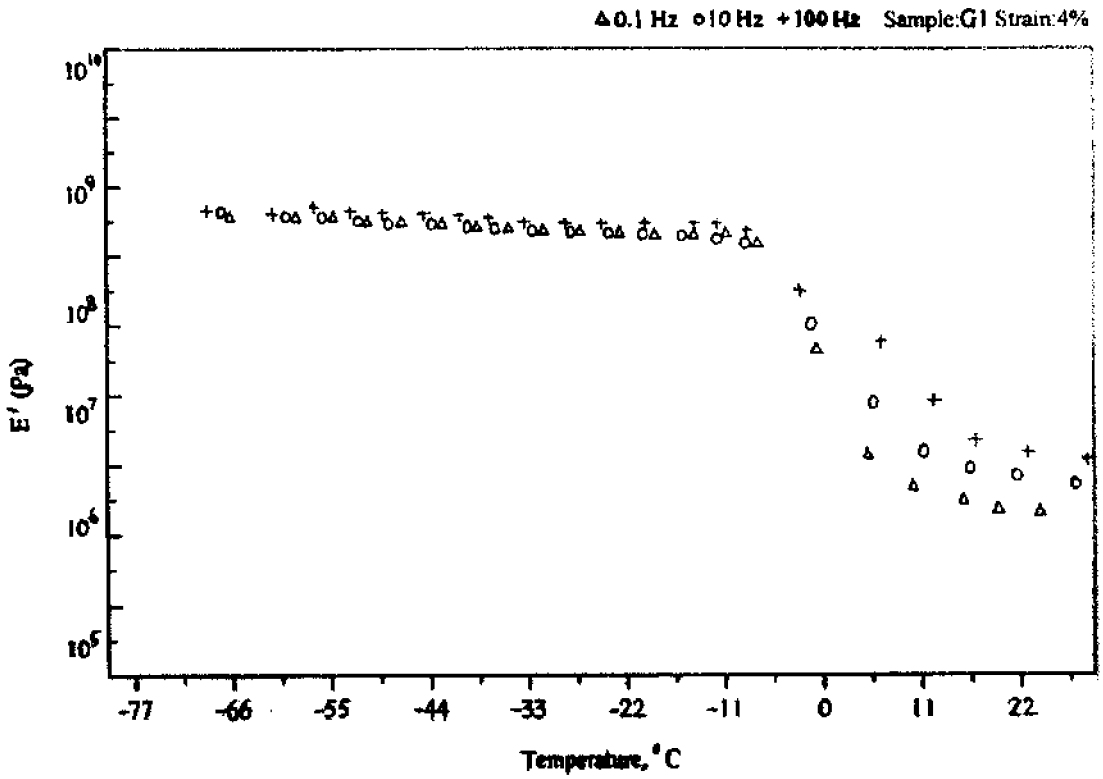

Figure 6.6. Variation of storage modulus of the gum ENR sample with temperature at different frequencies.

Prophylactics filler as well as particulate fillers (sample G3, G5-Carbbon black, G7-silica, G9-marble powder) also are found to be causing such a forward shift in the onset temperature for the main transition with increased frequency. They show slightly higher modulus values at all the frequencies below and above the main transition. The decrease in the storage modulus with temperature is due to the loss in stiffness of the material with temperature. The minimum loss in the stiffness and increase in the storage modulus of the particulate filled materials is due to the reinforcing action of the respective filler in the samples.

It can be seen that in the transition region, the effect of frequency will be intense. Therefore the plot of E' verses frequency at three different temperatures is plotted in **Figure 6.7**. The slope values of (trend lines not shown) all the samples at –30 and + 30 ^{0}C are found to be similar **(Table 6.4)**. The slope values are found to be maximum at 0 ^{0}C

which is nearer to the transition region than any other temperatures.

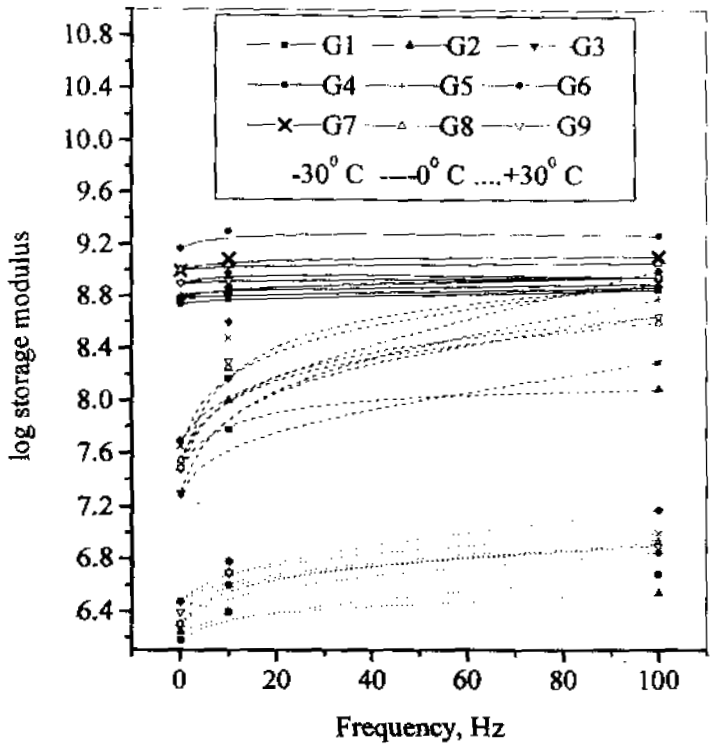

Figure 6.7. Variation of storage modulus with frequency at selected temperatures

Table 6.4. Slope values of log E' vs. frequency plots

Temperature (^{0}C)	SLOPE VALUES X 10^{-3}								
	G1	G2	G3	G4	G5	G6	G7	G8	G9
-30	0.97	1.34	0.81	0.47	0.76	0.17	0.75	0.45	0.43
0	8.33	4.08	100	11	10	9.75	9.4	12.7	8.61
+30	4.4	2.47	4.5	4.42	4.04	6.1	4.11	4.75	4

The transitions in molecular mobility requiring higher energy are attributed to the peaks in the plots. For pure gum ENR, only one peak at -5 to –10 ^{0}C range is observed while for other samples, two peaks can be seen. The observation of two peaks in the E'' verses temperature plots indicates the heterogeneous nature of the samples.

Typical plots showing the variation of loss modulus (E") Vs. temperature for ENR and ENR filled with prophylactics filler (G1-G3) are presented in **Figure 6.8**.

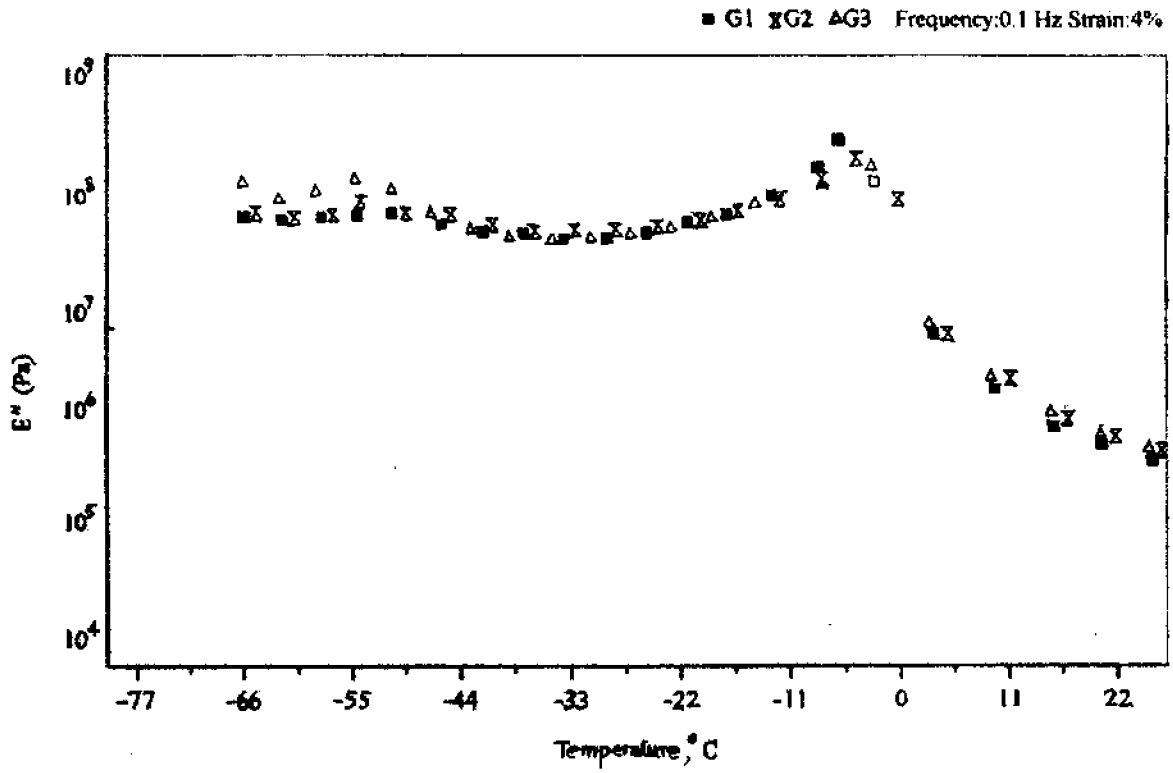

Figure 6.8. Variation of loss modulus of ENR/prophylactics samples with temperature

As the concentration of prophylactics in ENR increases from 10 to 40 phr (G2 and G3), the maximum in the prophylactics peak increases slightly while that of ENR peak decreases. For the samples G2 and G3, the loss modulus variation before and after the transition deserves much attention. For the ENR vulcanisate with 10 phr prophylactics (G2), the loss modulus values before the first peak are almost similar to that of gum ENR but after that the values become higher. As the temperature increases, the values are again coming close to that of ENR. But after the ENR transition, the E'' values again rise above that of gum ENR. Similar observations can be seen for the ENR vulcanisate with 40 phr prophylactics (G3) as well. The peak at –9 ^{0}C corresponds to the Tg of gum ENR. This damping peak is associated with the partial loosening of polymer structures leading to the movement of small chains near Tg at low frequencies (0.1 Hz here).

Tg is usually determined by the experiments that correspond to a time scale. If the experiments are carried out rapidly, time scale is shortened and frequency is increased. Then Tg value will be raised. On the contrary, if the reverse is done, Tg will be lowered. So Tg is not a true constant but is just an operational reference temperature for the onset of segmental rearrangements. For the present discussions, Tg values are taken from E'' Vs temperature plots because as per the recent literature[16] the temperature for maximum damping is not Tg but it is erroneously taken to be so. The temperature at the maximum in loss modulus is more close[16] to Tg.

The Tg values noted from the plots are presented in **Tables 6.5a** and **6.5b**. The increase in the Tg (at 10 Hz) of ENR (from –5 to –2 ^{0}C) with the addition of prophylactics is due to the increased stiffness of the system **(Table 6.5a)**. For the G2 sample at 10 Hz, the temperature corresponding to the maximum of prophylactics peak increases from –53 to –45^0 C with the further addition of prophylactics (G3) **(Table 6.5b)**.

Table 6.5a. Glass transition values of ENR

Frequency	Tg (^{0}C) from ENR peak								
Hz	G1	G2	G3	G4	G5	G6	G7	G8	G9
10	-5	-5	-2	3	-1	3	1	-1	-4
100	-3	-3	3	6	3	5	5	2	-1

Table 6.5b. Glass transition values of Prophylactics

Frequency	Tg (^{0}C) from Prophylactics peak								
Hz	G1	G2	G3	G4	G5	G6	G7	G8	G9
10	-	-53	-45	-46	-47	-50	-46	-48	-49
100	-	-53.5	-42	-43	-45	-47	-42	-46	-47

The plots for samples with particulate fillers are presented in **Figure 6.9.**

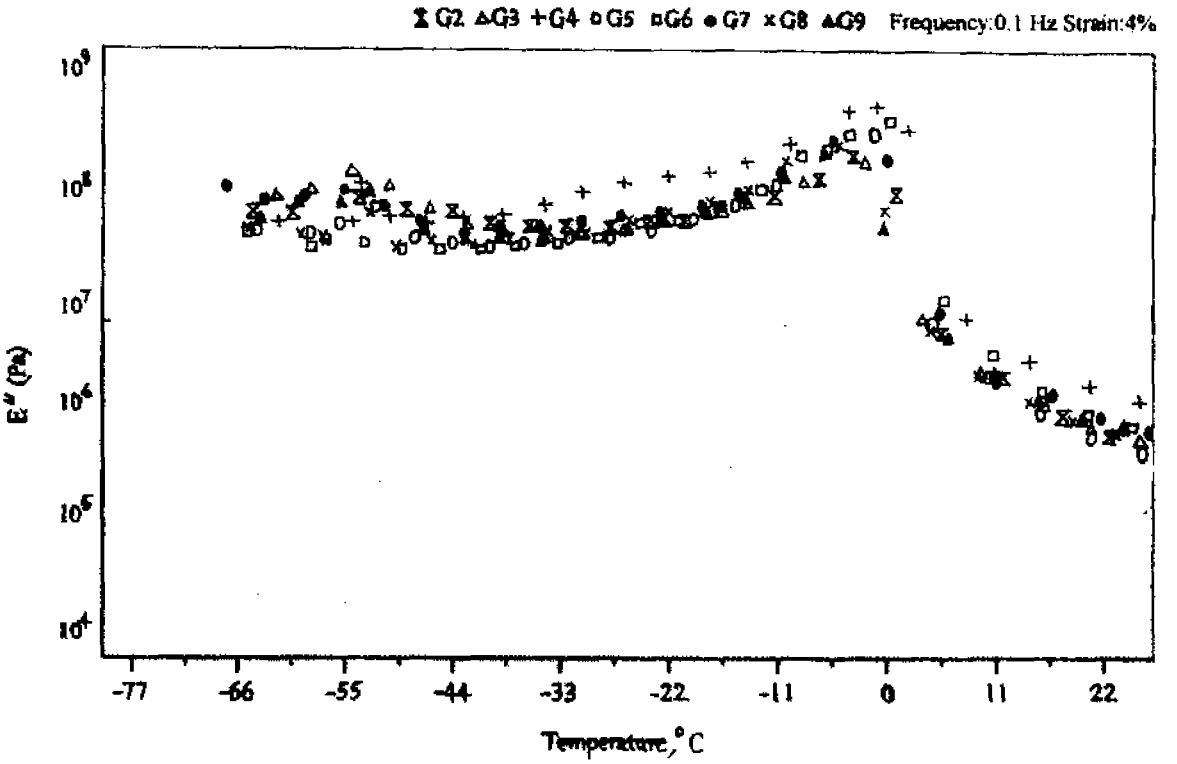

Figure 6.9. Variation of loss modulus of ENR/prophylactics/particulate filled samples with temperature

The presence of black causes different shifts in different systems at different frequencies. In the case of ENR/10 and 40 phr prophylactics systems at 10 Hz, black (G4&G5) as well as silica (G6&G7) increases the Tg of ENR. The increase in the concentration of prophylactics in ENR samples with particulate filler decreases Tg values

In the case of ENR/10 phr prophylactics system at 10 Hz, presence of marble powder (G4) increases the Tg of ENR from –5 to -1^0 C. But in the case of ENR/40 phr prophylactics sample, it decreases further. The increase in the concentration of prophylactics in marble powder containing samples (G8 and G9) decreases Tg values to –1 and -4^0 C. Tg of prophylactics phase at 10 Hz also shows increase with increasing concentration of prophylactics. With the presence of particulate filler, an increase in Tg of prophylactics is noted only in the case of ENR/10 phr prophylactics system.

The variation of loss modulus with temperature for the gum ENR sample (G1) for different frequencies is presented in **Figure 6.10**.

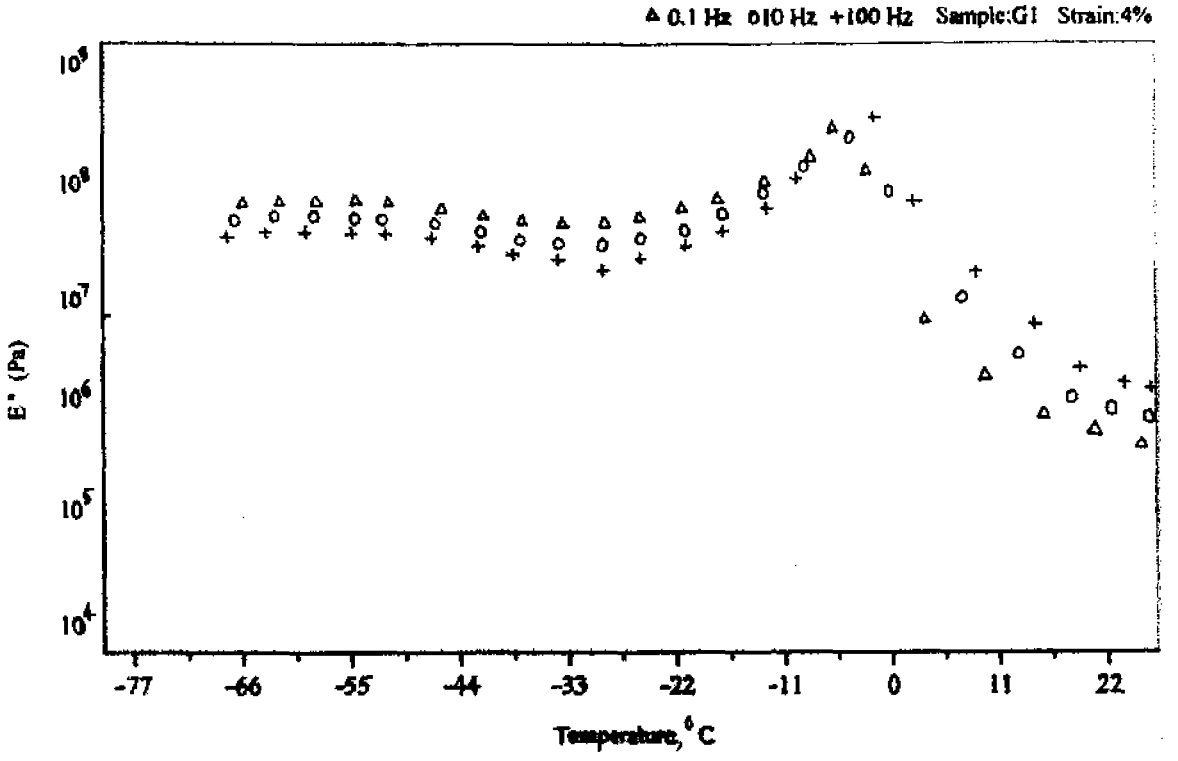

Figure 6.10. Variation of loss modulus of the gum ENR sample with temperature at different frequencies.

It is a general observation that, below the main transition, the loss modulus deceases with increase in frequency while above it, a reverse trend is observed. Moreover the influence of frequency is reflected in the E'' values, mainly above the transition. This phenomenon gives a twisted staircase or wave like appearance to the plots. On increasing the frequency **(Figure 6.10)**, the glass transition temperature of ENR slightly increases from –5 to –3 ^{0}C **(Table 6.5a)**. Increase in the frequency increases the Tg of ENR from –2 to +3 ^{0}C in the case of G3 sample. The Tg of prophylactics also increases from –45 to –42 ^{0}C. Moreover, the glass transition temperatures of ENR obtained from our experiments agree very well with the values previously reported from the works of Gelling[17,18]

In the case of black filled sample, increase in the frequency increases the Tg of

ENR peak **(Table 6.5a)** of ENR/40 phr prophylactics/10 phr black from –1 to +3 ^{0} C and that of prophylactics peak from –47 to –45^0 C. The observation of two peaks in the E'' verses temperature plots indicates the heterogeneous nature of the samples.

Shifts in Tg observed are due to the effective utilisation of carbon black surface by the polymer molecules **(Figure 6.11)**.

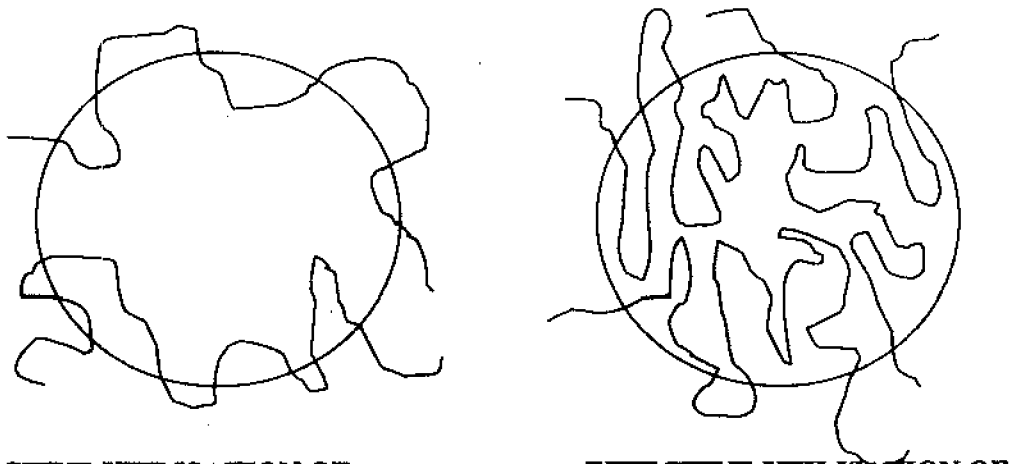

INEFFECTIVE UTILISATION OF FILLER SURFACE BY POLYMER CHAINS

EFFECTIVE UTILISATION OF FILLER SURFACE BY POLYMER CHAINS

Figure 6.11. Utilisation of filler surface by polymer chains

In the case of silica filled samples, increase in the frequency increases the Tg of ENR peak from +1 to +5 ^{0} C (for ENR / 40 phr prophylactics / 10 phr silica) and that of prophylactics peak from –46 to –42^0 C (for ENR / 40 phr prophylactics / 10 phr silica) are observed. Increase in the Tg of ENR is due to the chemical interaction of silanol groups in silica with epoxy groups in ENR. Shifts in Tg observed are again, due to the effective utilisation of silica surface by the polymer molecules. This is possible due to the ring opening of epoxy groups in ENR by the silanol groups of silica filler[19] given in **Figure 6.12**. Such an effective utilisation reduces the mobility of ENR phase considerably and this causes the Tg values to increase above that of the gum ENR.

In the case of marble powder filled samples, on increasing the frequency, the glass transition temperature of ENR peak increases slightly from –4 to -1^0 C (for ENR / 40 phr prophylactics / 10 phr marble powder) and that of prophylactics peak from –49 to –47^0 C (for ENR / 40 phr prophylactics / 10 phr marble powder).

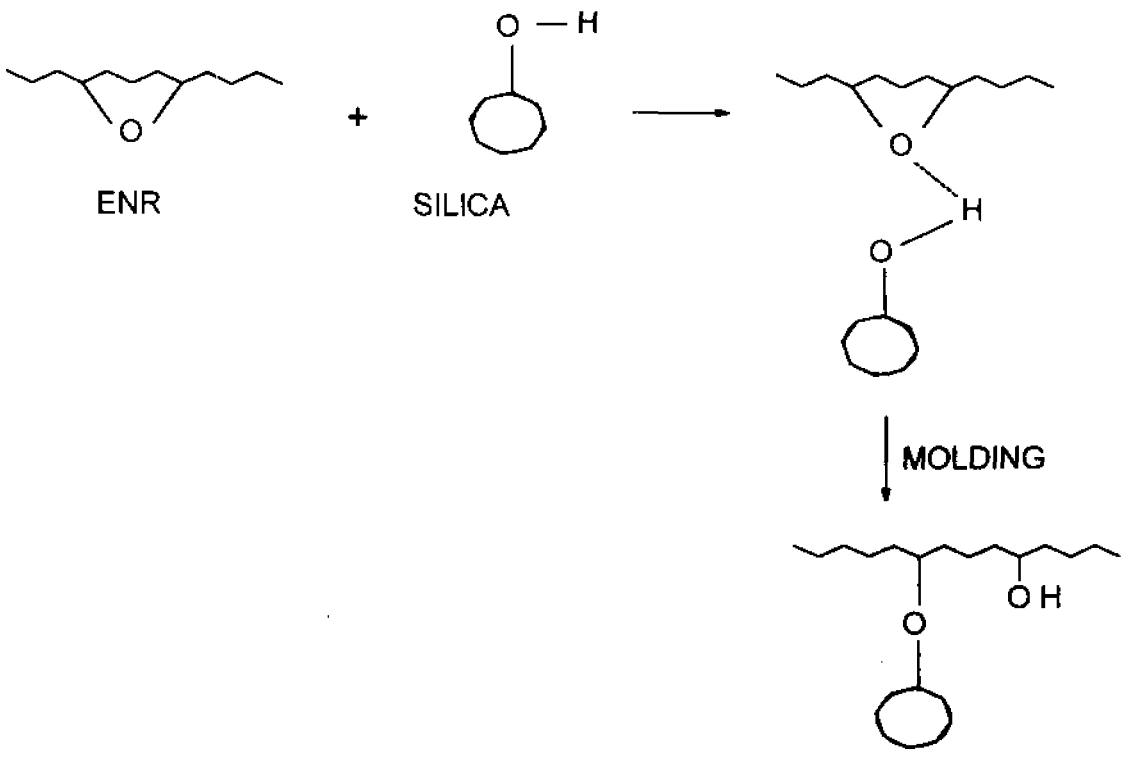

Figure 6.12. Interaction of silica with epoxy groups

Studies by Ahsan et al[20], identified the particles of $CaCO_3$ forming marble powder to have a heterogeneous surface with exposed polar cationic sites, which are capable of interaction with unsaturated hydrocarbons. Such interactions, even though very weak, can lead to effective utilisation of marble powder filler surface by the polymer molecules, which intern can result in the shifts in Tg values. Since such interactions are weaker compared to those of silica, shifts in Tg are not very considerable, for e.g., in the case of ENR/40 phr prophylactics system, even a decrease in Tg is observed which would not have occurred otherwise. Since marble powder reduces the relaxation of the prophylactics phase also, slight increase in prophylactics Tg values (–53 ^{0} C) are also observed. It is clear from these discussions that the interaction between the filler and one of the components of a mix is a major factor in deciding the damping properties similar to other effects such as the selective accumulation of the filler in one of the phases.

Figure 6.13 represents the variation of tan δ with temperature at 100 Hz frequencies for ENR samples of different compositions. Although polymer composition is the key parameter determining the damping properties, other factors such as morphology, crosslink density, interaction between different polymer components and the phase continuity etc. will affect damping[21]. Since the Tg values of the samples were discussed earlier using the loss modulus-temperature plots, the discussions here are limited to the damping behaviour (tan δ_{max}) alone. It is a general observation from **Figure 6.13** that as the temperature increases beyond ENR transition, tan δ values decrease.

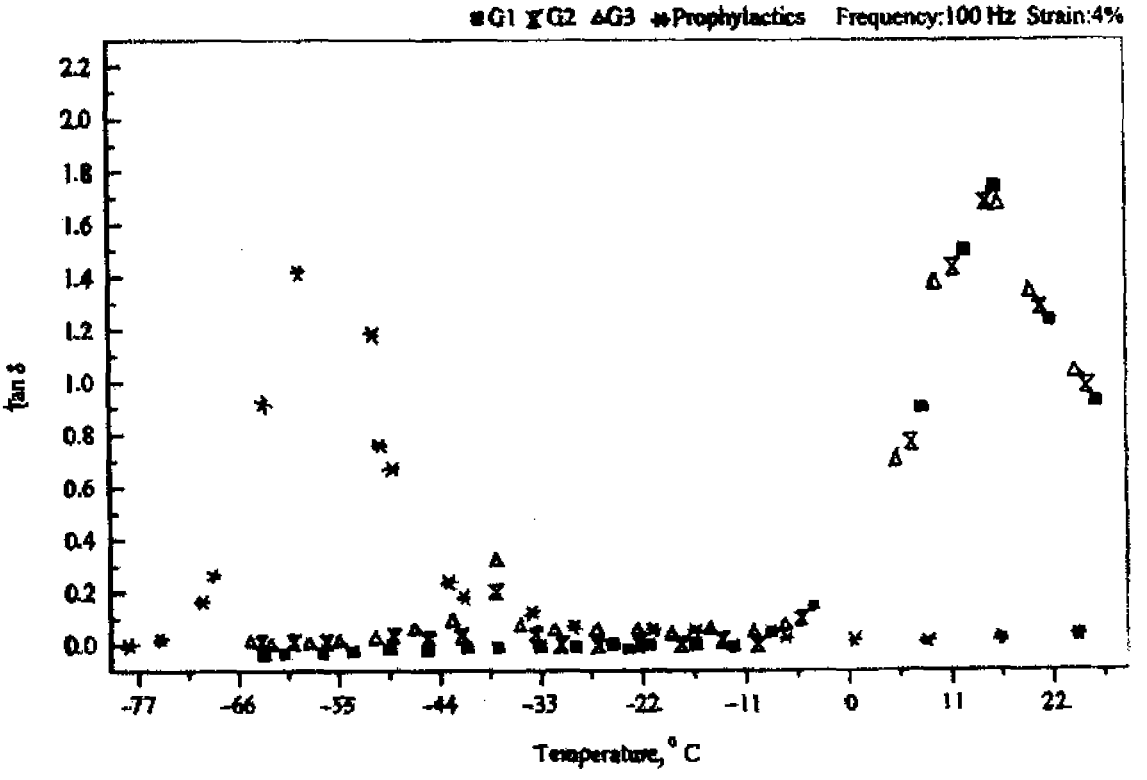

Figure 6.13. Variation of tan δ of ENR/prophylactics samples with temperature

It can also be observed from the **Figure 6.13** that the addition of prophylactics to ENR (G1 for gum ENR, G2 and G3 for ENR with 10 and 40 phr prophylactics), the tan δ_{max} of ENR slightly decreases while that of prophylactics increases. In these systems the prophylactics forms the dispersed and discontinuous phase in a continuous ENR phase. The dispersed phase, immobilises the continuous phase (ENR), in the relaxation process[22].

This intern causes a reduction in the tan δ_{max} of ENR with the increasing loading of prophylactics.

It is very interesting to see from **Table 6.6** that the tan δ_{max} for both ENR and prophylactics peaks in the filled ENR samples at a particular frequency is less than the corresponding single systems for most of the cases. This is found to be more pronounced for prophylactics peak. This fact reveals that ENR also repays the immobilisation to prophylactics more intensely than it received the same from prophylactics.

Table 6.6. tan δ_{max} values

Sample	Frequency Hz	tan δ_{max}	
		ENR peak	Prophylactics peak
G1	0.1	1	
	10	1.25	
	100	1.75	
G2	0.1	1.1	0.2
	10	1.6	0.2
	100	1.7	0.2
G3	0.1	0.93	0.3
	10	1.5	0.35
	100	1.65	0.35
G4	0.1	1.1	0.15
	10	1.45	0.13
	100	1.6	0.1
G5	0.1	0.8	0.3
	10	1.2	0.25
	100	1.3	0.3
G6	0.1	1.3	0.2
	10	1.4	0.15
	100	1.4	0.13
G7	0.1	1	0.38
	10	1.1	0.33
	100	1.25	0.33
G8	0.1	1.53	0.2
	10	1.6	0.19
	100	1.65	0.15
G9	0.1	1.25	0.37
	10	1.3	0.3
	100	1.35	0.3
Prophylactics	100		1.45

Figure 6.14 represents the variation of tan δ with temperature at 100 Hz frequency for different ENR samples with particulate fillers. It can be observed from the **Table 6.6** that the presence of carbon black, silica and marble powder filler in both ENR / 10 phr and 40 phr prophylactics causes a reduction in the tan δ_{max} of ENR and prophylactics peaks at 10 and 100 Hz. But at 0.1 Hz, a slight increase in tan δ_{max} is observed.

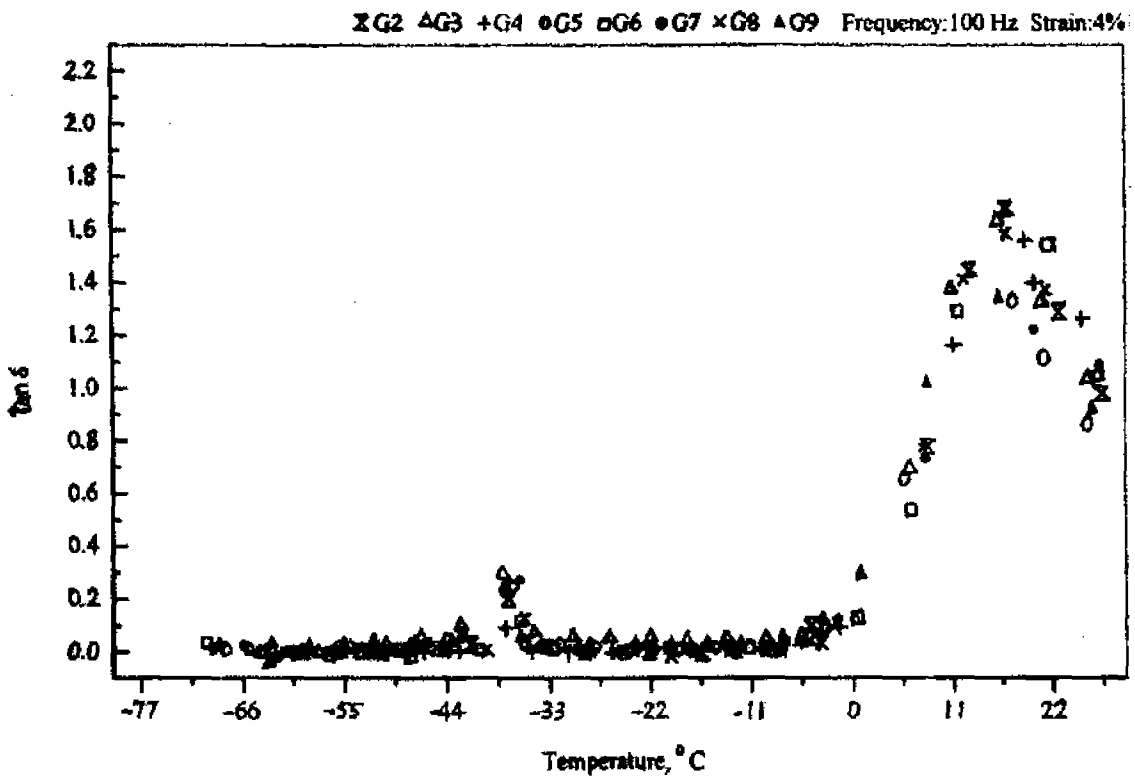

Figure 6.14. Variation of tan δ of ENR / prophylactics / particulate filled samples with temperature

Nielsen[23] reported that the reduction in tan δ_{max} in most of the cases is due to the additional restrictions caused by the filler to the respective phases in their relaxation in the sample. It can be seen that this depends on the frequency of the measurement also. Moreover the addition of filler needs more polymer for the wetting of filler surfaces. This causes a reduction in the effective volume of polymer available for relaxation, which finally results in a low value for tan δ_{max}. The reduction in tan δ_{max} denotes an improvement in the hysteresis of the system.

The influence of frequency on the tan δ - temperature plots is presented in **Figure 6.15.**

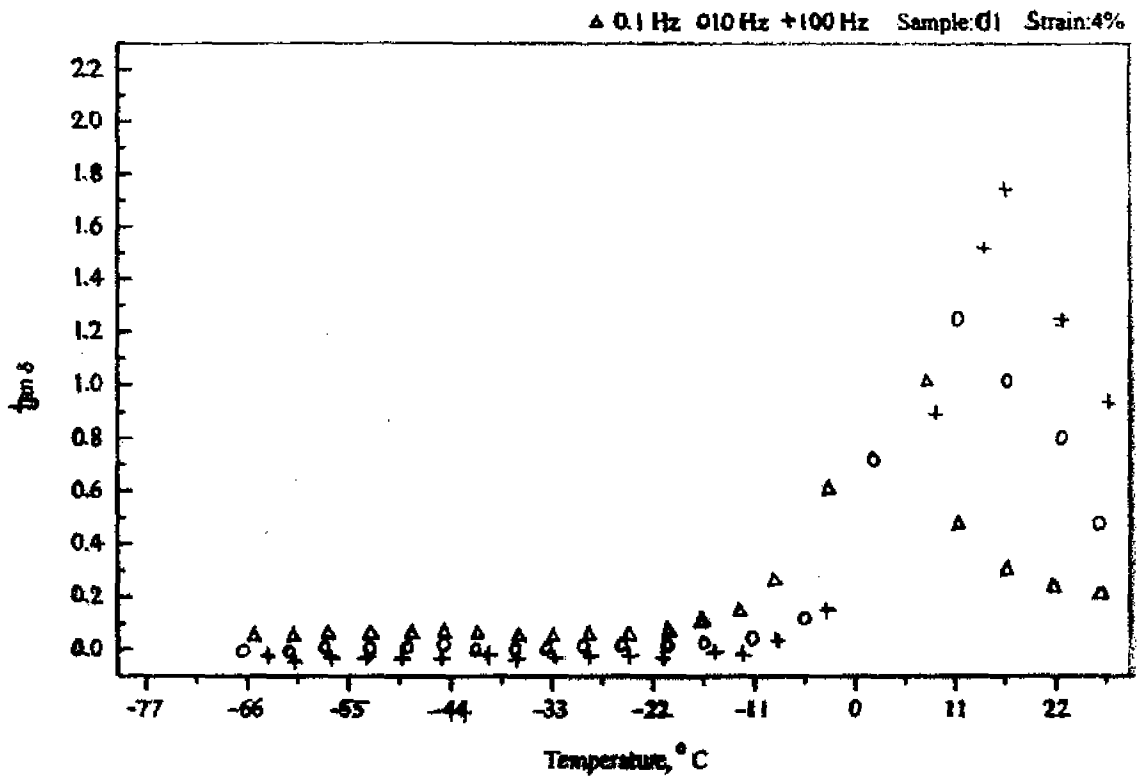

Figure 6.15. Variation of tan δ of the gum ENR sample with temperature at different frequencies

In **Figure 6.15**, it can be seen that the tan δ_{max} of ENR (G1) increases from 1 to 1.75, as the frequency increases from 0.1 to 100 Hz **(Table 6.6)**. But in the case of prophylactics peak, there is no notable change in tan δ_{max} with frequency. In the case of ENR vulcanisate containing 40 phr prophylactics (G3) also, tan δ_{max} of ENR and prophylactics increases with frequency **(Table 6.6)**. But in the case of prophylactics peak, the values level off after a frequency of 10 Hz. In the case of mixes with particulate filler also, such an increase in tan δ_{max} is observed but the magnitude of increase is less. It is very interesting to note from **Table 6.6** that the tan δ_{max} of both ENR and prophylactics peaks in the mixes is less than the corresponding single systems at most of the frequencies. This is found to be more pronounced for prophylactics peak. In addition, it is reported that

the addition of a solid elastic filler can either increase or decrease the mechanical damping of a polymer[24]. Here it is found to be true because different trends are observed at different frequencies. At most of the frequencies, either a leveling off or a decrease in tan δ_{max} is observed with the addition of particulate filler.

The variation in the tan δ_{max} of a component with filler loading can be used to find the relative distribution of filler among the blend components. The method involves the calculation of a parameter 'R' using tan δ_{max} variation.

$$R = \frac{\tan \delta g_{max} - \tan \delta f_{max}}{\tan \delta g_{max}} \qquad (6.1)$$

where

g – gum system

f - filled system

R is also related to the weight fraction of filler in the polymer (w) as,

$$R = \alpha w \qquad (6.2)$$

where α is polymer –filler interaction parameter.

On extending this equation to ENR, prophylactics individual component systems and their mixes, we get;

$$\left.\begin{aligned} R1 &= \alpha w \\ R2 &= \alpha w \\ R1' &= \alpha 1' w1' \\ R2' &= \alpha 2' w2' \end{aligned}\right\} \qquad (6.3)$$

where the subscripts represent the ENR and prophylactics systems and prime indicates the blend systems. w1 and w2 are the weight fraction of filler to total polymer in the blend distributed in ENR and prophylactics respectively. The total weight fraction 'w' of filler in the blend is given by;

$$w = w1' + w2' \qquad (6.4)$$

Assuming $\alpha 1 / \alpha 2 = \alpha 1' / \alpha 2'$; we get

$$\frac{w1'}{w2'} = \frac{R1'\,R2}{R2'\,R1} \qquad (6.5)$$

From above equations

$$w1' = \frac{R1'\ R2\ w}{R1'\ R2 + R2'\ R1} \qquad (6.6)$$

The analysis reveals that a major portion of the particulate filler (carbon black (94.8%), silica (94.3%) and marble powder (95.6%)) remains in prophylactics phase.

The addition of prophylactics increases the storage modulus E' of the samples. Since the modulus is a direct measure of the crosslink density, enhanced modulus can be attributed to the higher crosslink density of the matrix in the presence of fillers. According to the statistical theory of rubber elasticity[25], the crosslink density nE' r for a tetrafunctional network can be calculated according to the equation[26].

$$nE'\ r = Er' / 6\ RT \qquad (6.7)$$

where E'r is the dynamic storage modulus measured from the rubbery plateau region. Similarly, the crosslink density from swelling studies can be determined using the method discussed in chapter 2 (equations 2.30 and 2.31).

The crosslink density from dynamic mechanical measurements and from swelling studies (at 28 and 40^0 C) are presented in **Table 6.7.**

Table 6.7. Crosslink density values

Sample	Crosslink density values		
	From dynamic mechanical data X 10^2	From swelling studies gm mols /cc X 10^{-5}	
		28^0 C	40^0 C
G1	0.96	5.66	6.24
G2	1.08	5.85	6.44
G3	1.28	6.05	6.49
G4	1.6	7	7.13
G5	1.66	7.35	8.03
G6	1.6	6.44	7.28
G7	1.92	6.74	7.52
G8	1.33	5.48	5.85
G9	1.66	4.95	5.62

In the case of the crosslink density values from dynamic mechanical results, it is observed that with the addition of prophylactics to ENR, the crosslink density increases. The presence of carbon black, silica and marble powder is found to be increasing the crosslink

density from mixes of similar compositions without particulate filler. As the prophylactics content increases in samples with particulate fillers, an increase in crosslink density is observed.

The crosslink density values from swelling studies also are presented in **Table 6.7**. A slight increase in crosslink density is observed at 28 and 40 ^{0} C with the addition of prophylactics filler to ENR. This is due to the very high solvent resistance of ENR-50. The crosslink density values from swelling studies are found to be increasing with the addition of carbon black and silica while a drop is observed for marble powder filled sample.

The presence of strain-induced crystallisation in the samples can be confirmed using Martin-Roth-Stiehler[27] plots **(Figure 6.16)** drawn according to the equation given below.

$$\ln \sigma\lambda^2 / \lambda^{-1} = \ln E_0 + A (\lambda-\lambda^{-1}) \qquad (6.8)$$

where σ is the stress value, and λ is the extension ratio, E_0 and A are constants.

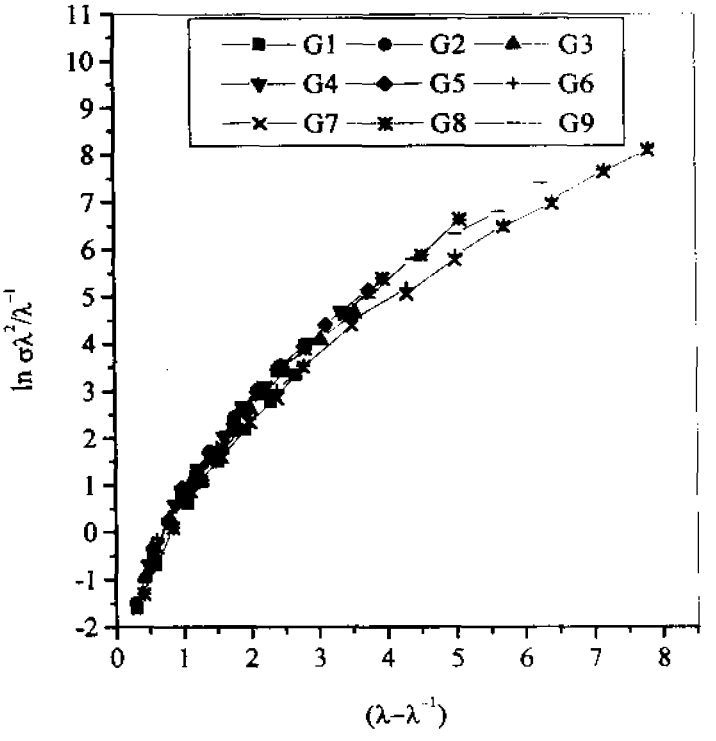

Figure 6.16. Martin-Roth- Stiehler plots

The plots of all the samples present changes in the slope. This is due to the strain-induced crystallisation of small prophylactics particles as well as ENR.

The activation energy E_{act} for the glass transition of the samples can be calculated using the Arrhenius equation given in chapter 2 (equation 2.9). E_{act} values are given in **Table 6.8**. The value is found to be decreasing with addition of prophylactics after an initial increase. The addition of particulate fillers decreases the E_{act} values. The most intense reduction is observed in the case of carbon black and least in the case of marble powder. The addition of prophylactics in the presence of particulate filler increases the E_{act} values.

Table 6.8. Energy of activation values

Sample	E_{act} (kJ)
G1	313
G2	543
G3	235
G4	163
G5	166
G6	247
G7	296
G8	279
G9	386

6.2 REFERENCES

1. A.M.Thayer, Chem.Eng.News, Jan 30, p.7 (1989).
2. S.J.Huang, Poly. Mater.Sci.Eng. 63, 633 (1990).
3. J.Tallman, Waste Age, 18, 141 (1987).
4. B. Wessling, Kunstoffe, 83, 7 (1993).
5. L.Slusarski and R. Sendlewski, Int. Polym. Sci. Technol, 9 (2), T/19 (1982).
6. K.Oliphant and W.E.Baker, Polym.Eng.Sci., 33 (3), 166 (1993).
7. J.R.M. Duhaime and W.E.Baker, Plast. Rubb. Compos. Process. Appln., 15 (2), 87 (1991).
8. P.Rajalingam, J.Sharp and W.E.Baker, Rubber Chem.Technol, 66, 664 (1993).
9. P.Rajalingam and W.E.Baker, Rubber Chem.Technol, 65, 908 (1992).
10. D.Gibala and G.R.Hamed., Rubber Chem.Technol, 67, 636 (1994).
11. I.Gawel and L.Slusarski., Prog.Rubb.Plast.Technol, 15(4), 235 (1999).
12. N.Sombatsompop., J.Elast.Plast, 31,271 (1999).
13. H.S.Liu, J.L.Mead and R.G.Stacer, Rubber Chem.Technol, 73,551 (2000)
14. Worldwide Rubber Statistics, International Institute of Synthetic Rubber Producers., Houston, TX, 1982.
15. A.A.Phadke, S.K.Chakraborty and S.K.De, Rubber Chem.Technol., 57,19 (1984).
16. L.E.Nielsen and R.F.Landel, "Mechanical Properties of Polymers and Composites", 2nd edn., Marcel Dekker, Inc, NY, 1994.
17. I.R.Gelling, Rubber Chem.Technol., 58,86 (1985).
18. I.R.Gelling, J.Nat.Rubb.Res., 6 (3), 184 (1991).
19. A.K.Manna, S.Dutta, M.K.Chatterjee, P.P.De, D.K.Tripathy and S.K.De., Proc. Internat. Conf. Rubb., Culcutta, India, Dec.12-14, 1997.
20. T.Ahsan, B.A. Colenutt, K.S.W.Sing., J.Chromatog, 479:17 (1989).
21. J.J.Fay, C.J.Murphy, D.A.Thomas and L.H.Sperling., Polym.Eng.Sci, 31, 1731 (1991).
22. M.Y.Boluk and H.P.Schreiber, Polym. Compos., 7, 295 (1986).
23. L.E. Nielsen, Mechanical Properties of Polymers and Composites, Vol 2, Marcel Dekker, Inc, NY, 1974.

24. G.L.Ball, SPE ANTEC, Tech. Papers, 17, 71 (1971).

25. L.R.G.Treolar, "The Physics of Rubber Elasticity", 3rd edn. Oxford, Clarendon Press, 1976.

26. B.Saville and A.A.Watson, Rubber Chem.Technol, 40, 100 (1967).

27. G.M.Martin, F.L.Roth and R.D. Stiehler., Trans. IRI., 32, 189 (1956).

Chapter 7

CHAPTER 7

DEVELOPMENT AND CHARACTERISATION OF NOVEL EPDM / NR PROPHYLACTICS WASTE COMPOSITES

ABSTRACT

The development and characterisations of novel ethylene propylene diene rubber (EPDM) compounds have been discussed in this chapter. The cure curves of EPDM compounds have been found to be the resultant of slow curing or marching cure curve of EPDM and that of fast curing 'S' shaped curing curve of natural rubber. The curing properties such as optimum cure time, scorch time and induction time have been found to be decreasing with the loading of prophylactics filler. But for most of the cases the values obtained for compositions with virgin natural rubber (ISNR-5) have been found to be lower than that with prophylactics filler. This behaviour is due to the difference in the curing behaviour of EPDM and ISNR-5. The increase in temperature has activated the cure process as can be seen from the increased cure rate index and cure rate constant values. These observations have been supported by the higher value of energy of activation for the gum EPDM compound. Thermal ageing produces mixed results regarding the improvement/deterioration in properties. Unaged tensile strength has been increased with the loading of prophylactics up to 30 phr. Samples with virgin natural rubber give better tensile strength compared to those with prophylactics. Crosslink density values determined from Mooney-Rivlin equation agree with the tensile strength values for most of the cases. An increase in the crosslinks density has been noted with the thermal ageing of the samples. The diffusion process in EPDM vulcanisate is found to be anomalous. The observed variation in the equilibrium swelling has been supported by the intrinsic diffusion coefficient and molar equilibrium sorption constant while at 40^0C sorption and permeation coefficients also has been found to be in agreement. The perfect linearity of the sorption kinetic plots at room temperature indicates a first order kinetic process of diffusion. But at high temperature of 40^0C, deviations from linearity have been observed.

CHAPTER 7

DEVELOPMENT AND CHARACTERISATION OF NOVEL EPDM / NR PROPHYLACTICS WASTE COMPOSITES

Results of this chapter have been communicated to J. Mater. Sci

Rubber products based on EPDM form a very interesting class of materials. EPDM differs from the general purpose elastomers like natural rubber in having a saturated hydrocarbon backbone, therefore, it offers unusually good, oxidation, ozone, thermal, electrical and chemical (weathering) and cut growth resistance[1,2]. These properties result mainly from its low content of unsaturation. Several research publications are available on EPDM focusing its chemical modification[3], detailed vulcanisation behaviour[4], and heat transfer model[5] calculations to predict mechanical properties. On the other hand, natural rubber finds use as a component in tire tread because of its excellent mechanical properties. It also differs from other elastomers in showing strain crystallising nature. It therefore offers good physical properties, but suffers from poor weathering and thermal resistance. All these properties result from its high content of unsaturation and ability for strain crystallisation.

A blend of EPDM and NR exhibits a useful combination of several properties such as good ozone and chemical resistance, better mechanical properties, reduced compression set and improved building tack properties[6] etc. They can give acceptable compromise between the properties of the components, e.g., NR phase can provide good physical properties without the use of highly reinforcing fillers and expensive coupling agents while EPDM phase can provide good heat aging and ozone resistance with out the use of antidegradants. Several studies in this area are available in the literature with special reference to the 60:40 ratio of NR:EPDM which can provide excellent ozone resistance without the addition of any antiozonant[7]. Apart from property benefits, the blends of EPDM and NR are also attractive in an economic point of view. The recycling of NR and EPDM giving emphasis to the process mechanism also is described in the literature[8].

This chapter reports some of the results on the development and characterisation of composite materials based on EPDM. The matrix EPDM was filled with two other elastomer inclusions such as natural rubber prophylactics waste and ISNR-5. The curing behaviour of the rubber compounds, physical properties and swelling behaviour of the vulcanisates were analysed with special reference to the influence of changes in temperature.

7.1. Results and discussions

The compound formulations used for the present work are given in **Table 7.1.**

Table 7.1. Basic formulation

Material	Loading (phr)						
	A0	**A1a**	**A1b**	**A2**	**A3**	**A4a**	**A4b**
EPDM	100	100	100	100	100	100	100
NR Prophylactics	0	10	0	20	30	40	
ISNR-5	0		10				40
ZnO	5	5	5	5	5	5	5
Stearic acid	2	2	2	2	2	2	2
MBTS	0.5	0.5	0.5	0.5	0.5	0.5	0.5
DPG	0.4	0.4	0.4	0.4	0.4	0.4	0.4
DCP	2.25	2.25	2.25	2.25	2.25	2.25	2.25
Sulphur	1.5	1.5	1.5	1.5	1.5	1.5	1.5

7.1.1. Curing properties

The rheographs which characterise the crosslinking process[9] of the rubber compounds at different temperatures (150, 160 and 170^0 C) are presented in **Figure 7.1** to **7.3**. Marching cure observable in the rheographs is characteristic of EPDM compounds.

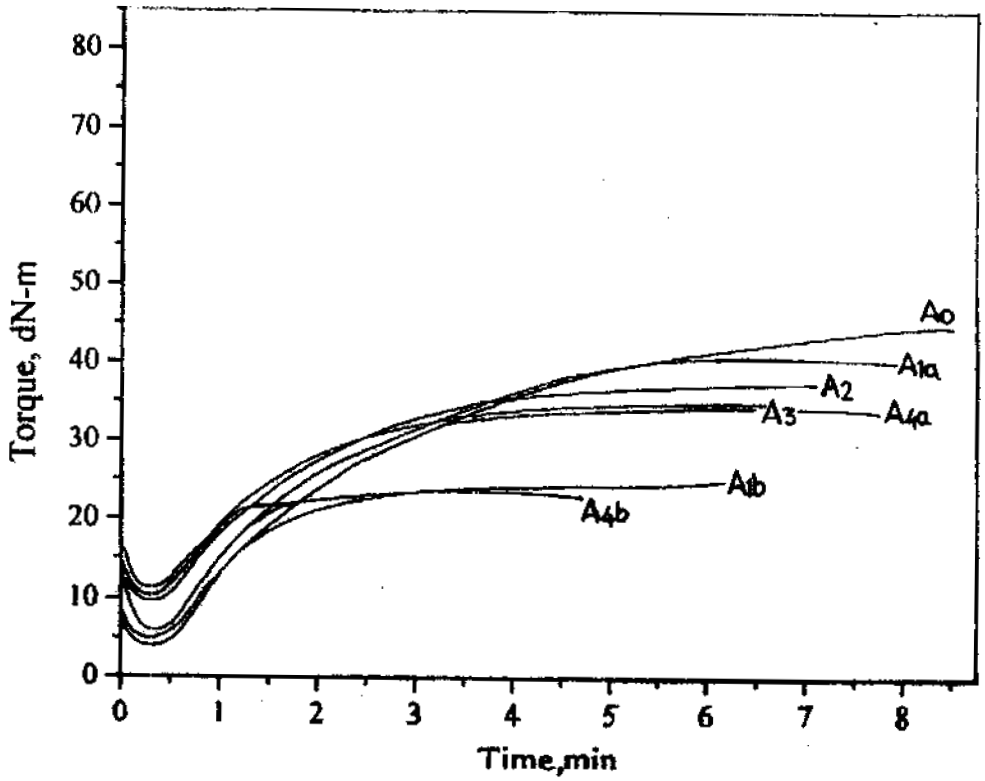

Figure 7.1. Rheographs of the EPDM/prophylactics filler compounds at 150° C

The initial (M_i), minimum (M_n) and maximum torque (M_h) values are presented in **Table 7.2.**

Table 7.2. Rheometric data

Sample	Initial Toque (M_i)			Minimum Torque (M_n)			Maximum Torque (M_h)		
	150° C	160° C	170° C	150° C	160° C	170° C	150° C	160° C	170° C
A0	7	10	12	4.5	6.5	5.5	44.5	42.5	41.5
A1a	11	10	13	6	8	6.5	40	38	32.5
A1b	9	7	6	4.5	3	3	25	21	19
A2	15	16	13	9.5	10	8	36.5	33	32
A3	17	17	15	10	12	10.5	35	33	31
A4a	17	17	15	11	12.5	11.5	35	33	32
A4b	8	11	7	4.5	6	6	23	22.5	21.5

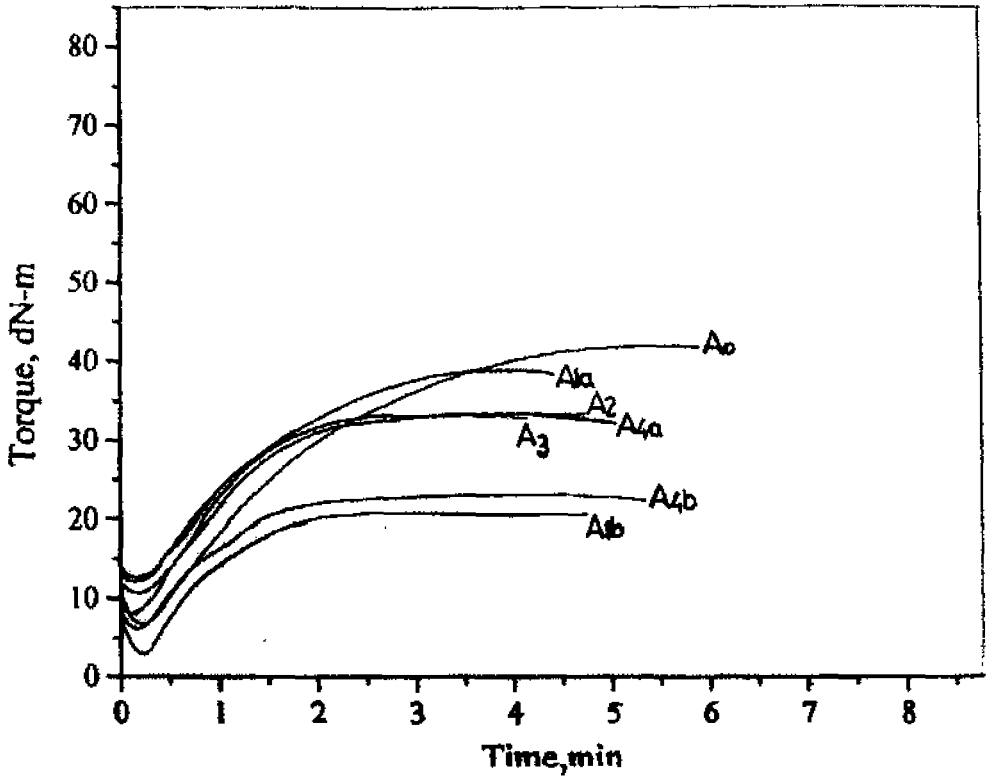

Figure 7.2. Rheographs of the EPDM/prophylactics filler compounds at 160^0 C

It can be seen from **Table 7.2** that as the amount of natural rubber prophylactics in EPDM increases, the initial torque increases. This can be made clear if a comparison of the values of A0, A1a, A2, A3 and A4a is made. The initial torque values shown by EPDM samples containing prophylactics are found to be higher than the corresponding ISNR-5 loaded samples (A1b and A4b). This is because of the lightly crosslinked nature of the prophylactics filler. Here, as the filler also is a rubber, only a slight increase in initial torque can be noted here.

It is clear from the **Table 7.2** that the substitution of natural rubber in the place of prophylactics filler results in a low value of minimum torque. This is true at both 10 and 40 phr loadings of the inclusions in EPDM. This is again due to the lightly crosslinked nature of the prophylactics. The maximum torque of the samples is found to be decreasing with prophylactics loading. In this case also lower values are obtained for the compositions with natural rubber such as A1b and A4b compared to prophylactics filled

samples (A1a and A4a).

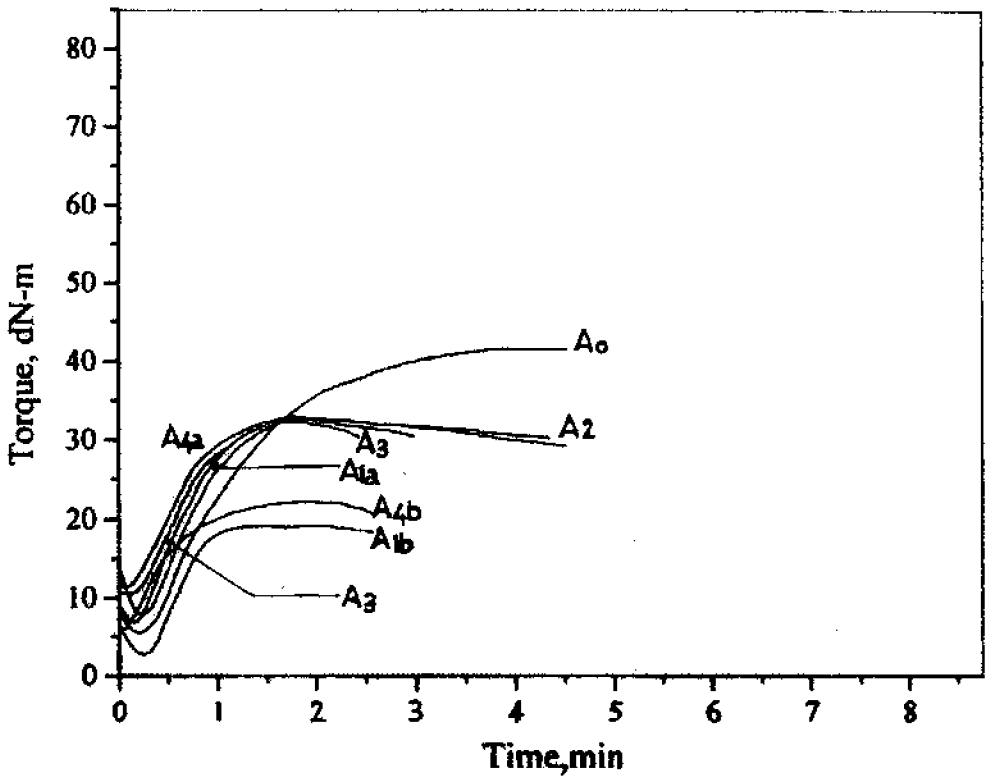

Figure 7.3. Rheographs of the EPDM/prophylactics filler compounds at 170^0 C

The influence of temperature on these properties also deserves much attention. As the temperature increases, the initial torque values of EPDM sample (A0) are found to be slightly increasing. But this trend is found to be becoming less predominant with increasing loading of prophylactics filler or ISNR-5. The values show an initial slight increase followed by a decrease at higher temperatures used in the study. In the case of minimum torque values also, the same behaviouris observed. A regular drop in the case of maximum torque is obtained with increasing temperature. The decreasing trend is due to the softening effect of temperature on the systems.

The variation of the curing properties such as optimum cure time (t_{90}), scorch time (t_2) and induction time (t_1) at 150^0 C are given in **Table 7.3**. These properties are calculated from the rheographs as reported earlier. It can be seen that, as the prophylactics

loading increases, t_{90} values show a decrease at 10 phr loading of prophylactics (A1a) and ISNR-5 (A1b). For further loadings of prophylactics, the value increases and then levels off at 40 phr prophylactics loading. In the case of t_2 and t_1 values also, an initial slight drop in the magnitude of the values are obtained, which is followed by a slight increase.

Table 7.3. Curing properties of EPDM compounds

Curing Property	Value						
	A0	**A1a**	**A1b**	**A2**	**A3**	**A4a**	**A4b**
Optimum cure time t_{90}, min							
150°C	29	20	12.3	18	18	18	9.5
160°C	19	11.5	11.2	10	9.5	9.5	8.5
170°C	13	6	5.8	5.8	5.3	5.5	4.8
Scorch time t_2, min							
150°C	3.3	3	2.5	2.75	2.75	2.75	3.5
160°C	2.3	1.8	1.9	2	1.75	2.25	2
170°C	2	1.5	1.65	1.75	1.5	1.25	1
Induction time t_1, min							
150°C	3	2.75	2.25	2.25	2.25	2.25	3
160°C	2	1.5	1.25	1.75	1.5	1.75	1.5
170°C	1.75	1.25	1	1.5	1.25	1	0.75

It can be seen that both at 10 and 40 phr loading of ISNR-5 (A1b and A4b), the optimum cure time values are below that of similar compositions with prophylactics (A1a and A4a). The initial reduction in optimum cure time with prophylactics loading is due to presence of unreacted accelerators or crosslink precursors in the prophylactics phase. However, the reduction in t_{90} values with the addition of 10 and 40 phr of natural rubber (ISNR-5) (A1b and A4b) is found to be more than that caused by prophylactics. This can be explained as follows. NR is very fast curing than both EPDM and prophylactics due to the higher concentration of unsaturation in it. This can be made clear by comparing the general nature of rheographs of EPDM and NR **(Figure 7.4)**.

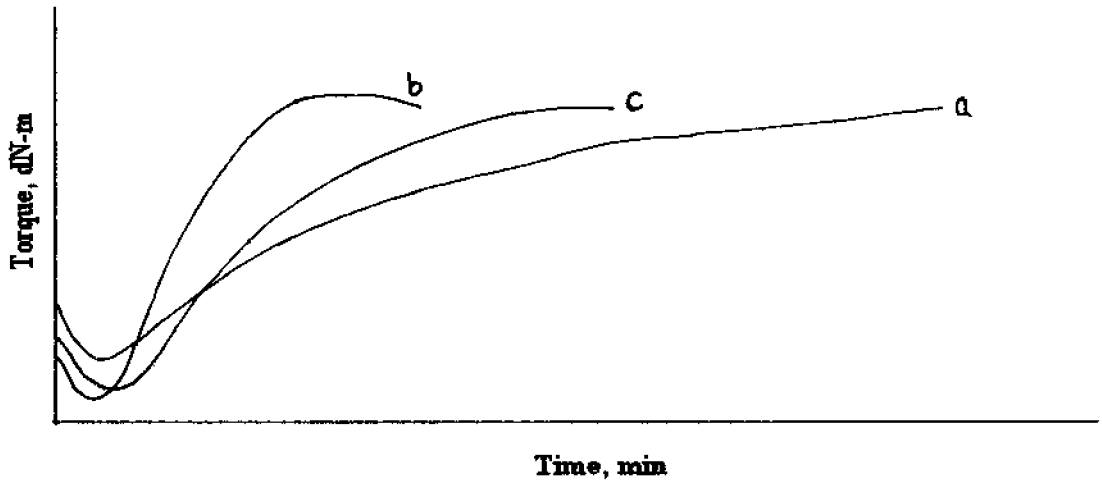

Figure 7.4. General nature of rheographs
(a). EPDM, (b). ISNR-5, (c). resultant rheograph

The rheographs obtained for a blend of EPDM and ISNR or NR prophylactics will be a resultant plot EPDM and NR. In a blend of EPDM and ISNR or prophylactics, the preference of curative will be in the order ISNR > NR Prophylactics > EPDM. So it is clear that when the curing of NR progresses fastly, the curing of EPDM and NR prophylactics lags behind. These factors are responsible for the lower t_{90}, t_2 and t_1 of ISNR-5 containing samples of EPDM than those with NR prophylactics.

The influence of temperature on the optimum cure time of the rubber compounds is presented in **Table 7.3**. The cure activating nature of temperature can be seen from here. There are two main observations connected with the influence of temperature on the crosslinking process of these systems. The primary one is that, at low temperature, an irregular drop in t_{90} is noted with the addition of prophylactics and ISNR 5. But at higher temperatures, the drop is almost in a regular manner. The second point to be noted is that, at low temperature, the difference in t_{90} values of EPDM – prophylactics system and EPDM - ISNR-5 system is higher than the corresponding difference at high temperature. This can be made clearer on comparing the t_{90} values of A1a & A1b and A4a & A4b.

In **Table 7.3**, observations on the influence of temperature on scorch time are presented. As already seen in the case of t_{90}, abnormalities in t_2 arise for the plots at

temperatures 150 and 160 ^{0} C. The addition of prophylactics filler initially reduces the scorch time values at 150^{0} C while at higher loadings, a leveling off is observed. At 160^{0} C, a slight increase in scorch time can be seen at higher loadings, while at the highest temperature a more regular drop is visible as the prophylactics loading increases. This is because of the complete decomposition of DCP at higher temperature. The vulcanisation system used here is a semi EV plus peroxide. The effect of peroxide will be shown predominantly at temperature 160^{0} C or above which is the decomposition temperature of DCP. So as the temperature increases, both sulphur and peroxide crosslinking occurs progressively and so the curing results present more regular trends than at low temperatures. The addition of 10 phr ISNR-5 (A1b) instead of natural rubber prophylactics (A1a), decreased the scorch time value at 150^{0} C while the addition of 40 phr ISNR-5 (A4b) increased it from a similar composition with prophylactics filler (A4a). On the contrary, a reverse trend could be seen at 160 and 170 ^{0} C. In the case of induction time **(Table 7.3)** also, an exactly similar observation is obtained.

The cure rate index **(Table 7.4)** and kinetics of cure reaction are analysed by the method explained earlier in chapter 2 (equations 2.2 and 2.6).

Table 7.4.Cure reaction kinetics data

Sample	Cure rate index CRI			Cure reaction rate constant (k)			Energy of activation (E_{act}) kJ / mol
	150^{0} C	160^{0} C	170^{0} C	150^{0} C	160^{0} C	170^{0} C	
A0	3.88	5.97	9.09	0.09	0.17	0.19	105.81
A1a	5.8	10.3	22.2	0.12	0.17	0.41	93.84
A1b	10.2	13	25	0.19	0.21	0.62	91.39
A2	6.5	12.5	25	0.10	0.18	0.34	92.36
A3	6.5	12.9	26	0.14	0.19	0.38	76.16
A4a	6.56	13.8	23.5	0.13	0.19	0.42	89.35
A4b	16.6	15.4	26.6	0.24	0.25	0.54	62.80

The plot of ln (M_h-M_t) verses time t of the elastomer compounds at 150 ^{0} C is shown in **Figure 7.5**. The plots are found to be linear which proves that the cure reactions

proceed according to first order kinetics. The cure reaction rate constants (k) are obtained from the slope of the respective linear equations. The cure rate index and cure rate constant values are presented in **Table 7.4**. At 150 and 160 ^{0} C, both CRI and k generally increases with increasing prophylactics loading. The CRI values obtained for natural rubber containing systems are much higher than the corresponding compositions with prophylactics filler. This is true for all the temperatures studied. The cure rate constants also show a slight increase with prophylactics loading. The intensity of this increase is found to be increasing with temperature. Also, comparatively high rate constant values are observed for compositions with ISNR-5.

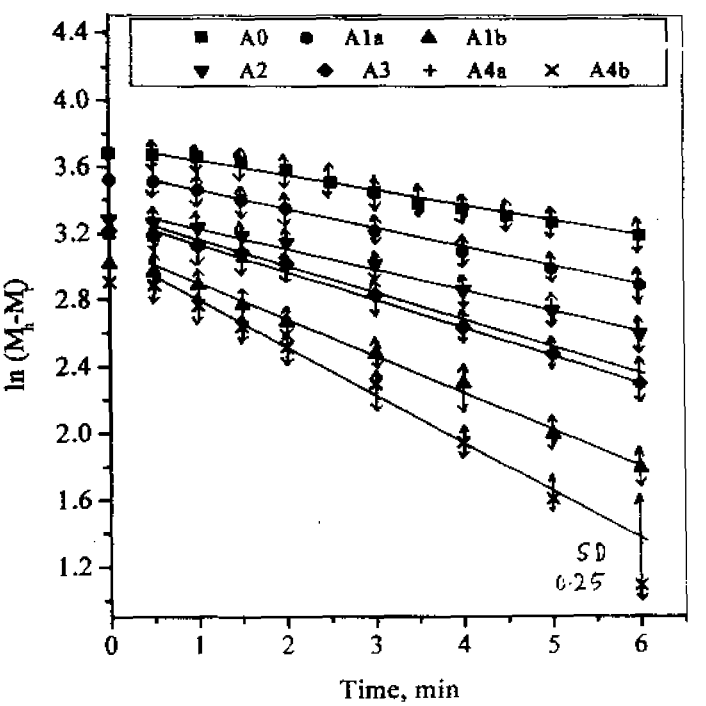

Figure 7.5. Plots of ln (M_h-M_t) Vs Time

The energy of activation values are calculated using Arrhenius equations given in chapter 2 (equation 2.7 and 2.8). The E_{act} values **(Table 7.4)** are calculated from the slope of a plot of log k verses 1 / T given in **Figure 7.6.** Normally fast reactions (higher k) yield lower values of E_{act}. In the case of EPDM gum sample, a high E_{act} value is observed. Also, as the loading of prophylactics filler increases, irregularly decreasing E_{act} values are

observed. The change in k values with the substitution of ISNR-5 (A1b and A4b) is well supported by the lower E_{act} values.

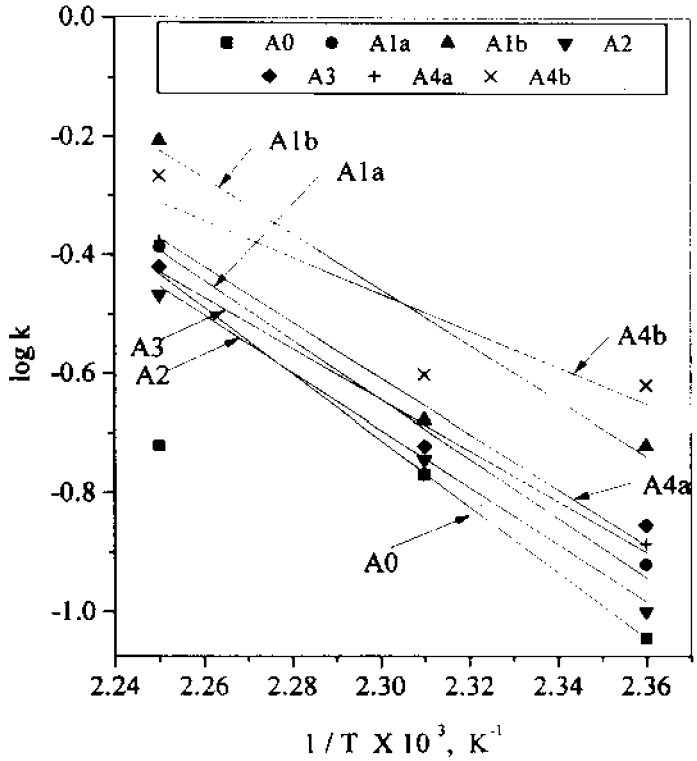

Figure 7.6. Variation of log k with absolute temperature

7.1.2. Technological properties

The stress-strain behaviour of a rubber network is mainly influenced by the presence of crosslinks and by constraints caused by the uncrossability of the network chains. The stress-strain curves of the unaged gum EPDM and prophylactics / ISNR-5 filled EPDM vulcansates are presented in **Figure 7.7**. The curves are slightly different from typical vulcanised low strength materials. This can be seen in the slightly rising stress value at higher strains while in the case of a low strength material such as SBR, the stress-strain plot will be parallel to the 'x' axis at higher strains.

It can be seen that at 10 phr loading of prophylactics (A1a), the initial linear portion of the curve is closer to 'y' axis. With the substitution of 10 phr ISNR-5 (A1b), the curve again bends towards 'y' axis. But as the prophylactics content increases further, the curve leans towards 'x' axis thus showing a drop in the rigidity of the vulcanisate.

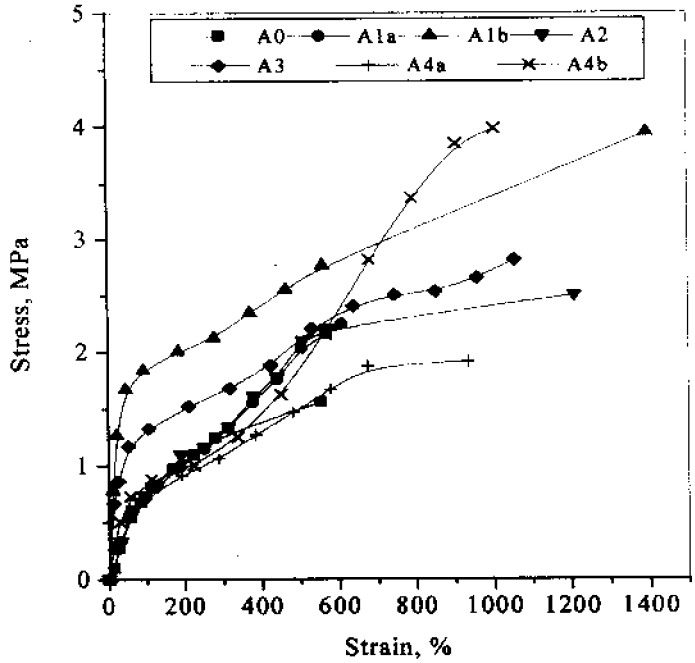

Figure 7.7. Stress-strain curves of unaged EPDM vulcanisates

The stress-strain curves after thermal aging is presented in **Figure 7.8**.

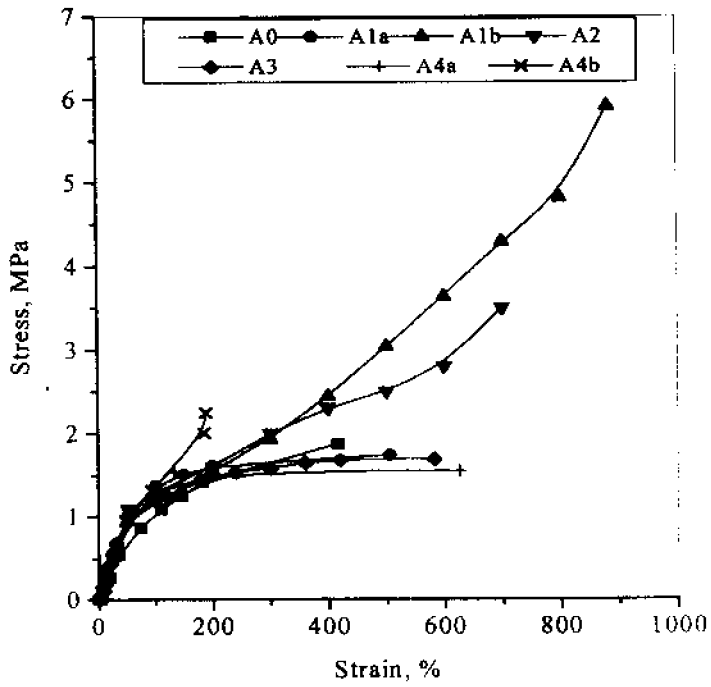

Figure 7.8. Stress-strain curves of aged EPDM vulcanisates

Here also similar behaviourcan be seen. But some samples such as EPDM with 30 phr natural rubber prophylactics (A3) presents a nature typical of vulcanised amorphous elastomers such as SBR.

The slope of the initial linear region of the stress- strain curve, presented as the Young's modulus is given in **Table 7.5.**

Table 7.5. Mechanical properties of EPDM vulcanisates

Mechanical Property	Sample code						
	A0	**A1a**	**A1b**	**A2**	**A3**	**A4a**	**A4b**
Young's Modulus (unaged), MPa	0.92	1.09	7.29	4.52	4.31	1.44	1.72
Young's Modulus (aged), MPa	1.25	1.45	2.29	2.01	2.13	1.65	1.88
Elongation at break (unaged), %	556	610	1396	1215	1056	936	1006
Elongation at break (aged), %	416	506	883	710	583	626	630
Tensile Strength (unaged), MPa	1.56	2.24	3.94	2.50	2.81	1.91 SD 0.08	3.98
Tensile Strength (aged), MPa	1.87	1.74 SD 0.02	5.9	3.5	1.69 SD 0.08	1.55 SD 0.25	2.25
Tear Strength, kN/m	8.19	10.6	13.5	13.2	13.4	13.9	13 SD 2.45
ν_{phys}, unaged, X 10^{-5}	4.7	13.1	21.5	19.6	13.1 SD 5.72	4.77	10.7
ν_{phys}, aged, X 10^{-5}	26.2	28	31	29.8	21.5	17.9	20.9

It is clear from table that for the unaged sample, the Young's modulus increases with the addition of 10 and 20 phr natural rubber prophylactics filler (A0, A1a and A2). This is due to the highly strain crystallising nature of the natural rubber prophylactics filler in the relatively weaker EPDM matrix. Further addition of prophylactics filler causes a decrease in Young's modulus. The values shown by ISNR-5 at 10 and 40 phr loadings (A1b and A4b) are higher than that by prophylactics filler. A similar observation is visible in the case of vulcanisates after thermal aging also. The Young's modulus is found to be affected to a great extent with thermal aging, except for certain samples such as A0, A1a, A4a and A4b, where a slight increase is observed. Even though generalisations cannot be made from these data, it is reasonable to think that addition of natural rubber prophylactics filler/ ISNR-5 can affect the thermal aging behaviourof EPDM.

The variation in elongation at break (e_b) is presented in **Table 7.5**. Elongation at break also is found to be increasing with the addition of 10 phr prophylactics. This is due to the ability of natural rubber prophylactics particles or ISNR-5 phases in EPDM matrix to elongate to high strains. Among the prophylactics loaded samples, the maximum value is obtained at a loading of 20 phr. Here also, the values are higher for the ISNR-5 filled samples at 10 as well as 40 phr loading. Even though thermal aging results in a decrease in the magnitude of the elongation at break values, the trend observed is the same.

The variation of unaged and aged tensile strength with the loading of inclusions is depicted in **Table 7.5**. As in the case of Young's modulus and elongation at break, here also the tensile strength initially increases at 10 and 20 phr prophylactics loading and then decreases. As in earlier cases, comparatively higher tensile strength values are shown by EPDM / ISNR-5 vulcanisates. The aged tensile strength also behaves in the same way. The superior aging resistance of the EPDM vulcanisates can be understood from the higher or comparable tensile strength values after thermal aging. This is noted for the samples A0, A1b and A2. This is due to the increase in crosslink density resulting from the influence of temperature during aging. Such results are reported in the literature[10,11]

The better aging resistance of gum EPDM sample is clear from the increased properties after thermal aging **(Table 7.6)**.

Table 7.6. Thermal aging data

Sample code	Percentage change in Young's modulus	Percentage change in Tensile strength
A0	35 (+)	19 (+)
A1a	33 (+)	28 (-)
A1b	68 (-)	49 (+)
A2	55 (-)	40 (+)
A3	50 (-)	66 (-)
A4a	14 (+)	23 (-)
A4b	9 (+)	77 (-)

(positive sign - increase in property, negative sign- decrease in property

The property variation observed after thermal aging varies from sample to sample. It is also important to note that the trend shown by Young's modulus and tensile strength are not similar. Better aging resistance shown by the EPDM samples, A0, A1a, A4a and A4b in the case of Young's modulus while in the case of tensile strength A0, A1b and A2

take that position. This can be analysed more clearly using **Table 7.6**, where percentage change in tensile strength after thermal aging of all the samples is presented. It is a general observation that as the content of natural rubber (as prophylactics or ISNR-5) in EPDM increases, the aging worsens the tensile strength while the trend is irregular in the case of Young's modulus. Sample A2 is an exception in the case of tensile strength variation. These observations reveal that in the case of present systems, there is no correlation between the stress-strain relation at low strain region (Young's modulus) and that at higher strain region (tensile strength). This is contrary to the behaviourshown by elastomer vulcanisates with particulate fillers where the common relation is "higher the Young's modulus, higher the tensile strength". This difference arises due to the difference in the mode of filler – elastomer interactions in these cases. In the case of an elastomer vulcanisate filled with some particulates, the property improvement is due to the adhesion between rubber layers and filler surfaces. This manifests in a number of phenomena such as bound rubber. On the other hand, in the present case, the property enhancement if any is due to the strain crystallising nature of the natural rubber prophylactics or ISNR-5 inclusion in a relatively low strength EPDM matrix. Therefore, any necessary correlation between Young's modulus and tensile strength need not be expected.

On increasing the loading of natural rubber prophylactics filler, tear strength increases sharply **(Table 7.5)** and levels off at higher loadings. Also better values are shown by the substitution of prophylactics filler with ISNR-5 only at 10phr. At 40 phr, the tear strength for EPDM / ISNR-5 system is lower than EPDM / prophylactics. The higher tear strength results from the ability of natural rubber prophylactics and ISNR-5 phases in EPDM to elongate to high strains and obstruct the advancing tear front.

The idea that one can obtain from these results is that the mechanical properties will be better if the inclusion also is allowed to vulcanise at the same cure cycle as the matrix. The difference between the properties of prophylactics and ISNR-5 filled EPDM systems occurs because vulcanisation of ISNR-5 takes place together with the vulcanisation of EPDM matrix while natural rubber prophylactics was already in a lightly crosslinked state during the mixing. ISNR-5 might have undergone an efficient mixing procedure with EPDM due to its low viscosity resulting from uncrosslinked state.

However, the lightly crosslinked nature of prophylactics and the resulting viscosity difference might be causing a number of secondary reasons for its inferior performance. Still, considering the economics aspects of the systems, better performing combinations of EPDM / Prophylactics /ISNR-5 reinforced with particulate fillers can be expected to produce better results.

7.1.3. Diffusion studies

The sorption curves of EPDM gum and prophylactics /ISNR-5 filled vulcanisates at room temperature and 40^0 C are presented in **Figures 7.9** and **7.10**, respectively. The mole% uptake, Qt of the solvent toluene is plotted vs. square root of time, t. The mole% uptake is calculated using equations given in chapter 2 (equation 2.14).

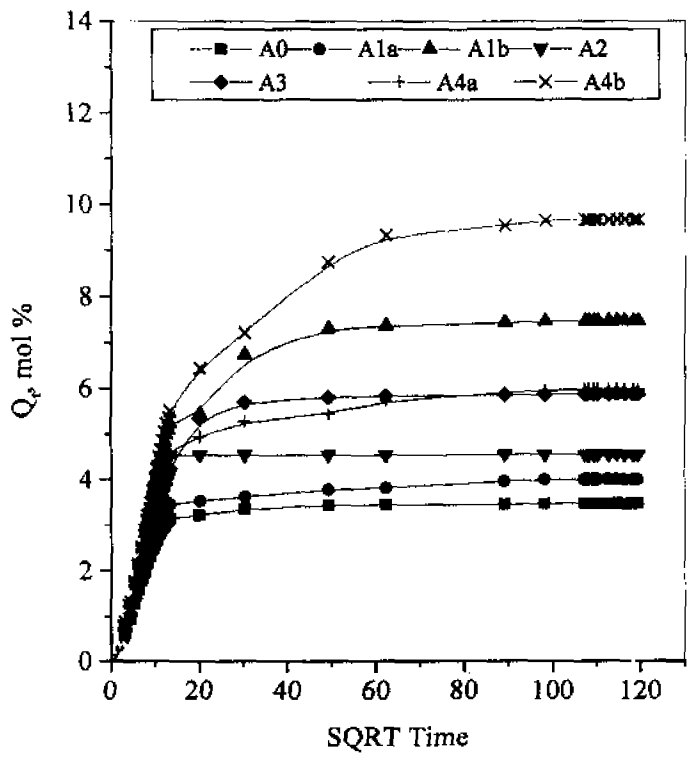

Figure 7.9. Sorption curves of EPDM vulcanisates at room temperature.

At equilibrium swelling, Q_t was taken as Q_∞ the mole% uptake at infinite time. It is clear from the figure that all the plots are sigmoidal. The sigmoidal shape is associated with the time taken by the polymer chains to respond to the swelling stress and rearrange themselves to accommodate the penetrant molecules[12]. It can be seen from the sorption

curves of the samples that the initial swelling rate is very high owing to the large concentration gradient. This keeps the polymer sample under intense solvent stress. But as the concentration gradient decreases with advancing swelling, the swelling rate decreases and the concentration difference becomes negligible at equilibrium swelling.

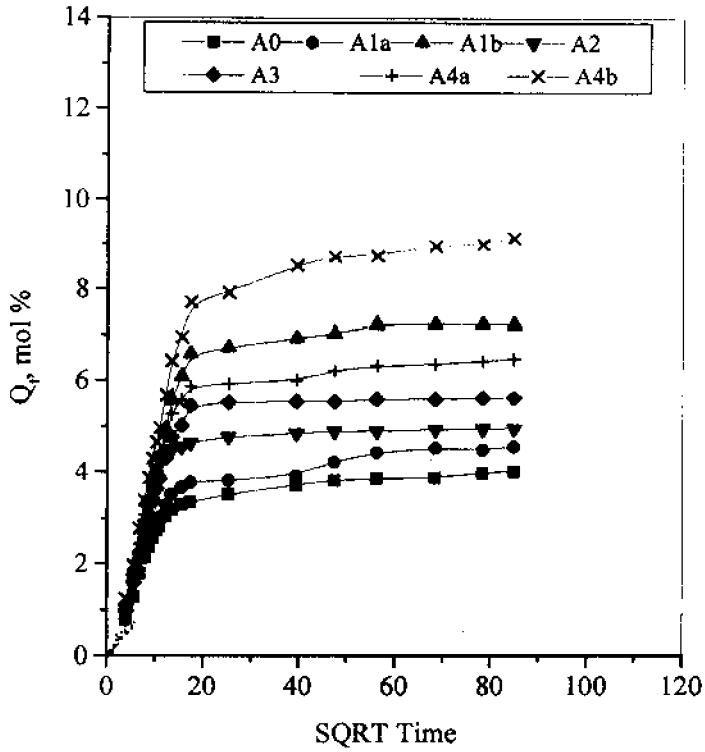

Figure 7.10. Sorption curves of EPDM vulcansates at 40^0 C.

The equilibrium mole% uptake value Q_∞ **(Table 7.7a)** of the samples at room temperature increase with increasing the content of second elastomer component, with very high values for EPDM vulcanisate filled with 10 and 40 phr ISNR-5. From this result we may be able to understand the inability of the prophylactics filler and ISNR-5 to restrict the solvent uptake just as other inorganic fillers do. But the analysis of other diffusion parameters such as k, K_s, D and D* shows uncomparable and abnormal trends.

The mechanism of penetrant transport into the elastomer network can be analy ed using the method[13] given in chapter 2 (equation 2.15). The factor k is a constant depending on the structural characteristics of the filler and polymer-solvent interaction. The parameter 'n' determines the mode of sorption mechanism. If the value of n is 0.5, it

means that the rate of diffusion of penetrant molecules is much less than the rate of relaxation of polymer chains. This mode of transport is termed as Fickian. On the other hand, if the value of 'n' is unity, the mode of diffusion is termed as non-Fickian where the rate of diffusion of penetrant molecules is much faster than polymer relaxation. When the rates of both processes are similar, value of 'n' will fall between 0.5 and 1, presenting an anomalous behavior. The computation of 'n' and 'k' is done by constructing the plots of log Q_t vs. log t followed by linear regression considering only the data upto 50% sorption. The values of 'n' and 'k' also are presented in **Table 7.7a**.

Table 7.7 a. Sorption data at 28^0 C

Sample Code	Q_∞ mol%	N	k gg^{-1} min^n x 10^{-2}	K_s min^{-1} x 10^{-2}	k_t min^{-1} x 10^{-3}	D X 10^{-5} cm^2s^{-1}	D* x 10^{-4} cm^2s^{-1}	ϕ	S gg^{-1}	P x 10^{-4} cm^2s^{-1}
A0	3.4597	0.6616	0.0378	0.0346	0.0056	5.70	16.7	0.2369	16.44	9.37
A1a	3.9895	0.6690	0.0335	0.0399	0.0047	4.82	18.0	0.2121	3.68	1.78
A1b	7.4491	0.7001	0.0214	0.0745	0.0028	2.17	27.0	0.1260	6.86	1.49
A2	4.5421	0.6711	0.0285	0.0421	0.0037	4.15	21.6	0.1824	5.24	1.73
A3	5.8616	0.6887	0.0229	0.0586	0.0029	3.10	24.1	0.1549	5.40	1.68
A4a	5.9587	0.6825	0.0262	0.0596	0.0035	3.22	25.8	0.1527	5.49	1.77
A4b	9.6554	0.6860	0.0178	0.0966	0.0019	1.78	38.2	0.1001	8.89	1.58

Since the value of 'n' obtained here falls in the range 0.5 to 1, the process can be considered to be anomalous. From the lower value of 'n' for EPDM gum vulcanisate, it is reasonable to think that in this sample, the diffusion of the permeant might have slowed down compared to that in filled vulcanisates. The parameter 'k', which characterises the polymer - solvent interaction is found to be reducing with the amount of prophylactics **(Table 7.7a)** which also is not in agreement with the observed trend in solvent uptake Q_∞. Since the value of 'n' obtained here falls in the range 0.5 to 1, the process can be considered to be anomalous. From the lower value of 'n' for EPDM gum vulcanisate, it is reasonable to

think that in this sample, the diffusion of the permeant might have slowed down compared to that in filled vulcanisates.

The effective diffusivity[14], D of the elastomer solvent system was calculated as described in chapter 2 (equation 2.16) Since extensive swelling was observed for most of the samples, correction to diffusion coefficients is necessary by calculating the intrinsic diffusion coefficients[15], D* given in chapter 2 (equation 2.17) The value of D and D* are given in **Table 7.7a**. It can be seen that D values of the prophylactics or ISNR-5 filled vulcanisates show a decreasing trend even though it is not in a regular manner. This trend shown by D values doesn't correlate with the swelling phenomena observed here from $Q\alpha$ results. Meanwhile the corrected D values (D*) are in agreement with the increased solvent uptake. When the higher Q_f value of ISNR-5 filled samples with respect to prophylactics filled samples is unsupported by D values, this also is supported by D* values. The importance of correction to diffusion coefficient can be understood from these results on diffusion of extensively swelling elastomer vulcanisates.

Another parameter called sorption coefficient, also is calculated from the equilibrium swelling using the relation[16] given in chapter 2. It can also describe both the initial penetration and dispersal of penetrant molecules into the elastomer network. Here $M\alpha$ is the mass of the penetrant sorbed at infinite time and M_0, the initial weight of the polymer sample. The values of sorption coefficient of the samples at room temperature also are presented in **Table 7.7a** and are found to be not in good agreement with the mole % uptake values in the same table. The permeation coefficient (P), which is a characteristic parameter reflecting the collective processes of diffusion and sorption is calculated as given in chapter 2. The permeation coefficient values given in the same table, also depicts similar abnormality as earlier denoted for D. Similar behaviour as D* is shown by the molar equilibrium sorption constant K_s **(Table 7.7a)**, which is defined by Hung[17] as

$$Ks = \frac{\text{No. of moles of solvent sorbed at equilibrium}}{\text{Mass of polymer sample}} \qquad (7.1)$$

Therefore in the present work, only D* and Ks are in agreement with observed increasing solvent uptake behaviour of the EPDM vulcanisates with increasing loading of prophylactics filler.

Sorption data at 40^0 C is given in **Table 7.7b**.

Table 7.7 b. Sorption data at 40^0 C

code	Q_∞ mol%	n	k gg^{-1} min^n x 10^{-2}	K_s min^{-1} x 10^{-2}	k_1 min^{-1} x 10^{-3}	D x 10^{-5} cm^2s^{-1}	D* x 10^{-4} cm^2s^{-1}	ϕ	S gg^{-1}	P x 10^{-4} cm^2s^{-1}
A0	4.0109	0.5907	0.0438	0.0401	0.0024	5.08	19.1	0.2112	3.69	1.88
A1a	4.5608	0.6209	0.0354	0.0456	0.0024	4.89	23.4	0.1906	4.20	2.06
A1b	7.2187	0.6926	0.0222	0.0722	0.0034	3.35	39.5	0.1295	6.65	2.23
A2	4.9543	0.6299	0.0356	0.0459	0.0031	5.11	29.1	0.1875	4.82	2.34
A3	5.6197	0.6456	0.0323	0.0562	0.0046	5.01	35.7	0.1605	5.18	2.59
A4a	6.4822	0.6241	0.0346	0.0648	0.0033	3.86	36.7	0.1421	5.97	2.31
A4b	9.1388	0.7223	0.0190	0.0914	0.0026	2.89	55.4	0.1052	8.42	2.43

The Q_∞ values also register an increase with prophylactics loading. It is also seen that at lower loadings of natural rubber prophylactics, increase in swelling temperature causes an increase in Q_∞, while at higher loadings, a decrease is obtained. But in the case of D, an increase is observed at all the systems except gum EPDM sample. The same is the case of D*, but all the samples behave in the same way without any exception. Another difference which observed for the diffusion behaviour at 40^0 C is the similar value of S for the EPDM gum sample to that of filled EPDM samples. On the other hand, for the experiment at 28^0 C, an abnormally high value of S was obtained for the gum EPDM sample. A bit different from what stated earlier for the diffusion at 28^0 C, here D*, K_s and in addition S and P also are found to be in agreement with the trend in Q_∞ with increasing prophylactics loading. Earlier in the case of curing parameters also, similar influence of higher temperature in clearing the abnormalities of the results was discussed. The observations here also supports this fact.

7.1.4. Sorption kinetics

In the case of a polymeric network, which is extensively being swollen by a penetrant, the diffusion process is characterised by linear kinetics. According to Thomas and Windle[18] a thermodynamic swelling stress is exerted by the penetrant on the polymer network, which therefore undergoes time dependant mechanical deformation. But in the early stages of swelling, this deformation is prevented[19] to some extent by the undeformed and unswollen polymer layers below. This factor extends the stress into two dimensions. But with the progress of swelling process, the magnitude of the stress is reduced and the equilibrium swelling of the surface layer occurs. Since the rate determining step of the process is the above said time dependent mechanical deformation, it can be confirmed that rate of sorption will be proportional to the difference in osmotic pressure inside and outside the polymeric materials[20]. Consequently, since this can be related to the concentration of the penetrant in the polymer, the first order kinetic equations given in chapter 2 (equation 2.22) can be used. The first order rate constant values (k_1) are obtained from a plot of log (C_α - C_t) Vs. time t for the experiment at room temperature **(Figure 7.11)** and 40^0 C **(Figure 7.12)**. It can be clearly understood from the linearity of the plots in **Figure 7.11** that the kinetics of diffusion of gum EPDM and natural rubber prophylactics/ISNR-5 filled samples follow first order kinetics at room temperature while at 40^0C, some deviation from linearity is observed **(Figure 7.12)**. The values of k_1 are a measure of the speed with which the polymer chain segments and penetrant molecules exchange their positions. The k_1 values are presented in **Tables 7.7 a** and **b**. The first order rate constant k_1 values decrease until 30 phr **(Table 7.7a)** loading of prophylactics waste while a higher value is obtained at 40 phr loading.

The initial decreasing trend in the k_1 values points out that the addition of natural rubber prophylactics slows down the initial rate of uptake of the solvent by the vulcanisate. Again, it is interesting to note how the present system behaves differently from other particulate filled vulcanisates. In the case of elastomer vulcanisates filled with particulate fillers, both the initial rate and equilibrium solvent uptake values vary in the same manner with increasing loading of the filler. But for the present case, such a correlation cannot be seen as equilibrium uptake value increases while rate of initial uptake

decreases with prophylactics loading. The drop in the initial rate of uptake reflected in first order the rate constant values is due to the heterogeneous nature of the composite samples. But as these prophylactics filler particles also start absorbing solvent at later stages of the diffusion process, the final uptake value increases with prophylactics loading.

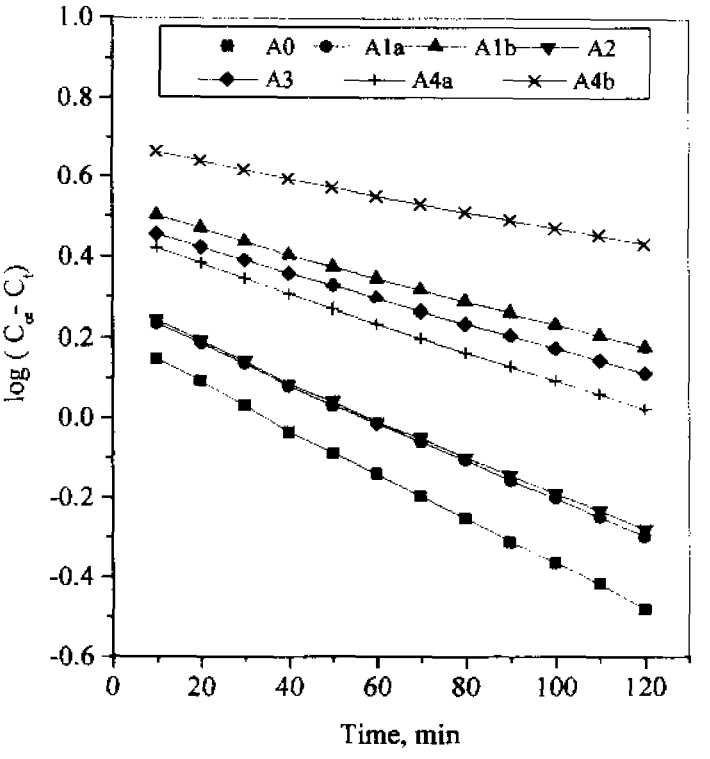

Figure 7.11. Plots of log (C∞ - Ct) Vs. time at 28^{0}C

The low rate of ISNR-5 filled samples compared to prophylactics filled samples can also be seen from **Table 7.7a**. The rate constant values of the diffusion at 40^0 C can be seen from **Table 7.7b**. A similar behaviour can be observed here also. As the temperature increases, the magnitude of the rate constant values decreases for the EPDM samples with 10 and 20 phr prophylactics loading. But after this loading, for the samples A3 and A4b, the values are found to be higher at higher temperature. Slightly lower values of k_1 at both temperatures are shown by the sample A4a.

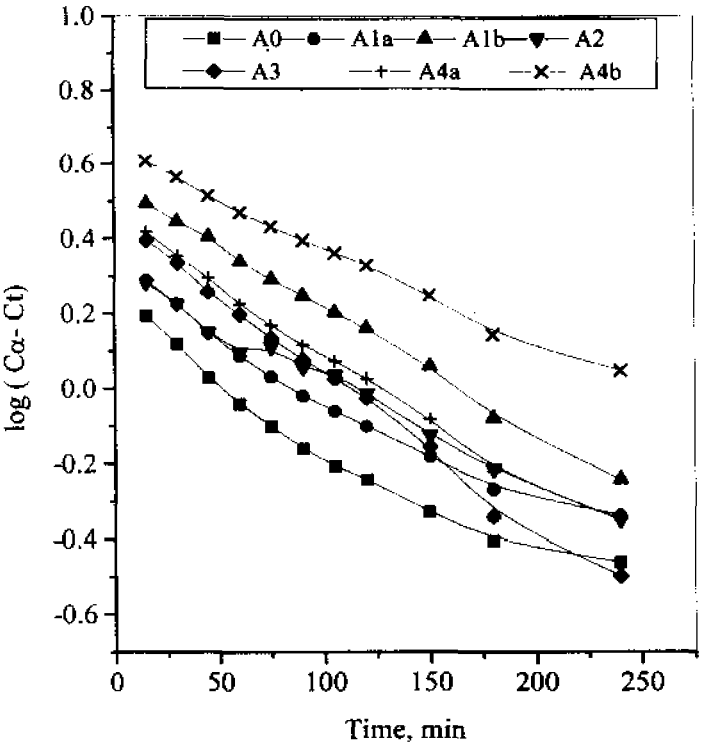

Figure 7.12. Plots of log (Cα- Ct) vs. time at 40^{0}C

7.1.5. Calculation of crosslink density

The crosslink density values were calculated from stress- strain data using Mooney -Rivlin equation[21]. The method is described in chapter 2 (equations 2.28 and 2.29). The plots obtained for both unaged and aged samples are given in **Figure 7.13** and **7.14** and the values of ν_{phys} are given in **Table 7.5**. The ν_{phys} values increase at 10 phr loading of prophylactics filler and then decrease for further loadings. Therefore, the maximum extent of physically effective crosslinks ν_{phys} can be seen for EPDM sample filled with 10 and 15 phr prophylactics filler. It can be seen from a comparison of values in **Table 7.5** that ν_{phys} gives better agreement with the observed tensile strength data. The higher ν_{phys} values of ISNR-5 filled samples compared to prophylactics filled samples at 10 and 40 phr loading (**Table 7.5**) are in agreement with the observed tensile strength values presented in the same table.

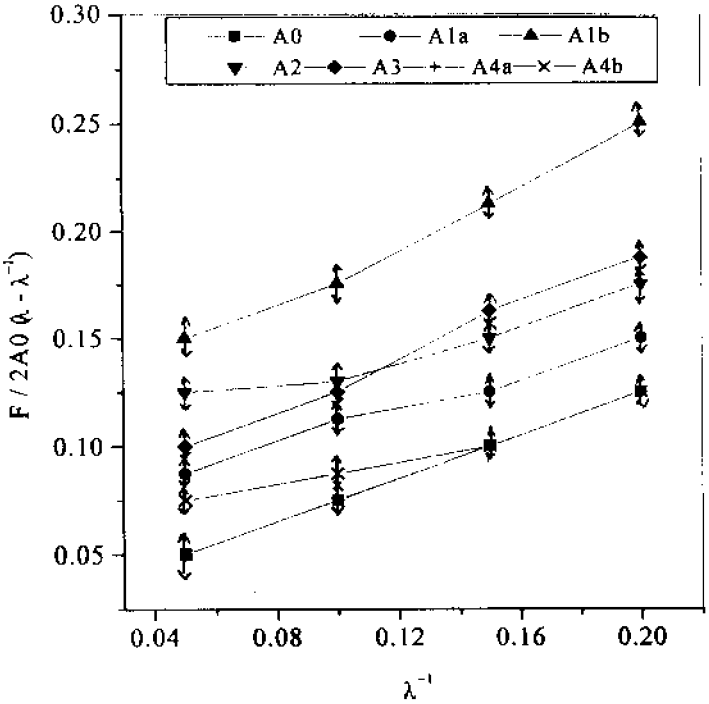

Figure 7.13. Plots of $F / 2A_0(\lambda - \lambda^{-1})$ Vs. λ^{-1} for unaged vulcanisates

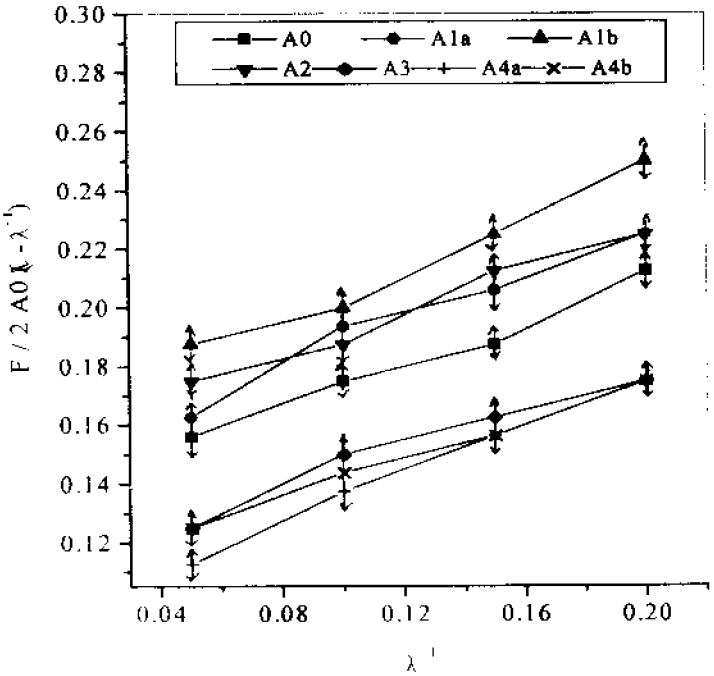

Figure 7.14. Plots of $F/ 2A_0(\lambda - \lambda^{-1})$ Vs. λ^{-1} for aged vulcanisates

7.2 REFERENCES

1. V.G.Costa and R.C.R.Nunes, Eur.Polym.J., 30(9),1025 (1994).
2. N.P.Cheremisinoff, Polym.Plast.Technol.Eng.31,713 (1992).
3. A.K.Ray, A.Jha and A.K.Bhowmick, J.Elast.Plast, 29,201 (1997).
4. J.L.M. Verschuuren, R. Zeeman, L.van der Does and A. Bantjes, Kautsch Gummi. Kunstst, 49(5), 336 (1996).
5. H.J.H. Beelen and L.R. Maag, Kautsch Gummi. Kunstst, 48(9), 617 (1995).
6. A.Y.Coran, Rubber Chem. Technol., 64,801 (1992).
7. S. Cook and R.M. Escolar, "Blends of Natural Rubber", First Ed. Andrew J.Tinker and Kevin P.Jones, Chapman and Hall, , Compounding NR/EPDM blends for light – coloured applications, chapter 16, p. 209, 1998.
8. M.A.L.Verbruggen, L.van der Does, J.W.M.Noordermeer, Rubber Chem. Technol, 72,731 (1999).
9. Worldwide Rubber Statistics, International Institute of Synthetic Rubber Producers., Houston, TX, 1982.
10. M. Baba, J. Lacoste, J.L. Gardette., Polym. Degrad. Stabil., 65, 421 (1999).
11. M. Baba, J. Lacoste, J.L. Gardette., Polym. Degrad. Stabil., 65, 415 (1999).
12. U. S. Aithal, T. M. Aminabhavi and P.E. Cassidy., J. Membr. Sci., 50, 225 (1990).
13. L. M.Lucht, and N.A.Peppas, J. Appl. Polym. Sci., 33, 1557 (1987).
14. T. M.Aminabhavi and R. S.Khinnavar, Res.Polym., 34(5), 1006 (1993).
15. T. M.Aminabhavi and R.S. Khinnavar, J.Chem Edn., 68, 343 (1994).
16. S. B. Harogoppad and T. M.Aminabhavi, Macromolecules, 24, 2595 (1991).
17. G. W. C. Hung, Microchem J., 19,130 (1974).
18. N. L. Thomas and A. H. Windle, Polymer., 18, 1195 (1977).
19. E. Southern, and A.G.Thomas., J. Polym. Sci. (A), 3, 641 (1965).
20. J. D. Cosgrove, T.G.Hurdley and T.Lewis, J., Polymer, 23, 144 (1982).
21. L. R. G. Treloar., "The Physics of Rubber Elasticity", 3rd Edn., Clarendon Press, Oxford, 1976.

Chapter 8

CHAPTER 8

IMPACT MODIFICATION AND DYNAMIC MECHANICAL ANALYSIS OF POLYSTYRENE / NR PROPHYLACTICS WASTE COMPOSITES

ABSTRACT

This chapter discusses the use of natural rubber prophylactics filler of varying particle sizes in a brittle plastic, polystyrene. It has been observed that pure polystyrene exhibits linear or near linear stress-strain behaviour while that of its composites deviates from linearity. The Young's modulus and tensile strength values have been decreased with the loading of prophylactics. Comparatively higher values of Young's modulus have been observed for samples with size 1 prophylactics filler at all the loadings. But such an observation is not obtained for tensile strength. The strain induced crystallisation of filled polystyrene composites has been proved by Martin-Roth-Stiehler plots. Good improvement in impact strength of polystyrene has been obtained with the loading of size 1 prophylactics. This observation has been supported by the scanning electron microscopic observations revealing the impact toughening mechanisms. Increase in the storage modulus value of pure polystyrene has been noted with increasing frequency of measurement. Loading of prophylactics (size 3) has been found to be decreasing the storage modulus values at temperatures below the polystyrene transition, while above this transition polystyrene presents a lower modulus. Among the different particle sizes of prophylactics filler used, 30 phr loading of size 3 presents a higher storage modulus at temperatures below the main transition while the minimum value has been shown by size 1. In loss modulus-temperature plots, pure polystyrene exhibits only one transition around 85^0C while all composite samples exhibit two transitions, one around –58 to -36^0 C range due to prophylactics and the other around 100^0C which is due to polystyrene. The phase-separated nature of the composite samples has been supported by both loss modulus-temperature and tanδ - temperature plots presenting two well-defined transitions. The glass transition values of polystyrene

determined from the loss modulus-temperature plots have been found to be increasing with the frequency of measurement except in the case of pure polystyrene. An increase in the Tg value of polystyrene has been observed with the loading of prophylactics even though it is in an irregular manner. Similar observation is noted with the addition of prophylactics of size 2 particle size also. Particle size of the prophylactics filler is not found to exhibit any clear trend in the variation of Tg values.

CHAPTER 8

IMPACT MODIFICATION AND DYNAMIC MECHANICAL ANALYSIS OF POLYSTYENE / NR PROPHYLACTICS WASTE COMPOSITES

Results of this chapter have been communicated to J. Polym. Recycl

The early part of this century considered polymeric materials as substitutes for traditional natural products. Later, with the development of advanced products with excellent physio-chemical properties, they began to perform important roles in other fields also. The use of polyolefin plastics leads to considerable savings in energy and time and among polyolefins, the position of polystyrene is noteworthy. Polystyrene is an engineering material but it suffers from a serious disadvantage which is its brittleness. Therefore, a considerable amount of impact resistance has to be introduced. This is usually achieved by combining the material with elastomers. Several works in this area are available from the lierature[1-17]. Research work also focused on the recycling of plastics[18], development of blends based on recycled plastics[19]. Similar studies on polystyrene also are available in the literature[20-25].

This chapter deals with the impact modification of polystyrene with increasing loading of natural rubber prophylactics waste of varying particle sizes such as size 1, 2 and 3. The particle size and size distribution were given earlier in chapter 3 **(Figure 3.3 and Table 3.2)**. Emphasis has been given to stress-strain behaviour, mechanical and dynamic mechanical properties and fractography of the composites.

8.1. Results and discussions

Solution mixing using toluene is used for the preparation of the composites. The recipe used for the study is given in **Table 8.1.**

Table 8.1. Basic recipe

Material	**Control (parts per hundred parts of plastic-php)**
Polystyrene	100
NR Prophylactics filler (Size 1,2 & 3)	Variable (0,5,10,15,20,25,30)

8.1.1. Technological properties

Figure 8.1 represents the stress-strain curves of polystyrene and its composites with NR prophylactics rejects (size 1).

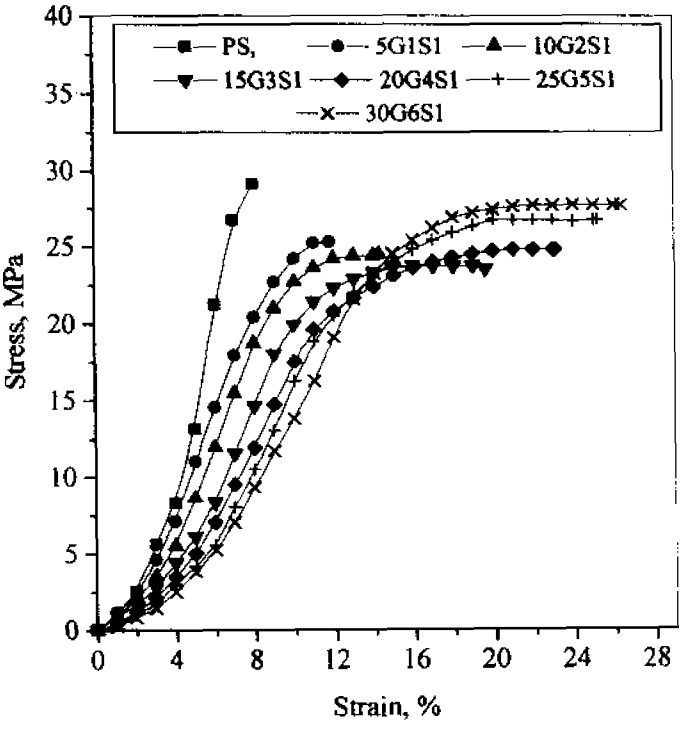

Figure 8.1. Stress-strain curves of polystyrene and composites

It can be seen that polystyrene presents its linear or near-linear stress-strain behaviour. As the content of NR prophylactics increases, the curves show a bending nature downward indicating a reduction in the modulus and an increase in the capacity of the material for

elongation. More over, the linearity of the curves also is affected in the composites. Similar behaviour is noted with the stress-strain curves of polystyrene composites containing NR prophylactics filler of higher particle sizes 2 (S2) and 3 (S3). The Young's modulus values calculated from the stress-strain curves are given in **Figure 8.2**. The value for polystyrene and composites fall in 120-440 MPa range. The values obtained for composites are below that of polystyrene. Also as the loading of NR prophylactics increases, there is a reduction in the modulus values. This is normal to be expected from the addition of an elastomer to a glassy plastic such as polystyrene. It can also be seen that comparatively higher Young's modulus values are obtained for polystyrene composite containing size 1 NR prophylactics filler. This proves the comparatively better performance of composite containing small size filler (S1).

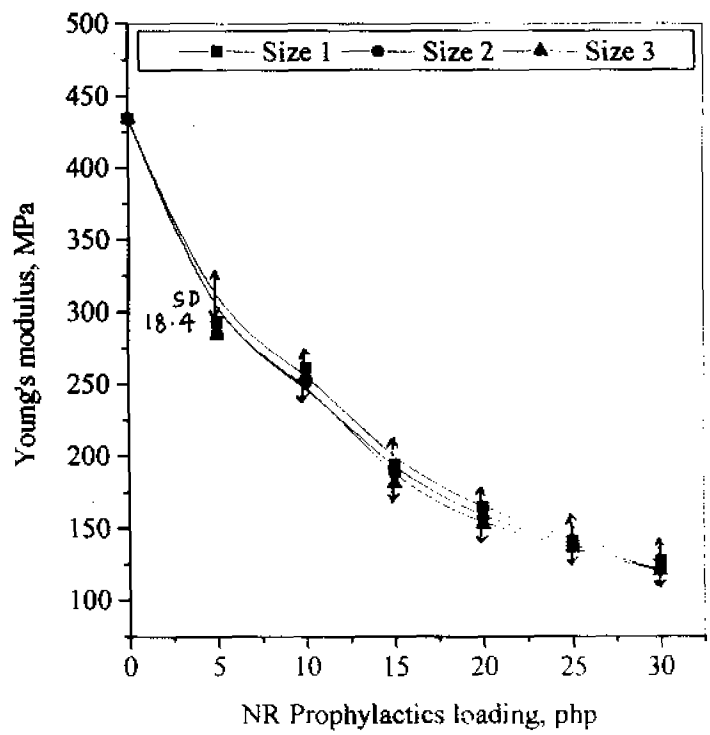

Figure 8.2. Variation of Young's modulus with NR prophylactics loading

The values of bulk modulus (K) are calculated from Young's modulus using the **Equation 8.1**.

$$K = E\,[3(1-2\nu)] \qquad (8.1)$$

where, E is the Young's modulus and ν, the Poisson's ratio of the matrix.

Plots obtained are given in **Figure 8.3**. It can be seen that the bulk modulus values falls in the range of 140-520 MPa. The equation predicts the constantly decreasing trend in the bulk modulus of the sample as the loading of NR prophylactics increases.

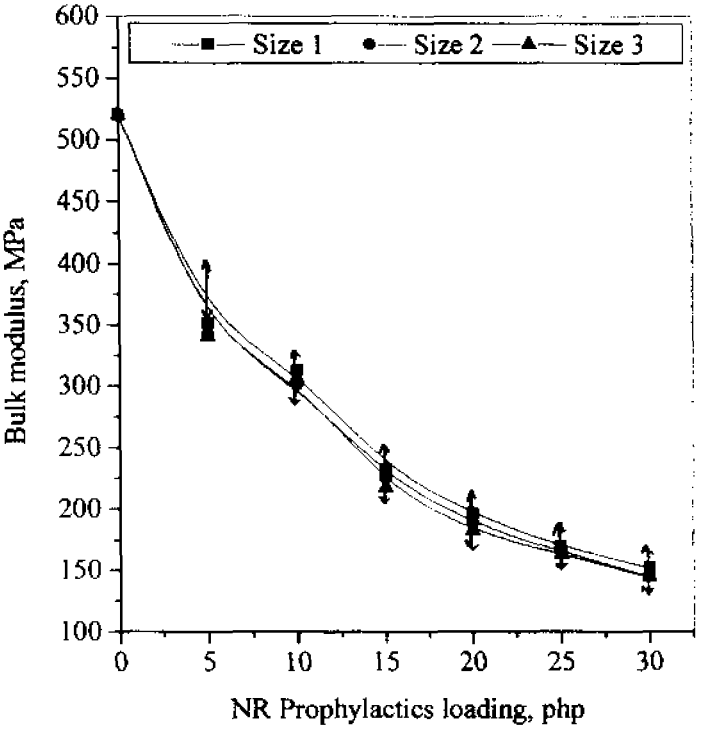

Figure 8.3. Variation of bulk modulus with NR prophylactics loading

The addition of NR prophylactics filler to polystyrene is found to increase the elongation at break values **(Figure 8.4)**. This is because the lightly crosslinked prophylactics filler particles elongate to high strains due to its strain crystallization tendency. Here also it can be seen that size 1 filler gives higher elongation at break. It is suggested[1] that the high elongation observed in the case of some commercial polystyrene samples is not at due to the rubber but due to the deformation of the continuous polystyrene matrix. This is because the rubber content in these samples is usually low (5-

10%). But this doesn't apply for the present cases because the rubber here is a lightly crosslinked one whose content is comparatively high. It can be seen in **Figure 8.4** that at higher loadings, increase in elongation at break is not very prominent (or even a leveling off can be noted (size 3). This is because of the coalescence of crazes to cracks in samples of higher loadings.

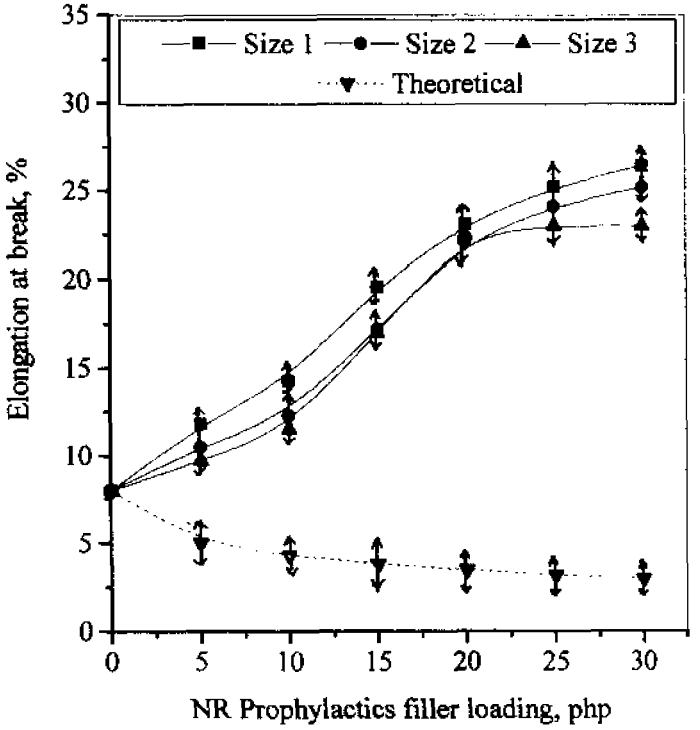

Figure 8.4. Variation of elongation at break with NR prophylactics loading

The behaviour of elongation at break observed here is entirely different from that of a system containing particulate fillers also. Elongation at break in the case of composites containing inelastic rigid filler follows an equation of the sort given below (dotted lines in **Figure 8.4**). This is because they do not deform under stress.

$$\varepsilon = \varepsilon 0\ (1 - \phi^{1/3}) \qquad (8.2)$$

where, ε is the elongation at break of the composite, $\varepsilon 0$, that of the matrix and ϕ, the filler volume fraction. The deviation of the present system from the dotted lines clearly indicates that in the case of polystyrene containing NR prophylactics filler, all the deformation is not

taking place in the polystyrene matrix alone.

The variation of tensile strength of the composites as a function of NR prophylactics loading is presented in **Figure 8.5.**

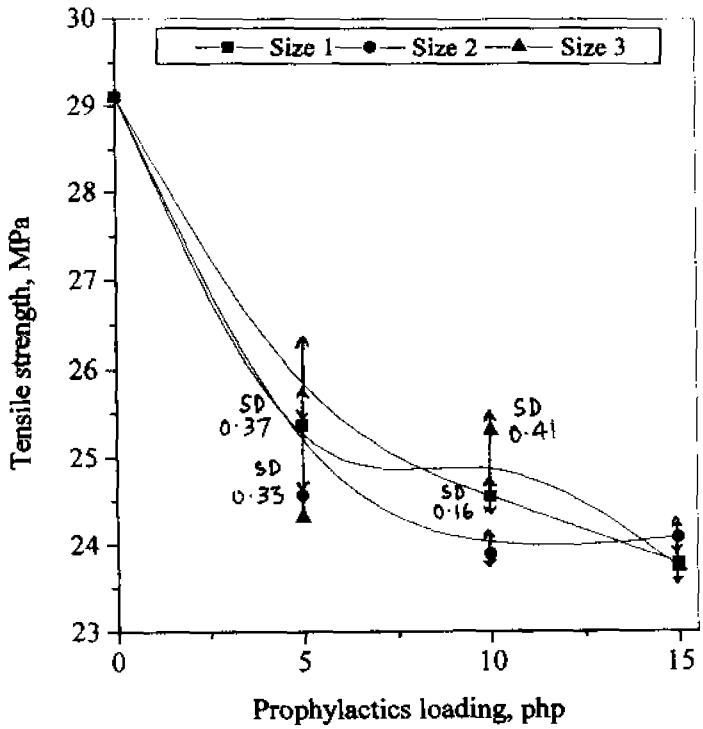

Figure 8.5. Variation of tensile strength with NR prophylactics loading

It can be seen that tensile strength values decrease with the loading of prophylactics filler. Better values are shown by size 1 at lowest loading. At 10 phr, size 3 and at 15 phr size 2 filler present better values of tensile strength. It can be generally seen that particle size is not presenting a clear trend in the results of tensile strength.

The strain induced crystallization in the composite samples can be confirmed by using Martin-Roth-Stiehler[26] plots given below **(Figure 8.6)**. These are drawn according to the **Equation 8.3**.

$$\ln \sigma\lambda^2 / \lambda^{-1} = \ln E_0 + A (\lambda - \lambda^{-1}) \qquad (8.3)$$

where σ is the stress value, and λ is the extension ratio, E_0 and A are constants.

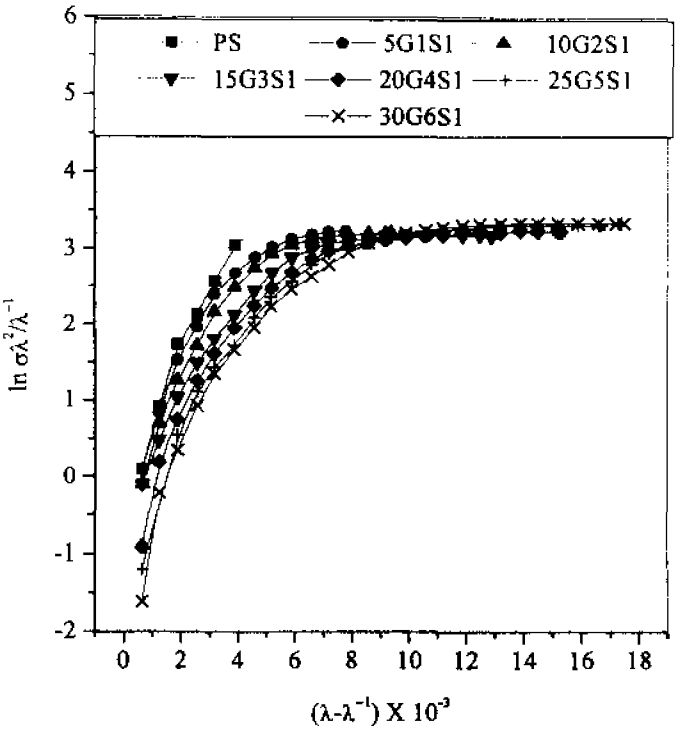

Figure 8.6. Martin-Roth-Stiehler plots

The plots of the composite samples present comparatively considerable changes in the slope. Even though polystyrene sample also presents very slight changes in the slope, this is no-way comparable to that of the composite samples. The changes in the slope of the plots clearly indicate the presence of strain induced crystallisation in the composite samples.

The impact strength values of polystyrene and its composites are shown in **Figure 8.7**. As the loading of NR prophylactics filler increases, only size 1 filler shows considerable increase. Other samples containing higher size fillers such as size 2 and 3 presents only either a very slight increase or leveling off behaviour. This is because size 2 and 3 are too large to show any effect on the impact strength of a brittle plastic such as polystyrene.

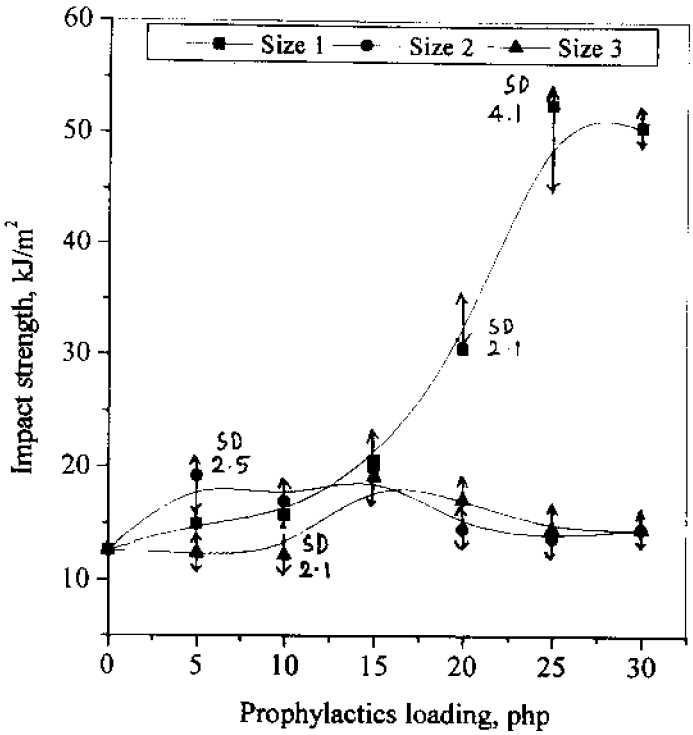

Figure 8.7. Variation of impact strength with NR prophylactics loading

The improvement in impact strength even if less (size 2 and 3) is due to the increase in the volume of rubber phase which reduces the interparticle distance. The rubber particles act as stress concentrators and catalyse the formation of fine craze structures in the surrounding matrix. These crazes prevent failure. The higher impact strength observed for composite sample with smaller (size 1) particle size can be attributed to the formation of more crazed matter during the failure. This arises from the increase in interfacial surface between NR prophylactics filler particle and polystyrene in the case of fine particle size filler.

8.1.2. Scanning Electron Microscopic Observations

The usefulness of a polymer in many applications is mainly determined by its predominant failure mechanism. **Figures 8.8a-i** represent the SEM photos of impact fractured samples. **Figures 8.8a-c** are that of pure polystyrene sample.

Rubber toughening can be successful only if the matrix is capable of yielding

and/or crazing. The massive crazes within the crack tip zone in the figure indicate that the matrix can be easily toughened by the addition of rubber. Crazing in polystyrene can be seen as clearly defined lines on the surface of the sample perpendicular to the direction of applied stress. Stress whitened regions also are visible in the figures. They are formed from the scattering of light by the many microscopic sized void regions of the crazes.

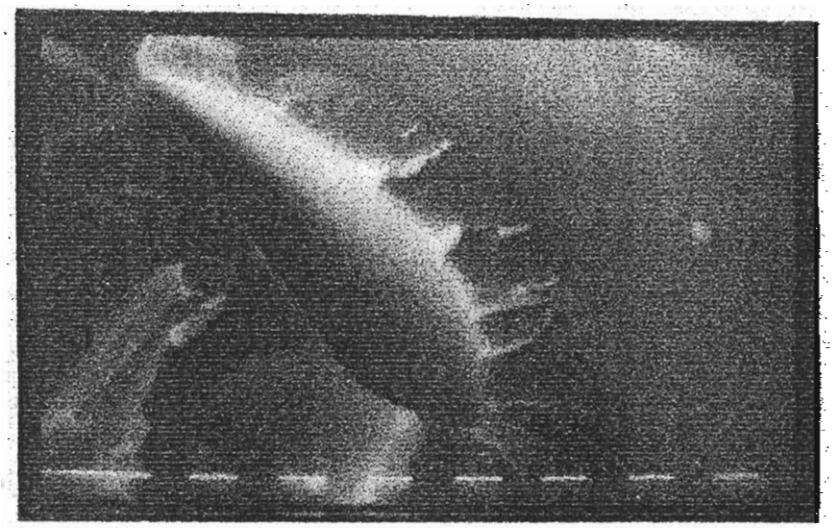

Figure 8.8 a. Fractured surface of pure polystyrene-Crazes in crack tip zone & stress whitening, Mag. X 600

Long crazes that nucleate within a crack tip zone are visible in **Figure 8.8b**.

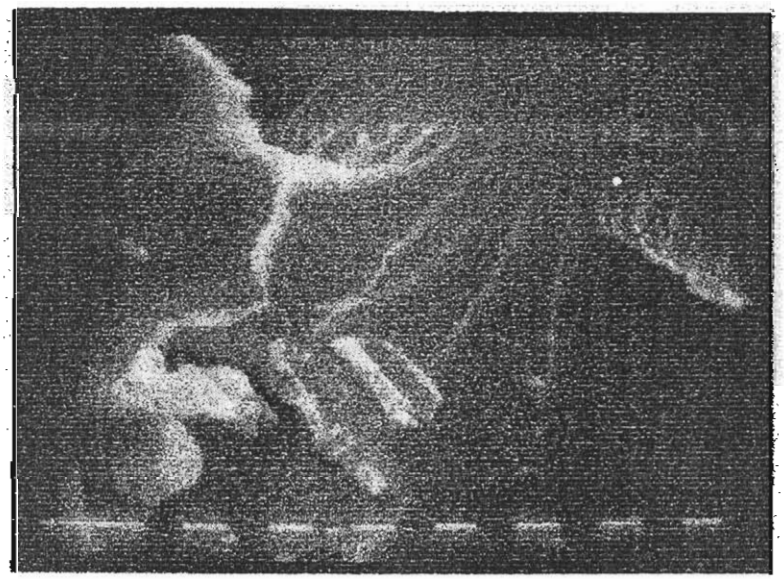

Figure 8.8 b. Fractured surface of pure polystyrene-long crazes in crack tip zone Mag. X 600

Cracks elongated in the direction of stress and the procedure of advancing crack by steps such as formation of localized plastic zone with stress build up, nucleation of voids, coalescence of individual voids etc also are visible in **Figure 8.8c**.

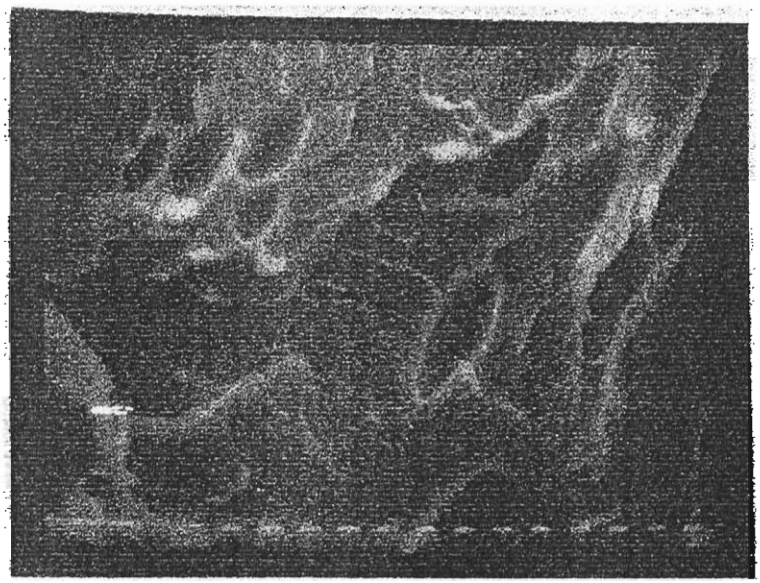

Figure 8.8c. Fractured surface of pure polystyrene-crack propagation mechanism. Mag. X 400

In the case of composite samples **(Figure 8.8d)**, stretching of rubber particles stabilize crack front and absorb energy. Here the Tg of NR prophylactics is in –40 to –60 ^{0}C range and this is lower enough to allow rapid stretching as the crack advances. The cavitations of rubber particles also relieve triaxial stresses. According to Bucknall[27,28] impact resistance depends on the rate at which matrix polymer can respond to stress by forming oriented fibrils. This happens because fibrillation is the most rapid mechanism available for extension of damage zone at crack tip.

Figures 8.8 d-i represent the polystyrene sample with 30 php size 1 prophylactics. In **Figure 8.8d**, fibrillation can be seen. For high impact polystyrene (HIPS), the critical size needed for this fibrillation is 1 μm. In the present cases of polystyrene/prophylactics composites, size 1 filler is found to be producing better results. It can be suggested here that for composites with size 1 prophylactics filler, combined effects of crazing, rubber particle cavitations and fibrillation are responsible for the impact toughening.

Figure 8.8d. Fractured surface of polystyrene composite-fibrillation. Mag. X 200

Two approaching microcracks can link each other by the origin and growth of secondary craze in the ligament (called bridge) which separates them **(Figure 8.8e)**. Finally the failure of this ligament also occurs in a brittle manner **(Figure 8.8f)**.

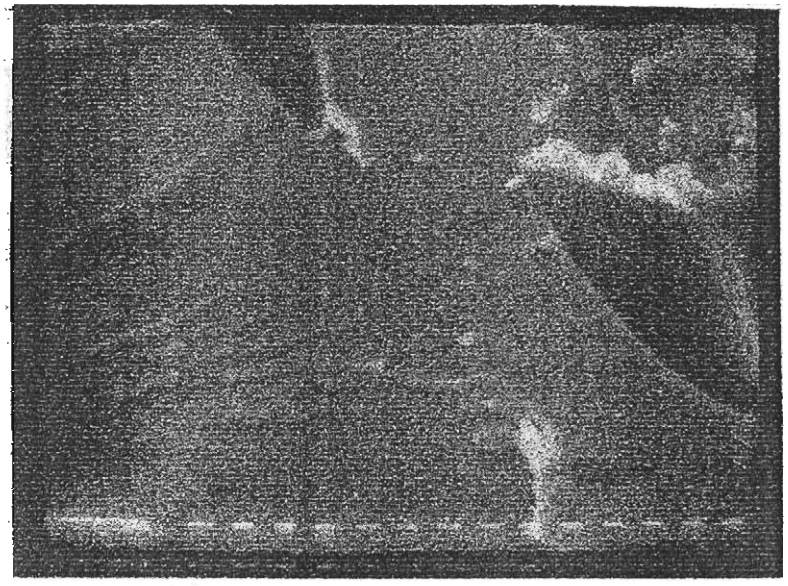

Figure 8.8e. Fractured surface of polystyrene composite-Crazing ligament between approaching cracks. Mag. X 400

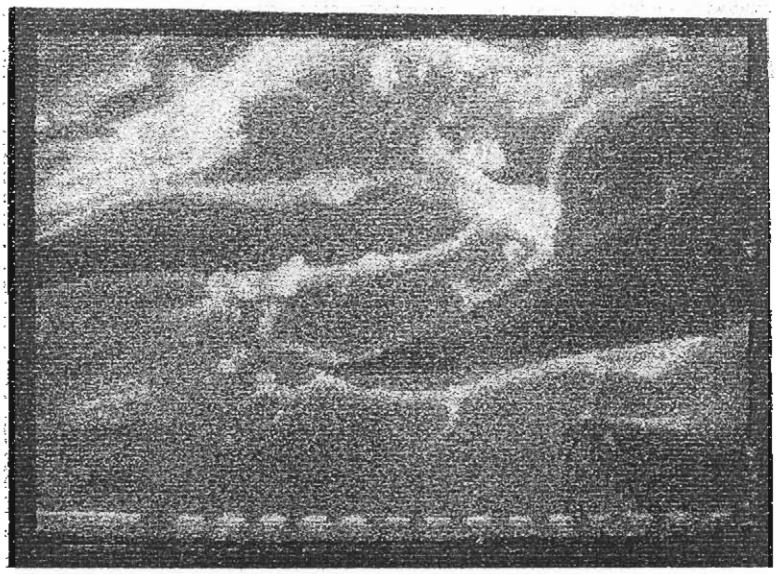

Figure 8.8f. Fractured surface of polystyrene composite-Brittle failure of crazed ligament. Mag. X 400

But when such as brittle fracture occurs, formation of 'cleavage stops' (chips) also occurs **(Figure 8.8g)**. These chips will sometimes spinter off also in the process.

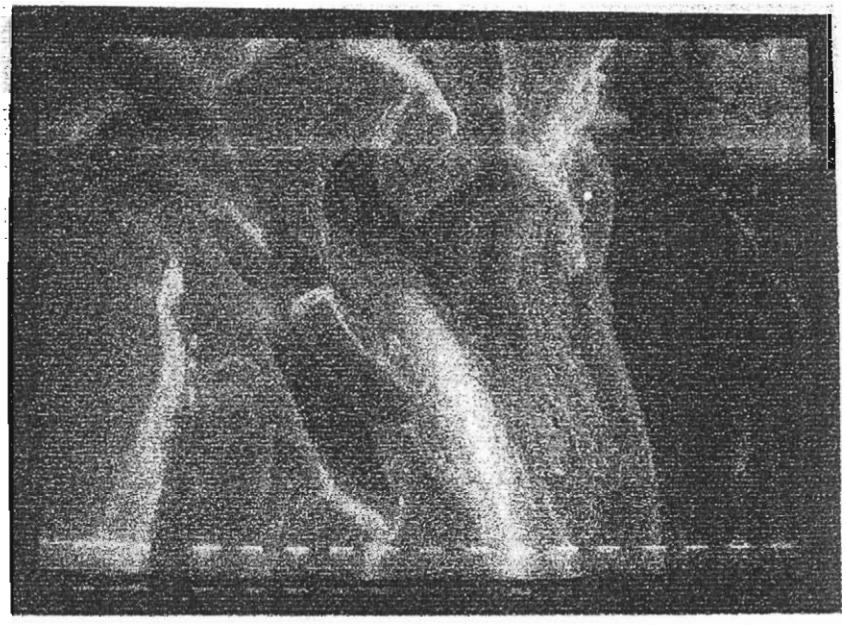

Figure 8.8g. Fractured surface of polystyrene composite-Brittle failure of crazed ligament-chip formation. Mag. X 400

The formation of stretched regions with a ductile failure mode is clearly visible in **Figure 8.8h**.

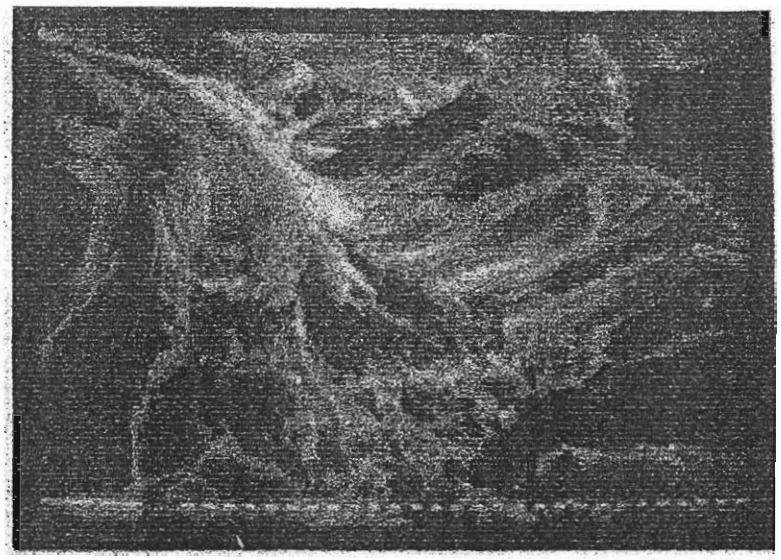

Figure 8.8h. Fractured surface of polystyrene composite-Ductile failure with stretched regions. Mag. X 200

Rubber particles in the matrix which are debonded in an effort to arrest sudden failure also can be seen. It can be seen that these particles also are pointing in the direction of cracks /stress **(Figure 8.8i)**.

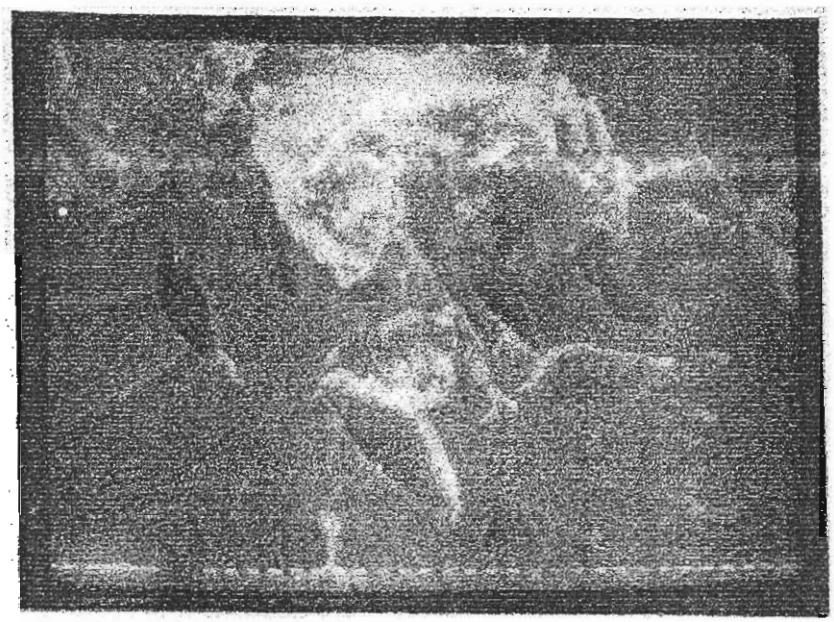

Figure 8.8i. Fractured surface of polystyrene composite-Particles arresting sudden failure of matrix. Mag. X 200

8.1.3. Dynamic mechanical analysis

Dynamic mechanical analysis is mainly used to check the variations in storage modulus, loss modulus and damping of the material and also the variation in Tg of the matrix. The plots are given in **Figures 8.9 –8.16. Figure 8.9** is the variation of storage modulus of polystyrene under different frequencies. It is a main observation that storage modulus of the samples decreases with rise in temperature. This is due to the loss in stiffness of the material at high temperature. Also as the frequency increases from 0.1 to 100 Hz, storage modulus increases and this is most noted for temperature above the transition. Similar effects could be observed with other samples also.

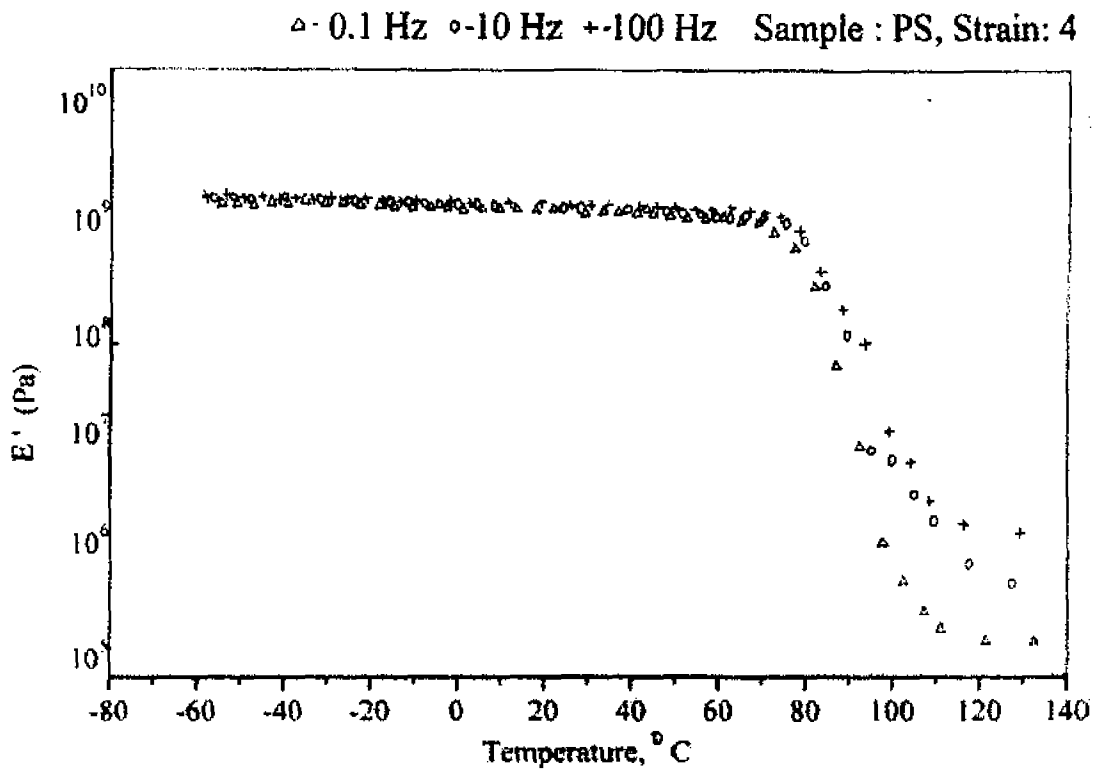

Figure 8.9. Variation of storage modulus with temperature: Influence of frequency

The variation of storage modulus with temperature (at 100 Hz) for different samples of increasing NR prophylactics loading (size 3) is presented in **Figure 8.10**. Below the transition point, highest modulus is shown by polystyrene sample while the least by polystyrene sample containing 25 php prophylactics filler. But at temperature above

transition, polystyrene softens considerably and therefore prophylactics containing composite samples give higher modulus values.

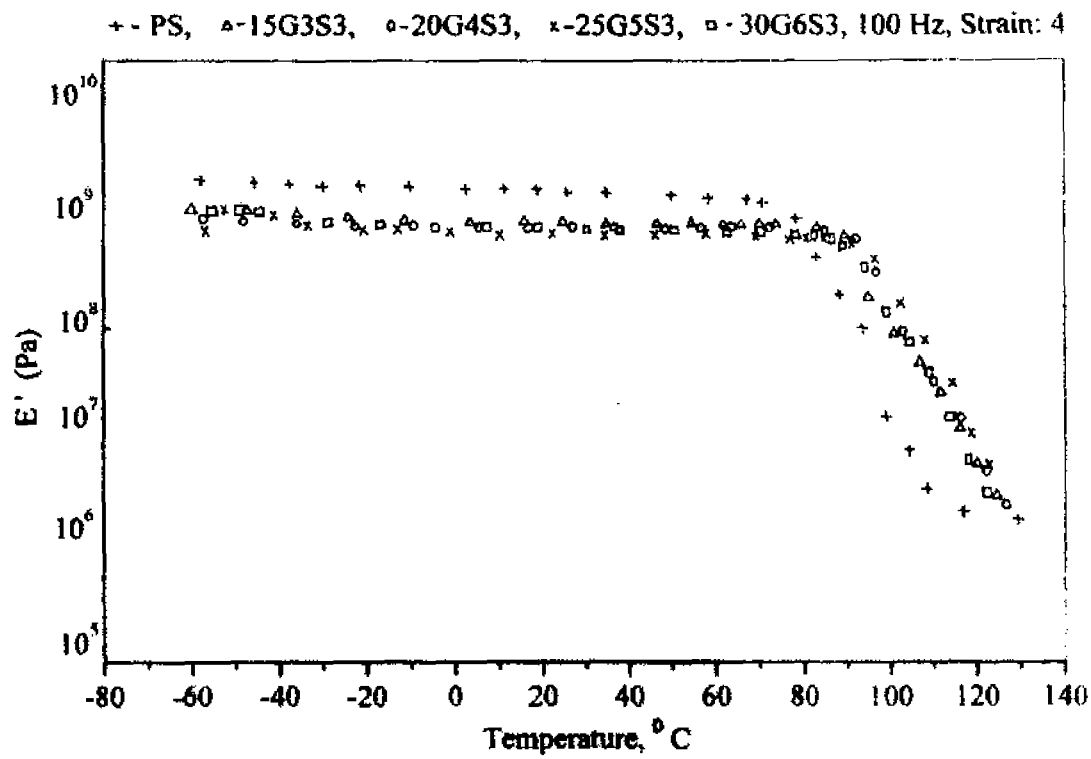

Figure 8.10. Variation of storage modulus with temperature: Influence of NR Prophylactics loading

Figure 8.11 depicts the influence of particle size of NR Prophylactics filler on the storage modulus. At a constant loading of 30 php, size 3 prophylactics containing samples presents a high modulus while size 1, the lowest.

The effect of frequency on the loss modulus–temperature plots of pure polystyrene is presented in **Figure 8.12**. Plots present one main transition around 85^0 C which is due to polystyrene. Below the main transition, the maximum value is observed at 0.1 Hz and the least at 100 Hz while above the transition, this order is reversed. This phenomenon gives a twisted staircase like appearance to the plots.

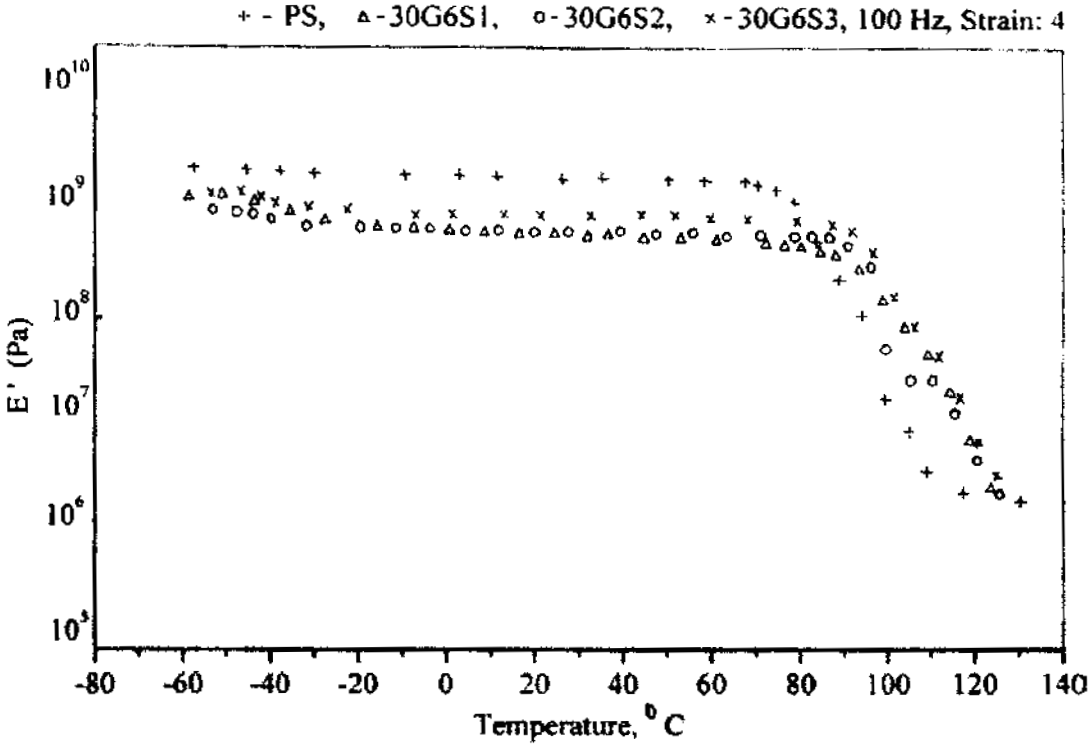

Figure 8.11. Variation of storage modulus with temperature: Influence of particle size of NR Prophylactics filler

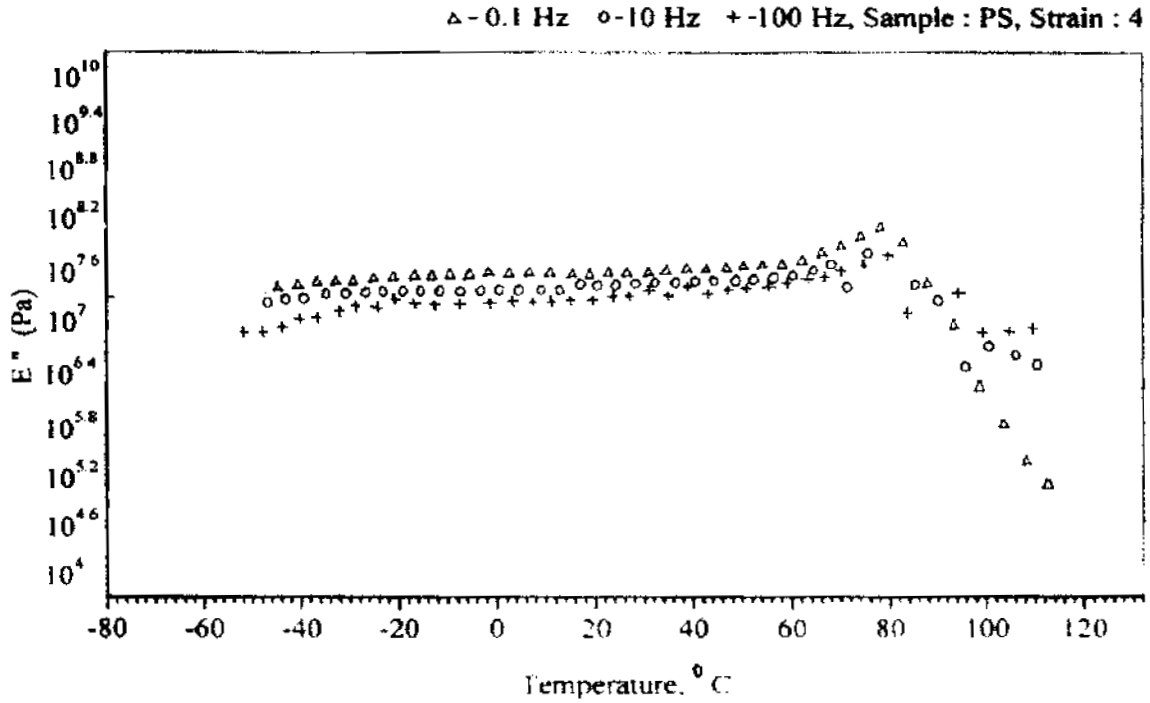

Figure 8.12. Variation of loss modulus with temperature: Influence of frequency

When pure polystyrene exhibits only one transition around 85^0 C, all composite samples exhibit two transitions, one around –58 to -36^0 C range and the other around 100^0 C **(Figure 8.13)**. The former is due to NR Prophylactics rejects and the latter is due to pure polystyrene. As the loading of prophylactics filler increases, the loss modulus decreases in the central region between the two transitions. But below the NR transition and above the PS transition, polystyrene presents a lower value. So as in the earlier case, the plots appear like a twisted staircase. Composite samples with size 2 NR prophylactics filler gives the lowest loss modulus **(Figure 8.14)** while the highest loss modulus is shown by samples with size 1 filler. Size 3 presents an intermediate behaviour.

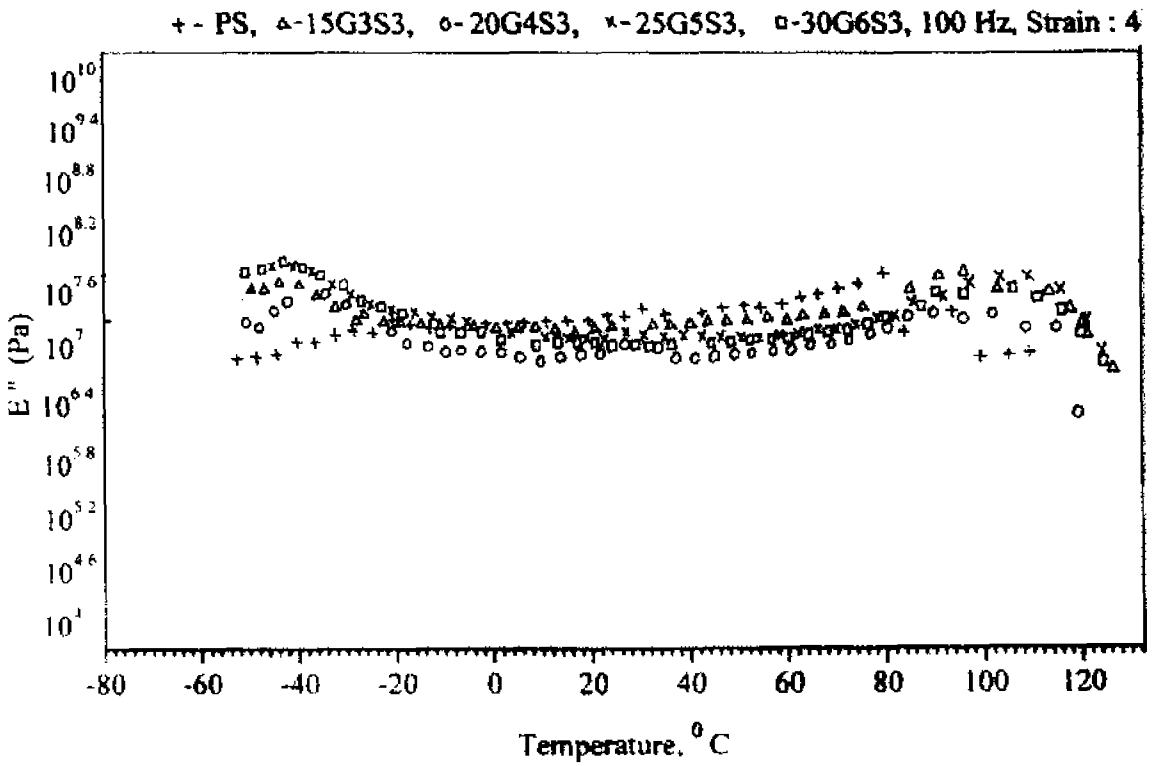

Figure 8.13. Variation of loss modulus with temperature: Influence of NR Prophylactics loading

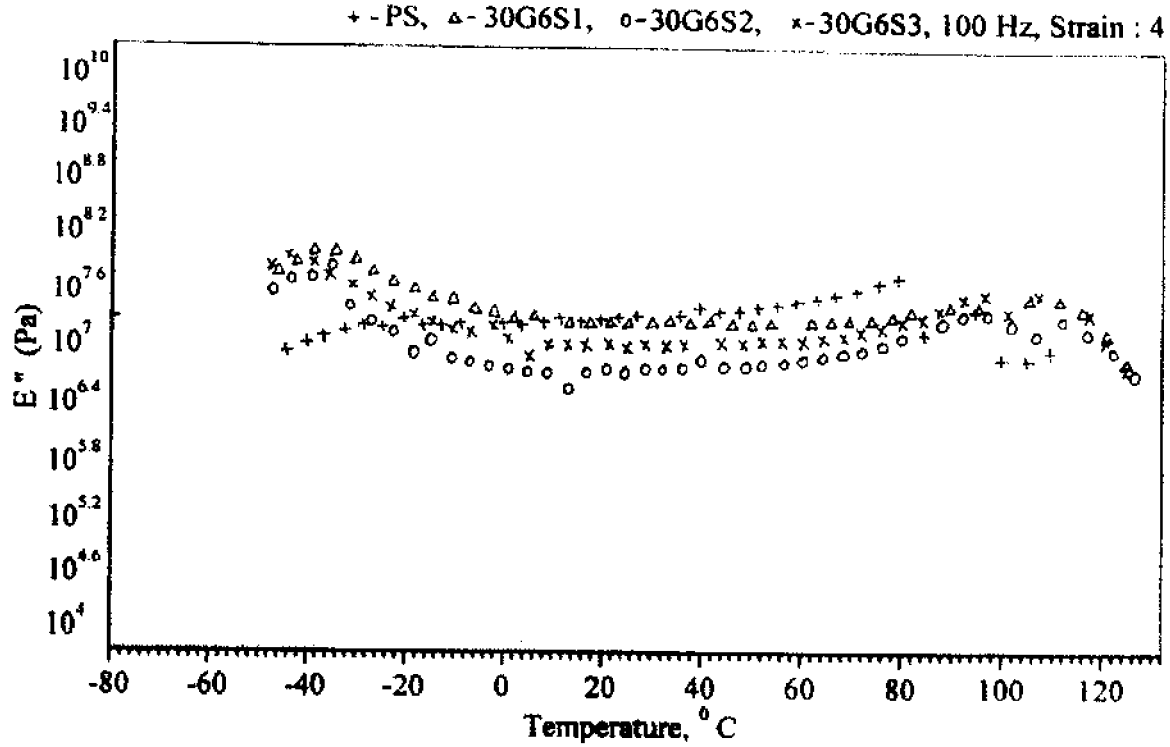

Figure 8.14. Variation of loss modulus with temperature: Influence of particle size of NR Prophylactics filler

It can be seen from **Figure 8.15** that tan δ value increases for all composites compared to that of polystyrene. The highest increase is shown at a loading of 25 php and the lowest at 15 php. Composites containing size 1 filler shows the highest tan δ value at most of the temperature regions **(Figure 8.16)** while the lowest is shown by size 2. But tan δ_{max} is highest for composites with size 3 prophylactics and minimum for composite with size 2 filler. The presence of two well-defined transitions clearly indicates that two separate phases exists in the system.

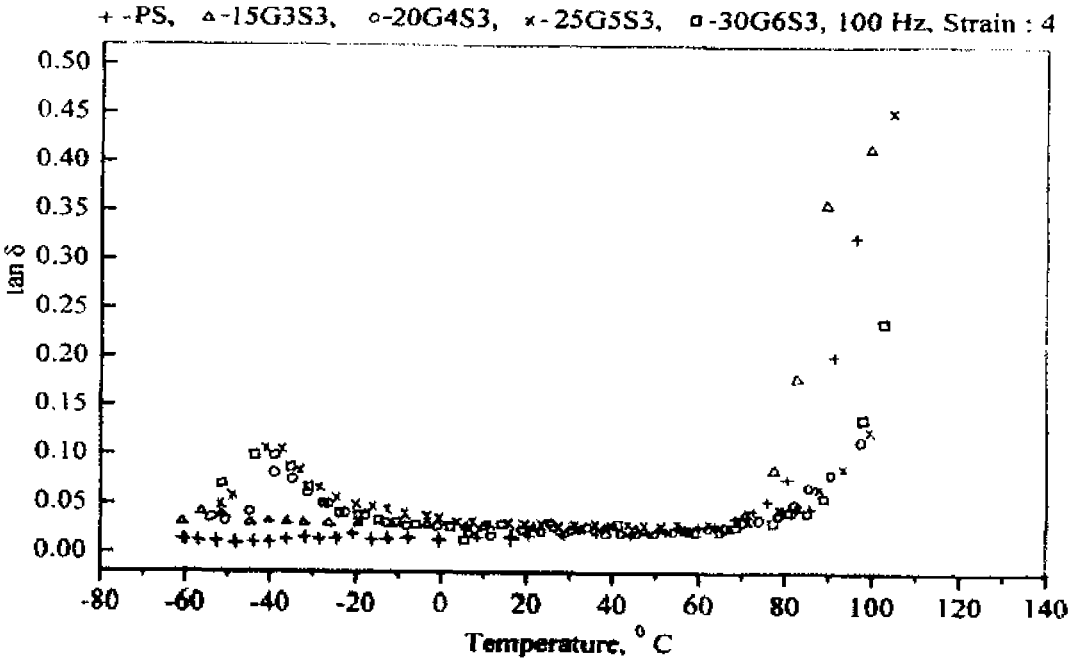

Figure 8.15. Variation of tan δ with temperature: Influence of NR Prophylactics loading

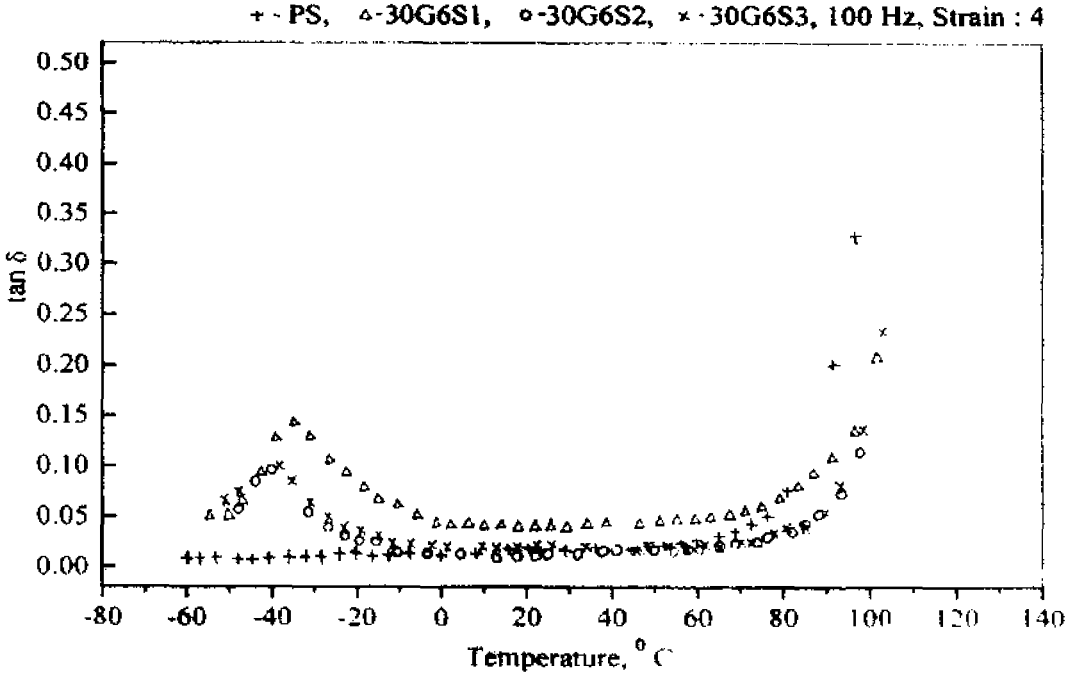

Figure 8.16. Variation of tan δ with temperature: Influence of particle size of NR Prophylactics filler

Tg is determined by experiments which correspond to a time sale. In the case of an experiment performed rapidly, time scale gets shortened, frequency is increased and then Tg will be raised. Here Tg values are taken not from tan δ-temperature plots but from E"-temperature plots. This is because it is reported[29] that temperature corresponding to the maximum damping is not Tg, but temperature corresponding to the maximum loss modulus is more close[29] to Tg. Tg values are given in **Table 8.2**.

Table 8.2. Glass transition values of samples

No	Sample	Glass transition values, ^{0}C		
		Frequency, Hz		
		0.1	10	100
1	PS	80	82	80
2	PS+15phpS3	90	93	98
3	PS+20phpS3	89	91	96
4	PS+25phpS3	91	99	109
5	PS+30phpS3	89	94	105
6	PS+30phpS2	89	94	97
7	PS+30phpS1	88	95	110
8	PS+10phpS2	84	88	94
9	PS+20phpS2	92	94	98

In the case of polystyrene, an expected increase in Tg with frequency cannot be seen. Composites have higher Tg values which indicate a tightening of the system. Also, as the frequency increases in each case, Tg increases. Generally it can be stated that the loading of prophylactics upto 25 php increases Tg (irregularly), which falls to a lower value at 30 php loading of size 3 filler. Also, as the particle size of filler increases, the variation in Tg doesn't follow any generalizations.

8.2. REFERENCES

1. C.B. Bucknall., "Toughened Plastics", Applied Science Publishers, London 1977; Adv.Polym.Sci., 27, 121 (1978).
2. A. Echte and F. Haaf, J. Hambrecht, Angew.Chem. 93,372 (1981).
3. A. Echte., Angew. Makromol.Chem.58/59, 175 (1977).
4. G. Riess and P. Gaillard., "Polymer Reaction Engineering-Influence of Reaction Engineering on Polymer Properties", K.H. Reichert, W. Geiseler (eds.), Hanser, Munich, p.221, 1983.
5. W. Retting, Angew. Makromol. Chem., 58/59, 133 (1977).
6. G.H. Michler and B. Hamann, J. Runge, Angew.Makromol. Chem., 180, 169 (1990).
7. G.H. Michler, "Kunststoff-Mikromechanik:Morphologie, Deformations- und Bruchmechanismen", Hanser, Munich, chap. 9, 1992.
8. R.P.Sheldon, "Composite Polymeric Materials", Applied Science Publishers, London, p. 44, 1982.
9. D.M. Bigg, Polym.Compos., 8,115 (1987).
10. L.E.Nielsen,"Mechanical Properties of Polymers", Reinhold, NewYork, Ch.6, 1962.
11. D. Braun, M. Klein, G.P.Hellmann, Polym. Compos, 1995.
12. R.P. Kambour, J.Polym. Sci., Macromol. Rev., 7, 1 (1973).
13. R.J. Seward., J.Appl.Polym.Sci., 14, 852 (1970).
14. G.H. Michler and K. Gruber, Plaste. Kautsch., 23, 496 (1976).
15. S. Shaw and R.P.Singh., J.Appl. Polym.Sci., 40, 685 (1990).
16. S. Shaw and R.P.Singh, J.Appl. Polym.Sci., 40, 701 (1990).
17. C. Maestrini, L.Monti and H.H. Kausch., Polymer, 37(9), 1607 (1996).
18. W.C.Mc Caffrey, D.G.Cooper and M.R.Kamal., Polym.Degrad. Stabil., 62,513 (1998).
19. C.S.Ha, H.D.Park, Y.Kim, S.K.Kwon and W.J.Cho., Polym.Adv.Technol., 7,483 (1995).
20. D.Ciesielska and P.Liu, Kautsch Gummi. Kunstst., 53(5), 273 (2000).

21. Dart Container Co, J. Environ. Health, 59(2), 30 (1996).
22. A.Kovski, Oil Daily, 9591,4 (1990).
23. M.J.Brues, M.R.Kamal and D.G.Cooper., ANTEC'95, Soc.Plast.Eng., 3(53), 3720 (1995).
24. D.Ciesielska and P.Liu, ANTEC'98, Soc.Plast.Eng., 3(56), 2906 (1998).
25. N.C.Liu and W.E.Baker., Polym.Eng.Sci., 32, 1695 (1992).
26. G.M.Martin, F.L.Roth and R.D. Stiehler., Trans. IRI., 32, 189 (1956).
27. C.B. Bucknall., Makromol Chem. Macromol Symp 16, 209 (1988).
28. C.B. Bucknall., "Fracture resistance in rubber-toughened polymers". Prague, July 1989, (appeared in Makromol Chem. Macromol Symp)
29. L.E.Nielsen and R.F.Landel., "Mechanical Properties of Polymers and Composites", 2nd edn., Marcel Dekker, Inc, NY, 1994.

Chapter 9

CHAPTER 9

RECLAMATION VERSUS CHEMICAL MODIFICATION OF NATURAL RUBBER PROPHYLACTICS REJECTS FOR RECYCLING IN POLYPROPYLENE

ABSTRACT

The use of reclaimed and chemically modified prophylactics rejects in unmodified and chemically modified polypropylene has been investigated. The room temperature epoxidation of prophylactics rejects has been carried out by in-situ formed performic acid using a mixture of formic acid and hydrogen peroxide. The dichlorocarbene modification of prophylactics at room temperature has been done using a mixture of chloroform and alkali in the presence of a phase transfer catalyst. The reclamation of prophylactics rejects has been carried out by the De Link process. The preparation of maleic anhydride modified and phenolic modified polypropylene in a hot two-roll mill is done using maleic anhydride/dicumyl peroxide mixture and dimethylol phenol/stannous chloride mixture respectively. The chemically modified prophylactics rejects as well as polypropylenes have been characterised by infrared spectroscopy, chemical analysis, glass transition and contact angle determinations. Epoxy group in the epoxidised sample is confirmed by the FTIR peaks around 870 cm^{-1} and 1300 cm^{-1} while dichlorocarbene modification is confirmed by the peaks at 1070 cm^{-1} (cyclopropane ring) and 746 cm^{-1} (C-Cl stretch). Improvement in epoxy values has been observed with increasing duration of the reaction up to 144 h. The highest epoxy value has been observed for the sample treated with 20 % epoxidation reagent. The chlorine content in the case of dichlorocarbene modified samples has been found to be increasing initially and levels off after 4 h of the reaction. Increase in the glass transition value has been observed with both chemical modifications due to the stiffening of polymer chains. Increased polarity resulting from the chemical modifications has been found to be reducing the contact angle of a sessile drop of water on the surface of chemically modified

materials. The thermal stability reduces with epoxidation due to the formation of acidic compounds during thermal degradation. Similar results have been noted with dichlorocarbene modified samples also. Tensile strength has been decreased with the addition of reclaimed prophylactics rejects while an increasing trend has been observed with the use of epoxidised prophylactics in both maleic anhydride and phenolic modified polypropylene and dichlorocarbene modified prophylactics in phenolic modified polypropylene. In the case of impact strength, reclaimed prophylactics has been found to be better than chemically modified forms. X-ray diffraction results reveal the α-monoclinic structure for polypropylene.

CHAPTER 9

RECLAMATION VERSUS CHEMICAL MODIFICATION OF NATURAL RUBBER PROPHYLACTICS REJECTS FOR RECYCLING IN POLYPROPYLENE

Results in this chapter have been communicated to J. Mater. Sci.

Polypropylene is a semicrystalline plastic,[1] which finds extensive use in many household articles, automobile parts, sterilisable equipments, film production etc. Now, it is the fastest growing usage thermoplastic[2] with a production of 1.5 mio tons in 1970's, 13 mio tons in 1990's, 19 mio tons in 1995 and 25 mio tons in 2000. The reason for such an uncontrollable and explosive growth in the usage of polypropylene is due to its various merits[3] such as low density, high vicat softening point, exceptional flex life, steam sterilisability, good surface hardness, scratch resistance, very good abrasion resistance, excellent electrical properties, low cost, chemical inocuity[4], resistance to biological organisms and availability in a wide range of MFI ranging from 0.25 to 800 g /10 min which reminds a roman saying 'Variety Delectat' (variety is delightful) which is true for polypropylene. Meanwhile it has some demerits also. These include its low impact strength, tendency to creep even at low stress and inert nature which makes its bonding, surface printing etc. a Herculean task. Such demerits can be overcome by its proper chemical modifications, which extensively appeared earlier in the literature [5-14]. Similarly natural rubber also can be subjected to several chemical modifications to attain better properties. Some of these are hydrogenation[15,16], chlorination[17,18], epoxidation[19-22], and dichlorocarbene modification[23,24]. Development of chlorinated rubber from crosslinked gloves waste also is reported in the literature[25].

The present chapter investigates the room temperature chemical modification (epoxidation and dichlorocarbene modification) of natural rubber prophylactics rejects and also its reclamation for recycling in unmodified and chemically modified polypropylene (MA-PP and Ph-PP). Powdered prophylactics rejects (size 2) having average size of 1.05

mm, most frequent size range of 0.6-0.9 mm, number average diameter Ln of 0.961 mm and weight average diameter Lw-1.083 mm was selected for the study.

9.1. Results and discussions

9.1.1. Characterisation of chemically modified prophylactics filler

9.1.1.1. Spectroscopic characterisation of epoxidised prophylactics

Epoxidation of natural rubber prophylactics rejects (LW) can be confirmed by comparing the FTIR spectrum of unmodified and chemically modified materials. The FTIR spectra of unmodified and epoxidised prophylactics are shown in **Figure 9.1.**

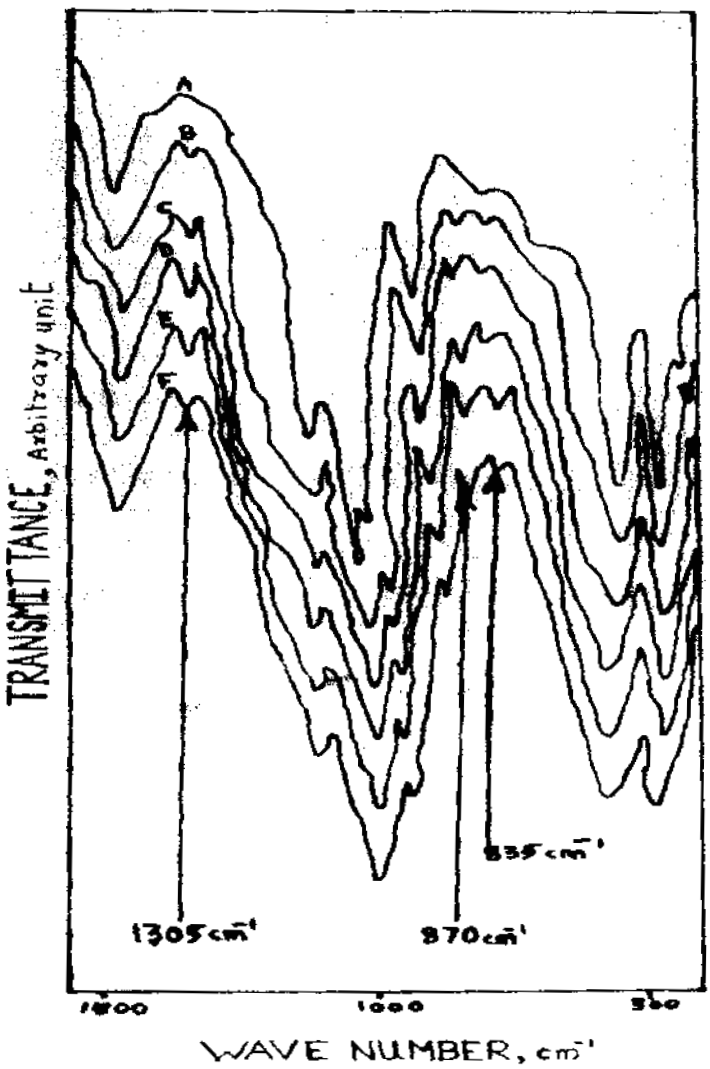

Figure 9.1. FTIR spectra of unmodified and epoxidised NR prophylactics rejects

[A-LW (0 h), B-ELW (0. 5h), C-ELW (1h), D-ELW (2 hr), E-ELW (6 h), F-ELW (24 h)]

It can be seen from **Figure 9.1** that the epoxidised materials (B-F) present two characteristic peaks, one around 870 cm^{-1} and the other around 1300 cm^{-1} while these are absent in the spectra of unmodified prophylactics material (A) given in the same figure. Slight variation in the intensity of the peak at 835 cm^{-1} also can be observed due to the involvement of unsaturation in the epoxidation reaction.

9.1.1.2. Spectroscopic characterisation of dichlorocarbene modified prophylactics

The FTIR spectra of unmodified and dichlorocarbene modified prophylactics is shown in **Figure 9.2.**

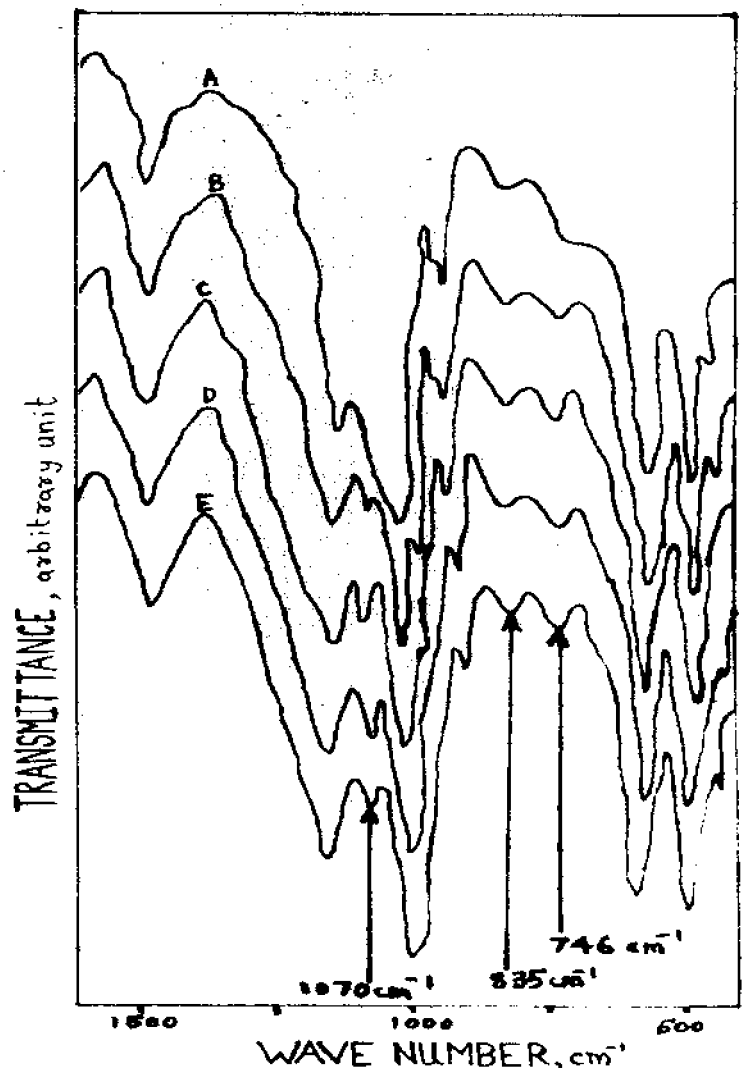

Figure 9.2. FTIR spectra of unmodified and dichlorocarbene modified NR prophylactics rejects

[A-LW (0 h), B-ClLW (2 h), C- ClLW (4 h), D-ClLW (8 h), E- ClLW (24 h)]

Dichlorocarbene modification of NR prophylactics rejects can be confirmed by FTIR peaks around 1070 m^{-1} and 746 cm^{-1} which corresponds to cyclopropane ring and carbon-chlorine stretching vibration respectively. As in the case of epoxidation, slight variations in the intensity of the peak at 835 cm^{-1} are observed due to the reaction of the unsaturation.

The general information regarding FTIR characterisations discussed above is presented in **Table 9.1** below.

Table 9.1. Important FTIR peaks

Peak position	Comments
3600-3400 cm^{-1}	broad transition - O-H str
3040 cm^{-1}	medium- C-H str
2918 cm^{-1}	strong- C-H str (asym)[CH2]
2854 cm^{-1}	strong- C-H str (sym)[CH3]
1664 cm^{-1}	medium- C ═ C
1455 cm^{-1}	strong- C-H def (asym)[CH3]
1382 cm^{-1}	strong- C-H def (sym)[CH3]
1305-1320 cm^{-1}	epoxy group
1070 cm^{-1}	cyclopropane ring
1032 cm^{-1}	medium- 1^0 alcohol (ali)
870 cm^{-1}	epoxy group
838 cm^{-1}	strong- C-H def (ofp) CHR −CCR1
746 cm^{-1}	C-Cl str

9.1.1.3. Epoxy values and percentage chlorine analysis

The reactions can be characterised also by using the chemical analysis methods using HBr and acetic acid which determines epoxy values[26] for epoxidised samples and chlorine content[27] [titration of the gas (from sample burned in Pd basket) absorbed solution] for dichlorocarbene modified samples. These results are presented in **Tables 9.2** and **9.3** respectively.

It can be seen from the epoxy values given in **Table 9.2** that there is a gradual increase in these values with the progress of the reaction and best results are obtained when the concentration of the reagent is 20%. It can be understood here that at the lowest concentration of reagent (10%), the extent of epoxidation is low and therefore the epoxy values are lower. At highest concentration of reagent (30%), sufficient epoxidation may be

occurring but the formed epoxy groups may be undergoing some side reactions, which leads to a low epoxy value. One important point to be kept in mind is that only the free unsaturation in these lightly crosslinked natural rubber prophylactics rejects are susceptible to these reactions.

Tables 9.2. Epoxy values

Time of Reaction h	Concentration of reagent, %		
	10	20	30
0	-	-	-
0.5	0.01	0.07	0.08
1	0.11	0.15	0.16
2	0.24	0.23	0.21
6	0.29	0.35	0.25
24	0.33	0.57	0.44
144	0.31	0.68	0.43

Similarly, as the time of reaction increases, the chlorine content in the sample also increases and finally levels off. This can be attributed to the reduced number of unsaturation sites for the reaction with its progress.

Tables 9.3. Chlorine content

Sample code	Time of reaction, h	Chlorine content, %
C0	0	-
C1	2	2.84
C2	4	4.70
C3	8	4.70
C4	24	4.72
C5	48	4.66
C6	72	4.71

9.1.1.4. Glass transition values

Evidences for the reaction can be also given by the variation in glass transition values (**Tables 9.4** and **9.5**). In the case of epoxidised samples, an increase in the glass transition temperature is observed with the advancing reaction. The increase is higher when the concentration of the reagent is 20%. The increase in the glass transition values indicates the stiffening of the chain due to the presence of epoxy groups. Similar increase in the glass transition values are observed for dichlorocarbene modified samples also. But

here the extent of the increase is higher (**Table 9.5**).

Table 9.4. Glass transition values of epoxidised samples

Time of reaction, h	Tg values, ^{0}C		
	Concentration of reagent, %		
	10	20	30
0	-62.2	-62.2	-62.2
1	-61.5	-61.2	-61.2
2	-61.6	-61.6	-61.1
6	-61.3	-60.8	-61.3
24	-61.4	-60.0	-60.9
144	-60.6	-53.0	-61.0

Table 9.5. Glass transition values of dichlorocarbene modified samples

Sample code	Time of reaction, h	Tg values, ^{0}C
C0	0	-62.2
C1	2	-60.8
C2	4	-58.0
C3	8	-58.0
C4	24	-47.0
C5	48	-39.0
C6	72	-39.5

9.1.1.5. Contact Angles

The surface modification of a polymer will change the wetting of a liquid on its surface. The extent of this wetting can be characterised by determining the contact angle of the liquid on the surface of the material. A liquid which wets intensively, spreads first and finally flows on the surface, making the contact angle zero. Therefore, the more the interaction between material surface and liquid molecules, the more will be the wetting of the liquid and then the less will be the contact angle. Contact angle values of a sessile drop of water on the surface of epoxidised sample are presented in **Table 9.6**. It can be seen from **Table 9.6** that the lowest contact angle is obtained for the sample epoxidised for 24 h using 20% reagent, indicating a higher extent of modification for this case. Similar determination of contact angle for the dichlorocarbene modified samples could not be carried out, as the sample surface was rough with several cracks after the reaction.

Table 9.6. Contact angles

Concentration of epoxidation reagent, %	Contact angles, ^{0}
0	73.0
10	66.0
20	56.5
30	58.3

9.1.1.6. Thermal stability of the prophylactics rejects

The thermogravimetric plots of unmodified and chemically modified (epoxidised using 20 % reagent) prophylactics rejects are given in **Figure 9.3a-c** and the results are summarised in **Table 9.7**. **Figure 9.3a** is the TGA plot, **Figure 9.3b** is the DTA plot and **Figure 9.3c** is the simultaneous difference temperature (SDT) plot.

It can be seen from a comparison of **Figure 9.3a & b** and **Table 9.6** that the unmodified NR prophylactics rejects undergo thermal degradation in mainly one stage. This is confirmed by the presence of one main peak in DTA **(Figure 9.3 b)** and SDT **(Figure 9.3c)**. **Figure 9.3c** represents the simultaneous difference temperature between the sample pan and empty reference pan. Therefore, the appearance of one peak in the SDT plots indicates that considerable energy is used up for the degradation of NR sample in that stage. It can also be seen from **Figure 9.3b** that the degradation process of unmodified NR prophylactics rejects starts at a temperature of 331^0 C and ends at 474^0 C and that the temperature at which the degradation rate becomes maximum is 395^0 C (temperature of the DTA peak referred to as peak temperature). The percentage residue analysis at four selected temperatures (300, 400, 500 and 1000 ^{0} C (char) indicates the regular degradation of the sample in the furnace. The net weight change in the degradation process of unmodified NR prophylactics rejects is 94.47 %.

In the case of samples epoxidised using 20% reagent for 2 hrs (code: G18), the degradation follows a two stage process **(Figure 9.3a)** with 2 peaks in DTA and SDT plots **(Figure 9.3b and c)**. The first degradation starts at an early temperature than the unmodified sample, i.e., at 279^0 C and ends at 479^0 C. The temperature at which the degradation rate becomes maximum is 389^0 C, which is lower than that of unmodified sample. The second minor degradation step starts at 492 ^{0}C and ends at 591 ^{0}C with the

maximum rate of degradation observable at 544 ^{0}C. Even though the percentage residue analysis at various temperature gives confusing results, the net weight change is found to be higher (96.96 %) than the unmodified sample. All the above data confirm the reduced thermal stability of the epoxidised sample and the increased span of the degradation process for the epoxidised sample.

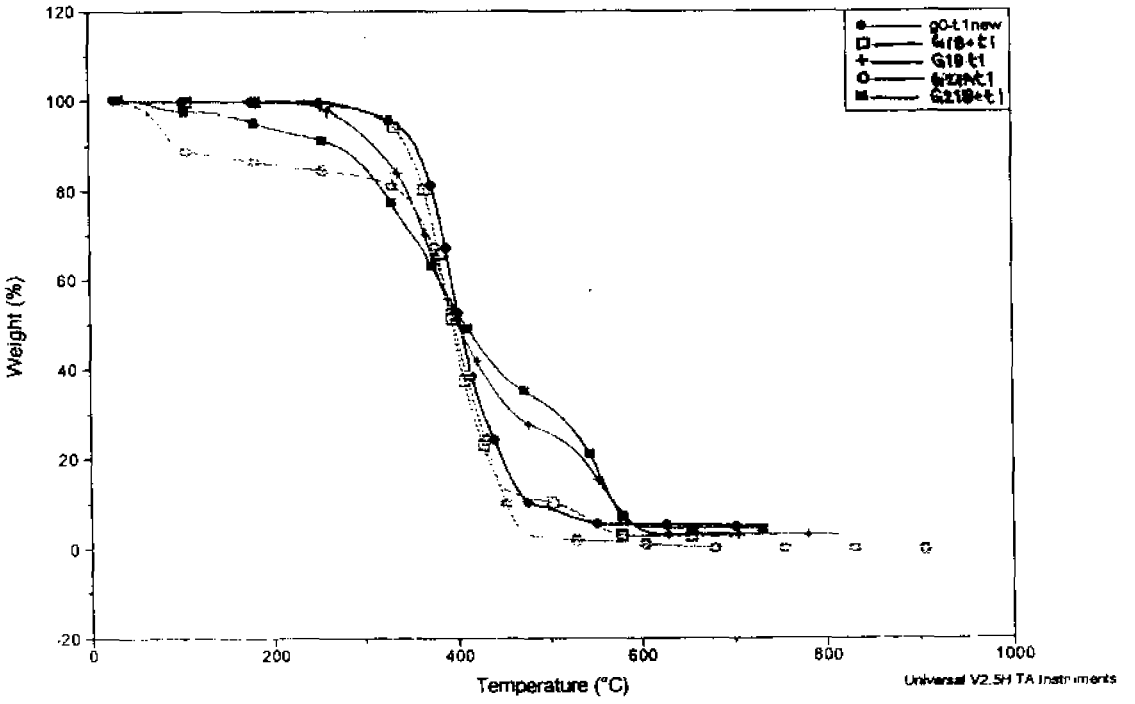

Figure 9.3a. Thermogravimetric (TGA) plots of unmodified and epoxidised NR prophylactics rejects

[G0-0 h, G18-2 h, G19-6 h, G21A-24 h, G21B-144 h]

In the case of sample with epoxidation time of 6 h also, the degradation is a two step process ranging from 216- 486 ^{0}C with peak temperature 372 ^{0}C (first step) and from 486-629 ^{0}C with peak temperature 557 ^{0}C (second step). This sample also presents its increased thermal degradation compared to the unmodified sample as far as net weight change and thermal data are concerned. The net weight change observed is 96.64%.

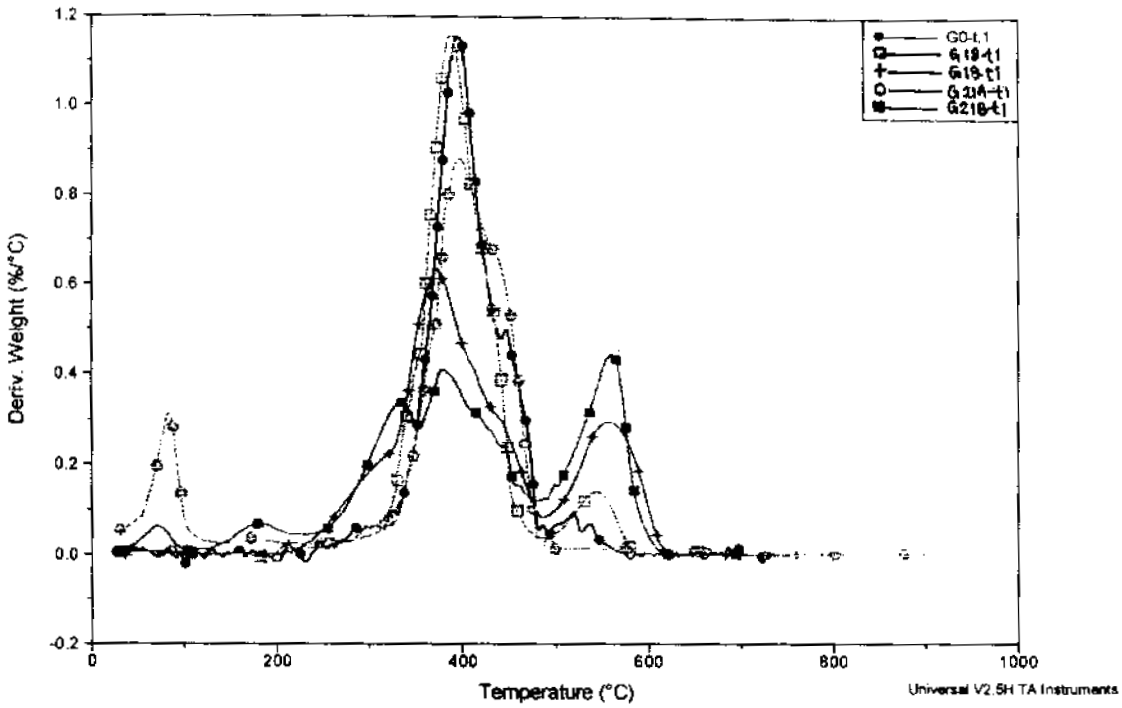

Figure 9.3b. Thermogravimetric (DTA) plots of unmodified and epoxidised NR prophylactics rejects

[G0-0 h, G18-2 h, G19-6 h, G21A-24 h, G21B-144 h]

It is now clear that in the case of epoxidised samples, the degradation follows a two step process presenting two peaks in the DTA peak. But the degradation of sample with an epoxidation time of 24 h presents only a single step. This is actually due to the forward shift of first degradation peak and backward shift of second peak which therefore appear similar to a single peak ranging from 292-500 ^{0}C with a peak value at 396 ^{0}C. Such merging or overlapping of DTA peaks is a common phenomenon in thermal analysis which causes several troubles to an analyst. In this case, the net weight change observed is 99.45%.

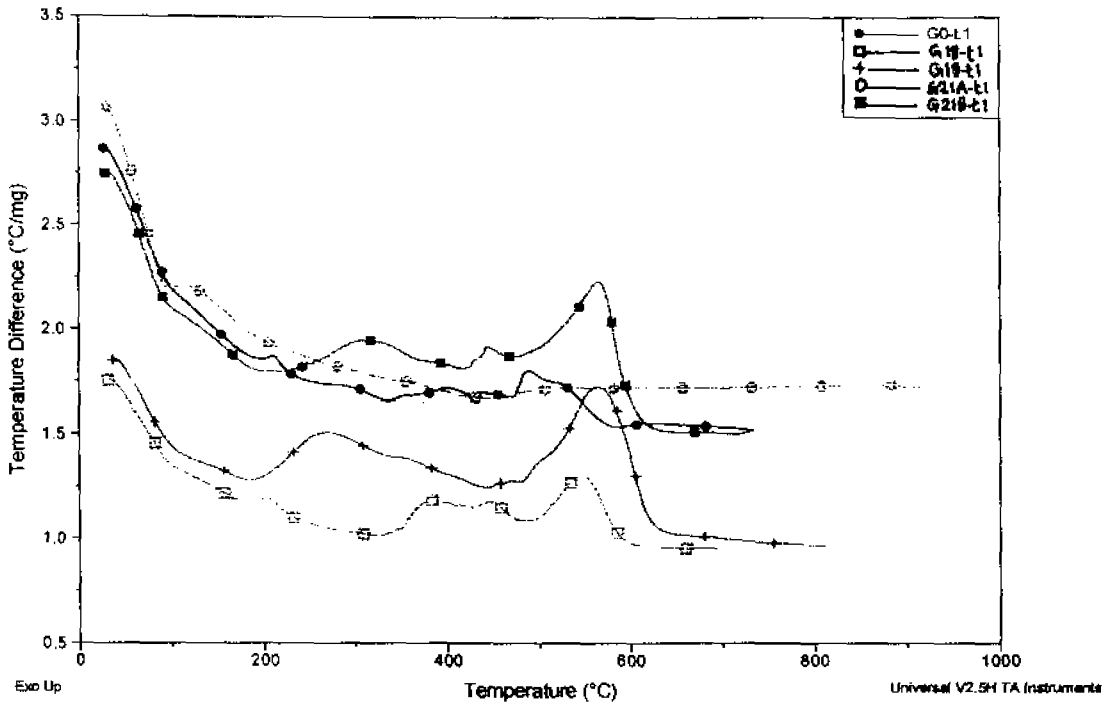

Figure 9.3c. Thermogravimetric (SDT) plots of unmodified and epoxidised NR prophylactics rejects

[G0-0 h, G18-2 h, G19-6 h, G21A-24 h, G21B-144 h]

But such a merging or overlapping of peaks is not observed in the sample epoxidised for 144 h. Here multistep degradation is observed with well resolved and separated peaks. The first one is in the range 230-352 ^{0}C, second one in 352-479 ^{0}C range and the last one in 479-620 ^{0}C range. The net weight change also is similar to other modified samples (95.39%) but only slightly higher than the unmodified sample. The irregular trend in the amount of residue at various temperatures reveals the possibility of formation of thermally stable crosslinked structures in the material during the degradation process. In the case of this sample, the rate constant values of different steps also are comparable.

Table 9.7. Thermogravimetric data of Epoxidised NR prophylactics rejects

Con: of reagent %	Time of reaction, h	Thermal data									
		Peak information		Temperature information, ^{0}C			% Residue analysis at selected temperatures, ^{0}C				
		No. of peaks-DTA	No. of peaks-SDT	Peak-temperature data	Degrad. starts at	Degrad. ends at	300	400	500	1000	Net wt change
0	0	2	2	395 518	331 474	474 578	97	53	8.6	4.9	94.47
20	2	2	2	389 544	279 492	479 591	97.6	43	10	2.6	96.96
	6	2	2	372 557	216 486	486 629	92	50	25	3.1	96.64
	24	2	2	82 396	33 292	124 500	83	47	2.3	1.1	99.45
	144	3	3	334 378 560	230 352 479	352 479 620	85	52	31	4.5	95.39

It can be seen here that the peak temperature decreases first with samples with increased reaction time upto 6 h and for the sample with reaction time of 24 hr, it increases. The value observed for the sample with reaction time of 144 h is the least. The reduction in peak temperature is due to the presence or formation of acidic components during thermal aging of the sample. The net weight change also presents an increasing trend with the reaction time even though slight abnormalities exist for the sample with 24 h reaction time.

Similarly, the thermogravimetric plots of unmodified and chemically modified (dichlorocarbene modified) prophylactics rejects are given in **Figure 9.4a** (TGA), **b** (DTA) and **c** (SDT) and the results are summarised in **Table 9.8**.

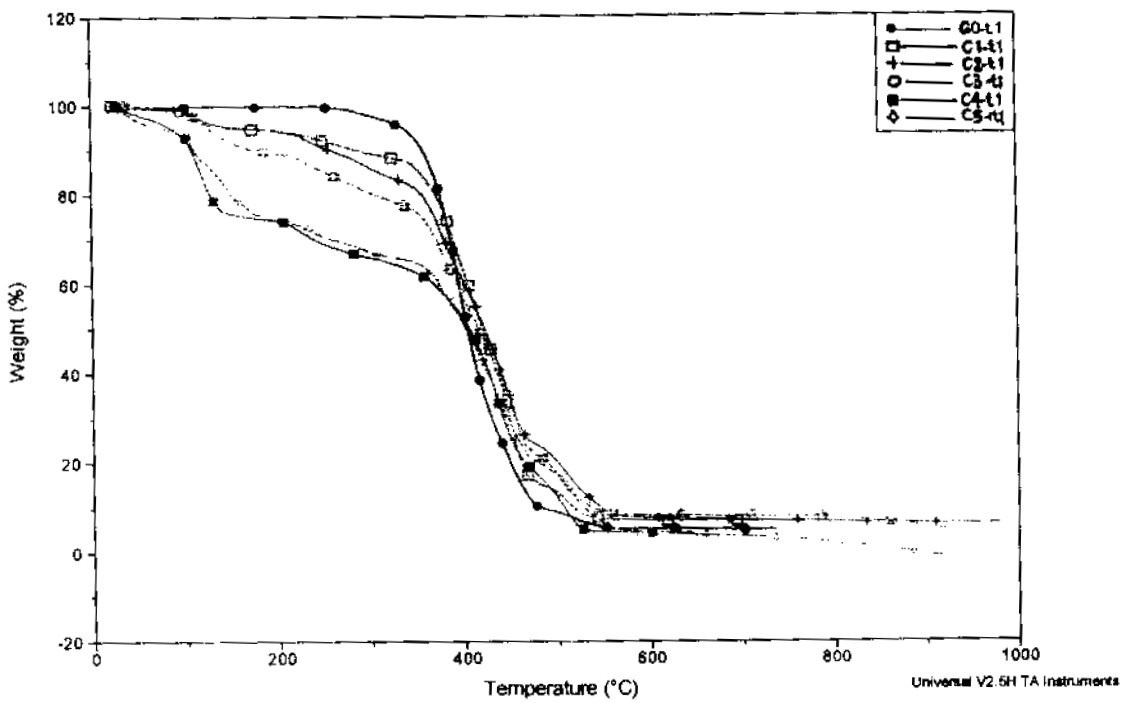

Figure 9.4a. Thermogravimetric (TGA) plots of unmodified and dichlorocarbene modified NR prophylactics rejects

[G0-0h, C1- 2h, C2-4 h, C3-8 h, C4-24 h, C5-48 h]

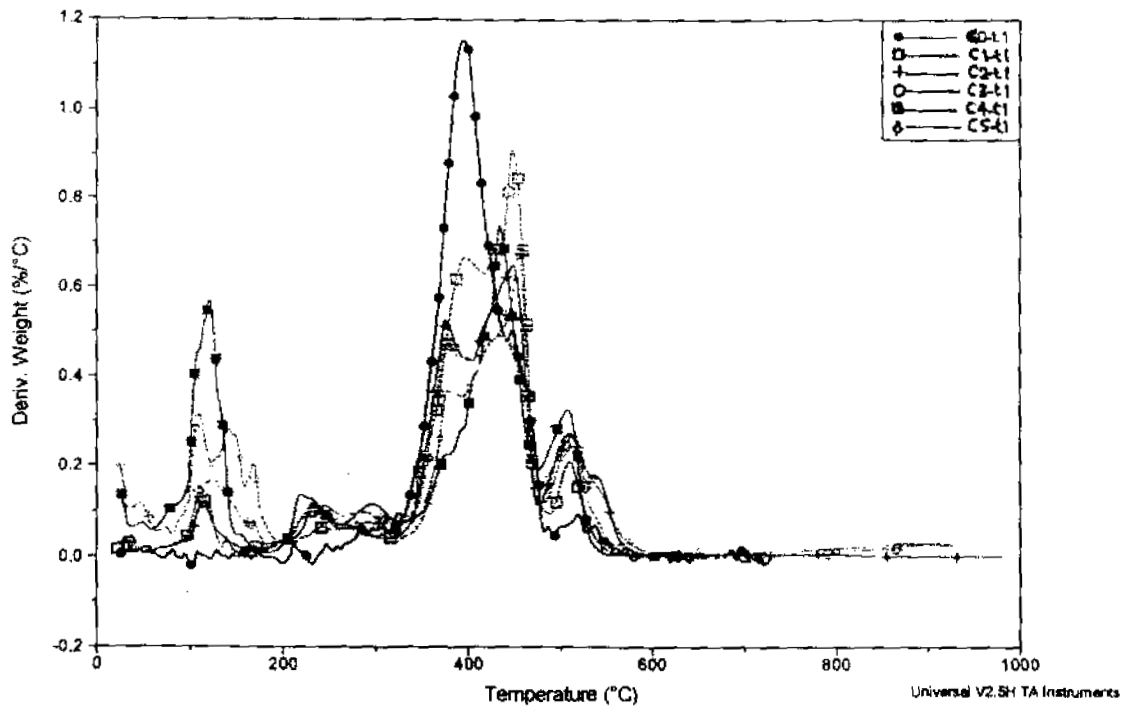

Figure 9.4b. Thermogravimetric (DTA) plots of unmodified and dichlorocarbene modified NR prophylactics rejects

[C0-0h, C1- 2h, C2-4 h, C3-8 h, C4-24 h, C5-48 h]

The degradations mainly consist of three stages. The first one is in 200-300 ^{0}C range, the second one in 300-470 ^{0}C and the last one in 470-550 ^{0}C range. It is a general observation that at a temperature of 300^0 C, the percentage residue goes on decreasing with the time of chemical modification. But the observation is different at higher temperatures. This leads to the possibility of the formation of some thermally stable structures in the dichlorocarbene modified NR prophylactics at higher temperatures studied. The reduced magnitude in the net weight change also points out this fact. It is interesting to see that the net weight change in the case of unmodified sample and the sample chemically modified for 72 h are similar. Therefore it is reasonable to think that any effects in thermal degradation pattern of dichlorocarbene modified NR prophylactics rejects are for the samples with intermediate reaction times such as 2-8 h at 500^0 C.

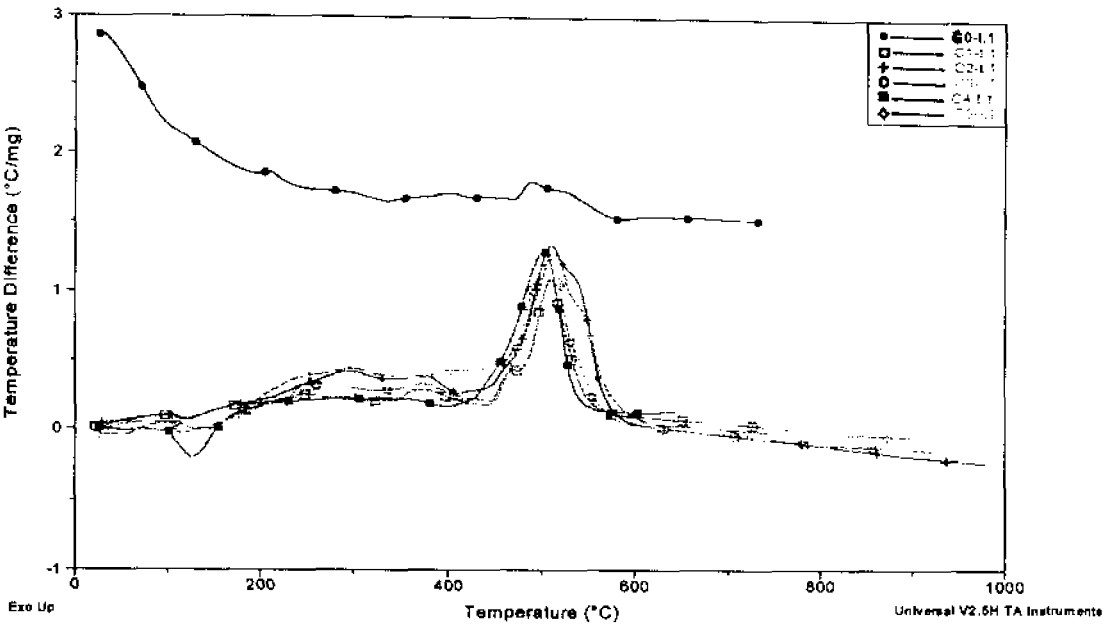

Figure 9.4c. Thermogravimetric (SDT) plots of unmodified and dichlorocarbene modified NR prophylactics rejects
[C0-0h, C1- 2h, C2-4 h, C3-8 h, C4-24 h, C5-48 h]

Table 9.8. Thermogravimetric data of dichlorocarbene modified NR prophylactics

Sample Code	Time of reaction, h	% Residue analysis at selected temperatures				
		300^0 C	400^0 C	500^0 C	1000^0 C	Net wt change
C0	0	97	53	8	4	94
C1	2	89	62	12	7.16	92.61
C2	4	85	60	19	7.22	92.22
C3	8	80	56	17	8.2	91.6
C4	24	65	52	11	4.3	95.6
C5	48	67	49	16	3.9	95.9
C6	72	-	-	-	5.4	94.7

9.1.2. Development and characterisation of polypropylene composites

Polypropylene composites are prepared using the chemically modified and unmodified polypropylene and chemically modified/reclaimed NR prophylactics rejects. The details are given in chapter 2 (sections 2.2.2 to 2.2.6). Epoxidised prophylactics sample used for the study is that obtained after reaction for 24 h using 20% epoxidation reagent, dichlorocarbene modified prophylactics sample used for the study is that obtained after reaction for 24 h (code C4). Reclaimed NR prophylactics rejects prepared as described in chapter 2 (section 2.2.4) also is used in the study. Mixes are selected wisely to study the influence of several parameters as given in **Table 9.9** and the recipe is given in **Table 9.10**.

Table 9.9. Mix numbers and aims

Mixes numbers	Aim
1	Control mix
1-4	To study the effect of loading of reclaimed prophylactics rejects in unmodified PP
5-8	To study the effect of loading of epoxidised prophylactics rejects in MA-PP
9-12	To study the effect of loading of epoxidised prophylactics rejects in Ph-PP
13	To study the effect of loading of epoxidised prophylactics rejects in unmodified PP to compare it with mixes 9-12
14-17	To study the effect of loading of dichlorocarbene modified prophylactics rejects in MA-PP
18-21	To study the effect of loading of dichlorocarbene modified prophylactics rejects in Ph-PP
22	To study the effect of loading of dichlorocarbene modified prophylactics rejects unmodified PP

9.1.2.1. Spectroscopic characterization of chemically modified polypropylene

The FTIR spectra of unmodified and chemically modified (MA-PP and Ph-PP) are given in **Figure 9.5.** MA-PP can be identified by the peaks at 1704 cm^{-1} (carbonyl group in MA), 1783 cm^{-1} (nonsym. stretch of carbonyl in MA) and 1860 cm^{-1} (5 membered cyclic anhydride carbonyl in MA-PP). Similarly, Ph-PP can be identified by the peaks at 1025 cm^{-1} (primary alcohol group CH_2-OH), 1205 cm^{-1} (C-O group), 3200-3600 cm^{-1} (phenolic OH) and 1500-1600 cm^{-1} (aromatic C---C). Other peaks of importance are 841 cm^{-1} (backbone vibration of C-CH_3 in polypropylene) and 1166 cm^{-1} (CH_3 group),

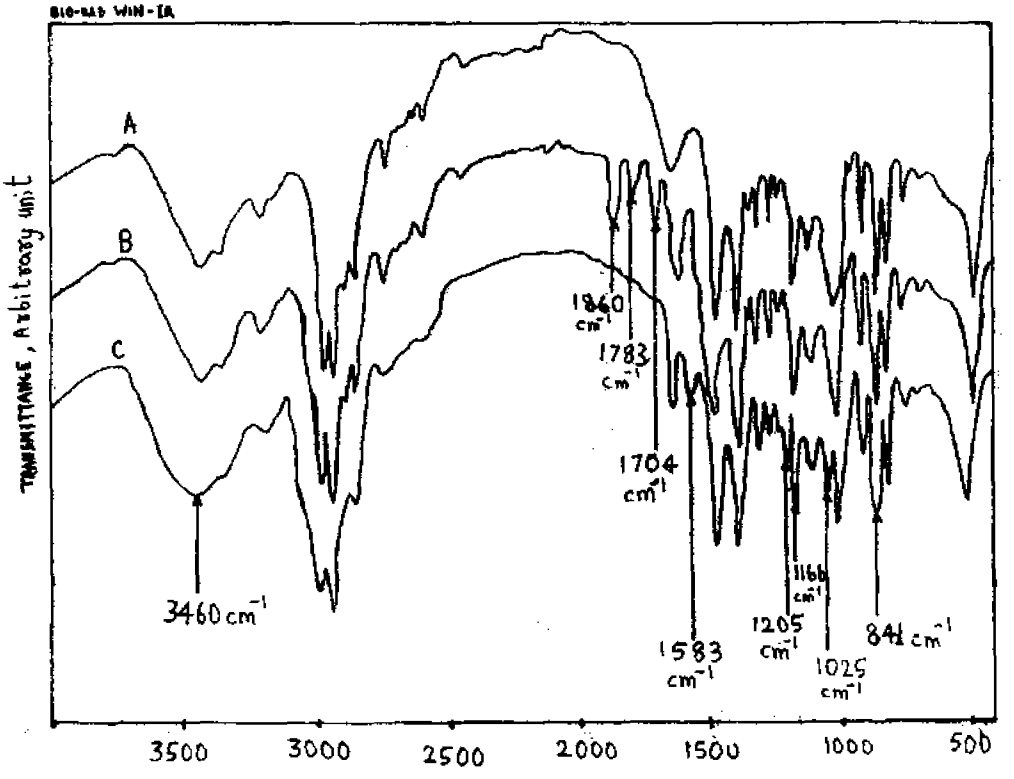

Figure 9.5. FTIR spectrum of PP, MA-PP and Ph-PP

[A –Pure PP, B-MA -PP, C – Ph-PP]

9.1.2.2. Characterisation of technological properties

The variation of tensile strength with the composition of the composites is interesting. It can be seen from **Table 9.10** that when the pure polypropylene presents a tensile strength of 30 MPa, the increasing concentration of reclaimed NR prophylactics

Table 9.10.Basic recipe and properties of the composite

Material	1	2	3	4	5	6	7	8	9	10	11	12	13	14	15	16	17	18	19	20	21	22
PP	100	100	100	100									100									100
MA-PP					100	100	100	100						100	100	100	100					
Ph-PP									100	100	100	100						100	100	100	100	
RLW		10	20	40																		
ELW					10	20	30	40	10	20	30	40	40									
CILW														10	20	30	40	10	20	30	40	40
AO	1	1	1	1	1	1	1	1	1	1	1	1	1	1	1	1	1	1	1	1	1	1
COMPOSITE PROPERTIES																						
TENSILE STRENGTH MPa	30 SD 2.5	32 SD 1.63	25	22	34	27 SD 2.4	30	30	26	23 SD 3.27	35	33 SD 2.4	26	24	22	23 SD 2.4	18	36	31	28	23	20.1
EB, %	6.4	7	10	9	4.4	4.9	5	6.1	4.6	4.9	4.5	4.1	4.8	5.9	6.2	8.1	8.4	6.4	7.8	9.1	9.2	6.2
IMPACT STRENGTH J/mm	50	71	98	123	61	75 SD 4.1	59	55	58	67	78	97	50	75	82	98	103	79	91	99	115	75
Tm 20 ° C/min	162	162	163	162	164	174	160	162	160	159	159	160	160	159	159	158	158	159	161	162	160	160
crystallinity DSC, %	59	53	49	45	57	58	52	50	48	47	44	42	44	44	41	38	44	51	47	46	46	40

rejects (RLW) regularly decreases the value to 22 MPa. In the case of composites comprising of chemically modified PP (MA-PP) and epoxidised NR prophylactics (ELW), the tensile strength shows a slight increase at all loadings compared to the virgin PP/RLW composites. The improved tensile strength may be due to the weak chemical interaction between MA-PP and epoxy groups in the chemically modified NR prophylactics (ELW). Also as the loading of epoxidised NR prophylactics (ELW) in MA-PP increases from 10 to 40 phr, the tensile strength decreases slightly. As the main matrix changes from MA-PP to phenolic modified PP (Ph-PP), addition of ELW presents higher values at 30 and 40 phr loadings. This may be due to the interaction between Ph-PP and epoxy groups in chemically modified NR prophylactics (ELW). But at lower loadings the effect is not observed and the values are lower than both PP/RLW and MA-PP/ELW composites of similar composition. A composite containing unmodified PP and ELW also gives a very low tensile strength. As the loading of ELW in Ph-PP increases, the tensile strength decreases slightly at 20 and 40 phr loadings while at 30 phr loading, it increases.

It is interesting to see that the composites made of MA-PP and dichlorocarbene modified NR prophylactics (ClLW) present lower tensile strength values compared to all above-mentioned samples of similar compositions. This inferior performance is most notable at 40 phr loading. This indicates the absence of any chemical interaction between the MA-PP and ClLW. Moreover, the increasing content of ClLW in MA-PP decreases the tensile strength values. On the other hand, composites of Ph-PP/ClLW show satisfactory tensile performance which is higher than most other compositions mainly at 10 and 20 phr loading and is comparable to MA-PP / ELW composites. Such a performance may be due to the slight interaction between Ph-PP and Cl groups in ClLW. But as observed earlier, the increasing loading of ClLW in Ph-PP decreases the tensile strength value. The reduced tensile strength value of unmodified PP/ClLW composite (40 phr) reveals that the better performance in the case of Ph-PP/ClLW is only due to the weak chemical interactions suggested earlier.

Another parameter of importance is the percentage elongation at break (eb%). It can be seen from **Table** 9.10 that the addition of RLW increases the value of eb% even though it is in an irregular manner. This is because of the presence of crosslinked

reclaimed rubber in PP. It is to be noted here that the reclaimed NR prophylactics can undergo crosslinking in the temperature range used for the melt preparation of the composites. In the case of MA-PP / ELW composites, the eb% values are lower at all loadings compared to the virgin PP/RLW composites. As the loading of ELW in MA-PP increases from 10 to 40 phr, the eb% increases slightly and regularly. When the main matrix is Ph-PP, addition of ELW gives eb% values which are comparable to that of MA-PP/ELW composites. It is also important to note that the values are much lower than PP/RLW composites. As the composite containing unmodified PP and ELW gives a better or comparable value of eb% to that of other samples such as PP/RLW, MA-PP/ELW and Ph-PP/ELW, it can be understand that the chemical modification of PP or prophylactics has no notable effect on eb%. The eb % can be considered to remain constant with the increasing loading of ELW in Ph-PP.

Composites of MA-PP and ClLW show higher values of eb% compared to all other samples at similar compositions. Still, the values are either comparable or slightly lower than PP/RLW systems. The increasing content of ClLW in MA-PP regularly increases the eb % values. Higher values compared to MA-PP/ClLW are shown by Ph-PP/ClLW composites. These values are found to be similar to that of PP/RLW systems. The increasing loading of ClLW in Ph-PP increases the eb % values regularly. When the matrix is unmodified PP, a lower value is observed at 40 phr loading.

The variation of impact strength also deserves much importance. It is a general observation in **Table 9.10** that the impact strength values of all composite samples are higher than that of the pure PP sample. This is due to the reduction in the average crystalline size in polypropylene by the dispersed rubber. As the concentration of RLW in PP increases, impact strength increases considerably in a regular manner. Compared to the virgin PP/RLW composites, the impact strength values are lower at all loadings in MA-PP/ELW systems. This points out the fact that the chemical interaction between MA-PP and ELW is not influencing the impact strength. With increase in the loading of ELW in MA-PP, the impact strength increases until 20 phr and then decreases slightly. After substituting the main matrix MA-PP with Ph-PP, addition of ELW presents higher values of impact strength at 30 and 40 phr loadings. This is similar to the observation in the case

of tensile strength. The values are lower than both PP/RLW and MA-PP/ELW composites of similar composition. Lower value of impact strength is observed in the sample of unmodified PP and ELW. The impact strength increases regularly as the loading of ELW in Ph-PP increases.

MA-PP/ClLW composites show higher impact strength values compared to most other samples of similar compositions. This clearly indicates that weak chemical interactions between the MA-PP and ClLW influence the impact performance of the samples. Better values are observed in Ph-PP/ClLW composites. The increasing loading of ClLW in Ph-PP regularly increases the impact strength value while unmodified PP sample presents lower impact strength with 40 phr ClLW.

9.1.2.3. Crystalline melting point

The crystalline melting point (T_m) of PP **(Table 9.10)** undergoes variation with the composition of the composites. In most of the cases, Tm falls around 160^0 C.

9.1.2.4. Percentage crystallinity of polypropylene composites

The variation in percentage crystallinity determined from DSC of the composites also is interesting **(Table 9.10)**. The percentage crystallinity is found to be reduced with the addition of unmodified and chemically modified NR prophylactics waste into PP. A regular decrease in the value is observed with the increasing content of RLW in PP. Even though higher values are observed in the case of MA-PP/ELW samples, here also a reduction in percentage crystallinity can be observed with the increasing loading of ELW in MA-PP. Again, lower values are obtained in the case of Ph-PP/ELW composites with a reducing trend with increasing loading of ELW. Similar value is presented by the PP/ELW sample also. The percentage crystallinity values shown by MA-PP/ClLW composites are again lower compared to most other systems of similar composition. Here, the value first decreases and then increases with increasing loading of ClLW in MA-PP. Ph-PP/ClLW samples give higher percentage crystallinity values compared to MA-PP/ClLW as well as Ph-PP/ELW systems but the values are lower (at most loadings) compared to MA-PP/ELW and PP/RLW samples. Also, it can be seen that the addition of ClLW to Ph-PP reduces the percentage crystallinity values. Addition of 40 phr ClLW to PP gives a composite with very low percentage crystallinity.

9.1.2.5. Crystalline structure of the composites

The XRD plots obtained for the composites are used to analyse the crystal structure of the polypropylene composites. Some typical plots are given in **Figure 9.6** and the data obtained for different composite compositions are given in **Table 9.11**.

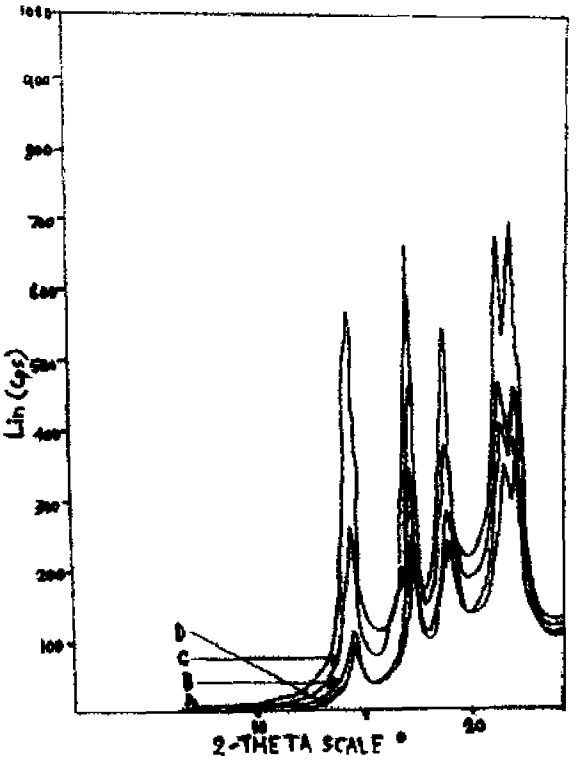

Figure 9.6. Typical XRD plots of polypropylene composites (PP/ RLW)

[A - PP, B – PP + 10 phr RLW, C – PP + 20 phr RLW, D – PP + 40 phr RLW]

The obtained diffractogram of polypropylene have 4 plane reflexes, 110, 040,130 and 111 which are characteristic of α monoclinic structure at 2θ of 14.4, 17.2,18.9, and 21.2 respectively. It can also be seen that the addition of prophylactics in reclaimed or in chemically modified forms is not changing the crystalline structure of polypropylene. In the case of polypropylene and the composite with 10 and 40 phr RLW, the highest intense peak is that at 21.2^0 while in the case of composite with 20 phr RLW, the intense peak is that at 17.2. It can be generally seen that the interplanar distance (d value) is generally decreasing as the loading of RLW in polypropylene increases. This reveals that the rubber

Table 9.11. XRD data

Material	1	2	3	4	5	6	7	8	9	10	11	12	13	14	15
PP	100	100	100	100							100				
MA-PP					100	100	100	100				100	100		
Ph-PP									100	100				100	100
RLW		10	20	40											
ELW					10	20	30	40	10	40	40				
CILW												10	40	10	40
AO	1	1	1	1	1	1	1	1	1	1	1	1	1	1	1
110															
2θ	14.47	14.45	14.53	14.47	14.36	14.38	14.47	14.51	14.51	14.58	14.62	14.54	14.59	14.39	14.46
d	6.11	6.12	6.08	6.11	6.16	6.15	6.11	6.09	6.1	6.1	6.05	6.08	6.06	6.15	6.12
040															
2θ	17.25	17.29	17.42	17.41	17.34	17.31	17.34	17.35	17.37	17.42	17.43	17.42	17.43	17.39	17.39
d	5.13	5.12	5.03	5.08	5.11	5.12	5.11	5.11	5.1	5.08	5.08	5.09	5.08	5.09	5.09
130															
2θ	18.94	18.96	19.13	19.18	19.06	19.06	19.01	19.08	19.08	19.11	19.17	19.06	19.11	19.09	19.14
d	4.68	4.67	4.63	4.62	4.65	4.65	4.66	4.65	4.65	4.64	4.62	4.65	4.63	4.65	4.63
111															
2θ	21.17	21.60	21.79	21.79	21.80	21.74	21.63	21.69	21.84	21.76	21.77	21.69	21.55	21.82	21.82
d	4.19	4.11	4.07	4.07	4.07	4.08	4.10	4.09	4.07	4.08	4.08	4.09	4.12	4.07	4.07

particles are not present in the interspherulitic region of PP and there is slight occlusion of rubber particles to interspherulitic regions. In the case of increasing loading of ELW in MA-PP also the observations are similar. But compared to PP/RLW samples of similar composition, here a general increase in 'd' value can be seen for most of the cases. In the case of Ph-PP / ELW samples, increased loading does not make any notable effect on 'd' value and the values are similar compared to PP/RLW and MA-PP/ELW cases. A composite sample containing PP/ELW also makes no difference. Composites containing MA-PP/ClLW compositions show a reducing trend in d value with increasing loading of inclusion in PP and with respect to similar compositions of PP/RLW and MA-PP/ELW and Ph-PP/ELW systems. Ph-PP/ClLW composite samples show mixed trends which depend on the composition.

9.2.REFERENCES

1. B. Monasse and J.M. Haudin, "Molecular structure of polypropylene homo and copolymers", Chapter 1, 'Polypropylene Structure, Blends and Composites', Ed. J. Karger-Kocsis, Chapman & Hall, London., 1995.
2. Edward P. Moore, Jr., "Polypropylene Handbook", Ed. Hanser Publications, Germany, 1996.
3. J. A. Brydson, "Plastic Materials", 3rd Edn, Newnes Butterworths, London, Ch. 11, 1975.
4. T.T. Lethi, J. Mater. Sci, Pure. Appl. Chem, A33 (12), 1997 (1996).
5. S.H.P. Bettini and J.A.M. Agnelli., Polym. Testing, 19(1), 3 (2000).
6. M. Lambla., Congresso Brasileiro de Polimeros, Vol. 1. Sao Paulo, p. 481, 5-7 Nov 1991.
7. J.P. Sang, K.K. Byung and M. J. Han., Eur. Polym. J, 26, 131 (1990).
8. J.R.Allan, J.G.Bonner and D.L.Gerrard., Rubb. Compos. Process. Appln., 24, 43 (1995).
9. A. Guyot., Polym.Adv.Technol., 7,61 (1994).
10. V.B.Gupta., Ind.J.Fibre.Textile.Res., 22,236 (1997).
11. P.Cheung, D. Suwanda and S.T. Balke., Polym. Eng. Sci., 30, 1063 (1990).
12. B.Kosikova, A.Revajova and V.Demianova., Eur.Polym.J., 31(10), 953 (1995).
13. S.H.P.Bettini and J.A.M. Agnelli., Polymer Testing., 19, 3 (2000).
14. J.M. Willis and B.D. Favis., Polym. Eng. Sci., 30, 1073 (1990).
15. N.K.Singha, P.P.De and S.Sivaram., J.Appl.Polym.Sci., 66,1647 (1997).
16. D.R.Burfield, K.L.Lim, P.K.Seow and C.T.Loo., Proc. Intern.Rubber.Conf., Kuala Lumpur, Vol. 2, p. 47, 1985.
17. L.B.Krentsel, S.O.Travin, A.D.Litmanovich and K.K.Yutujan., Eur.Polym.J., 21(4), 405 (1985).
18. M.V.Eskina, A.S.Khachaturov, L.B.Krentsel and A.D. Litmanovich., Eur.Polym.J., 26(2), 181 (1990).
19. N.V.Bac, M.Mihailov and L.Terlemezyan., Eur.Polym.J., 27(6), 557 (1991).
20. N.V.Bac, L.Terlemezyan and M.Mihailov., J.Appl.Polym.Sci., 50, 845 (1993).

21. L.H.Gan and S.C.Ng., Eur.Polym.J., 22(7), 573 (1986).

22. N.V.Bac, L.Terlemezyan and M.Mihailov., J.Appl.Polym.Sci., 42, 2965 (1991).

23. S.T.M.Sang., J.Rubb. Res. Inst.Malaysia., 26 (2), 48 (1978).

24. J.Lai and W.M.Saltman., J. Polym.Sci., Pt.A, 4, 1637 (1966).

25. M. Joseph, R.Joseph and K.E.George, "Production of Chlorinated Rubber from Latex Waste", paper presented at 7th Kerala Sci. Congress.27-29 Jan, 1995, Palakkad, Proceedings Paper no 02-01, p. 60-62.

26. A.J. Durbetaki.., Anal. Chem., 28, 2000 (1956)

27. "Estimation of chlorine content", Elemental Analysis Lab, National University of Singapore, Singapore.

Chapter 10

CHAPTER 10
CONCLUSIONS

This chapter discusses the main points of all the results contained in this thesis. Also the scope for further studies in the field of polymer recycling has been indicated, focusing the topics still to be explored in this field.

CHAPTER 10
CONCLUSIONS

Owing to strict regulations in the quality of most of the polymer products, the formation of rejects from polymer industries is considerably high. Since, these materials are stable to most common degrading agencies, their decomposition is a very slow process. The open burning of these rejects creates serious environmental problems due to the release of zinc compounds into the atmosphere. The present work is a study on the recycling of mechanically ground prophylactics rejects as filler in synthetic elastomers and plastics. NR prophylactics filler is prepared by the powdering of waste condom material. Synthetic elastomers involved in the study are an amorphous elastomer, 'styrene butadiene rubber' (SBR), a relatively novel strain crystallising elastomer, 'epoxidised natural rubber' (ENR-25 and 50) and ethylene propylene rubber (EPDM). Synthetic plastics involved are an amorphous brittle plastic, 'polystyrene' (PS) and a semi-crystalline plastic 'polypropylene' (PP). The main results in the whole thesis can be concluded as given below.

Prior to the use of natural rubber prophylactics waste as filler in styrene butadiene rubber, it has been ground in a toothed wheel mill to get a rubber powder polydispersed in size. This has been sieved and separated into four different size fractions such as size 1 to 4. A mill-sheeted form of natural rubber prophylactics has also been prepared using a two-roll mill. Different size fractions of prophylactics filler have been characterised by observing their surface morphology using scanning electron microscopy and by analyzing the average particle size, most frequent size range, number and weight average diameters and particle size distribution curves. Scanning electron microscopic photograph of the prophylactics filler reveal that the particles are irregularly shaped with rough surface. From size 1 to 4, the particle size increases and the size distribution widens. Assessment of processing, curing, mechanical, solvent swelling and tensile/tear fractography etc. of styrene butadiene rubber have been done by adding varying loadings (0,10,20,30 and 40 phr) of each fraction to it. In a conventional vulcanisation system, curing characteristics of the styrene butadiene rubber compounds such as optimum cure time, scorch time and induction time have been found to be decreasing with the addition of natural rubber prophylactics filler. This has been identified to be due to the presence of unreacted accelerator in natural rubber prophylactics rejects.

Analysis of rheometric cure curves also shows that the cure reactions follow first order kinetics. The Stress-strain behaviour observed is typical of vulcanised low strength materials, i.e., the stress value is found to be increasing slowly at higher strains. Young's modulus values are found to be unaffected at lower loadings of the prophylactics filler while a slight decrease is observed at higher loadings for most of the cases. The secant modulus M-300 (300 % elongation) decreases up to 30 phr and then increases slightly for 40 phr filler loading. Compared to finer filler particles, better tensile performance has been shown by large prophylactics particles. But tear strength shows superior performance in the case of SBR vulcanisate with smaller filler particles. The comparatively better tensile performance of large sized fillers and mill-sheeted form of the prophylactics filler has been supported by swelling index, cross-link density values, Kraus, Cunneem-Russell equations as well as scanning electron fractography. IN these vulcanisates, prophylactics filler particles have been observed as phase separated entities.

The melt rheological behaviour of styrene butadiene rubber compounds filled with natural rubber prophylactics rejects and selected particulate fillers such as carbon black, silica, and marble powder also have been investigated. Irrespective of the composition, prophylactics particle size, mixing conditions and temperature, all the rubber compounds exhibit pseudoplastic behaviour. The increase in the melt viscosity of styrene butadiene rubber compounds with the increasing loading and varying particle size of prophylactics as well as loading of particulate filler has been found to be shear rate dependent. At the highest shear rate, among the particulate fillers used, the order of increasing the viscosity has been found to be marble powder<silica=black. At low and intermediate shear rates and at a temperature of 150^0C, the compound mixed for 5 minute showed least viscosity but at highest shear rate the curves converge to a point due to 'spurt' or sudden combined flow. In the case of samples without particulate fillers, the influence of temperature has been found to have a notable effect on viscosity only in the case of gum styrene butadiene rubber compounds. Except at 160^0C all the samples filled with particulate fillers have been found to be less pseudoplastic than gum and other prophylactics filled samples. Compared to other equations tried, Eiler van Dyck equation has been found to be giving closely agreeing values of viscosity to that of experimental values while the least agreement is shown by Guth

equation. A decrease in the extrudate distortion also has been observed with the addition of prophylactics and particulate fillers to styrene butadiene rubber compounds.

Use of varying concentrations (0,10,20 30 and 40 phr) of prophylactics filler of varying particle sizes, size 1, 2, 3 and 4 and mill-sheeted form in epoxidised natural rubber (ENR25) has been discussed. Discussions focus on the processing, mechanical and solvent swelling behaviour of gum and prophylactics filled epoxidised natural rubber compounds. The increase in the fastness of cure reaction with the loading of prophylactics has been found to be due to the presence of unreacted accelerator in the prophylactics rejects. In the case of ENR-25, better tensile and tear properties have been exhibited by smaller size prophylactics fillers, especially size 1 at most of the loadings. Among the theoretical models used for the prediction of Young's modulus, Mooney and Guth equations have been found to be giving close values to that of experimentally observed values, mainly at higher loadings of 30 and 40 phr of prophylactics filler. Swelling studies, Kraus, Cunneem-Russell and Lorenz-Park equations and the scanning electron fractography of the samples have supported the comparatively better performance of size 1 prophylactics filler in epoxidised natural rubber vulcanisates. As prophylactics filler particles remain as phase separated entities in ENR-25, these are considered as filled composite systems than as blend systems.

The processing aspects, mechanical and dynamic mechanical analysis of epoxidised natural rubber, ENR 50 containing prophylactics (size 2 fraction) and particulate fillers (carbon black (HAF), silica and marble powder) also have been studied. All the rheographs obtained are typical 'S' shaped curves. The variation of minimum rheometric torque with the loading of prophylactics and particulate fillers is dependent on the composition of the system. Among the particulate fillers, only black has been found to be increasing the minimum torque in ENR/40 phr prophylactics system. Only carbon black and silica have been found to be increasing the maximum rheometric torque. The decrease in optimum cure time and increase in the speed of the vulcanisation reaction also has been observed with prophylactics and particulate fillers in most of the cases. The stress-strain curves of the gum and prophylactics filled ENR vulcanisates are different from typical vulcanised low strength materials due to the strain crystallising nature of ENR. With the addition of prophylactics filler, the young's modulus values show a slight increase. The addition of carbon black, silica and marble powder also increases the young's modulus. The addition of prophylactics in

particulate containing systems increases the young's modulus except in the case of silica. Improvement in the overall mechanical properties of ENR-50 composites with the loading of prophylactics and particulate fillers has been evidenced by the increase in tensile and tear strengths. As the concentration of prophylactics increases, storage modulus values also increase. This is normal to be expected from the presence of crosslinked particles in elastomer matrices. The storage modulus increases with increasing frequency also. Addition of prophylactics filler to epoxidised natural rubber has been found to be increasing the glass transition temperature of epoxidised natural rubber while the presence of carbon black and silica increases it further. An improvement in the hysterisis of the filled ENR-50 samples has been indicated by the reduced damping maximum values of ENR-50 at 100 Hz. Increased concentration of particulate filler in the prophylactics phase has been noted from the analysis of filler distribution by damping maximum values. Good agreement between the tensile strength values and crosslink densities obtained from dynamic mechanical data and swelling studies at room temperature have been observed. Addition of particulate fillers decrease the energy of activation for glass transition of the ENR-50 samples while the loading of prophylactics filler in the presence of particulate filler increase the values.

The development and characterisation of novel ethylene propylene diene rubber (EPDM) compounds have been discussed. Studies in this section makes a comparison between EPDM samples containing NR prophylactics as well as ISNR-5.The cure curves of EPDM compounds have been found to be the resultant of slow curing or marching cure curve of EPDM and that of fast curing 'S' shaped curing curve of natural rubber. Minimum torque in rheographs shows a slight increase with prophylactics loading. Substitution of natural rubber in the place of prophylactics filler results in a low value of minimum torque. This is true at both 10 and 40 phr loadings of the inclusions in EPDM. This is due to the lightly crosslinked nature of the prophylactics. The maximum torque (M_h) of the samples is found to be decreasing with prophylactics loading. The curing properties such as optimum cure time, scorch time and induction time have been found to be decreasing with the loading of prophylactics filler. But for most of the cases the value obtained for compositions with virgin natural rubber (ISNR-5) has been found to be lower than that with prophylactics filler. This behaviour is due to the difference in the curing behaviour of EPDM and ISNR-5. Increased cure rate index and cure rate constant values with the addition of prophylactics and increased

temperature clearly indicates the presence of unreacted accelerator in the prophylactics rejects and the cure activation at high temperature. These observations have been supported by the higher value of energy of activation for the gum EPDM compound. The cure kinetic plots are found to be almost linear which proves that the cure reactions proceed according to first order kinetics. Thermal ageing produces mixed results showing the improvement/deterioration in properties. Unaged tensile strength has been increased with the loading of prophylactics up to 30 phr. Samples with virgin natural rubber give better tensile strength compared to those with prophylactics. Physical cross-links determined from Mooney-Rivlin equation agree with the tensile strength values for most of the cases. Tear strength increases sharply with the loading of prophylactics and levels off at higher loadings. Better values are shown by the substitution of prophylactics filler with ISNR-5 only at 10phr. At 40 phr, the tear strength for EPDM / ISNR-5 system is lower than EPDM / prophylactics. The diffusion process in EPDM vulcanisate is found to be anomalous. The observed variation in the equilibrium swelling has been supported by the intrinsic diffusion coefficient and molar equilibrium sorption constant while at 40^0C sorption and permeation coefficients also has been found to be in agreement. The perfect linearity of the sorption kinetic plots at room temperature reveals the first order kinetic process.

It has been observed that pure polystyrene exhibits linear or near linear stress-strain behaviour while that of its composites with prophylactics show deviations from linearity. A drop in the Young's modulus and tensile strength values has been observed with the loading of prophylactics. The better performance of size 1 prophylactics filler in the case of Young's modulus and impact strength has not been observed in the case of tensile strength. The strain induced crystallisation of prophylactics particles in filled polystyrene composites has been proved by Martin-Roth-Stiehler plots. Scanning electron microscopic observations has been proved to be useful to understand the operating mechanism of impact toughening in polystyrene composites. In loss modulus-temperature plots pure polystyrene exhibits only one transition around 85^0C while all composite samples exhibit two transitions, one around – 58 to -36^0 C range due to prophylactics and the other around 100^0C which is due to polystyrene. The phase-separated nature of the composite samples has been supported by both loss modulus-temperature and tanδ - temperature plots presenting two well-defined transitions. The glass transition values of polystyrene determined from the loss modulus-

temperature plots have been found to be increasing with the frequency of measurement except in the case of pure polystyrene. An irregular increase in the Tg value of polystyrene has been observed with the loading of prophylactics. Particle size of the prophylactics filler is not found to exhibit any clear trend in the variation of Tg values.

The use of reclaimed and chemically modified prophylactics rejects in unmodified and chemically modified prophylactics rejects also has been investigated. Epoxidation of prophylactics rejects at room temperature has been carried out by in-situ formed performic acid using a mixture of formic acid and hydrogen peroxide. A mixture of chloroform and alkali in the presence of a phase transfer catalyst has been used for the dichlorocarbene modification of prophylactics at room temperature. De Link process has been employed for the reclamation of prophylactics rejects in a two roll mixing mill. The preparation of maleic anhydride modified and phenolic modified polypropylene in hot two-roll mill is done using maleic anhydride/dicumyl peroxide mixture and dimethylol phenol/stannous chloride mixture respectively. The characterisation of chemically modified prophylactics and polypropylene has been characterised by infrared spectroscopy, chemical analysis, variation of glass transition temperatures and contact angle determinations. Epoxy group in the epoxidised sample is confirmed by the presence of FTIR peaks around 870 cm^{-1} and 1300 cm^{-1} while dichlorocarbene modification is confirmed by peaks at 1070 cm^{-1} (cyclopropane ring) and 746 cm^{-1} (C-Cl stretch). Up to a reaction time of 144 h, increase in epoxy values has been observed. The magnitude of epoxy value has been found to be highest for the sample treated with 20 % epoxidation reagent. Similarly, up to 4 h an increase in the chlorine content of dichlorocarbene modified samples has been found with a leveling off behaviour afterwards. Stiffened of polymer chains after chemical modifications show increase in the glass transition values. Increased polarity resulting from the chemical modifications has been found to be reducing the contact angle of a sessile drop of water on the surface of chemically modified materials. The thermal stability has been found to be reduced with epoxidation due to the formation of acidic compounds during thermal degradation. Similar results have been noted with dichlorocarbene modified samples also. A reduction in tensile strength has been observed with the addition of reclaimed prophylactics rejects while an increasing trend has been observed in the case of epoxidised prophylactics with both maleic anhydride and phenolic modified polypropylene and dichlorocarbene modified prophylactics with phenolic

modified polypropylene. Impact modification of polypropylene has been found to be more effective with reclaimed prophylactics than chemically modified forms. α-Monoclinic structure of polypropylene has been proved by the results of X-ray diffraction.

Scope for further studies

Further studies in this area may focus on the following aspects.

1. Development of compatibilised blends based on ENR/PVC, NR/PVC and Nylon/EPDM blends involving NR prophylactics rejects.
2. Development of NR prophylactics vulcanisates filled with particulate fillers and reinforced with natural fibres for non-critical applications.
3. Development of toughened polystyrene materials by soaking NR prophylactics rejects in styrene (compounded with polymerising and crosslinking agents) and thermal treatment.

GEORGE MATHEW

Thevervelil House
Kozhencherry P.O.
Pathanamthitta Dist
Kerala State
India 689 641

Ph. 0473-313834
e-mail: gmathew7@rediffmail.com

OBJECTIVE: Seeking a challenging position in the field of Polymer Science

EDUCATION: MSc in Polymer Chemistry and Technology, School of Chemical Sciences, Mahatma Gandhi University, India. 1993.

BSc in Chemistry, Mahatma Gandhi University, India. 1990

COURSE WORK: Polymer Chemistry, Advanced Organic Chemistry, Physical Chemistry, Analytical Chemistry and Spectroscopy.

SKILLS: Proficiency in using standard and modern polymer analytical equipments.

Experience in IR, NMR, TGA, DSC, Universal Testing Machine, Rheovibron, Rheometer, Flexometer, Abrader and most other polymer testing instruments.

Computer Skills: Chemdraw, Chemwindow, Chemoffice Chem Sketch, MS Windows, Microcall Origin, CPP programming.

EXPERIENCE: **6/99 – 5/2000:** Visiting Scientist, Department of Chemistry, National University of Singapore.

Performed chemical modification of prophylactics waste and chracterised the material using various techniques such as IR, TGA, DSC. Successfully prepared and characterized composite materials consisting of chemically modified Polypropylene and modified waste rubber rejects.

10/96 – 9/98: School of Chemical Sciences (Technology Lab)

Council of Scientific and Industrial Research (CSIR) - Senior Research Fellow

Engaged in finding alternate ways to recycle waste rubber and to reuse it effectively in new elastomers such as SBR, ENR, EPDM and for the impact modification of Polystyrene.

Involved in the development and characterization of natural fiber (sisal, jute, coir, banana, oil palm) and synthetic fiber (carbon and glass) reinforced plastic (PE, PP), rubber and thermoset composites, thermal and x-ray diffraction characterizations.

Synthesis, characterization and performance evaluation of a novel Binary accelerator system for accelerated sulphur vulcanization of Natural Rubber.

Evaluated the use of waste marble powder from marble industries as effective filler for natural rubber, experimentally and then, theoretically.

Collaborated with the synthesis, characterization and evaluation of chemically modified SBR as a compatibiliser for SBR/CR blends.

2/95 – 9/96: School of Chemical Sciences

Junior Research Fellow (Technology Lab)

Development of Cabin Bush from waste rubber for heavy vehicles.

3/93- 9/93: Rubber Research Institute of India

Project Assistant, Rubber Chemistry Physics Technology (RCPT) Division.

Development of cost effective and flame resistant Elastomer Composites.

AWARDS:

1. **Jawaharlal Nehru Memorial Award** for Asian Research Scholars. **1998.**
2. **Senior Research Fellowship, CSIR. 1996.**

PUBLICATIONS:

(1) Effect of selected inorganic fillers on the Processing Characteristics,Mechanical properties and flammability of Natural rubber Vulcanisates

G.Mathew, B.Kuriakose and S.Thomas

J. Elast. Plastics, 29,2,163(1997).

(2) Use of Natural rubber Prophylactics waste as potential filler in Styrene Butadiene rubber Compounds

G.Mathew, R.P.Singh, R.Lakshminarayanan and S.Thomas

J.Appl.Polym.Sci., 61, 2035(1996).

(3) Recycling of Natural Rubber Latex Waste and its Interaction in Epoxidised Natural Rubber,

Polymer 42, 2137 (2001).

G.Mathew, R.P.Singh, N. Radhakrishnan Nair and S.Thomas.

(4) Thermal Conductivity of Styrene Butadiene Rubber Compounds with Natural Rubber Prophylactics Waste as Filler.

N.S.Saxena, P.Pradeep, G.Mathew, S.Thomas, M.Gustafsson, S.E.Gustafsson., Eur.Polym.J.35, 1687(1999).

(5) A New Binary Accelerator System for Sulphur Vulcanization of Natural Rubber

A.S.Aprem and G.Mathew Kottayam, K. Joseph and G.Mathew, Changanacherry, and S.Thomas

Kautsch. Gummi Kunstst.(9/99, p. 586)

(6) Compatibilisation of SBR/NBR Using Chemically Modified Styrene Butadiene Rubber.

M.T. Ramesan, C.K. Premalatha, G.Mathew and R. Alex.

J. Polym.Sci., Phys. Ed (submitted).

(7) Role of dichlorocarbene Modified Styrene Butadiene Rubber in Compatibilization of Styrene Butadiene Rubber and Chloroprene Rubber Blends.

M.T. Ramesan, G.Mathew, B. Kuriakose and R. Alex.

Eur. Polym.J, 37, 719 (2001).

(8) Thermal Conductivity and Thermal Diffusivity Analyses of Low Density Polyetehylene Composites Reinforced with Sisal, Glass and Intimately Mixed Sisal/Glass Hybrid Fibres.
G.Kalaprasad, P.Pradeep, G.Mathew, C.Pavithran and S.Thomas
Compos.Sci. Technol., 60, 2967 (2000).

(9) Melt Rheological Behavior of Intimately Mixed Short Sisal/Glass Hybrid Fiber Reinforced Low Density Polyethylene Composites
G.Kalaprasad and S.Thomas, C.Pavithran, S.C.Schit and Murukesan
Compos.Sci. Technol (Accepted-in press)

REFERENCES:

Prof. Suat Hong Goh
Department of Chemistry
National University of Singapore
10 Kent Ridge Crescent
Singapore 119 260

Dr. R.P Singh
Scientist
Polymer Chemistry Division
National Chemical Lab, Pune, India

Prof. V.N. Rajasekharan Pillai
Former Vice Chancellor
Mahatma Gandhi University
Kottayam
Kerala, India 686 560

PERSONNEL DETAILS

1. **Permanent Address**

George Mathew
Thevervelil House (oppo YMCA)
College Road, Kozhencherry P.O.
Pathanamthitta Dist, Kerala State
S. India, Pin. 689 641.
Ph. 91-0473-313834 (Res), **E mail: gmathew7@rediffmail.com**

2. Date of birth : 26 March 1971
3. Sex : Male
4. Nationality : Indian
5. Religion : Christian-Orthodox
6. Marital Status : Single

ADDRESS

George Mathew
Thevervelil House(oppo YMCA)
College Road, Kozhencherry P.O.,
Pathanamthitta Dist, Kerala State
S. India 689 641.
Ph. 91-0473-313834
E mail: gmathew7@hotmail.com

Use of Natural Rubber Prophylactics Waste as a Potential Filler in Styrene–Butadiene Rubber Compounds

GEORGE MATHEW,[1] R. P. SINGH,[2] R. LAKSHMINARAYANAN,[3] and SABU THOMAS[1,*]

[1]School of Chemical Sciences, Mahatma Gandhi University, Priyadarshini Hills P.O., Kottayam 686 560, Kerala, [2]Polymer Chemistry Division, National Chemical Lab, Pune, and [3]Elastomer Technical Services, Pudur, Madurai, India

SYNOPSIS

Owing to the unstable nature of the latex compound and the strict specifications in the quality of latex products such as condoms and examination gloves, the rejection in the latex industry comes to about 10 to 15% of the rubber consumed. These latex rejects contain about 95% rubber hydrocarbon of very high quality. A cost-effective technique has been developed for the reuse of natural rubber (NR) prophylactics waste in styrene–butadiene rubber (SBR). The influence of powdered latex rejects on the curing characteristics, mechanical properties, and failure behavior of SBR has been investigated. More emphasis is placed on the effect of both particle size and the loading of latex waste filler. Swelling studies were carried out to establish the degree of crosslinking of SBR and to assess the extent of interaction between the matrix and latex waste filler of varying particle sizes. A three layer model has been set up to study the diffusion of sulfur from the matrix phase to the filler phase. Scanning electron microscopy has been used to analyze the particle morphology, filler dispersion, and filler–matrix interface adhesion. The results of the study revealed that NR prophylactics rejects can be used effectively as a potential filler in SBR up to about 40 phr loading. © 1996 John Wiley & Sons, Inc.

INTRODUCTION

In recent years, there has been a great deal of interest in polymer industry about the development of cost effective techniques to convert waste and used rubber in to a processable form.[1–6] Many efforts have been made to lower rubber compound cost and to conserve raw materials and energy by the use of reclaimed rubber. Researchers have used various techniques, such as chemical,[1,7] thermomechanical,[3,6] and cryomechanical[2,4,8,9] processes. Even though the use of reclaimed rubber claims economic advantages, it constitutes only a small percentage of the raw rubber consumption because of its inferior physical properties.

Compared to reclaimed rubber, scrap latex rejects have recently become a focus of attention because of the lightly crosslinked and the high quality nature of the rubber hydrocarbon. As a result of the unstable nature of the latex compound and the strict specifications in the quality of latex products such as condoms and gloves, the rejection in the latex industry comes to about 10% to 15% of the rubber consumed. The reuse of natural rubber latex waste is not only a matter of economy but a matter of ecology also because natural rubber takes several decades to decompose. Discarded prophylactics, which are rich in rubber hydrocarbon, should be returned to the production cycle as long as latex industries are faced with the problem of disposal. The papers published in this broad field of recycling may be generally divided into the following areas.

- Studies on the various recycling techniques.[1–5]
- Methods of characterization of rubbercrumbs.[10–14]
- Studies on the interface of rubber crumbs/polymer matrix.[11–15]
- Influence of shape, size, and loading of crumb particles on the properties.[16–18]

* To whom correspondence should be addressed.

Journal of Applied Polymer Science, Vol. 61, 2035–2050 (1996)

CCC 0021-8995/96/112035-16

- Effect of chemical modification of rubber crumbs.[17-19]

In addition to these, Acetta and Vergnaud[20,21] tried to upgrade scrap rubber powder by vulcanization without new rubber. Phadke et al.[22,23] studied the mechanical properties and rheological behavior of cryoground rubber–natural rubber blends. Sharapova et al.[24] investigated the role of sulfur diffusion in the vulcanization of rubbers containing comminuted scrap using a three layer model. Onouchi et al.[25] reclaimed crushed tire scrap with dimethyl sulfoxide. The Rubber Research Institute of India[26] and the Rubber Research Institute of Malaysia[27,28] have independently developed a technique for reclaiming latex rejects. However, more in-depth studies on the influence of particle size and loading of latex waste filler in rubber compounds are lacking. In this paper, we report on an economic method to convert latex rejects to a processable form and to reuse them as a filler in styrene butadiene rubber. Emphasis has been given to understand the influence of both particle size and loading of filler on the curing characteristics and mechanical performance of the vulcanizates. Swelling studies were carried out to understand the interaction of the latex waste filler with the SBR matrix. Sulfur diffusion in these compounds has been analyzed by the help of a three layer model. Particle morphology, filler dispersion, and filler–matrix interface adhesion were analyzed using scanning electron microscopy (SEM).

EXPERIMENTAL

Materials

Styrene-butadiene rubber (SBR; Synaprene 1502) was supplied by Synthetics and Chemicals Ltd, Bhitaura, Bareilly, UP, India. Styrene Content was 25.5%. NR latex waste filler was prepared from waste latex condom rejects supplied by Hindustan Latex Ltd., Thiruvananthapuram, Kerala, India. Rubber additives were as follows: zinc oxide, stearic acid, *N*-cyclohexylbenzthiazyl sulphenamide (CBS), trimethyl dihydroquinolin (TDQ), and sulfur (all are commercial grades). A reagent grade of toluene was also used.

Preparation and Characterization of Powder Rubber

Our size reduction system for powdering NR latex waste doesn't involve any expensive machinery. The size reduction was carried out by a mechanical grinding process in a fast rotating toothed wheel mill to get a polydispersed rubber powder. The powder was separated into three different particle sizes, with size increases in the following order: size 1 (S1) < size 2 (S2) < size 3 (S3).

We have prepared size 4 filler by passing the latex waste through a hot two-roll mixing mill for a fixed time (5 min). The particle size reduction in this technique is very much lower than the first technique; hence, we got comparatively larger particles of sizes ranging from 5–15 mm. Each set of these sizes were characterized for particle size distribution, most frequent size range, average size, and specific gravity. Particle size distribution analysis was done using an optical microscope. A mill sheeted form (M) of the latex rejects also were prepared by passing the rejects through a two-roll mixing mill for 10 min.

Compounding

Compounding of SBR and NR prophylactics filler was done on a two-roll mixing mill (friction ratio 1 : 1.4), according to ASTM D 15-627. The basic formulation used is given in Table I. We have analyzed the effect of adding up to 40 phr of rubber powder of varying sizes, as well as the mill sheeted form, into SBR.

Sample Preparation and Testing

Uncured rubber compound was characterized by determining the optimum cure time, scorch time, and induction time using a Monsanto Rheometer, R_{100}. The cure reaction rate constant was calculated from the cure curves, and, thus, the kinetics of vulcanization also was studied. The Wallace plasticity of the rubber compounds was determined using a Wallace rapid plastimeter.

Curing of the rubber compounds was carried out in an electrically heated hydraulic press at 150°C. Dumbbell shaped tensile and angular tear specimens

Table I Basic Formulation

Material	Loading (phr)
SBR	100
Zinc oxide	5
Stearic acid	2
CBS	1
TDQ	1
Sulfur	2.2
Filler	Variable

MODEL TO STUDY SULFUR MIGRATION

THREE - LAYER MODEL SPECIMEN

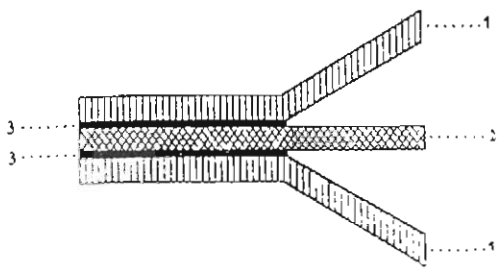

1. GUM SBR MIX
2. NR LATEX WASTE
3. ALUMINIUM FOIL

DIMENSIONS OF THE SAMPLE

		LENGTH (cm)	BREADTH (cm)	THICKNESS (cm)
1.	GUM SBR MIX	16	8	0.2
2.	NR LATEX WASTE	16	8	0.2
3.	ALUMINIUM FOIL	8	8	0.004

Figure 1 Model to study sulfur migration.

were punched out from the compression molded sheets along the mill grain direction. The tensile properties and the tear resistance of the compounds were measured on an Instron Universal Tensile tester, at a crosshead speed of 500 mm/min, as per ASTM D 412-80 and ASTM D 624-81, respectively. Hardness (IRHD) of the cured sheets was also tested.

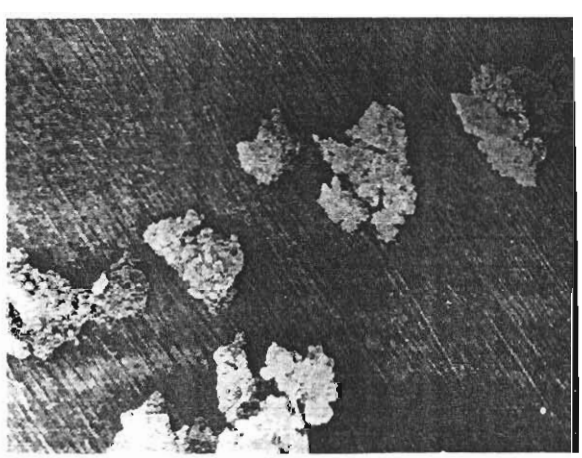

Figure 2 SEM photograph of latex waste filler particles (size 1; magnification ×60).

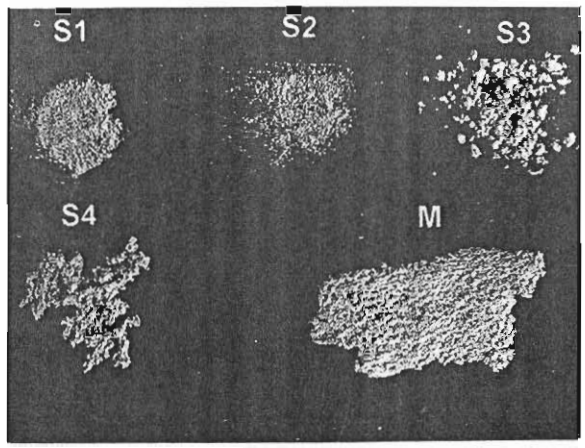

Figure 3 Photograph of varying particle sizes and mill sheeted form of latex waste filler.

Swelling Studies

To assess the swelling resistance of gum and filled SBR vulcanizates, swelling index values were determined. Circular samples of 2 cm diameter were allowed to swell in toluene at room temperature (28°C) for 72 h. The variation of crosslink density with increasing filler loading also was analyzed using swelling experiments. The equation of Kraus,[29] as well as the Cunneen and Russell equations[30] were used to assess the reinforcement of SBR matrix by latex waste filler of varying particle sizes.

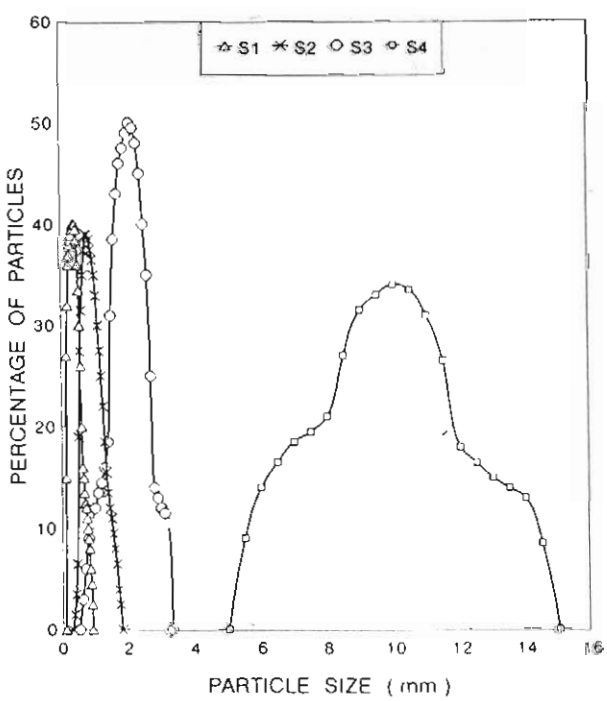

Figure 4 Particle size distribution curves.

Table II Particle Size Data

Particle Size	Most Frequent Size Range (m^2)	Average Size (m^2)
Size 1 (S1)	0.3–0.5	0.5
Size 2 (S2)	0.6–0.9	1.05
Size 3 (S3)	1.7–2.5	1.9
Size 4 (S4)	9–11	10

Sulfur Diffusion Studies

A three-layer model[24] as shown in Figure 1 was set up to study the diffusion of sulfur from the matrix phase to the filler phase. A layer of NR latex waste (containing 80 phr of size 1 filler) was sandwiched between two layers of gum SBR compounds. Size 1 filler was selected because of higher sulfur diffusion rate due to increased contact surface area with SBR matrix. In one half of the specimen, the layers of the gum SBR and latex waste were separated by an aluminium foil; in the other half, the foil was not placed. The region of the latex waste layer with the aluminium foil that will be out of contact with the two outer gum SBR layers is named as the "area not in contact"; the region of the latex waste layer without aluminium foil that will be in contact with the two outer gum SBR layers is named as the "area in contact". The system was then subjected to vulcanization at low pressure. The middle layer was separated, and the swelling index, as well as the crosslink density values were determined, by cutting circular samples from (1) the area in contact with outer gum SBR layers (denoted by CS) and (2) the area not in contact with outer gum SBR layers (denoted by NCS).

Morphology and Fractography

Morphology, filler distribution, and fractography were done using a JEOL JSM 35 C model scanning electron microscope. After tensile and tear testing, the fractured surface was carefully cut out from the failed specimen. The samples were stored in a desiccator to avoid contamination and then sputter coated with gold within 24 h prior to the examination through SEM.

RESULTS AND DISCUSSION

Physical Characteristics of Ground Latex Waste

Particle Morphology

Figure 2 represents the SEM of the NR prophylactics filler particles (size 1) used in the present work. The particles are irregularly shaped with rough surface.

Particle Size Distribution

The photograph of the latex waste filler of different particle sizes and the mill sheeted form used in this study is presented in Figure 3. It is clear from the photograph that as we move from size 1 to size 4, particle size increases. Since it is possible for particles with somewhat large diameters to also penetrate the meshes due to their elasticity, it is better to represent them by size distribution curves, as given in Figure 4. Size 4 shows the most broad distribution. Size 1 and size 2 have narrow distribution, while size 3 takes the intermediate position. The most frequent size range and average particle sizes are presented in Table II. Both these values exhibit an increase as we move from size 1 to size 4. The specific gravity of the latex waste filler is determined to be 1.1529.

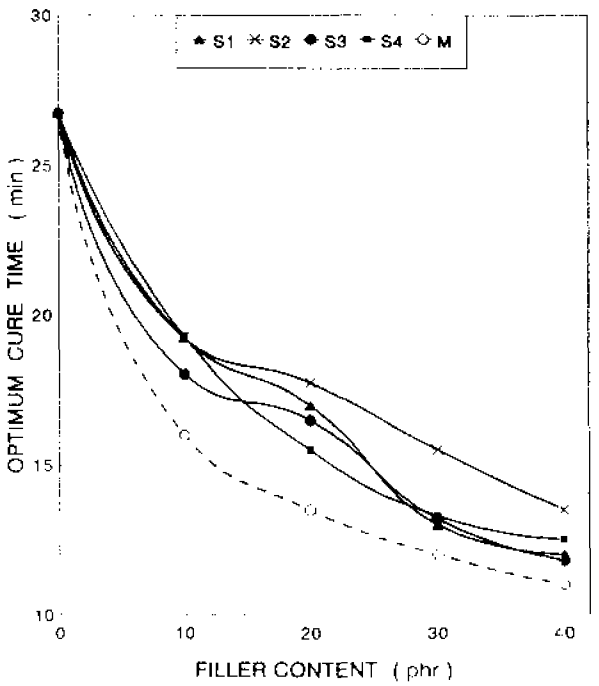

Figure 5 Variation of optimum cure time of SBR compounds with particle size and loading of filler.

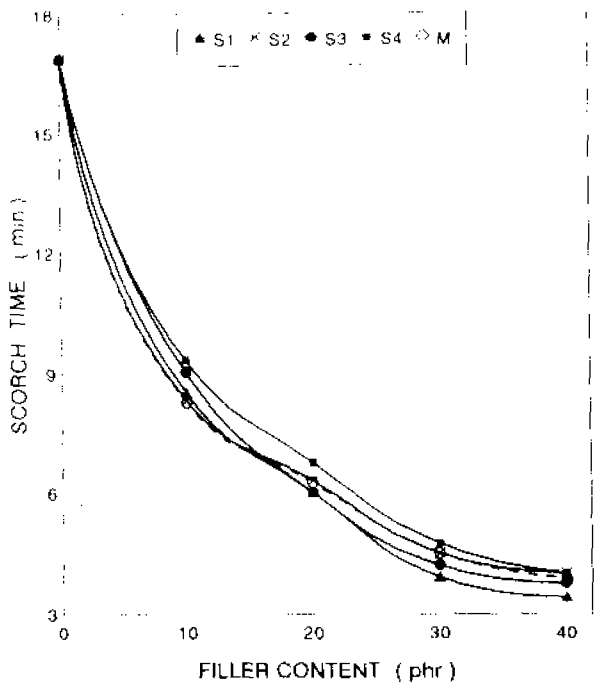

Figure 6 Variation of scorch time of SBR compounds with particle size and loading of filler.

Processing Characteristics

The processing characteristics of the blends are shown in Figures 5–9. The variation of optimum cure time (time for attaining 90% of the maximum torque), scorch time (premature vulcanization time), and induction time (time needed to start vulcanization) are presented in Figures 5, 6, and 7, respectively. A considerable decrease in all these three parameters is noted with increasing loading of filler in SBR. This is due to the presence of unreacted curatives in the latex rejects. Prophylactics, as well as gloves, are manufactured by a latex dipping process, which needs a very fast accelerator. The accelerator used by the company is ZDEC, i.e., zinc diethyl carbamate having the structure:

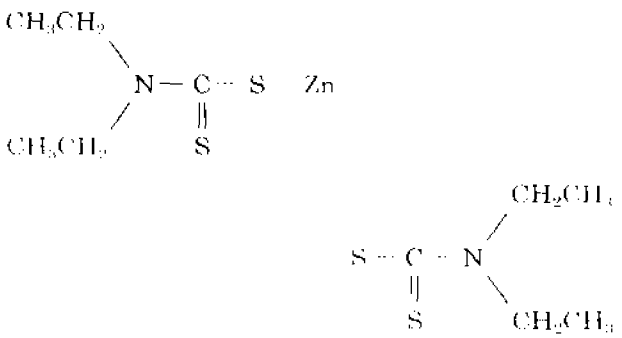

Some of this accelerator will remain unreacted after the curing process. This is extracted using spectroscopic grade acetone, and the spectrum of the dry sample is given in Figure 8. The peak at 790–770 cm^{-1} indicates the presence of ethyl chain ($-CH_2CH_3$), and that at 700–600 cm^{-1} is due to $C-S_{str}$. The $C=S_{str}$ is clearly visible at the 1250–1020 cm^{-1} range, and the peak at 2820–2760 cm^{-1} confirms the presence of N–CH_2 group in the compound. This observation indicates the presence of unreacted accelerator in the NR prophylactics. As the loading of NR prophylactics increases, the availability of the unreacted accelerator also increases, which leads to further reduction in curing characteristics, such as optimum cure time, scorch time, and induction time. The decrease in optimum cure time is minimum for SBR filled with size 2 filler and maximum for SBR loaded with mill sheeted form. The reduction in scorch time as well as induction time is maximum for SBR filled with size 1 filler and minimum for that with size 4 filler.

The general equation for the kinetics of a first-order chemical reaction can be written as

$$\ln(a - x) = -kt + \ln a \qquad (1)$$

where a = initial reactant concentration, x = reacted quantity of reactant at time t, and k = first-order

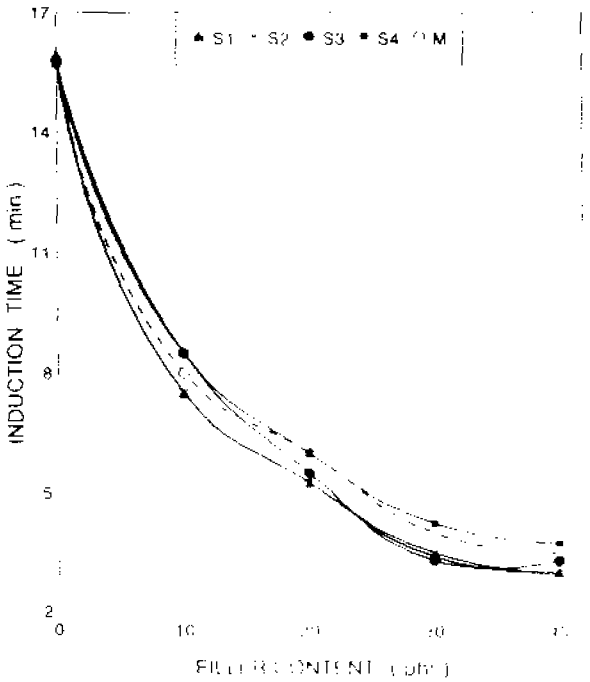

Figure 7 Variation of [illegible] of SBR [illegible] pounds with particle [illegible] loading of filler.

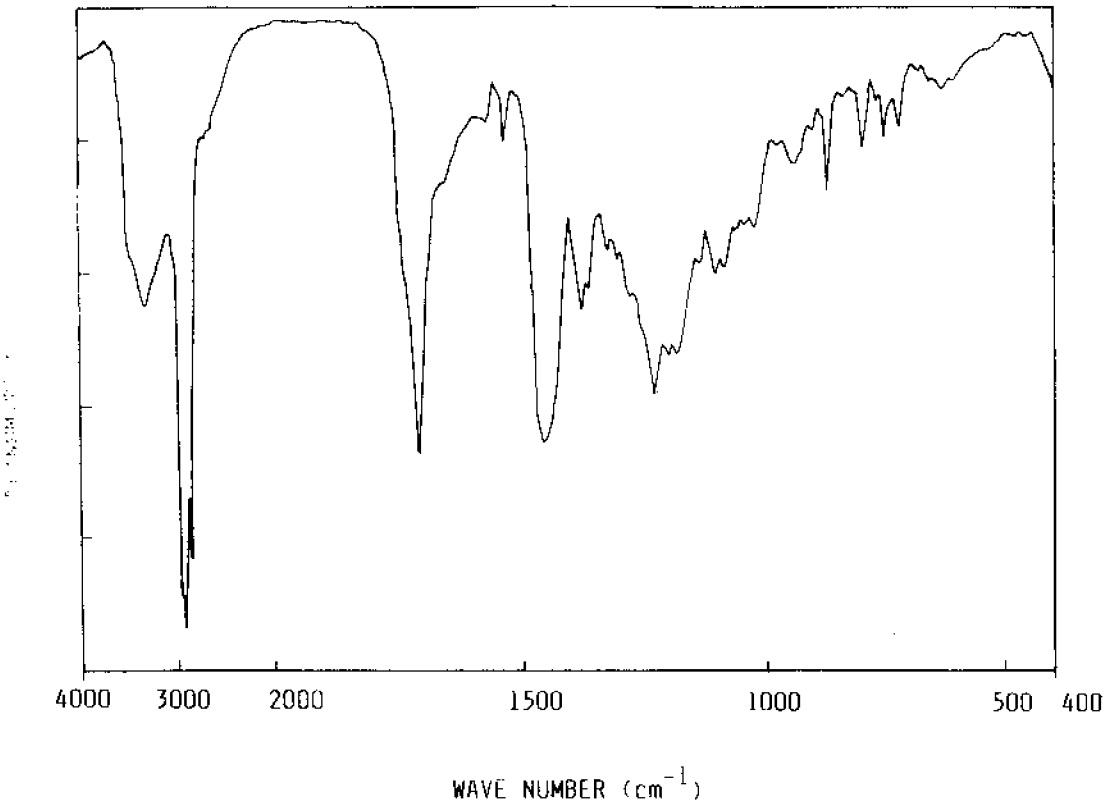

Figure 8 IR spectrum of the unreacted accelerator (ZDEC).

reaction rate constant. For the vulcanization reaction of rubber, the rate of crosslink formation is usually monitored by measuring the torque developed during vulcanization. The torque values so obtained are proportional to the modulus of the rubber. So if the change in a physical property such as modulus is measured, rather than the change in reactant concentration, the following substitutions can be made.

$$(a \quad x) = (M_{\infty} - M) \tag{2}$$

$$a = M_{\infty} \quad M_0 \tag{3}$$

where M_{∞} is the maximum modulus, M_0 is the minimum modulus, M is the modulus at time t. Substituting torque values for modulus, we get

$$(a \quad x) = (M_t \quad M_0) \quad \text{and} \quad a \quad M_{\infty} \quad M_0 \tag{4}$$

where M_{∞} is the maximum torque, M_0 is the minimum torque and, M_t is the torque at time t. When $\ln(M_{\infty} \quad M_t)$ is plotted against t, a straight line graph is obtained as shown in Figure 9, which proves that the cure reaction of the gum and filled SBR compound follows first-order kinetics. The cure reaction rate constant (k) values are obtained from the slope of the straight lines. These values are presented in Table III. The rate constant values generally increase with increasing filler loading. The higher the loading, the greater the amount of curatives available. This indicates an increase in the rate of crosslinking. This increase of rate constant is most noted for SBR loaded with mill sheeted form of the filler.

Figure 10 represents the variation of Wallace plasticity (100°C) with increasing loading of filler. Since Wallace plasticity is a direct measure of the elastic recovery of the rubber compound, its increase with increasing filler loading is extremely advantageous as far as rubber compound is concerned. The Wallace plasticity at 40 phr filler loading is found to be minimum for SBR loaded with mill sheeted form of the filler.

Mechanical Properties

Figure 11 represents the stress strain curves of the gum and filled (size 1 filler) SBR compounds. The stress strain behavior of filled SBR vulcanizate is

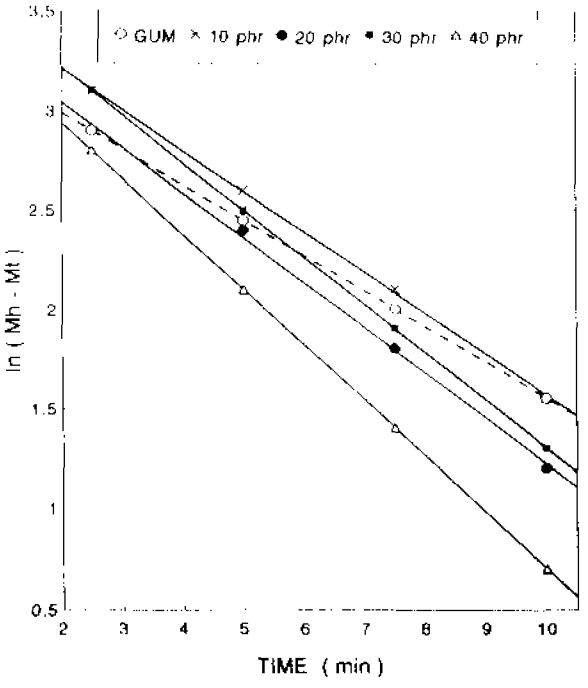

Figure 9 Plots of $\ln(Mh - Mt)$ versus time (min) of gum and filled (size 1) SBR compounds.

controlled by the characteristics of the filler and the matrix. The deformation behavior seen from the curves is almost similar for gum and filled samples. At higher strains, the stress value is found to be increasing slowly, rather than exhibiting yielding behavior. This behavior is typical of vulcanized low strength materials. The elongation at break exhibits a good increase with increasing filler loading (Fig. 12). At higher loadings of the filler, this increase is predominant for SBR vulcanizates filled with size 2, 3, and 4 fillers, while size 1 shows lower values. Mill sheeted form stands midway between these two extremes. The observed increase in elongation at break with increasing filler loading may be due to the ability of NR latex waste filler particles to elongate to high strains. The decrease in crosslink density with increasing filler loading also contributes to the increase in elongation at break values. The crosslink density values are given in the following section. The Young's modulus values are shown in Table III. They are found to be unaffected at lower loadings of the filler, while a slight decrease is observed at higher loadings for most of the cases. The modulus at 300% elongation (M 300) presented in Table III decreases up to 30 phr and then increases slightly for 40 phr filler loading. The above said abnormal nature of moduli values may be due to two opposing factors, namely, crosslink density reduction and reinforcement, with increasing loading of the filler. When reduction in crosslink density with filler loading tends to decrease the modulus, the reinforcement by the filler tends to increase it. These factors compete with each other. Therefore, the observed behavior is the net effect of these two factors.

A remarkable increase in tensile strength is observed with increasing filler loading as shown in Figure 13. This points out the fact that latex waste filler has some reinforcing effect in SBR matrix. This reinforcing effect observed with increasing loading of NR prophylactics is due to the strain crystallization behavior of crosslinked NR latex filler. In a weak matrix like SBR, NR latex filler is found to retain its strain crystallizing nature, even if it is in the form of a fine filler. But contrary to the usual behavior of fine filler (size 1) being more reinforcing, here, the largest size (size 4) and mill sheeted form show relatively good tensile properties. This is due to the sulfur diffusion phenomena noted here and reported earlier in similar systems.[24] For the fine filler (size 1), the contact surface area with the SBR matrix is more. This can lead to an increase in sulfur migration from the matrix to the filler phase. Enhanced sulfur migration weakens crosslinks in the matrix, so the tensile properties which were expected to be superior for size 1 filler actually become inferior. The extent of sulfur migration is controlled not only by the particle size of the filler but also by the degree of polysulfidic linkages in the filler. The degree of polysulfidic linkages in the filler has a direct relation with the extent of sulfur migration.[15] Mill sheeted form of the latex waste filler is prepared by passing the waste through a two-roll mill for 10 min. This leads to substantial breakdown of the polysulfidic linkages resulting in a low degree of polysulfidity for mill sheeted form.[15] It is obvious that mill sheeted form also undergoes size reduction during the mixing procedure. Still the extent of sulfur diffusion is least in SBR compounds filled with mill sheeted form. Owing to this, they show better values of tensile strength over others.

The tear strength of SBR compounds (Fig. 14) also show an increase with increasing loading of filler. The particles of NR latex waste filler present in the tear path elongate to high strains and obstruct tear front. Among the filler sizes used, smaller sizes S_1, S_2, and S_3 show the maximum tear strength at 40 phr loading. Size 4 filler is inferior to these both at low and high filler loading. For SBR compounds containing fillers of smaller sizes, there will be a large number of filler particles present per unit area to elongate to high strains and to obstruct the advancing tear. As far as tear strength is concerned,

Table III Rate Constant and Modulus Values

SBR Compound	Cure Reaction Rate Constant (k) (sec^{-1})	Young's Modulus (MPa)	M_{300} (MPa)
Gum SBR	0.18	1	0.92
Size 1 Filler			
10 phr	0.21	1	0.91
20 phr	0.22	1	0.88
30 phr	0.24	1	0.90
40 phr	0.28	0.77	0.97
Size 2 Filler			
10 phr	0.23	1	0.92
20 phr	0.29	1	0.79
30 phr	0.24	1	0.79
40 phr	0.25	1	0.86
Size 3 Filler			
10 phr	0.24	1	0.91
20 phr	0.25	1	0.88
30 phr	0.24	1	0.86
40 phr	0.34	0.85	0.95
Size 4 Filler			
10 phr	0.20	1	0.79
20 phr	0.26	0.80	0.78
30 phr	0.23	0.80	0.86
40 phr	0.30	0.70	0.70
Mill Sheeted Filler			
10 phr	0.36	1	0.94
20 phr	0.37	0.85	0.92
30 phr	0.33	0.80	0.87
40 phr	0.42	0.80	0.95

the performance of compounds containing fillers of smaller particle sizes is superior to others. The effects of filler loading on IRHD hardness are shown in Figure 15. The observed decrease in IRHD hardness with increasing filler loading is due to the decrease in crosslink density.

Swelling Studies and Crosslink Density Determination

Swelling index values represent the swelling resistance of rubber compound and are calculated using the equation

$$\text{Swelling index } \% = \frac{W_2 - W_1}{W_1} \times 100 \qquad (5)$$

where W_1 is the initial weight of the circular specimen cut from the cured rubber slabs, and W_2 is the final weight of the specimen (after equilibrium swelling in toluene). The swelling index values are shown in Table IV. The value obtained for the gum SBR compound is lower than that of any other filled system. This indicates that the gum compound has more resistance to swelling than the filled SBR compounds. This observation points to the decrease in crosslink density in filled compounds, which again, is a consequence of sulfur migration. With increasing filler loading, swelling index values are found to be increasing, but the increase is not always uniform. For a fixed filler loading, the value is minimum for the SBR compound filled with the mill sheeted form of the filler. This indicates comparatively better reinforcement in SBR vulcanizates loaded with mill sheeted form of the filler. The crosslink density ($1/2M_c$) was determined using the following Flory–Rehner equation

$$M_c = \frac{\rho_r V_s (\phi^{1/3} - \phi/2)}{\ln(1-\phi) + \phi + \chi\phi^2} \qquad (6)$$

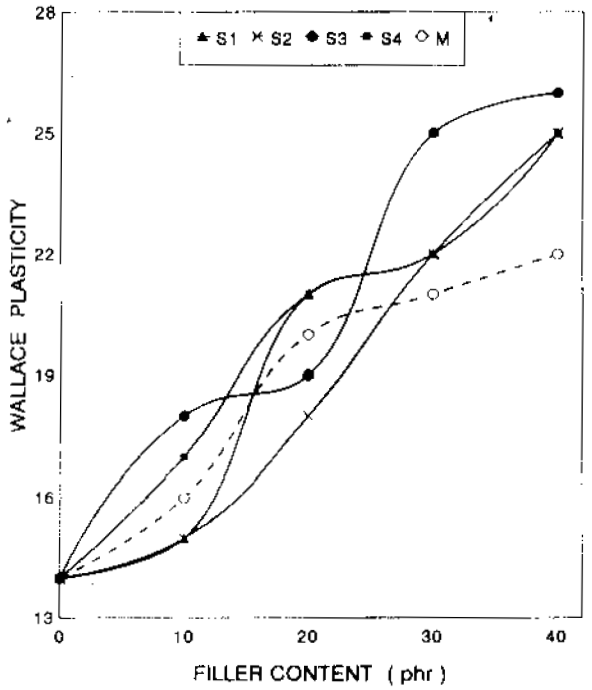

Figure 10 Variation of Wallace plasticity of SBR compounds with particle size and loading of filler.

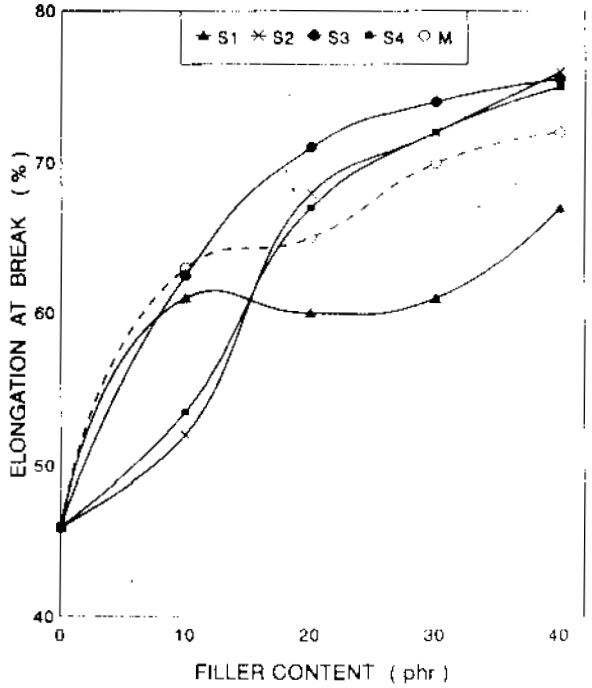

Figure 12 Effect of the size and loading of filler on the elongation at break of SBR vulcanizates.

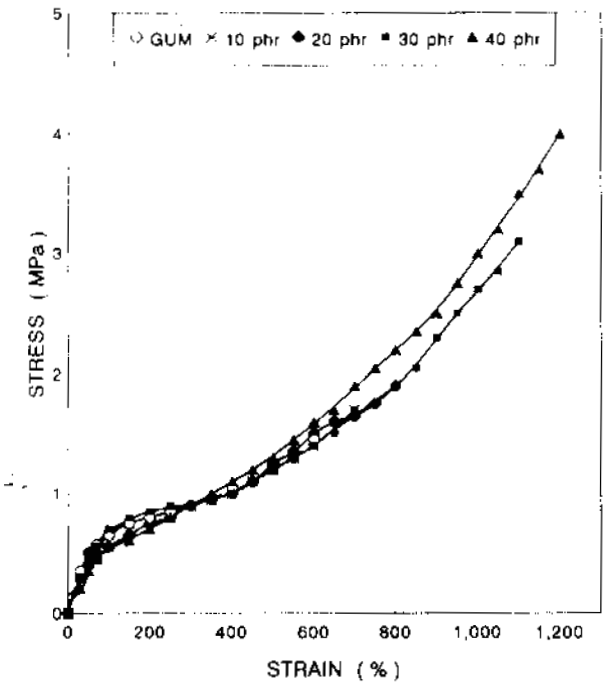

Figure 11 Stress–strain curves of gum and filled (size 1) SBR vulcanizates.

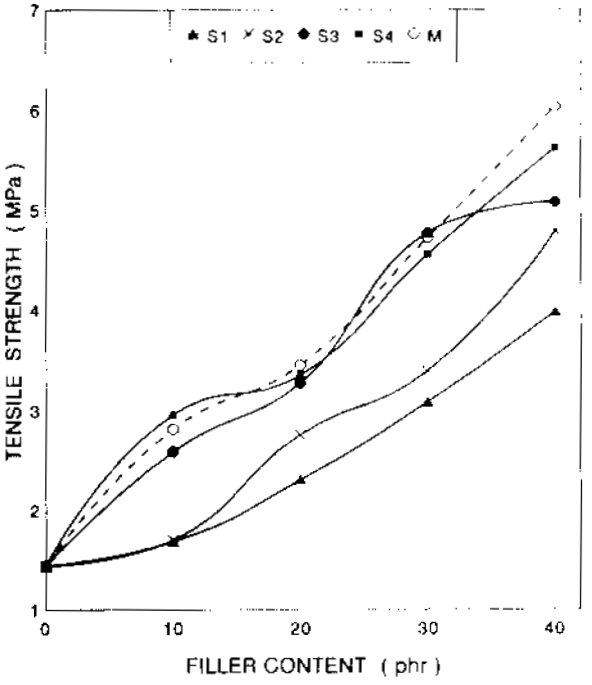

Figure 13 Effect of the size and loading of filler on the tensile strength of SBR vulcanizates.

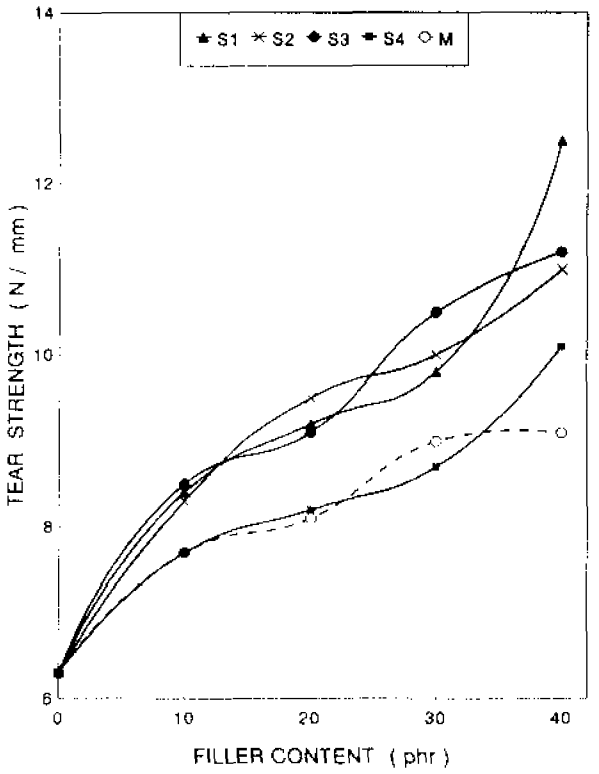

Figure 14 Effect of the size and loading of filler on the tear strength of SBR vulcanizates.

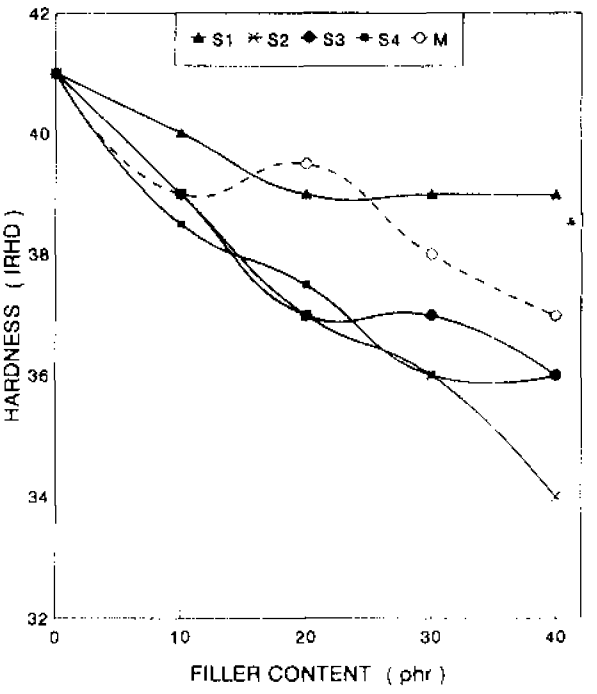

Figure 15 Effect of the size and loading of filler on the hardness (IRDH) of SBR vulcanizates.

where ρ^r is the density of the polymer; V^s, the molar volume of the solvent; V^{rf}, the volume fraction of elastomer in solvent swollen filled samples; and χ, the interaction parameter, which is given by the equation

$$\chi = \beta + (V^s/RT)(\delta^s - \delta^p)^2 \qquad (7)$$

where β is the lattice constant; R, the universal gas constant; T, the absolute temperature; δ^s is the solubility parameter of the solvent; and δ^p, the solubility parameter of the polymer.

The variation of crosslink density as a function of increasing filler loading is given in Figure 16. As a result of sulfur migration from the SBR matrix to the filler phase, the crosslink density of the matrix phase decreases. This can lead to a decrease in the swelling resistance of filled systems. This crosslink density decrease is minimum for SBR vulcanizates containing mill sheeted form of the filler. This is due to the lower degree of polysulfidic linkages in the mill sheeted form, which always retards sulfur migration.[15] For SBR vulcanizates loaded with fillers of smaller particle sizes, enhanced sulfur diffusion causes much reduction in crosslink density.

Extent of Reinforcement

The extent of reinforcement is assessed by using Kraus and Cunneen and Russel equations

According to Kraus equation,[20]

$$V^m/V^{rf} = 1 - m\left[\frac{f}{1-f}\right] \qquad (8)$$

where V^{rf} is the volume fraction of rubber in the solvent swollen filled sample and is given by the equation

Table IV Effect of the Size and Loading of Filler on the Swelling Index Value of SBR Compounds

	Swelling Index Values (%) Filler Loading (phr)				
Sample	0	10	20	30	40
Gum	427				
Size 1		439	469	503	463
Size 2		447	489	520	526
Size 3		461	497	485	497
Size 4		462	476	477	468
M		431	428	449	449

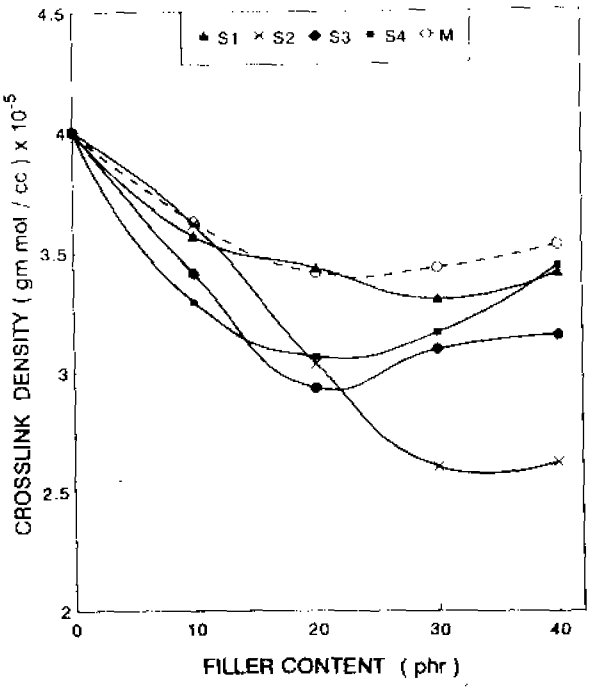

Figure 16 Variation of crosslink density of SBR vulcanizates with particle size and loading of filler.

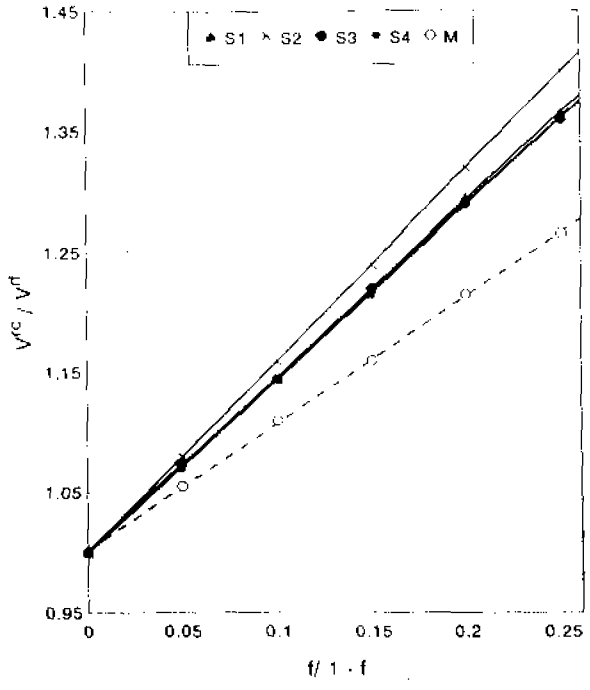

Figure 17 Plots of $\frac{V^{rv}}{V^{rf}}$ vs. $\frac{f}{1-f}$ of SBR vulcanizates.

$$V^{rf} = \frac{(d - fw)\rho_p^{-1}}{(d - fw)\rho_p^{-1} + A^s\rho_s^{-1}} \tag{9}$$

where d is the deswollen weight of the sample; f, the volume fraction of the filler; w, the initial weight of the sample; ρ_p, the density of the polymer; ρ_s, the density of the solvent; and A^s, the amount of solvent absorbed. For an unfilled system, $f = 0$. If we substitute $f = 0$ in eq. (9), we get the expression for the volume fraction of rubber in the solvent swollen unfilled sample (V^{ro}).

$$V^{ro} = \frac{d\rho_p^{-1}}{d\rho_p^{-1} + A^s\rho_s^{-1}} \tag{10}$$

Since eq. (8) has the general form of an equation for a straight line, a plot of V^{ro}/V^{rf} as a function of $f/1 - f$ should give a straight line, whose slope (m) will be a direct measure of the reinforcing ability of the filler used. The more the reinforcing ability of the filler, the more will be the swelling resistance caused by that filler. A constant C, which is characteristic of the filler, is also calculated using the equation

$$C = \frac{m - V^{ro} + 1}{3(1 - V^{ro1/3})} \tag{11}$$

where m is simply the slope of the line plotted, according to eq. (8). The plots of Kraus equation for various particle sizes of fillers are shown in Figure 17, and the values of slopes and C are presented in Table V. According to the theory developed by Kraus[29] for highly reinforcing carbon blacks, negative higher slope values indicate a better reinforcing effect. In the present study, we observed that as the filler loading increases, the amount of solvent absorbed (A^s) also increases considerably. This increase will cause a reduction in the V^{rf} value calculated using eq. (9). Since V^{ro} remains unaffected with filler loading, the ratio V^{ro}/V^{rf} increases considerably with the increasing loading of filler, which gives rise to a positive slope. It is clear from Figure

Table V Values of Slopes and C

	Kraus Equation		Cunneen and Russell Equation
Particle Size	Slope (m)	C	Slope (a)
S1	1.16	1.67	2.8
S2	1.6	1.7	3.3
S3	1.44	1.64	1.9
S4	1.43	1.63	1.3
M	1.1	1.31	1

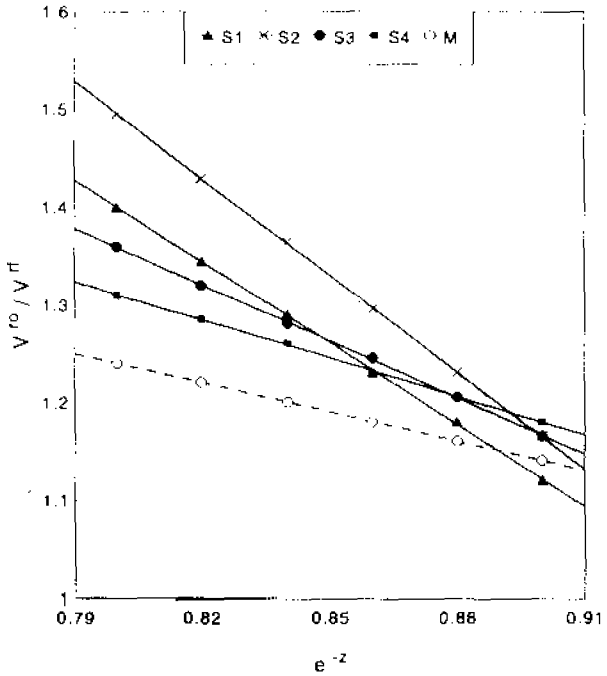

Figure 18 Plots of V^{ro}/V^{rf} vs. e^{-z} of SBR vulcanizates.

17 that the slopes are positive and are higher for SBR loaded with smaller sized fillers. The slope is found to be the lowest for SBR filled with mill sheeted form. So it is clear that SBR vulcanizate containing the mill sheeted form of the filler absorb a minimum amount of solvent. Therefore, the decrease in V^{rf} is comparatively less; hence, the ratio V^{ro}/V^{rf} is the least at a particular loading. This compound therefore presents a lower positive slope compared to others. This suggests that as far as the extent of reinforcement is concerned, the mill sheeted form is superior to other fillers.

The Cunneen and Russell equation[30] is given by

$$V^{ro}/V^{rf} = ae^{-z} + b \qquad (12)$$

V^{ro} and V^{rf} has the same meaning as explained above, and z is the weight fraction of the filler used. A plot of V^{ro}/V^{rf} versus e^{-z} should give a straight line whose slope, a, will be directly proportional to the reinforcing ability of the filler. The plots of the Cunneen and Russell equation are shown in Figure 18, and the slope a values are presented in Table V. In this case, V^{ro}/V^{rf} also increases with increasing filler loading, and this increase is most noted for fillers of smaller particle sizes. Comparatively highly reinforcing mill sheeted form of the filler absorb minimum amount of solvent. Therefore, the SBR vulcanizate loaded with the mill sheeted form of the filler shows the lowest V^{ro}/V^{rf} value at a particular loading and presents a smaller positive slope. Both Kraus and Cunneen and Russell equations point out the comparatively higher reinforcing nature of the SBR vulcanizates containing the mill sheeted form of the filler.

Three Layer Model for Sulfur Diffusion Experiment

The diffusion of sulfur from the SBR matrix to the filler phase is analyzed by using a three layer model,[24] as shown in Figure 1. The dimensions of the model are also given. The crosslink density of the sample obtained from the contact area of the middle latex waste layer is found to be higher than that of the sample obtained from the noncontact area. This is clear from Table VI. The same trend is reflected in the swelling index values presented in the same table. This is because of the sulfur diffusion from the outer gum SBR layers to the middle latex waste layer. This sulfur diffusion causes an increase in the crosslink density of the middle layer at the area in contact with outer SBR layers. At the area of the middle latex waste layer, which is separated from the outer gum SBR layers by the aluminium foil, sulfur diffusion cannot occur, so the crosslink density values here are found to be comparatively lower.

Morphology and Fractography

The tensile as well as tear strengths of the polymers are related to the morphological features of the fracture surface. Figures 19–23 represent the SEM pictures of tensile and tear fractured surfaces. In all the figures, it is possible to see the filler particles as phase separated entities, and this observation confirms the noncompatible nature of these filled samples; so these systems can be considered only as a natural rubber prophylactics filled SBR composite, not a true compatible blend of NR and SBR. It can also be seen from these figures that latex waste particles have undergone size reduction during mixing. The SEM of the failed tensile gum vulcanizate is presented in Figure 19(a). Here, the fracture is

Table VI Swelling Index and Crosslink Density Values From Sulfur Diffusion Experiment

Sample	Swelling Index (Q_f)	Crosslink Density (g mol/cc $\times 10^{-5}$)
CS	4.27	2.75
NCS	5.56	1.65

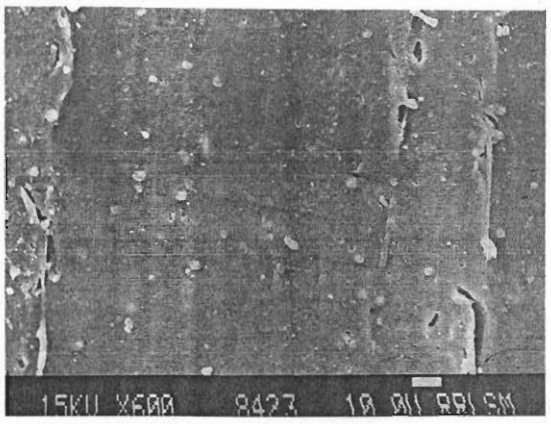

(a)

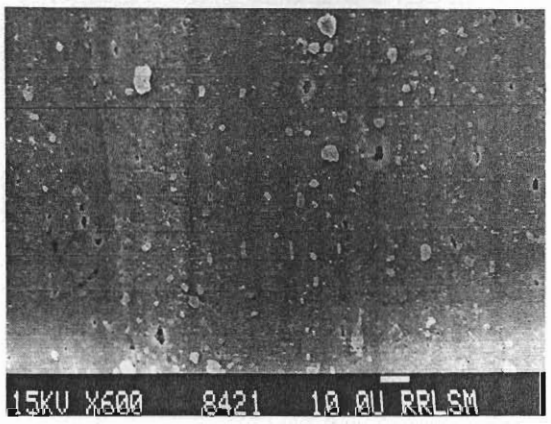

(b)

Figure 19 SEM photographs of the tensile fractured surface of gum SBR vulcanizate (a) and the tear fractured surface of gum SBR vulcanizate (b).

smooth without any deviation. This observation is in agreement with the low tensile strength of the gum SBR vulcanizate. The SEM of the failed tear gum vulcanizate, shown in Figure 19(b), also presents smooth torn areas. This indicates its low tear properties.

The tensile fractured surface of filled (40 phr of size 1) SBR vulcanizate are presented in Figure 20(a). Here, the fracture is not smooth as in the case of gum. As a result of enhanced sulfur migration, dewetting is observed in this case, as shown in Figure 20(b).

Figure 21(a) represents the torn surface of the SBR vulcanizate filled with 40 phr of size 1 filler. The figure shows crack deviation due to the restriction to crack propagation by filler particles. In this case also, dewetting is observed, as can be seen from Figure 21(b). The observation of dewetting is in agreement with the noncompatibility behavior of these filled systems discussed earlier.

The tensile and tear fractured surface of SBR vulcanizate loaded with 40 phr (size 4) filler is shown in Figures 22(a) and (b), respectively. In both cases, extensive crack deviation can be seen.

Figure 23(a) is the tensile fractured surface of the SBR vulcanizate filled with the 40 phr mill sheeted

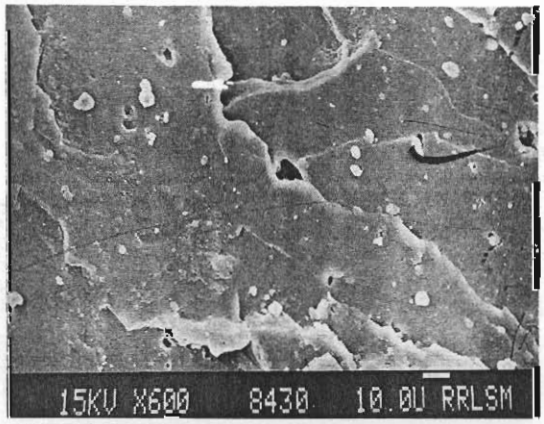

(a)

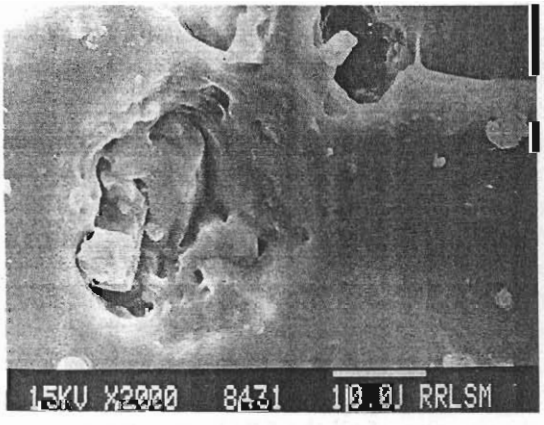

(b)

Figure 20 SEM photographs (a) and (b) of the tensile fractured surface of filled (size 1) SBR vulcanizate.

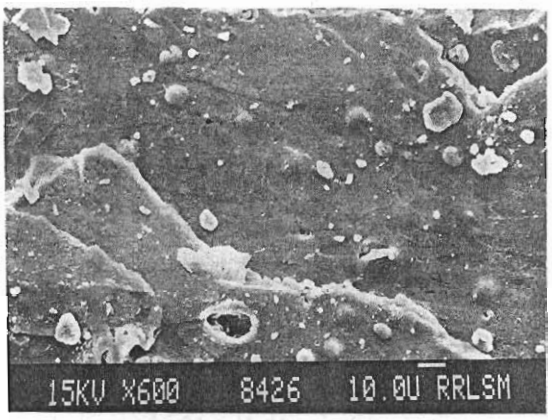

(a)

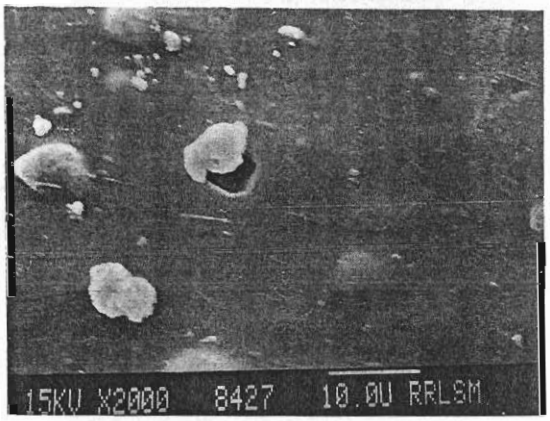

(b)

Figure 21 SEM photographs (a) and (b) of the tear fractured surface of filled (size 1) SBR vulcanizate.

form of the filler. Since sulfur diffusion is minimum in this case, filler–matrix adhesion is fairly good, and, hence, dewetting is less predominant. In this case also, filler particles obstruct the crack propagation and cause crack deviation. The torn surface of the SBR compound loaded with 40 phr of the mill sheeted form is presented in Figure 23(b). A sinusoidal wavy pattern at the fracture surface is a characteristic feature of high tear-resistant material

In the case of all the filled compounds, torn surfaces show much crack deviation and present a series of parabolic tear lines distributed randomly. These parabolic tear lines result from the interaction of main fracture fronts with subsidiary fracture fronts and from the obstruction to tear propagation by filler particles. Reduced sulfur migration causes increase in filler–matrix adhesion in SBR vulcanizates filled with size 4 filler and mill sheeted form. The SEM pictures also indicate that the latex waste particles are not completely compatible with the SBR matrix. In all cases, the particles could be seen as phase separated entities.

CONCLUSION

The use of NR prophylactics waste as a potential filler in SBR is very attractive because of the sim-

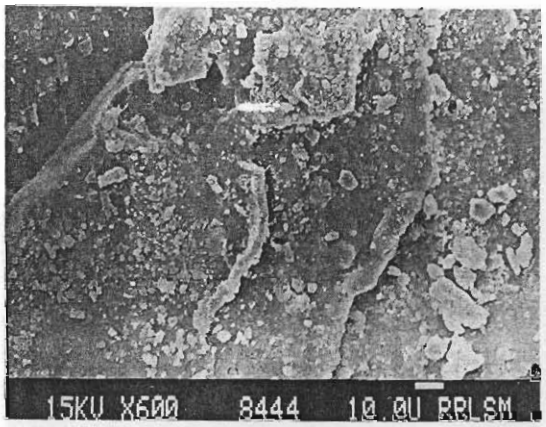

(a)

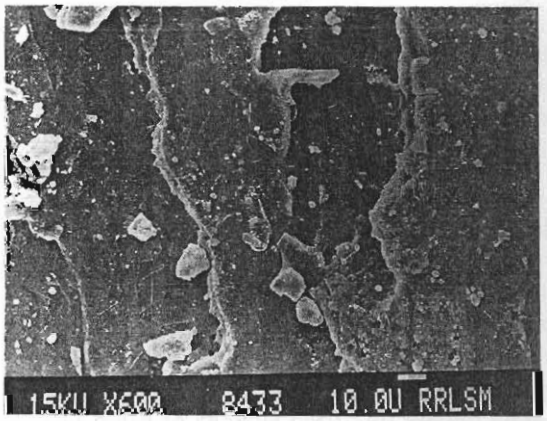

(b)

Figure 22 SEM photographs of tensile fractured surface of filled (size 4) SBR vulcanizate (a) and the tear fractured surface of filled (size 4) SBR vulcanizate (b).

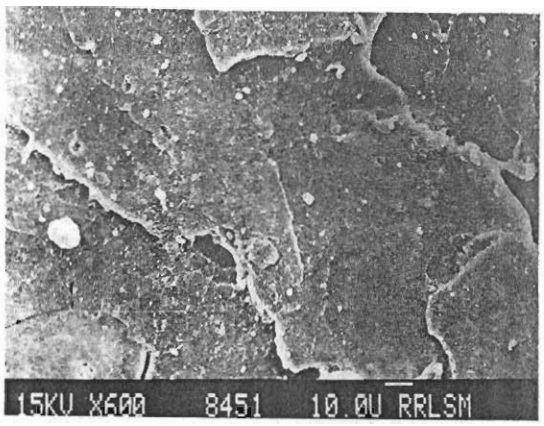

(a)

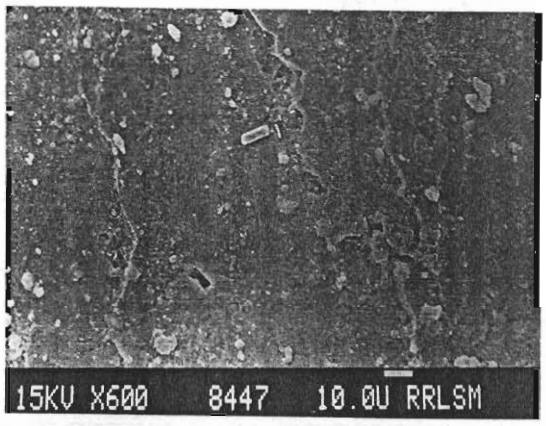

(b)

Figure 23 SEM photographs of the tensile fractured surface of filled (mill sheeted filler) SBR vulcanizate (a) and the tear fractured surface of filled (mill sheeted filler) SBR vulcanizate (b).

plicity of the latex waste grinding technique and the surplus nature of the NR prophylactics. NR latex waste has been ground into particles of various sizes. The particle size morphology and size distribution are analyzed. It has been noticed that with increasing filler loading, there is a reduction in optimum cure time, scorch time, and induction time and an increase in cure reaction rate constant. The Wallace plasticity, which is a measure of elastic recovery of rubber compound, increases with increasing filler loading. The above observations are advantageous as far as productivity and processability are concerned. Up to 40 phr filler loading, the tensile and tear properties show good improvement. The size 4 and mill sheeted form of the filler are found to exhibit superior tensile properties over others. The IRHD hardness values are found to be decreasing with increasing filler content. The swelling index values show a considerable increase, while the crosslink density shows a gradual reduction with increasing filler loading. The Kraus and Cunneen and Russell equations have been used to analyze the extent of reinforcement. These theories support the superior filler–matrix interaction in SBR vulcanizates loaded with the mill sheeted form of the filler. A three layer model has been developed to study the sulfur diffusion in filled SBR compounds. The results emanating from the sulfur diffusion experiment explain the reduction in crosslink density in filled SBR compounds. Compared to the production of fine rubber powder, the production of mill sheeted form of the filler is easy and economic. By wisely selecting the mill sheeted form of the filler, sulfur diffusion can be minimized, and the filler–matrix adhesion can be improved. The SEM examination of the tensile and tear fractured surfaces strongly supports the improved mechanical performance of the SBR vulcanizates filled with the mill sheeted form of the filler. The SEM studies also indicate that the crumb rubber particles are not completely compatible with the SBR matrix. Further studies are in progress to improve the adhesion of the rubber particles with the SBR matrix.

REFERENCES

1. A. A. Harshaft, *Environ. Sci. Technol.*, **6**, 412 (1972).
2. M. C. Kazarnowics, E. C. Osmundson, J. P. Boyle, and R. W. Savage, Paper presented at Rubber Div. Mtg., Am. Chem. Soc., Cleveland, Ohio, Oct 4–7, 1977; *Rubber Chem. Technol.* (abstr.), **51**, 386 (1978).
3. T. C. P. Lee and W. Millens, U.S. Patent 4,046,834 (1977) (to Gould Inc.).
4. L. E. Peterson, J. T. Moriarty, and W. C. Bryant, Paper presented at Rubber Div. Mtg., Am. Chem. Soc., Cleveland, Ohio, Oct. 4–7, 1977; *Rubber Chem. Technol.* (abstr.), **51**, 386 (1978).
5. N. R. Braton and J. A. Koutsky, *Chem. Eng. News.*, **52**, 21 (1974).
6. A. A. Phadke, A. K. Bhattacharya, S. K. Chakraborthy, and S. K. De, *Rubber Chem. Technol.*, **56**, 726 (1983).
7. A. Ratcliffe, *Chem. Eng.*, **79**, 62 (1972).
8. M. W. Biddulph, *Conserv. Recycl.*, **1**, 169 (1977).
9. P. J. Zolin, N. B. Frable and J. F. Gentilcore, Paper presented at Rubber Div. Mtg., Am. Chem. Soc.,

Cleveland, Ohio, Oct 4–7, 1977; *Rubber Chem. Technol.* (abstr.), **51**, 385 (1978).
10. R. P. Burford and M. Pittolo, *Rubber Chem. Technol.*, **56**, 1233 (1983).
11. R. P. Burford, in *Energy Recovery and Utilization of Solid Wastes*. Nagoya, 1982, p. 507.
12. R. P. Burford and M. Pittolo, Talk 56, presented at Rubber Div. Mtg., Am. Chem. Soc., Philadelphia, 1982.
13. L. Slusarski and R. Sandlewski, *Int. Polym. Sci. Technol.*, **11**, 6 (1984).
14. K. Fujimoto and T. Nishi, *Int. Polym. Sci. Technol.*, **8**, 25 (1981).
15. K. Fujimoto, T. Nishi, and T. Okamoto, *Int. Polym. Sci. Technol.*, **8**, 30 (1981).
16. S. Yamashita, *Int. Polym. Sci. Technol.*, **8**, 77 (1981).
17. K. Fujimoto, T. Nishi, and T. Okamoto, *Int. Polym. Sci. Technol.*, **8**, 65 (1981).
18. S. V. Usachev et al., *Int. Polym. Sci. Technol.*, **12**, 30 (1985).
19. P. Elfferding, *Int. Polym. Sci. Technol.*, **9**, 30 (1982).
20. A. Acetta and J. M. Vergnaud, *Rubber Chem. Technol.*, **54**, 302 (1981).
21. A. Acetta and J. M. Vergnaud, *Rubber Chem. Technol.*, **55**, 961 (1982).
22. A. A. Phadke, S. K. Chakraborty, and S. K. De, *Rubber. Chem. Technol.*, **57**, 19 (1984).
23. A. A. Phadke and B. Kuriakose, *Kautschuk Gummi Kunststoffe*, **38**, 694 (1985).
24. L. N. Sharapova, A. A. Chekanova, N. D. Zakharov, and E. Yu. Borisova, *Int. Polym. Sci. Technol.*, **10**, 4 (1983).
25. Y. Onouchi, S. Inagaki, H. Okamoto, and J. Furukawa, *Nippon. Gomu. Kyokaishi*, **55**, 439 (1982).
26. N. M. Claramma, K. T. Thomas, and E. V. Thomas, Paper presented at the Rubber Conf., Jamshedpur, Nov. 6–8, 1986.
27. Y. Aziz, Paper presented at the Plastic Rubber Inst. Seminar, Aug. 4, 1990, Kuala Lumpur, Malaysia.
28. Y. Aziz, Paper presented at Polymer 90, Sept. 23, 1990, Kuala Lumpur, Malaysia.
29. G. Kraus, *J. Appl. Polym. Sci.*, **7**, 861 (1963).
30. J. I. Cunneen and R. M. Russell, *Rubber Chem. Technol.*, **43**, 1215 (1970).

Received July 10, 1995
Accepted April 5, 1996

PERGAMON

European Polymer Journal 35 (1999) 1687–1693

EUROPEAN POLYMER JOURNAL

Thermal conductivity of styrene butadiene rubber compounds with natural rubber prophylactics waste as filler

N.S. Saxena [a], P. Pradeep [b,*], G. Mathew [c], S. Thomas [c], M. Gustafsson [d], S.E. Gustafsson [d]

[a] *Condensed Matter Physics Laboratory, Department of Physics, University of Rajasthan, Jaipur, India*
[b] *Department of Physics, Sree Narayana College, Quilon, Kerala, 691001 India*
[c] *School of Chemical Sciences, Mahathma Gandhi University, Kottayam, Kerala, India*
[d] *Department of Physics, Chalmers Institute of Technology, University of Gothenburg, S-412 96, Gothenburg, Sweden*

Received 24 February 1998; accepted 28 September 1998

Abstract

Efforts on a large scale have been made by the polymer industry to develop cost effective techniques to convert waste and used rubber into processable forms. Some of the authors have developed a cost effective technique for the reuse of natural rubber (NR) latex condom waste as a potential filler in styrene butadine rubber (SBR). It has been proved that waste NR particles do reinforce SBR matrix. For optimizing cryosystem performance of the blends, characterization of the composites in terms of thermal behaviour is important. Thermal conductivity of SBR filled with lightly cross-linked NR latex waste is measured using the transient plane source (TPS) method in the temperature range of 100–300 K. It has been found that the thermal conductivity of SBR composites increases linearly with temperature to a peak value at a temperature which lies well within the glass transition region of SBR. With further increase of temperature the thermal conductivity decreases asymptotically to a constant value near 300 K. The variation in the thermal conductivity is empirically correlated with the present experimental data by the equation, $\lambda(T) = a + bT + cT^2$, where a, b and c are parameters which are polymer dependent and have different values below and above the glass transition. The observed variation in thermal conductivity is explained on the basis of various phonon scattering mechanisms, namely structure scattering and cooperative motion of repeat units, as also by considering structural features and the effect of temperature on structural units in a phenomenological manner.

1. Introduction

It has been well established that polymer composites and blends are effective answers to the challenge of developing new polymers for a specific set of properties [1]. These materials give cost effective and easily available compounds and are widely used in the cryogenic temperatures, especially around their glass transition, T_g. Since the T_g of both SBR and NR lie within the region of 100–300 K, a study of thermal conductivity of these materials would yield valuable information which would be of considerable help in optimizing cryosystem performance, heat transfer and cooling load calculations and determination of different state points. The study of low temperature thermal properties and the generation of practical design data between 100 and 300 K will contribute much to the understanding of the thermal equilibrium processes and hence to optimize cryo-components.

Considerable work has been reported on the variation of pure polymers [2,3] but data on polymer composites are limited. Efficient application at cryo-

* Corresponding author. Fax: +91 474-741793; e-mail: aravukad@md2.vsnl.net.in

0014-3057/99/$ - see front matter
PII: S0014-3057(98)00247-X

genic temperatures depends not only on their mechanical properties but also on their thermal properties such as thermal conductivity, diffusivity etc. Also attempts have been made to make rubber compounds cheaper and to conserve raw materials and energy by the use of reclaimed rubber [4–7]. Some of the authors [8] have developed a cost effective technique for the reuse of NR latex waste as filler in SBR. In contrast to inferior technological properties of reclaimed rubber, scrap latex rejects contain high quality rubber hydrocarbon and are lightly cross linked. From the ecological point of view also the reuse of NR latex waste as a potential filler in SBR is interesting since NR takes several decades to decompose. Various types of studies on the NR latex waste filled SBR compounds have already been conducted [8] and in this paper we report the thermal conductivity studies on five samples of SBR/NR including SBR gum and SBR filled with 10, 20, 30 and 40 phr of NR prophylactics waste having average particle size of 5 mm.

2. Experimental

Finely powdered NR latex waste is blended with SBR by the following technique. Powdering of NR latex waste is done by an inexpensive size reduction mechanism. The size reduction was carried out by a mechanical grinding process in a fast rotating toothed wheel mill to get a polydispersed rubber powder. Compounding of SBR and latex waste filler was done on a two roll mixing mill according to ASTMD 15-627. Curing of the rubber compounds was carried out in an electrically heated hydraulic press at 150°C. Samples of diameter 18 mm and thickness 10 mm are prepared by moulding. Details of the sample specification, basic formulation and composition are given in Tables 1–3. Thermal conductivity measurement of the samples has been made using transient place source (TPS) method in the temperature range of 100–300 K. The technique is based on three-dimensional heat flow inside the sample, which can be regarded as an infinite medium by limiting the total time of transient recording. A disc-shaped TPS element with diameter 7 mm and thickness 0.07 mm is placed between two cylindrical pieces of the sample material of diameter 18 mm each.

Table 1
Specification of SBR/NR composites

Specification	
Styrene butadience rubber (SBR)	*Source*: Synthetics and Chemical Ltd, Bhitaura, Bareilly, India. Strene content 25.5%
NR Latex waste filler	Prepared from waste latex condom rejects. *Source*: Hindustan Latex Ltd, Thiruvanandapuram, India
Rubber additives	Zinc oxide, Stearic acid, *N*-cyclo hexyl benz-thiazyl'sulphenamide, trimethyldihydroquinolin sulphur [all are commerical grades]
Toluene	Reagent grade is used

Table 2
Basic formulation

Material	Loading (phr)
SBR	100
Zinc oxide	5
Stearic acid	2
CBS	1
TDQ	1
Sulphur	2.2
Filler	Variable

The sample holder containing these samples is placed in a thin-walled steel tube having slightly bigger diameter than the sample holder and is left in the cryostat containing liquid nitrogen until all temperature gradients in the sample have disappeared. After achieving the isothermal conditions in the sample a constant current pulse is passed through the heating element and resistance or temperature of the element is recorded simultaneously by recording its voltage increase.

2.1. Theory of the TPS method

In the TPS technique the source of heat is a hot disc made out of a bifillar spiral (shown in the Fig. 1), which also serves as a sensor of the temperature increase in the samples. Assuming that the conducting pattern is in the y–z plane of a coordinate system placed inside an infinite solid with a thermal conductivity λ, a thermal diffusivity κ, and a specific heat per unit volume ρC, the rise in temperature at a point y, z at time t, due to an output power per unit area Q is given by [9, 10]:

Table 3
Composition of the samples

Sample I	SBR (gum)
Sample II	SBR + 10 phr NR
Sample III	SBR + 20 phr NR
Sample IV	SBR + 30 phr NR
Sample V	SBR + 40 phr NR

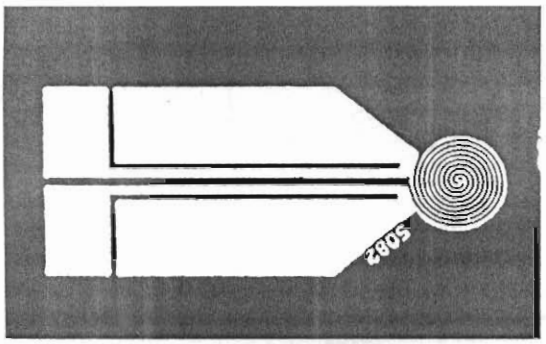

Fig. 1. TPS sensor.

$$\Delta T(r,z,\tau)=\frac{1}{4\pi^{3/2}a\lambda}\int_0^{\tau}\frac{d\sigma}{\sigma^2}\int_A dy'\,dz'Q\left(y'z't-\frac{\sigma^2a^2}{x}\right)\times\exp\left[\frac{-(y-y')^2-(z-z')^2}{4\sigma^2a^2}\right] \quad (1)$$

where $x(t-t')=\sigma^2a_1^2$, $\theta=(a^2/x)$, $\tau=(t/\theta)^{1/2}$, a is a constant (radius of the disc) which gives a measurement of the overall size of resistive pattern and is known as the characteristic time. The temperature increase $\overline{\Delta T(\tau)}$, because of flow of current through the sensor, gives rise to a change in the electrical resistance $\Delta R(t)$ which is given as [10]

$$\Delta R(t)=\alpha R_o\overline{\Delta T(\tau)} \quad (2)$$

where R_o is resistance of TPS element before the transient recording has been initiated, α is the temperature coefficient of resistance (TCR) and $\overline{\Delta T(\tau)}$ is the mean value of the time-dependent temperature increase of the TPS element. $\overline{\Delta T(\tau)}$ is calculated by averaging the increase in temperature of TPS element over the sampling time because the concentric ring sources in the TPS element have different radii and are placed at different temperatures during the transient recording. Following Gustafsson [10],

$$\overline{\Delta T(\tau)}=\frac{P_o}{\pi^{3/2}a\lambda}D_s(\tau) \quad (3)$$

where

$$D_s(\tau)=[m(m+1)]^2\times\int_0^{\tau}\frac{d\sigma}{\sigma^2}\left[\sum_{i=1}^{m}I\left\{\sum_{k=1}^{m}k\sigma^{\frac{-(i^2+k^2)}{4\sigma^2m^2}}L_o\left[\frac{ik}{4\sigma^2m^2}\right]\right\}\right] \quad (4)$$

P_o is the total output of power, L_o is the modified Bessel function. To record the potential difference variations, which normally are of the order of a few millivolts during the transient recording, a simple bridge arrangement, as shown in Fig. 2, has been used. If we assume that the resistance increase will cause a potential difference variation $\Delta U(t)$ measured by the voltmeter in the bridge, the analysis of the bridge indicates that:

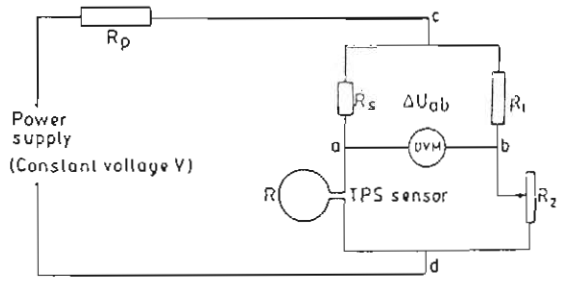

Fig. 2. Bridge circuit for TPS method.

$$\Delta E(t)=\frac{R_o}{R_s+R_o}I_o\Delta R(t)=\frac{R_s}{R_s+R_o}\frac{I_o\alpha R_oP_o}{\pi^{3/2}a\lambda}D_s(\tau) \quad (5)$$

where

$$\Delta E(t)=\Delta U(t)[1-C\cdot\Delta U(t)]^{-1} \quad (6)$$

and

$$C=\frac{1}{R_sI_o\left[1+\frac{\gamma R_p}{\gamma(R_s+R_o)+R_p}\right]} \quad (7)$$

The definition of various resistances is found in Fig. 2, R_o is a standard resistance with a current rating that is much higher than I_o, which is the initial heating current through the arm of the bridge containing the TPS element. γ is a constant which is chosen to be 100 in the present measurement. Calculating $D_s(\tau)$ using a computer programme and recording the change in potential difference, $\Delta U(t)$, one can determine λ.

3. Results and discussion

The variation of thermal conductivity with temperature for SBR/NR composites with varying NR content is shown in Fig. 3. It is seen that the thermal conductivity of all the composites shows a similar trend of increasing almost linearly with temperature to a peak value. The peak values are observed at around 215 K for all compositions, which is well within the glass transition range of SBR and NR. The value of thermal conductivity then decreases and begins to fall to a temperature-independent value at 290 K.

In these types of polymers it is a general characteristic that they show a marked conductivity maximum in the glass transition region. It is known that SBR and NR are incompatible rubbers. Although the rubbers are not miscible, no separate peaks are found in the thermal conductivity values of the composites

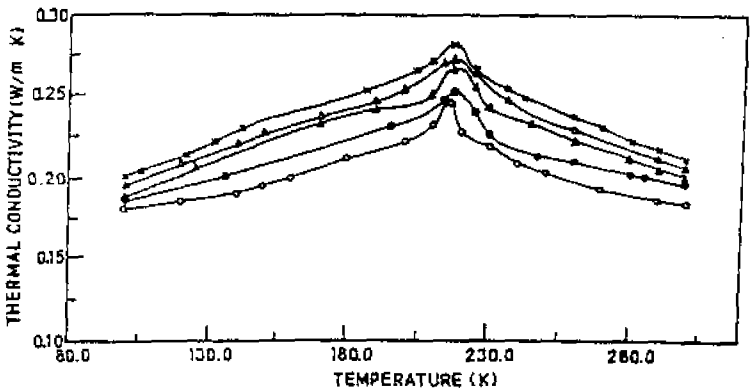

Fig. 3. Temperature variation of thermal conductivity of different SBR/NR compositions (× sample I, • sample II, ○ sample III, ▲ sample IV, and △ sample V).

studied here. This can be explained on the basis of the fact that the appearance of single glass transition cannot be taken as unambiguous evidence of miscibility [11]. If the respective T_gs are close (ca. 10°C), they may appear as a single broad transition. Here this point appears to be true since the T_gs of SBR (209–214 K) and NR (190–210 K) are close enough not to show separate peaks. Another aspect to be considered is that the elastomer pair is not miscible, but vigorous mechanical mixing overcomes the small potential barrier to unlike segmental interaction and so gives rise to a morphology that is homogeneous, at least down to the level accessible to standard analytical techniques.

By means of least square fit to the experimental data as a function of temperature (as plotted in Fig. 3), empirical relationships have been established for the theoretical prediction of thermal conductivity as given in the form

$$\lambda(T) = a + bT + cT^2 \tag{8a}$$

(for temperature region below T_g) and

$$\lambda(T) = a + dT + eT^2 \tag{8b}$$

(for temperature region above T_g) where a, b, c, d and e are parameters which are polymer dependent and T is the absolute temperature. The observed variation in thermal conductivity can be explained by considering structural features and the effect of temperature on the structural units in a phenomenological manner [12].

Even in amorphous polymers like SBR there exist some local order which is termed as intermediate range order (IRO) [13]. In the low temperature region below T_g, the temperature dependence of λ is controlled by variation of phonon mean free path. During cooling certain defects are also created in the system, such as bends in chains, gaps between two chains in line, chains of smaller lengths than the others etc. Hence below T_g structure scattering and chain-defect scattering are the main phonon scattering mechanisms. In the former case lattice wave propagate uniformly inside each small domain with dimensions equal to the size of the IRO region and then are abruptly scattered by a sudden change of refractive index at the boundary. The dimensions of IRO at T_g depend mainly on the processing conditions and degree of polymerization, hence it does not vary with temperature. Therefore the contribution to thermal resistance corresponding to these processes is temperature-independent. The first term a in both empirical equations represents the contribution to thermal resistance of structure scattering.

As for the chain defect scattering [14], defects introduced by bends and relatively smaller lengths of chain segments also scatter phonons, i.e. the elastic wave propagating along the chain finds itself at a point beyond which it can no longer proceed in the same direction with the same velocity. Therefore it is reflected along the same chain or is refracted along some other permitted direction. In the temperature region below T_g, with a rise in temperature the polymeric chains straighten out more and more, increasing the corresponding mean-free path and thus the contributions to the corresponding thermal resistance decreases linearly with the rise of temperature. The chain defects are effectively identical to stacking faults [15] and hence are expected to show similar temperature dependence for thermal resistance. The constant b in Eq. (8a) represents the thermal resistance by chain-defect scattering. The constant c can also be attributed to represent the contribution to thermal resistance by other possible stray scattering mechanisms. The constants a, b, c, d and e are polymer dependent parameters. This means that they should change systematically with NR content in the composite and the

Table 4
Values of constants for empirical Eqs. (8a) and (8b) developed for thermal conductivity

Composite	a	b	c ($\times 10^{-6}$)	d	e ($\times 10^{-5}$)
SBR	0.1510	0.0003	0.6604	0.00098	2.6884
SBR + NR (10 phr)	0.2203	−0.0007	4.1487	0.00002	0.3312
SBR + NR (20 phr)	0.1777	−0.0001	2.1290	0.00052	1.5499
SBR + NR (30 phr)	0.1283	0.0005	0.1403	0.00089	2.1701
SBR + NR (40 phr)	0.1306	0.0006	−0.1120	0.00118	−3.0538

obtained values of these constants supports this dependency (Table 4). Also these values depend on the extent of IRO in the polymer at T_g, lengths of the backbone chain and branch chains, the strength of the primary bonds and the molecular weight of the side groups.

A close look at the values of these constants would provide interesting information about the contributions of various scattering mechanisms at play in determining the thermal resistance of the composites. It has already been mentioned that the term a in Eq. (8) represents structure scattering and the contribution of this to thermal resistance is temperature independent and that the factors contributing to the structure scattering depend mainly on processing conditions and degree of polymerization. The values of constant a for various composites show a more or less increasing trend with the amount of thermal resistance offered by the composites. However the constants b and d which represent the chain-defect scattering and vacant-site scattering follow a different pattern. These values are inversely proportional to experimentally observed thermal resistance of the composites. However the constants c and e, which represent contribution to thermal resistance due to stray scattering mechanisms other than structure and chain-defect (vacant-site) scattering, again follow an increasing trend with the amount of thermal resistance offered by the composites. Thus this may be interpreted as an indication that the scattering mechanisms represented by these constants (c and e) are arising out of the interaction of the SBR matrix phase with the NR filler and although not exactly temperature independent, they have something more to do with processing conditions and degree of polymerization.

At temperatures above glass transition region, scattering by microvoids (vacant-site scattering) becomes predominant besides structure scattering. As temperature increases and the polymer passes to rubbery through leathery state, gradually individual units, atomic groups and small chain segments undergo intensive thermal motion and large torsional rotations, and the sliding of chain segments starts to play a dominant role in governing the variation of properties with temperature. This has a two-fold effect on the structure of the system; initially the dominant chain moments create some vacant sites or microvoids which scatter phonons in the similar way to the point defects [5]. With the rise of temperature, the number and size of these microvoids increases and consequently, the contribution of vacant site scattering to thermal resistance would increase linearly with temperature. Thus structure scattering and vacant-site scattering become the predominant scattering processes over certain range of temperature above T_g resulting in a decrease in the thermal conductivity with a rise of temperature. The constant d in Eq. (8b) represents the contribution to thermal resistance by vacant-site scattering and e other stray scattering mechanisms.

Fig. 4 shows the thermal conductivity variation of the composites with filler content measured at room temperature (300 K). It is interesting to note that the thermal conductivity shows a sharp decrease to a minimum value at 10 phr of NR content and then a linear increases with filler content. NR being less thermally conductive than SBR, the decrease in thermal conductivity of SBR with the addition of NR is natural due to the superposition effect, but the increasing trend in the thermal conductivity values of the composites containing NR content greater than 10 phr is rather interesting. This could be explained with reference to the modification in crosslinking density of the matrix produced by the filler content.

Fig. 5 shows the calculated crosslinking density ($1/2\,M_c$) of the composites using the following Flory–Rehner equation

$$M_c = -\frac{\rho_r V^s (V^{rf})^{1/3}}{\ln(1 - V^{rf}) + \chi V^{rf2}} \tag{9}$$

where ρ_r is the density of the polymer, V^s is the molar volume of the solvent, V^{rf}, the volume fraction of elastomer in solvent swollen filled samples, and χ the interaction parameter, which is given by the equation,

$$\chi = \beta + (V^s/RT)(\delta^s - \delta^p) \tag{10}$$

where β is the lattice constant. R is the Universal gas constant; T, the absolute temperature; δ^s is the

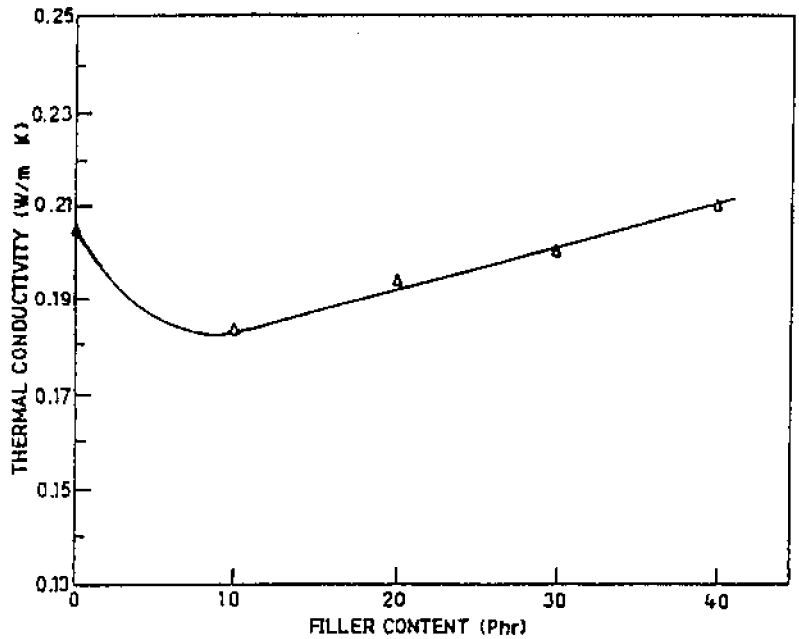

Fig. 4. Plot of thermal conductivity variations of composites with NR content at 303 K.

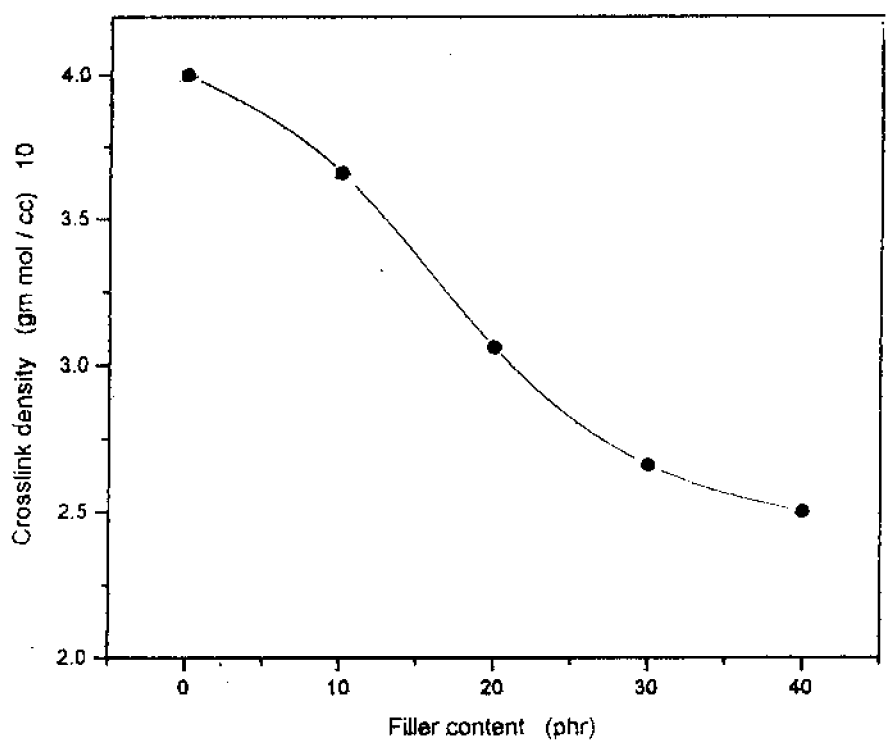

Fig. 5. Variation of crosslink density of SBR/NR composites with filler loadings.

solubility parameter of the solvent; and δ^V the solubility parameter of the polymer. Detailed description of the calculation of the crosslinking density was given elsewhere [8]. It can be seen from Fig. 5 that the crosslinking density of the matrix decreases with increasing filler content. This decrease can be attributed [8,17] to the sulphur diffusion from the SBR matrix to the filler phase. As the filler content increases, the sulphur migration also increases, resulting in a progressive fall in crosslinking density of the composites. The decrease in crosslinking density results [17] in an increase in the thermal conductivity. The initial fall in thermal conductivity of the composite may be attributed to the blending of the rubbers having different thermal conductivity values (NR is less thermally conductive than SBR) and the resulting superposition effect. It may be that this reduction in the resultant thermal conductivity of the composite gradually gets compensated by the increase in thermal conductivity due to the decrease of crosslinking at higher filler contents.

4. Conclusions

Thermal conductivity variation of SBR filled with various amounts of NR filler shows broad peak values of thermal conductivity in the glass transition region. It has been found that the thermal conductiveness of the SBR composites falls to a minimum at 10 phr of NR particle content and further addition of NR particles results in compensating this fall in thermal conductivity due to the decrease in crosslinking density of the composites with increasing filler content.

Acknowledgements

One of the authors (PP) is grateful to Mr Biju Mon, Computer Centre, Sree Narayana College, Quilon for his help in the preparation of the manuscript

References

[1] Seymour RB. Polymers for engineering applications. ASM International, 1985.
[2] Rees W. J Appl Phys 1962;37(2):864.
[3] Choy CL, Hunt RG, Salinger GL. J Chem Phys 1972;52:3629.
[4] Harshaft AA. Environ Sci Technol 1972;6(15):412.
[5] Lee TCP, Millens W. (To Gould Inc.). US Patent 834, 4046, 1977.
[6] Bruton NR, Koutsky JA. Chem Engng News 1974;52(6):211.
[7] Phadke AA, Bhattacharya AK, Chakraborthy SK. Rubber Chem Technol 1983;56:726.
[8] Mathew G, Singh RP, Thomas S. J Appl Polym Sci 1996;61:2035.
[9] Carslaw HS, Jaegar JC. Conduction of heat in solids. Oxford: Oxford University Press, 1959.
[10] Gustafsson SE. Rev Sci Instrum 1991;52:197.
[11] Hottman JD, William G, Pasaglia E. Transitions and relaxations in polymers. New York: Interscience, 1996.
[12] Dasora P. Phys Scripta 1994;46:611.
[13] Encyclopedia of polymer science engineering, vol. 1–6. 2nd ed. New York: Wiley, 1985.
[14] Perpechoko II. An introduction to polymer physics. Moscow: Mir, 1981.
[15] Hayden W, Moffatt WG, Wulft J. The structure and properties of materials, vol. III. New Delhi: Wiley Eastern, 1968.
[16] Sharapova LN, Chekanova AA, Zakharov ND, Borisova EYu. Int Polym Sci Technol 1983;10:49.
[17] Evseeva LE, Tanaeva SA. Cryogenics 35 1995;277:.

ELSEVIER

Polymer 42 (2001) 2137–2165

polymer

www.elsevier.nl/locate/polymer

Recycling of natural rubber latex waste and its interaction in epoxidised natural rubber

G. Mathew[a], R.P. Singh[b], N.R. Nair[c], S. Thomas[d,*]

[a]*Department of Chemistry, C.M.S. College, Kottayam 686001, Kerala, India*
[b]*Polymer Chemistry Division, National Chemical Lab, Pune 411008, India*
[c]*Rubber Research Institute of India, Kottayam 686009, Kerala, India*
[d]*School of Chemical Sciences, Mahatma Gandhi University, Kottayam 686560, Kerala, India*

Received 27 October 1998; received in revised form 5 April 2000; accepted 13 June 2000

Abstract

The waste rubber formed in latex-based industries is around 10–15% of the rubber consumed. The formation of a higher percentage of waste latex rubber (WLR) in latex factories is due to the unstable nature of the latex compound and the strict specifications in the quality of latex products. These latex rejects contain about 95% rubber hydrocarbon of very high quality, which is only lightly cross-linked. These rejects, if not properly used, can create serious ecological and environmental problems. The authors have developed a cost-effective technique for the reuse of WLR in epoxidised natural rubber (ENR). The effect of powdered rejects on the curing behaviour, mechanical performance and swelling nature has been investigated. The cure characteristics such as optimum cure time, rheometric scorch time and induction time, are found to decrease with increasing concentration of latex waste filler. When the vulcanisation system is conventional, the finest size filler shows superior mechanical performance while the order of performance is reversed when the vulcanisation mode changes to efficient. The applications and limitations of several theoretical models in describing the tensile modulus of the samples have been demonstrated. A three-layer model has been used to study the migration of sulphur from ENR to the latex filler phase. The extent of sulphur migration in the case of different particle sizes of latex waste filler in two different vulcanisation systems has been analysed. The failure behaviour of the samples was analysed using scanning electron microscopy. The study shows that waste latex rubber can be used as filler in ENR economically.

Keywords: Rubber recycling; Epoxidised natural rubber; Processing characteristics

1. Introduction

Elastomers are a major class of materials having a wide range of applications, ranging from footwear to space vehicles. This is because of their unique mechanical properties such as elastic behaviour even at very large deformation and energy absorbing capacity. By properly controlling the compounding ingredients in rubber, its ultimate properties can be made to match the requirements. The potential properties of an elastomer can be improved by the addition of certain fillers like silica, carbon black, mica [1,2], etc. As a result of the severe energy crisis, and the need to reduce compound cost, rubber product manufacturers were forced to increase the proportion of filler in the rubber compound without adversely affecting the mechanical properties. This approach, however, always resulted in a rubber compound with very high specific gravity [3], which is not fair, as far as elastomers are concerned. In order to overcome this problem and also to make the rubber compound cheaper, new materials have been considered for use as fillers. Just like waste plastic, waste rubber also is becoming a worldwide problem. The disposal/utilisation of tyres, whose life span has ended, is a great economic and ecological problem. The earlier approach to this problem was to reclaim [4] or remove the cross-links in the rubber rejects and then use the latter as new rubber. However, the use of reclaimed rubber was limited owing to three main reasons:

(i) Easy reclamation was not possible in the case of waste tyres due to the presence of steel belts or plies [5].
(ii) The properties of reclaimed rubber were inferior due to its degradation during reclamation.
(iii) The various components of a tyre or blend may not respond in the same way to reclamation [6].

Meanwhile the authorities prohibit the open burning of this waste because of the release of zinc compounds into the

* Corresponding author. Tel.: +91-481-598503; fax: +91-481-561190.
E-mail address: sabuthomas4@sancharnet.in (S. Thomas).

0032-3861/01/$ - see front matter
PII: S0032-3861(00)00392-4

atmosphere [7]. Therefore, nowadays researchers pay more attention to scrap latex rejects compared to reclaimed rubber. This is because of the lightly cross-linked and high-quality nature of the rubber obtainable from latex rejects. Moreover, these rejects are available in huge quantities. The two main reasons for this surplus nature are the unstable nature of latex and the strict specifications regarding the quality of latex products. Therefore, these scrap latex rejects are now considered as the best potential candidate for recycling.

Many reviews regarding the disposal problem of rubber rejects and possible solutions are available from the literature [8–11]. Another method to reuse large volumes of scrap latex rejects to use it as an impact modifier in brittle plastics like polystyrene [5,12]. This can be done simply, either by solution or melt blending techniques, or by polymerising the monomer in the presence of swollen crumb, as done by Freeguard [13]. Researchers [14] have analysed the reactive blending of plastics and scrap rubber also. The use of cryoground rejects, as filler in rubbers [8,9] and polyolefins [15] is well known. Recently, many new methods for the devulcanisation of waste rubber have become available. The most important among these is the devulcanisation process using ultrasonic irradiation. A number of studies in this field have been reported by Tukachinsky [16], Levin [17] and Isayev et al. [18,19]. They found that in the presence of heat and temperature, the ultrasonic waves were able to break up the three-dimensional network in cross-linked rubbers. The resulting devulcanised rubber could be reprocessed, shaped and revulcanised just like virgin rubber. In addition to this ultrasonic devulcanisation technique, there are several surface modifications, which are possible on the latex waste. Chemical [20,21], mechanical [22,23], plasma [24,25], corona [26,27] and electron beam radiation [28,29] are reported to be useful to improve the matrix filler adhesion. Epoxidised natural rubber or ENR is a relatively new rubber, having properties similar to those of synthetic rubbers rather than natural rubber. It has low air permeability [30] (comparable to that of butyl rubber), good oil resistance [31] (comparable to that of nitrile rubber) and good dynamic properties. It exhibits strain-induced crystallisation [32] similar to natural rubber.

In this article, we evaluate the effects of using powdered latex rejects as filler in ENR. The influence of filler loading on the curing characteristics is discussed. Also, the effect of both particle size and loading of the filler on the mechanical properties, swelling and failure behaviour are compared and presented. A comparative study based on the mode (conventional and efficient) of the vulcanisation system and its effect on the tensile strength of the vulcanisates also is carried out. The dependence of filler–ENR matrix adhesion on the particle size of the filler also is examined on the basis of sulphur migration phenomena. Several theoretical models have been used to fit the experimental tensile modulus values. The filler particle morphology, filler dispersion and filler–matrix interphase adhesion are analysed using scanning electron microscopy.

2. Experimental

2.1. Materials

The basic material used in this work is ENR-25, epoxidised natural rubber having 25% epoxidation, manufactured and supplied by the Rubber Research Institute of India, Kottayam, India. Its composition is given in Table 1. NR latex filler was prepared from WLR, supplied by Hindustan Latex Ltd, Thiruvananthapuram, Kerala, India. Other compounding ingredients such as zinc oxide, stearic acid and CBS (*N*-cyclohexyl benzthiazyl sulphenamide) were of reagent grade and obtained from local rubber chemical suppliers. Toluene (reagent grade) was used for carrying out swelling studies.

2.2. Methods

2.2.1. Preparation of powder rubber

The ground vulcanisate preparation was done in a fast-rotating toothed-wheel mill. The advantage of this technique is that one can obtain a fine elastic rubber powder, unlike cryoground rubber (CGR), which is stiff [33]. Therefore, CGR will not permit easy diffusion of curatives into it. The powder rubber was found to be polydispersed in particle size. It was then sieved into four different particle sizes, ranging from 0.3 to 0.5 mm (size 1 or S1), 0.6 to 0.9 mm (size 2 or S2), 1.7 to 2.5 mm (size 3 or S3) and 9 to 11 mm (size 4 or S4). A mill-sheeted form (M) of the latex rejects also was prepared by passing the rejects through a hot two-roll mill for 10 min. Various particle sizes and mill-sheeted form of the filler are presented in Fig. 1.

2.2.2. Mixing, rheometry and preparation of test samples

Mixing of ENR and filler were carried out using a laboratory size two-roll mixing mill having a friction ratio 1:1.4, as per ASTM D 15-627. The recipe used is given in Table 2. The effect of addition of up to 40 phr of latex filler in ENR is investigated, with emphasis on the size of the filler and its influence on sulphur migration.

The cure characteristics of the mixes were determined using a Monsanto Rheometer model R-100 at 150°C by

Table 1
Composition of ENR-25

Constituent/properties	%/Value
Epoxy content (%)	25
Density (gm/cc)	0.97
Mooney viscosity	80–90
Protein content (%)	0.001–0.0004
Molecular weight	10^5
Colour	Yellow

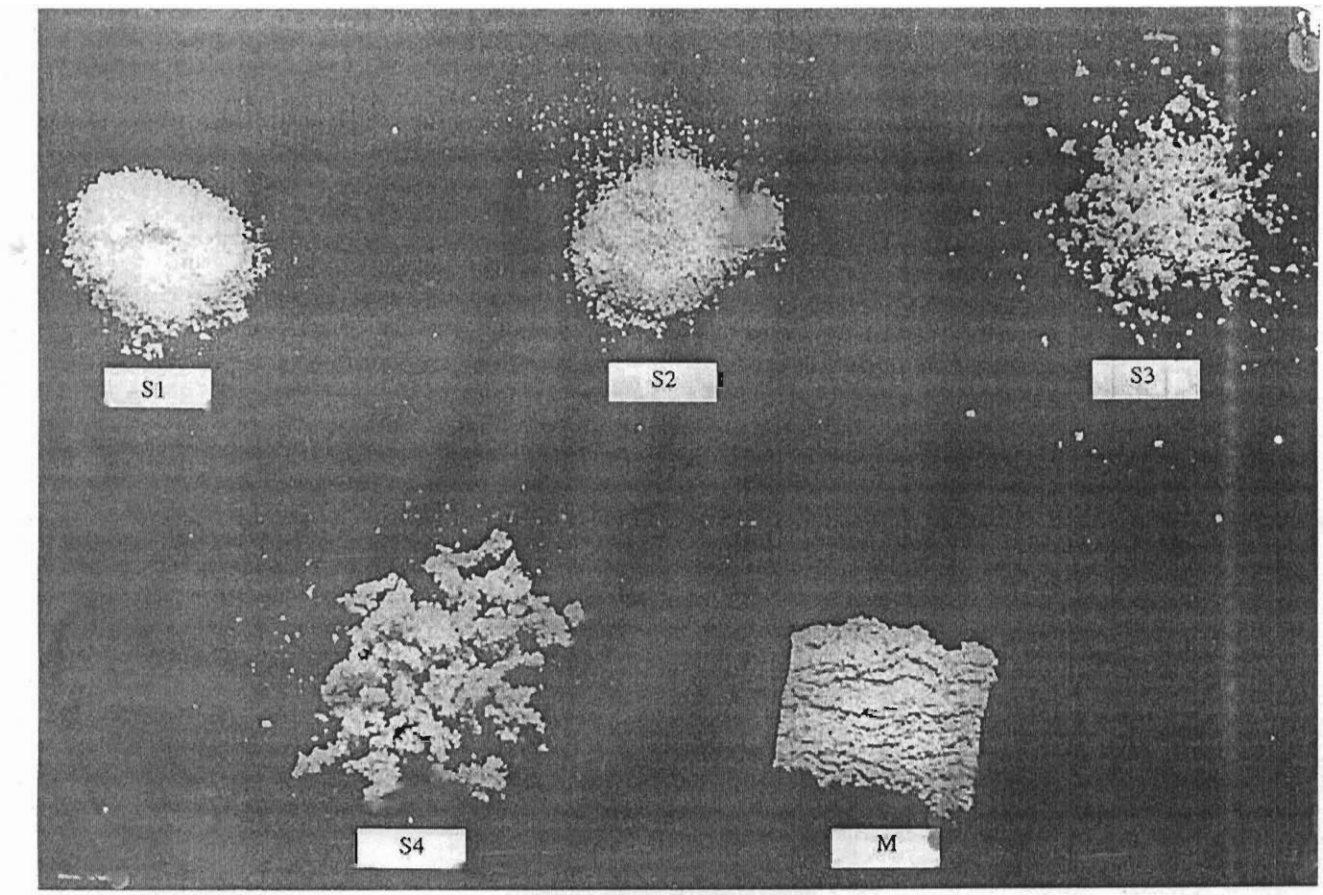

Fig. 1. Different particle sizes (sizes 1–4) and mill-sheeted form of the filler.

measuring the optimum cure time, scorch time and induction time. The kinetics of vulcanisation [22] was also studied from the rheographs and correlated with cure rate index values.

The compounds were then compression-moulded at 150°C using an electrically heated hydraulic press for their respective cure times (t_{90}). Dumbbell-shaped tensile and angular tear specimens were punched out from the compression-moulded slabs along the mill grain direction.

2.2.3. Physico-mechanical testing of the samples

Stress–strain was determined on an Instron Universal Testing Machine, using a C-type dumbbell specimen, according to ASTM D 412-80. The tear strength was determined as per ASTM D 624-81 using angular tear specimens. Both the tests were done at 28°C and at a cross-head speed of 500 mm/min.

Table 2
Base formulation

Material	Control (phr)
ENR-25	100
Zinc oxide	5
Stearic acid	2
CBS	0.6
Sulphur	2.5
Calcium stearate	1
WLR	Variable (0,10,20,30,40)

2.2.4. Swelling studies

Equilibrium swelling [34] measurements of the vulcanisates was performed in toluene at room temperature. The samples were allowed to equilibrate for 7 days and again the solvent was renewed after 3 days, to remove soluble materials from the vulcanisates. The variation of cross-link density with filler loading was analysed. In order to assess the ENR matrix–filler interaction previously established, Kraus [35], Cunneen and Russell [36] and Lorenz–Park [37] models were applied.

2.2.5. Sulphur diffusion studies

The sulphur migration phenomena that takes place between ENR and the filler phases was studied using a three-layer model [38] (Fig. 2) system. It consists of three layers, one layer of NR latex waste (all sizes 1–4 and M were tried) was sandwiched between two layers of gum ENR compounds. In one half of the specimen, the outer ENR layers were separated from the inner latex waste layer by using aluminium foils (non-contact surface) and

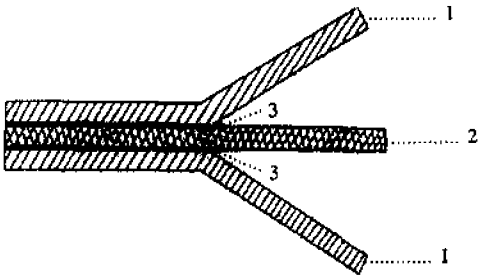

THREE LAYER MODEL

1. GUM ENR MATRIX
2. NR LATEX WASTE
3. ALUMINIUM FOIL

DIMENSIONS OF THE SAMPLE

	LENGTH (cm)	BREADTH(cm)	THICKNESS (cm)
1. GUM ENR MIX	16	8	0.2
2. NR LATEX WASTE	16	8	0.2
3. ALUMINIUM FOIL	8	8	0.004

Fig. 2. Model to analyse sulphur migration.

in the other half, the aluminium foil was omitted (contact surface). The system was then subjected to vulcanisation at low pressure. Then the middle layer was separated. The cross-link density and swelling index values of this layer were determined by swelling the samples taken from the contact and non-contact regions. If sulphur migration occurs from the outer ENR matrix to the middle latex waste layer, the cross-link density of the latex waste layer at the contact surface will be increased. The extent of increase will be a direct measure of extent of sulphur migration.

2.2.6. Scanning electron microscopic studies

The SEM observations of filler morphology and distribution were made in a direction transverse to the grain direction, using a JEOL JSM-35C model scanning electron microscope. Fracture surfaces of the test samples were carefully cut from the failed test pieces without touching the surfaces. These specimens were sputter coated with gold, within 72 h of observation.

3. Results and discussion

3.1. Processing characteristics

The powdered filler particles are found to be almost spherical in shape with fissured surfaces (Fig. 3). Since particles of larger diameter also can penetrate through the meshes because of their elasticity, the particle size data can be presented as distribution curves (Fig. 4). The distribution broadens as we go from sizes 1 to 4. The average size and most frequent size range are given in Table 3. The number average (D_n) and weight average (D_w) diameters are calculated using the equations given below and are also presented in Table 3.

$$D_n = \sum N_i D_i / \sum N_i \quad (1)$$

$$D_w = \sum N_i D_i^2 / \sum N_i D_i \quad (2)$$

where N_i is the number of rubber particles having a certain diameter D_i.

It is clear from the table that all these parameters show an increase from size 1 to size 4. The shape factor p and its significance will be discussed later.

The processability characteristics of the compounds (Table 4) can be studied from the rheographs. The finest size filler (size 1) is selected for the determination of processing/curing characteristics. The minimum torque in the rheograph is a measure of filler content in the rubber and is presented as the minimum viscosity value M_n. These values first register an increase with increase in filler content, but later they decrease (Table 4). The initial increase is due to the presence of cross-linked rubber

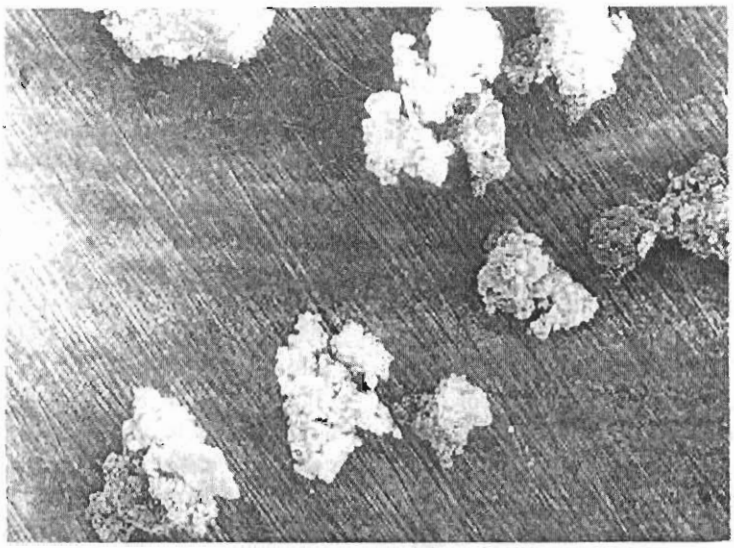

Fig. 3. Scanning electron micrograph of powdered rubber rejects.

particles in ENR and the decrease at 40-phr loading may be because of the higher extent of mastication during mixing. The maximum torque in the rheograph is a measure of cross-link density in the rubber and is presented as the maximum viscosity value M_h. It is found that the presence of particulate inclusions increases the maximum torque. However, in our case, where the inclusion itself is a rubber, the variation may be a result of the combined effect of cross-link density variation and the presence of cross-linked particles. At 10-phr loading, the presence of cross-linked particles increases M_h, but at later stages of loading, the sulphur migration (which will be discussed later) becomes predominant, which leads to reduced cross-link densities. This causes the reduction in M_h values.

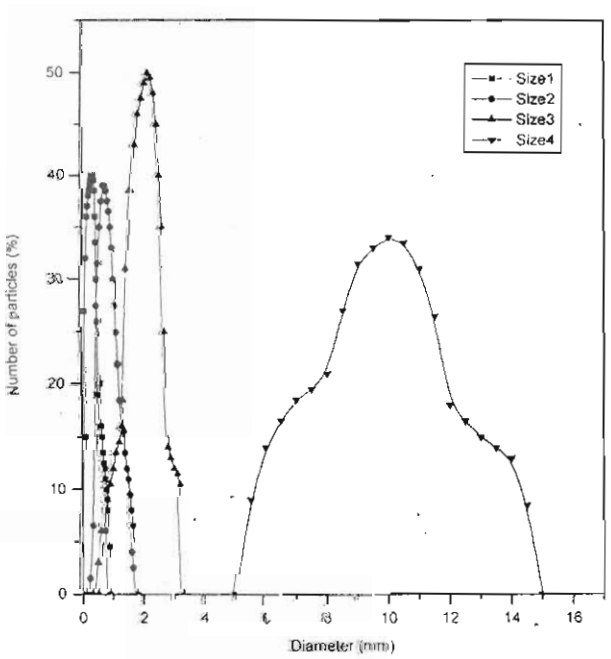

Fig. 4. Particle size distribution curves.

As the filler content increases, the optimum cure time, t_{90} (time needed for the formation of 90% cross-links), scorch time t_2 (premature vulcanisation time) and induction time, t_1 (time to start the vulcanisation process) are found to decrease. These results are presented in Fig. 5. This is due to the presence of unreacted accelerator zinc diethyldithiocarbamate (ZDEC) in the latex waste. ZDEC is one of the important accelerators currently used in the manufacture of condoms. Its structure is shown in Fig. 6a. In order to confirm its presence we have extracted the unreacted ZDEC from the latex waste, and it has been evaluated by IR. The spectrum is presented in Fig. 6b. The peaks at 700–600 cm^{-1} are due to C–S stretching and that at 790–770 cm^{-1} indicates the presence of ethyl chain ($-CH_2-CH_3$). The C=S stretching peak is visible at 1250–1020 cm^{-1} and the peak at 2820–2760 cm^{-1} indicates the presence of $N-CH_2$ group in the compound. All these confirm the presence of unreacted accelerator in the latex rejects. Therefore, it is clear that the rubber compound contains the accelerator CBS (*N*-cyclohexyl benzthiazyl sulphenamide) added in the formulation (Table 2) and the unreacted accelerator ZDEC, already present in the latex rejects. As a result of the combined accelerating effect, the three parameters, namely t_{90}, t_2 and t_1, decrease with loading of filler.

The increase in speed of the curing reaction with filler loading can be analysed systematically, by calculating two parameters, namely the cure rate index (CRI) and reaction rate constant (k). The cure rate index values (CRI) are calculated using the equation:

$$\mathrm{CRI} = 100/t_{90} - t_2' \tag{3}$$

Table 3
Particle size data

Particle size	Average size (mm)	Most frequent size range (mm)	No. average diameter (mm)/D_n	Wt. average diameter (mm)/D_w	Shape factor p
Size 1	0.5	0.3–0.5	0.401	0.489	2.2951
Size 2	1.05	0.6–0.9	0.961	1.083	2.0067
Size 3	1.9	1.7–2.5	2.11	2.34	2.1667
Size 4	10	9–11	10.09	10.72	1.6513

where t_{90} is optimum cure time and t_2 is rheometric scorch time.

CRI values are given in Table 4 and its variation with filler loading will be discussed later. The kinetics of cure reaction is analysed by the method [22] explained below.

The general equation for the kinetics of a first-order chemical reaction can be written as:

$$\ln (a - x) = -kt + \ln a \tag{4}$$

where a is the initial reactant concentration, x is the reacted quantity of reactant at time t and k is the first-order reaction rate constant.

The rate of cross-link formation during the vulcanisation of rubber is usually monitored by measuring the developed torque. Since these torque values are a direct measure of the modulus of the rubber, the following substitutions can be made.

$$a - x = M_\infty - M \tag{5}$$

$$a = M_\infty - M_0 \tag{6}$$

where M_∞ is the maximum modulus, M_0 is the minimum modulus and M is the modulus at time t.

Substitutions of torque values for modulus give the equations:

$$a - x = M_h - M_t \tag{7}$$

$$a = M_h - M_0 \tag{8}$$

where M_h is maximum torque, M_0 is minimum torque and M_t is the torque at time t.

The plots of $\ln (M_h - M_t)$ versus time, t, are presented in Fig. 7. Even though linearity is claimed for the plots theoretically, deviations from linearity are experimentally observed for certain points. The observed linearity in the plots confirm that the cure reaction of the samples follow first-order kinetics. The slope of the respective straight lines gives the cure reaction rate constant (k) and are presented in Table 4.

It is clear from Table 4 that both CRI and k values show an increase up to 30-phr latex waste loading and later they decrease at 40-phr loading. The initial increase is again due to the presence of unreacted accelerator in the latex waste. This cure-activating nature of latex filler is an advantage, since a faster curing sample will have a high production rate. However, this cure activation is found to level off at higher loadings of latex waste. Since the filled ENR compound is more stiff and non-tacky, the compound is easy to handle for further processing. On the other hand, the unfilled ENR is very tacky, making it difficult to handle.

3.2. Mechanical properties

The mechanical properties of elastomers filled with powder rubber depend on many factors, such as the following.

(i) Strain crystallising nature of the filler.
(ii) Adhesion [39] of the filler with matrix.
(iii) Particle size of the filler.
(iv) Extent of sulphur migration from matrix to filler phase, which is controlled by many factors such as:
  (a) The concentration of polysulphidic linkages in the matrix and filler. If the concentration of polysulphidic linkages in the matrix is higher than that of filler, sulphur migration will be less, but it will be extensive if the reverse is true [22].
  (b) The particle size of the filler. As the particle size of the filler decreases, the contact surface area with the ENR matrix increases, leading to more sulphur diffusion.

As the filler content increases, the tensile strength (Fig. 8)

Table 4
Cure characteristics

Loading (phr)	Minimum viscosity (M_0) ($dN - m$)	Maximum viscosity (M_h) ($dN - m$)	Cure rate index (CRI) (min^{-1})	Rate constant (k) (min^{-1})
0	3	35	12.5	0.266
10	4	44	33.3	0.631
20	4.5	44	33.3	0.675
30	6	43	36.4	0.810
40	4	42	32.1	0.800

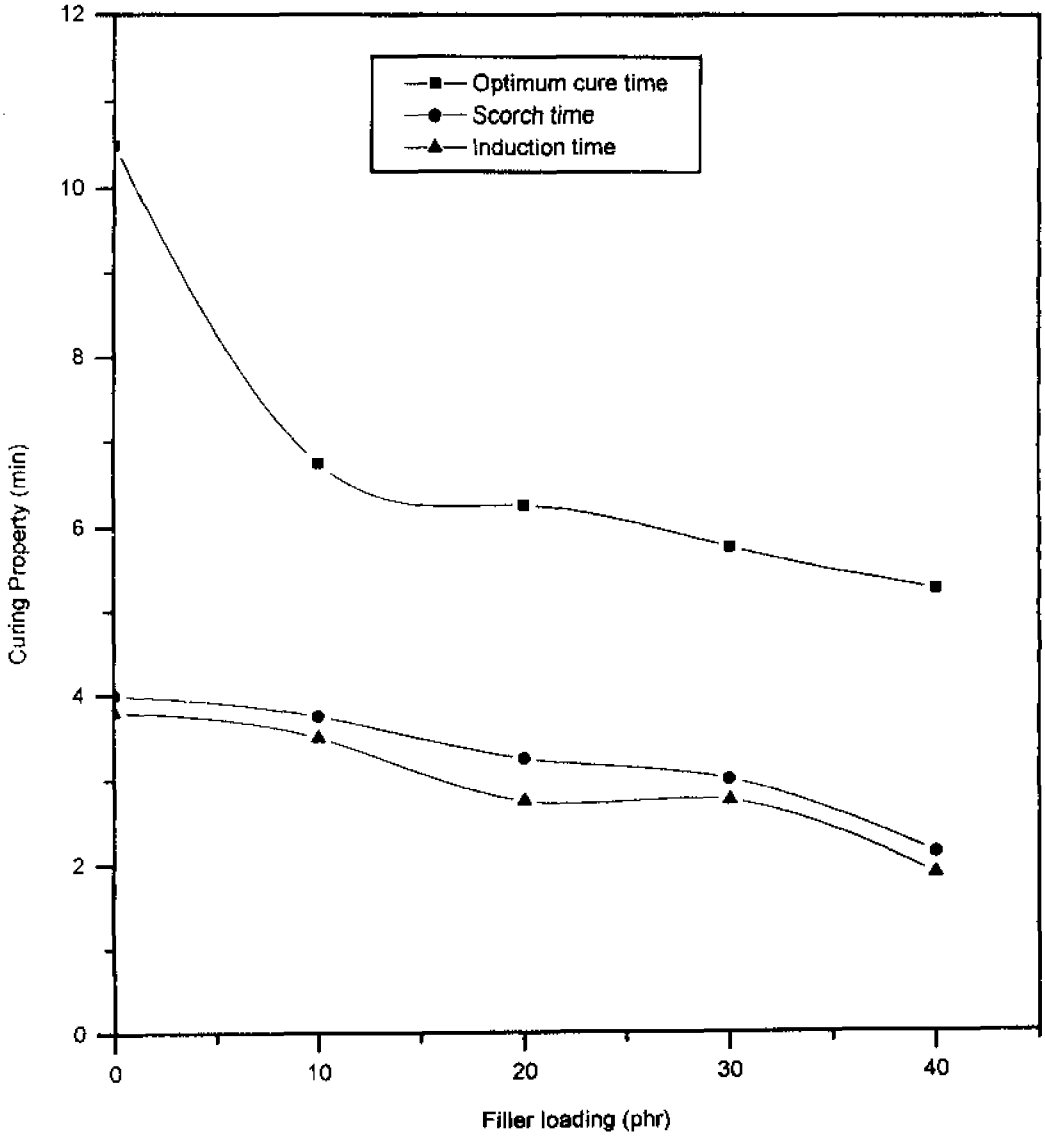

Fig. 5. Effect of filler loading on curing characteristics.

increases dramatically and reaches a maximum value at 30-phr loading. Beyond 30-phr loading, the tensile strength values show a decrease or levelling-off behaviour. For size 1, the increase is about 300%. The increase in tensile strength is due to the strain crystallising nature of NR latex filler particles. The threshold value of strain, required for strain crystallisation of natural rubber (NR), is 500%. Since the filler particle is very small, it will cover this value even at the initial stages of extension. The increase in tensile strength with loading confirms the fact that NR retains its strain crystallising nature, even if it is in the form of fine filler, Lewis and Nielsen [40] postulated that as the particle size decreases, the contact surface area increases, providing a more efficient interfacial bond, leading to better properties. At high filler loading, there will be an increased tendency for agglomeration, which may weaken the interfacial bonds. It is also important to mention that the tendency for agglomeration increases with the decrease of particle size. At 40-phr loading of size 1 filler, the latter effect exceeds the former and, therefore, tensile strength drops suddenly. Such a sharp drop is noted only for size 1. Agglomerates as described above, tend to contain voids, so that their apparent volume will be considerably greater than their true volume. If the agglomerates are hard with appreciable strength, then the filled material will have a higher strength than expected. Soft disintegrated agglomerates, however, as in the present case, produce a reverse effect, which manifests as a sharp drop in tensile strength at higher filler loading. Since such an agglomeration is less probable for higher particle sizes, a sharp drop in tensile strength is not observed.

We have noted many interesting behaviours associated with the particle size–performance relationship. In the case of fine filler, the contact surface area with the matrix is more. This can lead to enhanced sulphur migration from

(a)

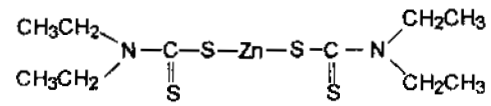

(b)

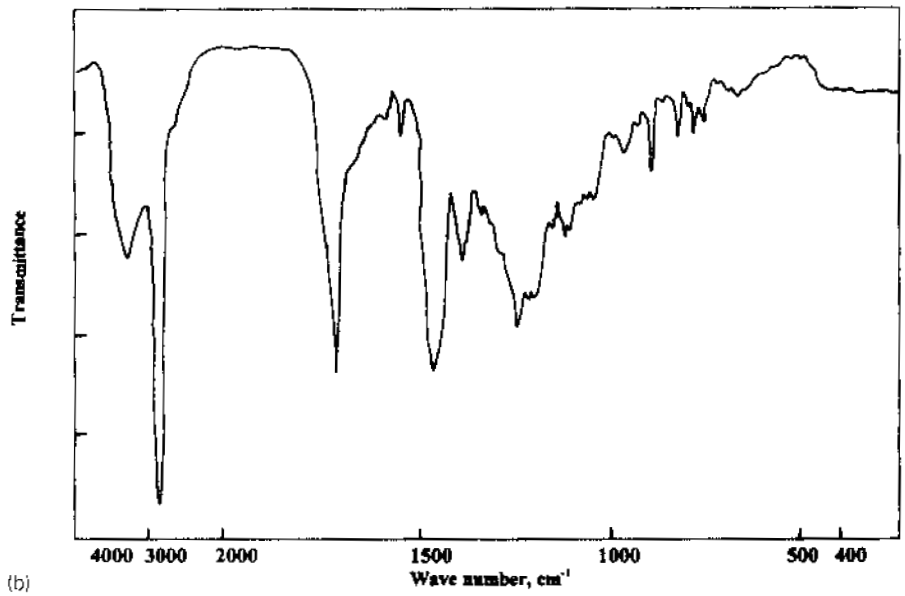

Fig. 6. (a) Structure of unreacted accelerator (ZDEC). (b) IR spectrum of unreacted accelerator (ZDEC).

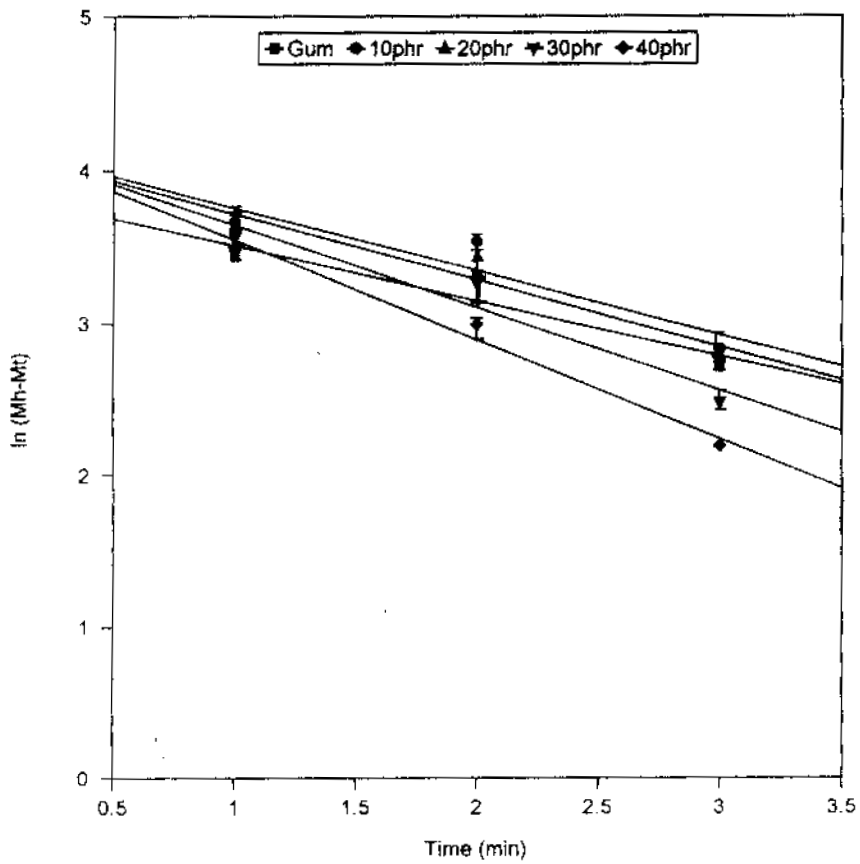

Fig. 7. Plots of ln $(M_h - M_t)$ vs. time, t.

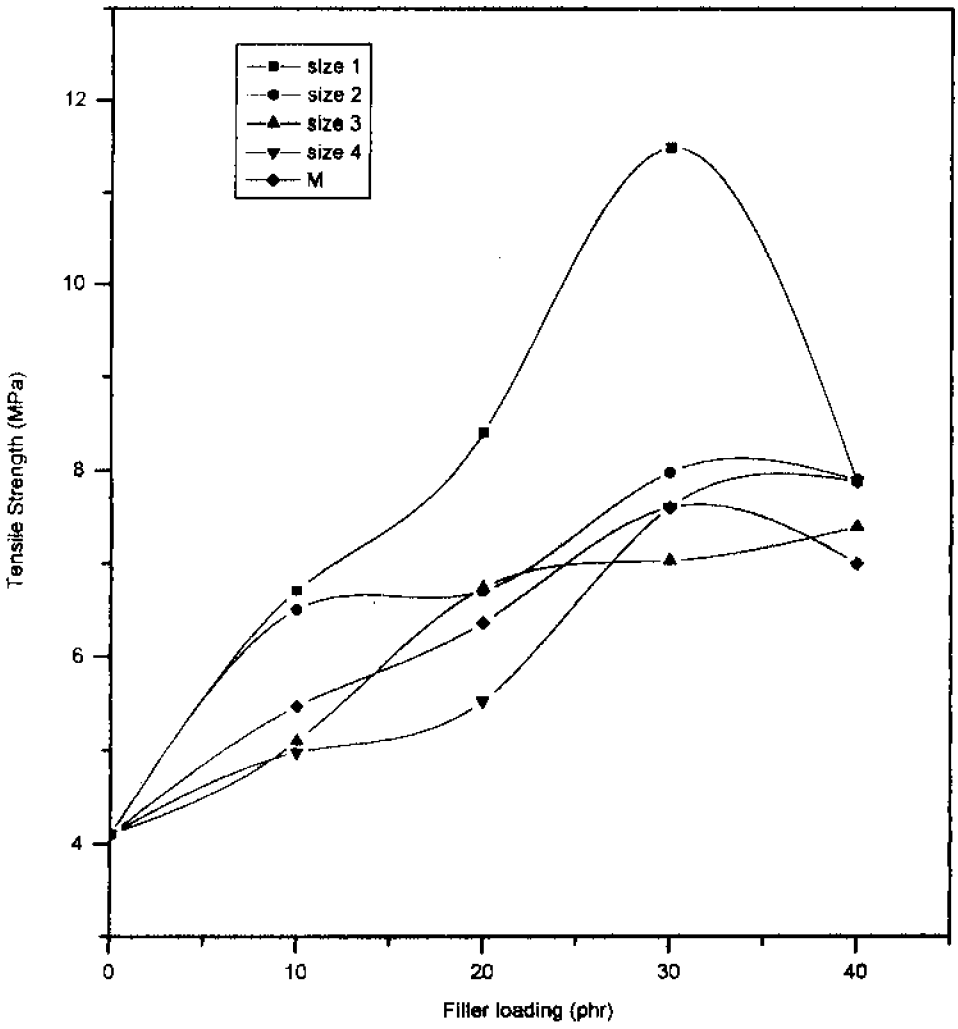

Fig. 8. Effect of filler loading and size on the tensile strength of ENR cross-linked by a CV system.

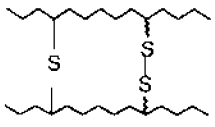

Efficient system (EV)

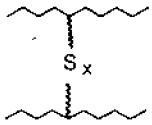

Conventional system (CV)

Fig. 9. Schematic sketch of sulphur linkages for different vulcanisation systems.

matrix to filler and worsening of tensile properties. So one expects inferior properties for ENR filled with size 1 filler. According to our studies, however, size 1 filler is found to be superior (Fig. 8). This is mainly because fine particles of size 1 will have a uniform distribution, which makes an efficient stress transfer possible. The second reason is the competition between polysulphidic linkages in the ENR matrix and filler. The basic formulation used here is a conventional vulcanisation (CV) system with high sulphur-to-accelerator ratio (Table 2). This provides a higher concentration of polysulphidic linkages in ENR, than that of the filler. A schematic sketch of the CV system is given in Fig. 9. When the concentration of polysulphidic linkages in the matrix is higher than that of the filler, sulphur migration from the matrix to the filler is less predominant [22]. Therefore, the tensile properties for fine fillers (sizes 1 and 2) become superior to those of large-size fillers (sizes 3, 4 and M).

In order to analyse this effect in detail, we have tried a recipe with a low sulphur-to-accelerator ratio

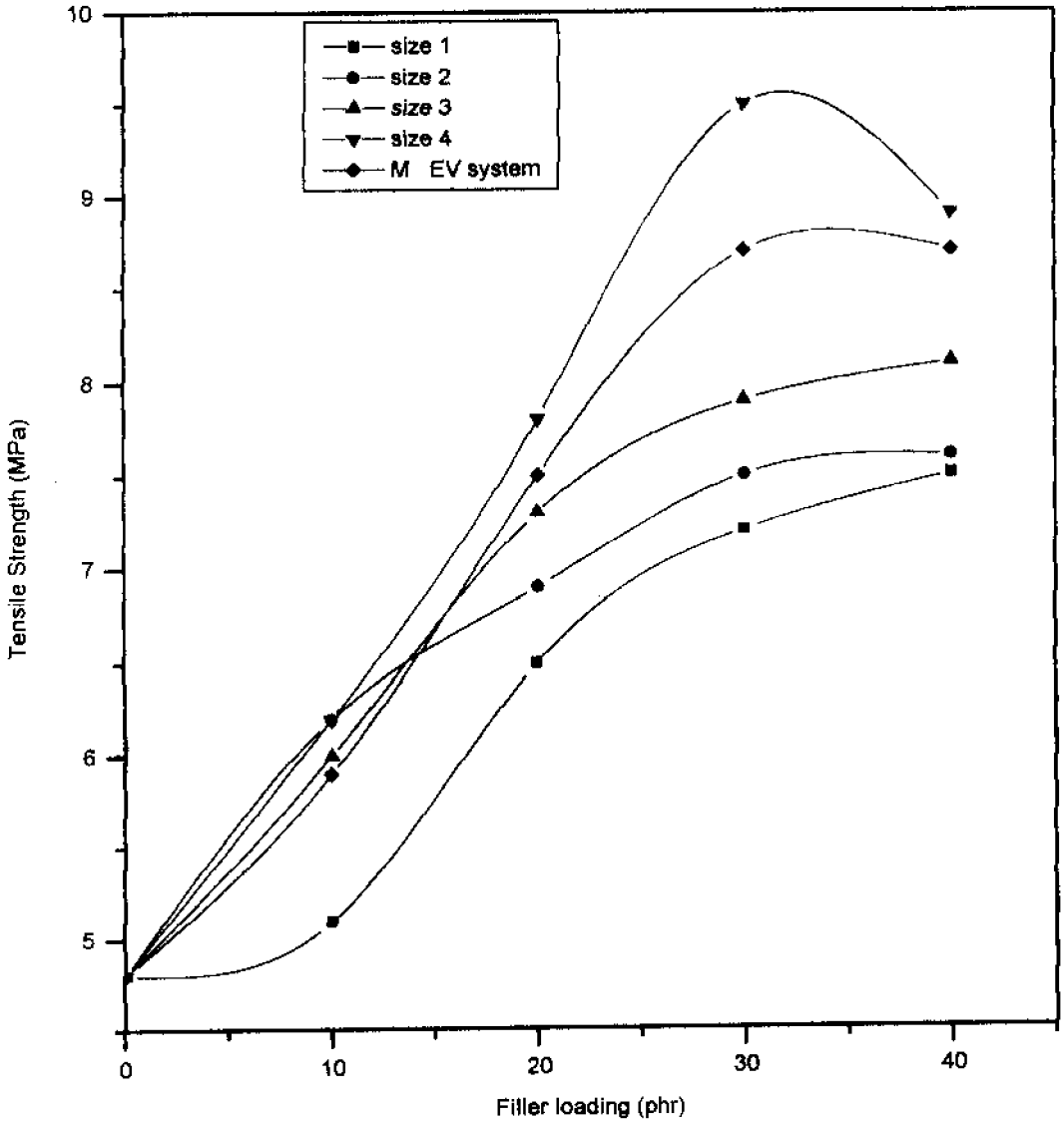

Fig. 10. Effect of filler loading and size on the tensile strength of ENR cross-linked by an EV system.

Table 5
Cross-link density values from sulphur migration studies

Vulcanisation system	Filler size	Cross-link density values $\times 10^{-5}$ (gm moles/cc) of middle layer	
		Contact surface (CS)	Non-contact surface (NCS)
CV	S1	1.14	1.18
	S2	1.16	1.15
	S3	1.15	1.14
	S4	1.15	1.16
	M	1.13	1.14
EV	S1	1.45	1.21
	S2	1.30	1.22
	S3	1.31	1.23
	S4	1.20	1.23
	M	1.25	1.24

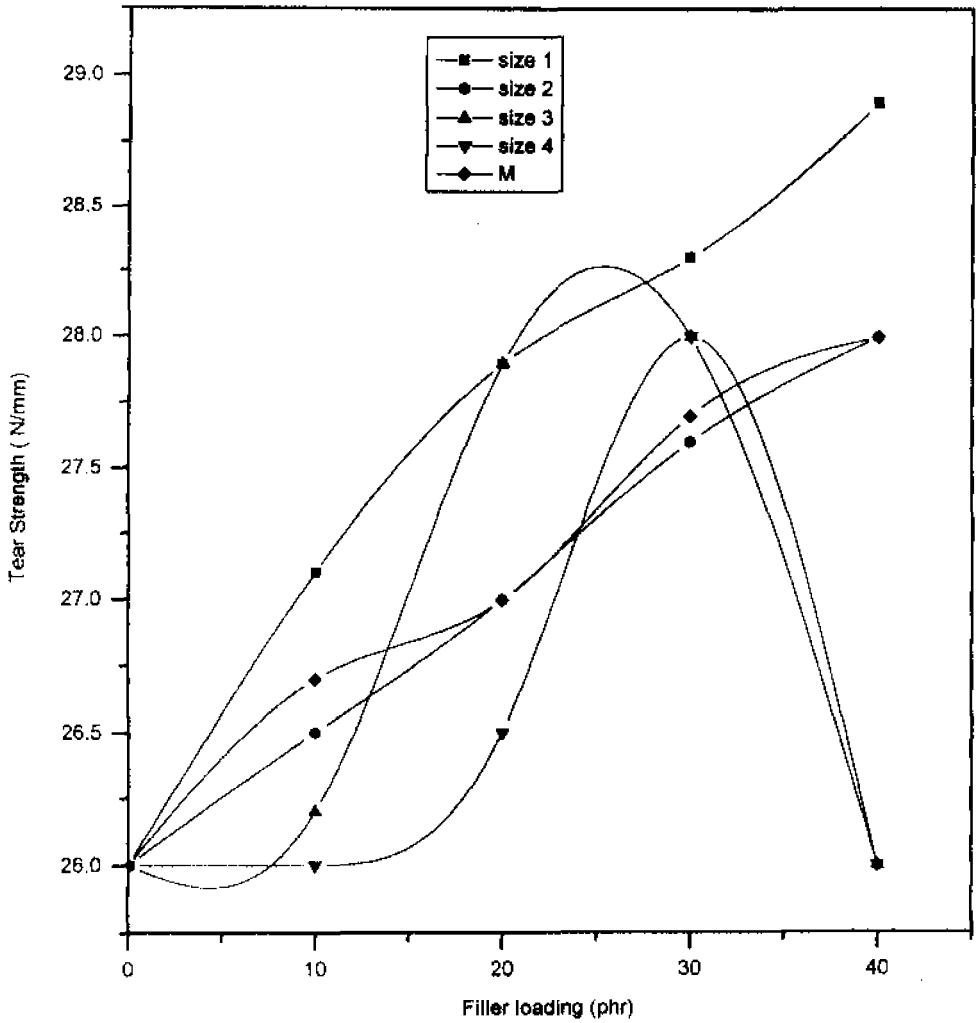

Fig. 11. Effect of filler loading and size on the tear strength of ENR vulcanisates.

(sulphur — 0.5 phr, CBS — 1.5 phr). This efficient vulcanisation (EV) system provides mainly mono and disulfidic linkages in the ENR matrix phase (Fig. 9). Here, since the concentration of polysulphidic linkages in the filler is more than that of the matrix, sulphur migration is extensive and is maximum in the case of size 1 (owing to the large contact area). Therefore, the tensile strength values for large-size fillers (sizes 4 and M) become higher than that of size 1. This is clear from Fig. 10. There is one more important reason for the superior properties of large-size fillers, mainly size 4. It is clear from Fig. 4 that the size 4 filler has the widest particle-size distribution. Such mixtures of particles with differing sizes can pack more densely than monodispersed particles because smaller ones can fill the interstitial spaces between the closely packed large particles to form an agglomerate. Such an agglomerate [41], which is formed from a polydispersed or ungraded system may be able to carry a large proportion of load and is, therefore, superior to the agglomerate discussed earlier. Such cases describing the superior performance of large particles were already reported by many researchers [42].

The absence of sulphur migration in the CV system as well as its presence and extent in the EV system is confirmed by using a three-layer model as shown in Fig. 2. The dimensions of the model are also shown in Fig. 2. For the CV system (Table 5), the cross-link density of the sample obtained from the contact surface of the middle latex waste layer is found to be almost the same as that from the non-contact surface. Moreover, the values are found to be similar for all the particle sizes of the filler. This data confirms the absence of sulphur migration in the CV system. Whenever sulphur migration is present in the system, the cross-link density of the sample from the contact surface must be higher than that of the non-contact surface. Owing to the higher concentration of polysulphidic linkages in the ENR matrix for the CV system, sulphur migration must be less and consequently, the cross-link density from the contact and non-contact surfaces must be comparable.

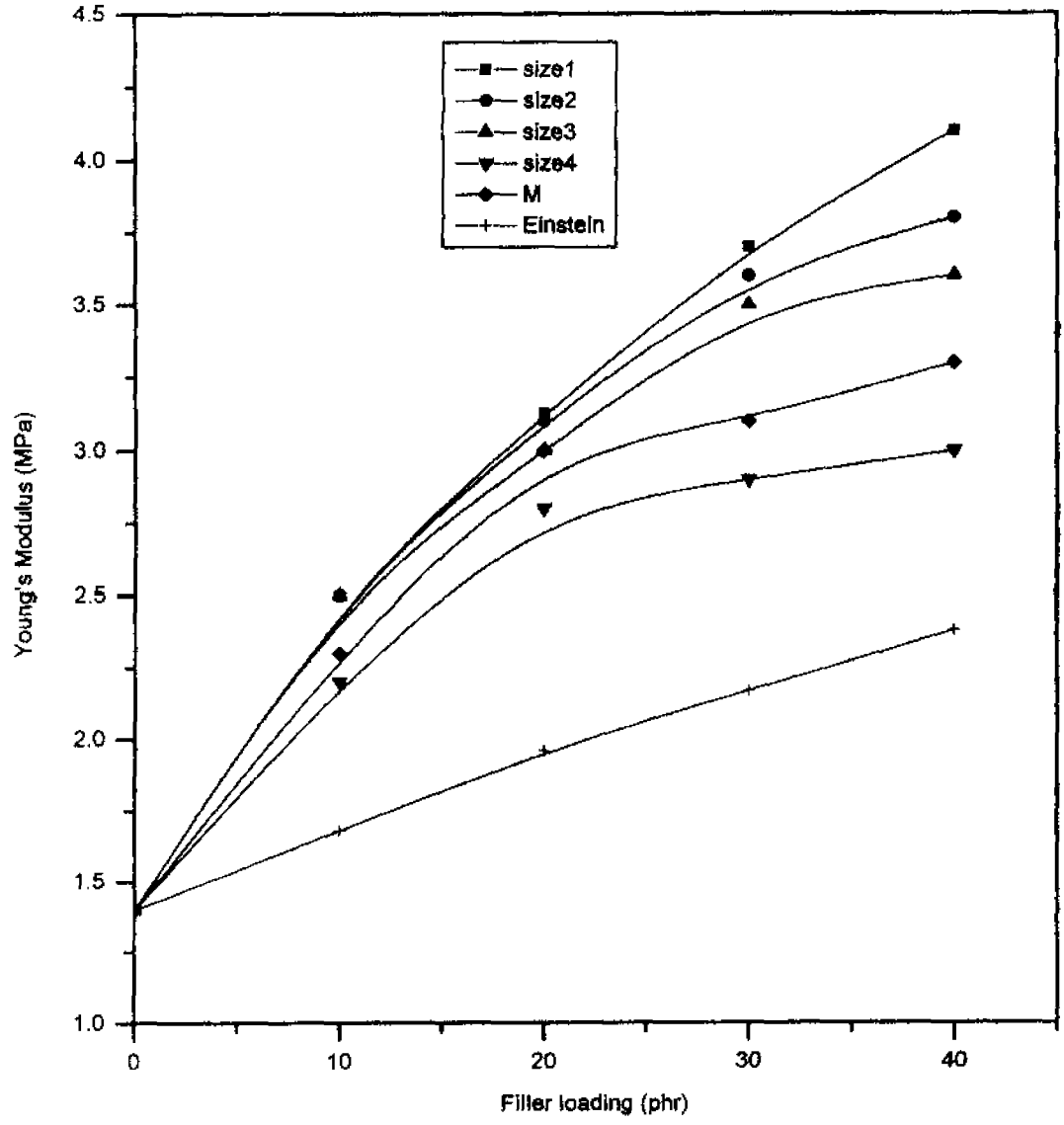

Fig. 12. Comparison of the experimental data with Einstein's model for a CV system.

This is found to be true for the present case. However, for the EV system with lower concentration of polysulphidic linkages in the ENR matrix, the sulphur migration must be predominant and consequently, the cross-link density from the contact surface must be higher than that from the non-contact surface. However, various additional factors, such as the differential swelling of prophylactic particles and the ENR matrix, the competition between the interaction parameters of the two polymers and the overall compact structure of the system deciding the diffusion characteristics, make the swelling results a bit irregular. The superior influence of the compact nature of the polymer matrix over the interaction parameter values on the swelling process will be discussed in a later section. Even in the case of the EV system, the cross-link density of the sample from the contact surface is found to be only slightly higher than that from the non-contact surface. Even though this proves the presence of sulphur migration, this factor alone is unable to support the observed changes in mechanical properties.

The tear strength of gum and filled ENR samples are presented in Fig. 11. With increase in loading of the filler, there is slight improvement in the tear strength of the samples up to 30-phr loading. This increase is due to the restriction in the advancement of the tear front. This restriction is caused by the elongation of filler particles in the tear path. The performance of size 1 filler is superior here. In the case of finer filler (size 1) there will be a large number of filler particles present per unit area to elongate to high strains and to resist tear propagation. As the particle size increases to sizes 2 and 3, the tear strength decreases and the values are minimum for size 4. However, at 40-phr loading, the value either drops or levels off for large filler sizes.

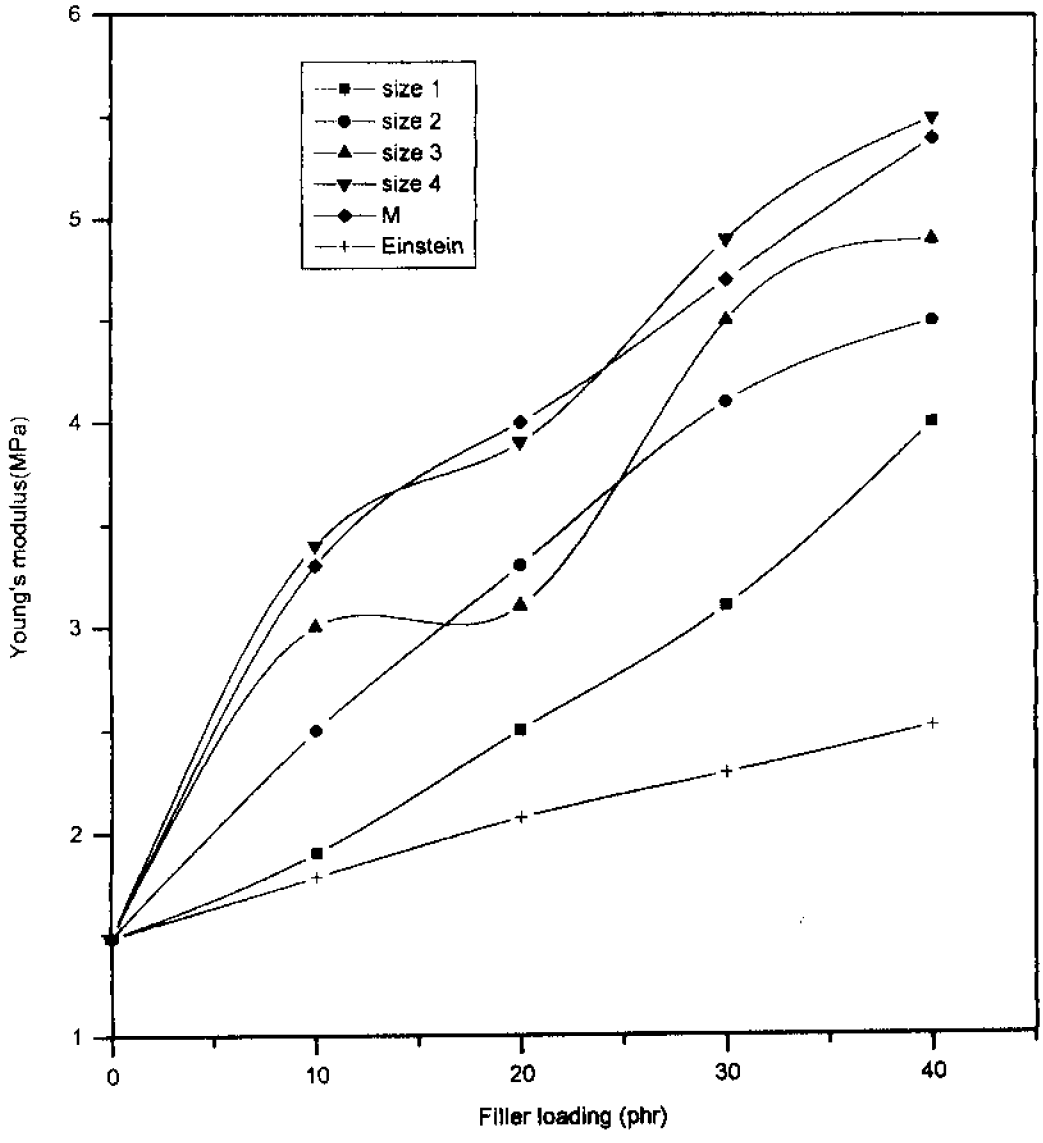

Fig. 13. Comparison of the experimental data with Einstein's model for an EV system.

3.3. Theoretical modelling of Young's modulus

Young's modulus of particulate-filled composites can be predicted using several theoretical models. Even though a large number of theoretical equations are generally available for composite materials, only a few are specially formulated for composites with non-rigid matrices. These include the Einstein, Mooney, Guth, Cohan, and Brodnyan models. The Einstein equation and its modifications are usually applied to predict the modulus of the composites containing rigid fillers such as black and silica. These theories are applied to systems with non-rigid fillers such as prophylactic particles, which undergo strain crystallisation on stretching.

The simplest theoretical equation for the reinforcement of a material with a filler is given by Einstein [43]. The equation is

$$M_c = M_m(1 + 2.5V_f) \quad (9)$$

where M_c is Young's modulus of the composite, M_m is Young's modulus of the matrix and V_f is the volume fraction of the filler. The Young's modulus values of all the four particle sizes and mill-sheeted form of the latex waste filler are correlated with the Einstein model in Figs. 12 and 13. Fig. 12 represents the conventional vulcanisation system, where the finest filler (size 1) is most reinforcing. Therefore, it presents a plot that is far above that given by the Einstein equation. It is a general observation from the figure that only large-size fillers such as sizes 3 and 4 are found to give close values to that of Einstein. With increasing loading of fillers, the deviation shown by the finer-size fillers such as sizes 1 and 2 goes on increasing, while that of large-size fillers

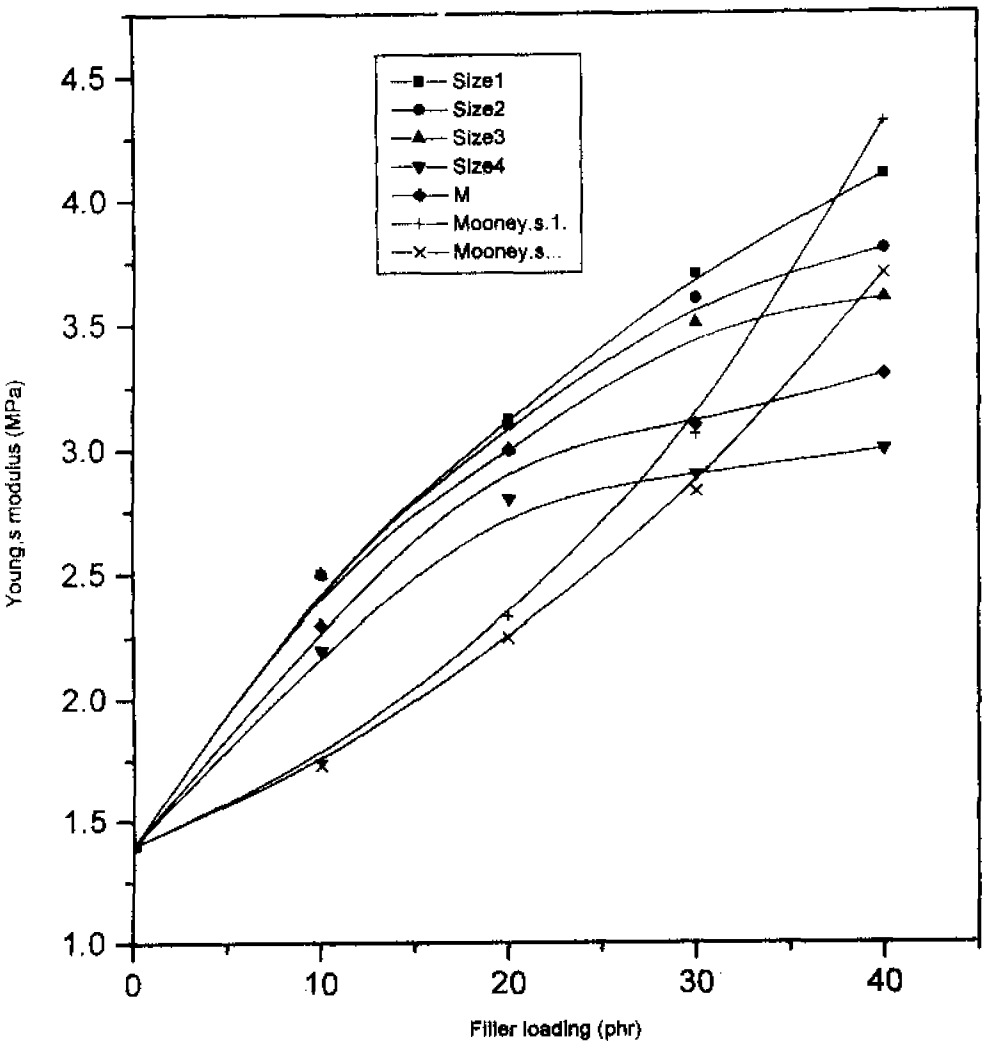

Fig. 14. Comparison of the experimental data with Mooney's model for a CV system.

(sizes 3 and 4) decreases. The behaviour shown by the mill-sheeted form (M) is in between finer- and large-size fillers.

Fig. 13 represents the Young's modulus correlation of all filler grades with the Einstein model, in an EV system. Here, the finest filler (size 1) is weakly reinforcing and, therefore, its plot is closer to that of Einstein, mainly at 10-phr loading. It is found that as the particle size increases to sizes 2–4, the deviation of the modulus values from those of the model increases. Also, as the loading increases, the magnitude of deviation also increases even though some irregularities are observed for the size 3 filler at 20-phr loading. It is a general observation that for CV and EV systems, none of the filler grades shows an exact correlation with the Einstein model.

The observed deviations from the model are due to the following reasons:

(1) The Einstein model assumes that the stiffening action of a filler is independent of its size, while it has already been established by many researchers [44] and also by our studies [45] that the reinforcement of the matrix by a filler changes with its particle size. Since this effect is not accounted for by the model, the experimental values for different size grades deviate differently from the model.

(2) The model assumes that the filler particles are spherical in shape and there is perfect adhesion between the filler and matrix. It is clear from the SEM photos of filler particles (Fig. 3) that the filler particles have non-uniform size distributions and shape. Also, we have noted from the scanning electron micrographs (Fig. 28a and b) that the filler particles are not firmly bonded to the matrix. The presence of an air pocket over the filler particles has already been confirmed by the work of Phadke et al., [46]. Therefore, the imperfect adhesion between filler and matrix also contributes to the observed deviations from the model.

(3) It is stated by Mooney [47] that the Einstein equation is valid only for low concentrations of filler. This is because at higher filler loading, the strain fields around filler particles can interact, causing deviations from the model.

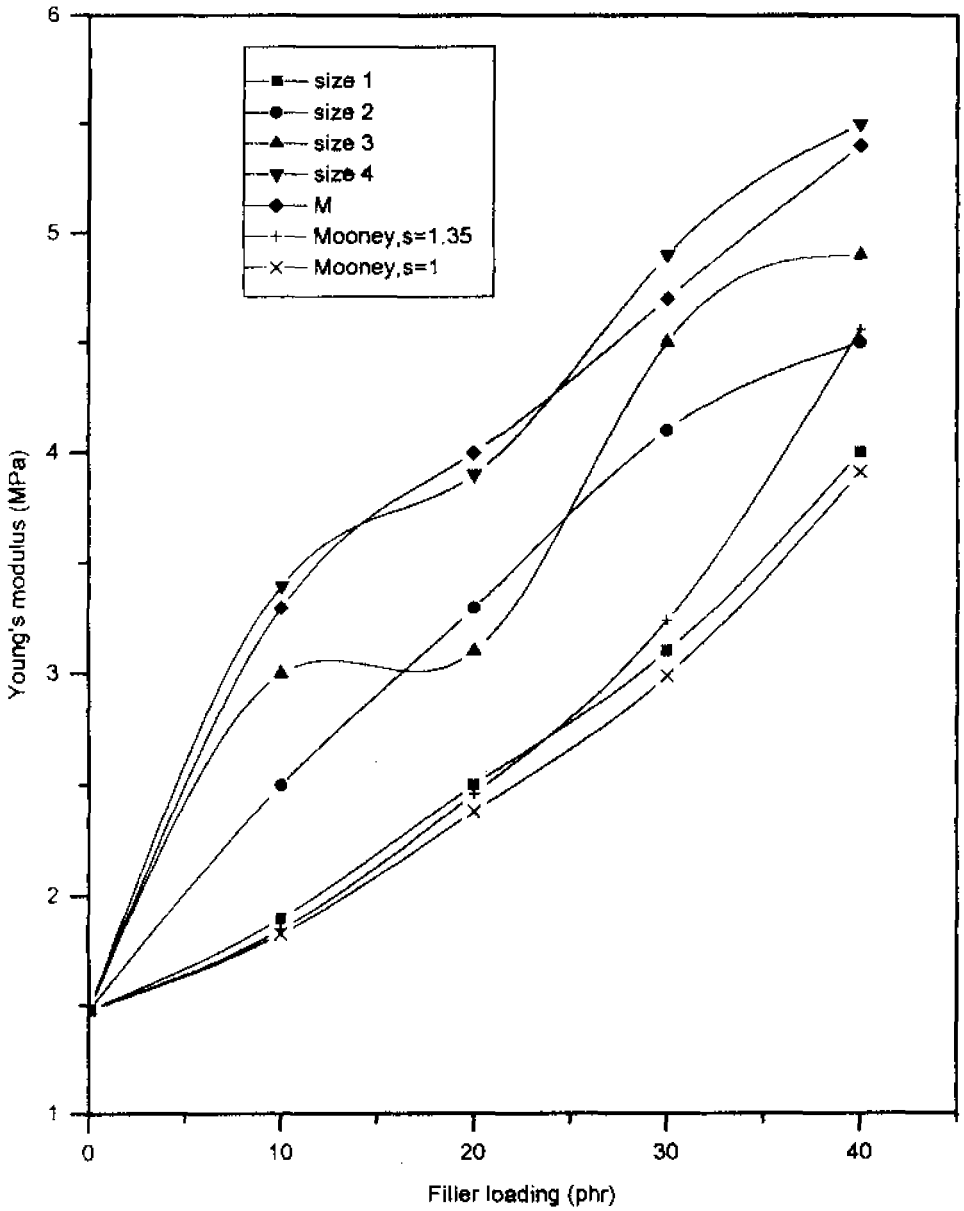

Fig. 15. Comparison of the experimental data with Mooney's model for an EV system.

(4) The final and most important reason for the deviation may be the lower rigidity of the filler compared to normal fillers such as carbon black or silica. Since it is assumed in the Einstein model that the filler is much more rigid than the matrix, this factor may cause a number of secondary reasons for deviations from the model. However, it has already been proved by Smallwood in the literature [48] that the Einstein equation is more useful for predicting the elastic behaviour of rubbers containing non- or less-reinforcing fillers. The correlation, even though less, between experimental and theoretical values observed in our case again proves this fact.

The Einstein equation does not account for the particle agglomerations. Therefore the equation has been modified by Mooney [47] by introducing a crowding factor S. The Mooney equation is given as;

$$M_c = M_m \exp\{2.5V_f/1 - SV_f\} \quad (10)$$

where M_c, M_m and V_f are the same as explained earlier. S is the crowding factor or relative sedimentation volume of the filler, which accounts for the agglomeration of filler particles. Agglomerates of filler particles tend to contain voids or air spaces so that their apparent volume will be higher than their true volume. S is defined as the ratio of apparent volume occupied by the filler to its true volume.

According to Mooney [47], the minimum possible value that S can have is unity while its experimental value ranges

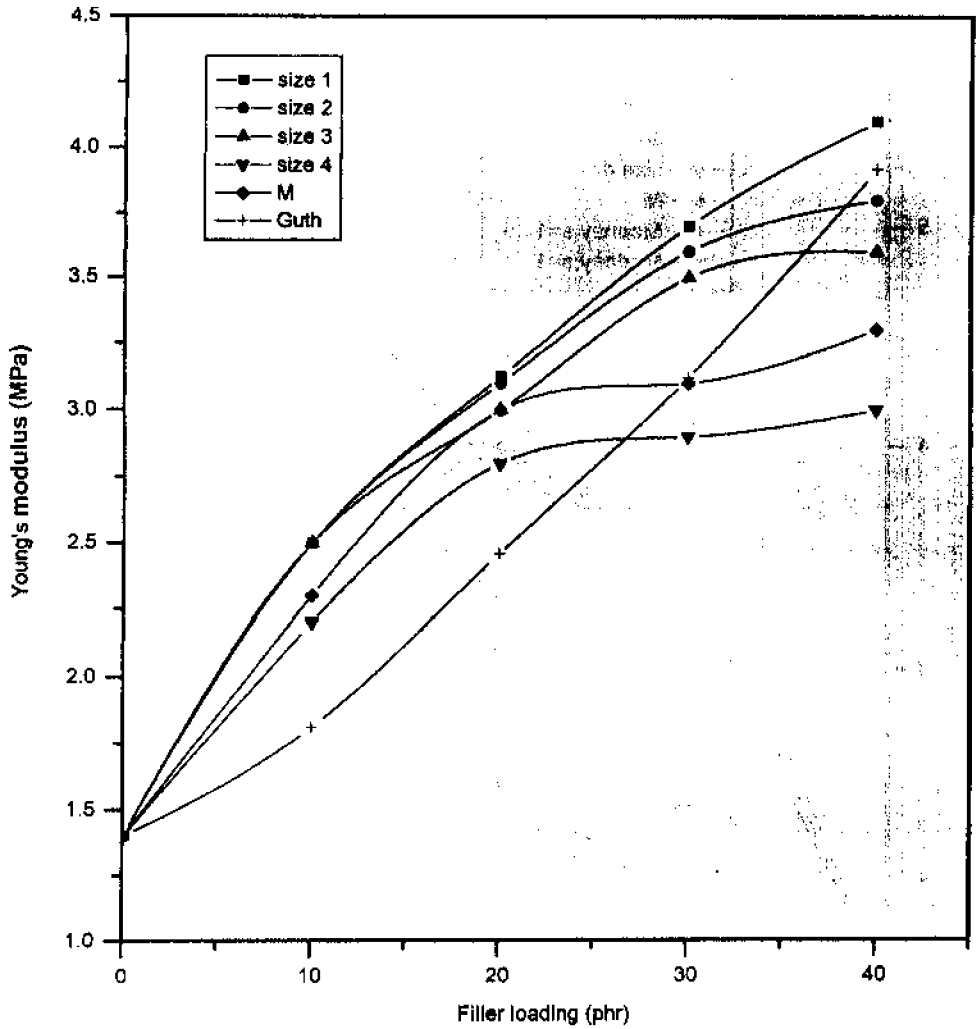

Fig. 16. Comparison of the experimental data with Guth's model for a CV system.

from 1.2 to 2. However, it has been reported [49] that up to $V_f = 0.5$, a value of 1.4 (or 1.35) can fit the best experimental values. For our system, we have made our calculations using two values of S, 1.35 and 1. Fig. 14 is the Mooney model fitting curves of different size grades of latex waste filler, in the conventional vulcanisation system. When the value of S is 1.35, the size 4 filler gives comparatively closer values than that given by the equation at 10- and 20-phr loading. However, as the loading increases to 30 phr, a better value is shown by the mill-sheeted form, while the size 4 filler gives a value below that of the model. All other filler sizes such as 1, 2 and 3, deviate greatly from the model mainly at lower loadings. As the filler loading increases to 40 phr, the model plot shoots up and, therefore, closer values are shown by finer filler sizes 1–3. Size 4 and mill-sheeted form values lie much below that of the model at highest loading. When the value of S is 1, the size 4 filler gives better agreement mainly at 30-phr loading and sizes 2 and 3, at 40-phr loading. Large-size fillers, size 4 and the mill-sheeted form, are below that of the Einstein model while finer sizes 1 and 2 are above. As far as the efficient vulcanisation system (Fig. 15) is concerned, for $S = 1.35$, the size 1 filler is closer to the values predicted by the Mooney equation. This is due to its weakly reinforcing nature in the EV system. Most other size grades and mainly sizes 4 and the mill-sheeted form deviate from the model at all the loadings. It is clear from the nature of the Mooney plots ($S = 1.35$) up to 40-phr filler loading, that it will steeply increase for further filler loadings. The general nature of the Mooney equation, i.e. a modulus value which tends to infinity at higher filler loadings, which has been reported previously [47,49] is observable here also. It has already been experimentally established by Nielsen [49] that S increases with decreasing particle size. This means that the tendency of finer filler to agglomerate is greater compared to large fillers. Therefore, it is clear that in order to have a reasonable fitting of tensile strengths of the size 1 filler with the Mooney model, different and variable values of S for different loadings, size, etc., must still be suggested. The above observed fitting of theoretical

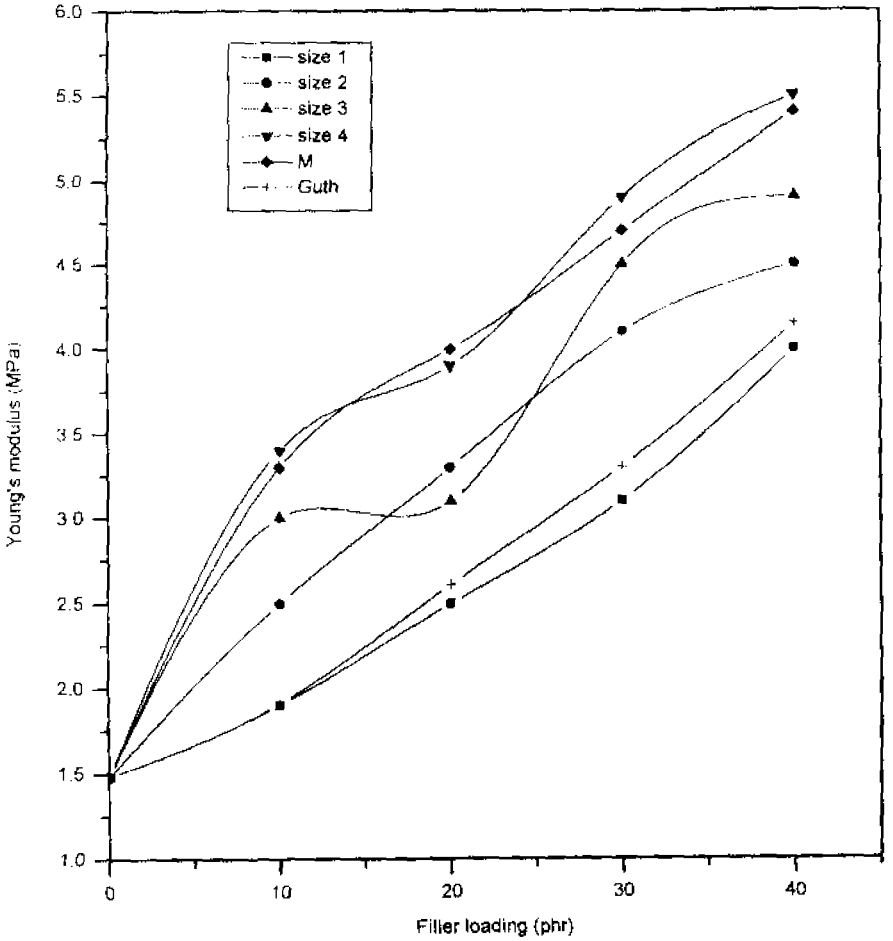

Fig. 17. Comparison of the experimental data with Guth's model for an EV system.

values, even though partial, may be due to the fulfilment of some of the assumptions connected with the Mooney model, such as Poisson's ratio of the matrix must be 0.5, etc. This model also assumes that filler particles are uniformly distributed spheres with good adhesion to the matrix and the modulus of the filler is infinitely greater than that of the matrix. Even when the value of S is 1, the deviations from the model shown by various particle sizes of fillers is almost the same.

Guth and Smallwood [50] generalised Einstein's concept and introduced a particle interaction term. This modified equation can be written as:

$$M_c = M_m(1 + 2.5V_f + 14.1V_f^2) \quad (11)$$

where M_c, M_m and V_f are the same as explained earlier.

For the conventional vulcanisation system, the Guth model gives similar values as given by large-size fillers (size 4) and the mill-sheeted form at 10 and 20 phr. This is clear from Fig. 16. Size 1 and 2 plots, owing to their superior reinforcing behaviour, lie above the model at 30-phr loading. However, at 40-phr filler content, finer fillers sizes 1 and 2 suffer from particle agglomerations and, therefore, their modulus values slightly bend towards the x-axis and lie equidistant from the model. Such a blending is observed for size 4 and the mill-sheeted form also. At higher filler loading, size 3 filler prefers an intermediate position. Since the model does not account for the agglomeration effects at higher loadings, the theoretical curve tends to infinite position, as in the case of the Mooney equation.

When the vulcanisation system changes to efficient mode (Fig. 17), most of the finest filler size (size 1), falls below the value predicted by the model. Agreement between theoretical and experimental values is observable at all the filler loadings. All the filler sizes except sizes 3 and 4, exhibit a constantly increasing deviation from the Guth model with loading. It is a general observation that when the vulcanisation system is conventional, good correlation with the model is shown by large particle-size grades of the filler; and when the vulcanisation system is efficient, the place is taken by the finer fillers.

The model assumes that the change in elastic constant of the rubber by embedded spheres is entirely analogous to the theory of viscosity. For example, when a carbon black suspension undergoes stretching, the suspended particles perturb the stresses and strains are set up in the body,

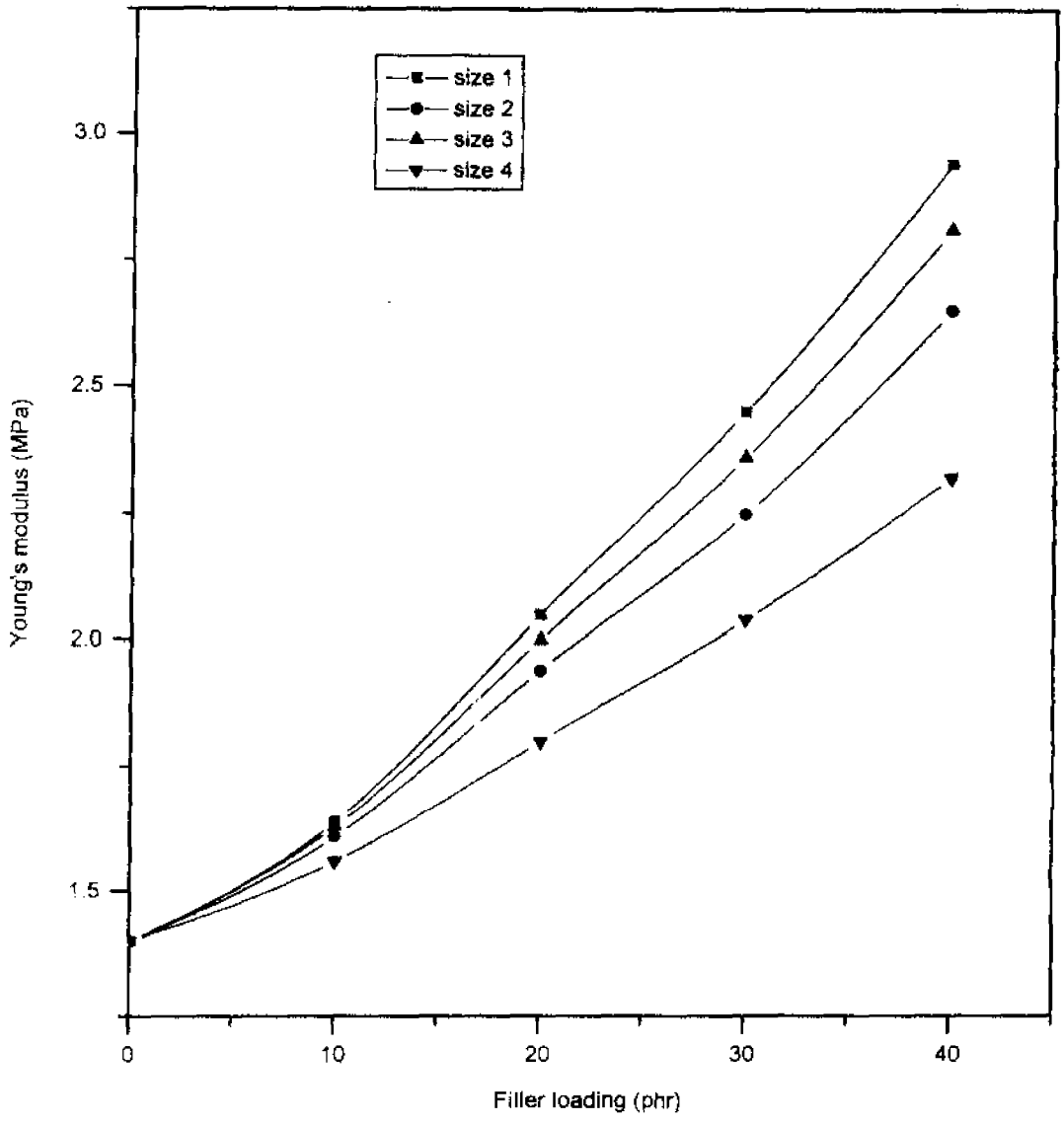

Fig. 18. Theoretical plots of tensile strength from Cohan's model (CV system).

which lead to an increased elastic energy and elastic constants. For this to happen, however, filler particles must be spherical and rigid. Even though sizes 3 and 4 assume a somewhat spherical shape, their non-rigid nature violates the assumption. Therefore, they deviate from the model mainly at higher loadings.

Most of the equations discussed above assume that the particulate inclusion is spherical in shape. Even though we have assumed that filler particles are spherical in the present case, they are not exactly so. Only large particle-size fillers can be considered as spherical, while smaller fillers possess different shapes. This can be understood from a comparison between Figs. 26a (size 1), 29a or 29c (size 4). Many studies have been reported in which the effect of particle shape on reinforcement is discussed. This effect must be treated separately from usual effects such as agglomeration and interphase adhesion.

Properties of composites are affected by changes in the shape of inclusion also. Bueche observes [51] that different filler shapes lead to different mechanical properties. A theoretical treatment was suggested by Wu [52], which could prove that disc-shaped particles can reinforce better than spherical or needle-shaped ones. The anisotropy associated with this, which Wu neglected, was taken into account by Chow [53]. Chow [53] modified the equation by introducing longitudinal and transverse moduli and proved that fillers with a high aspect ratio show a better reinforcement, than those with high particle symmetry. This aspect ratio also is included in the Guth equation modified by Cohan.

The Cohan model [54] is given by the equation:

$$M_c = M_m(1 + 0.675pV_f + 1.62p^2V_f^2) \quad (12)$$

where M_c and M_m are the same as explained earlier and p is

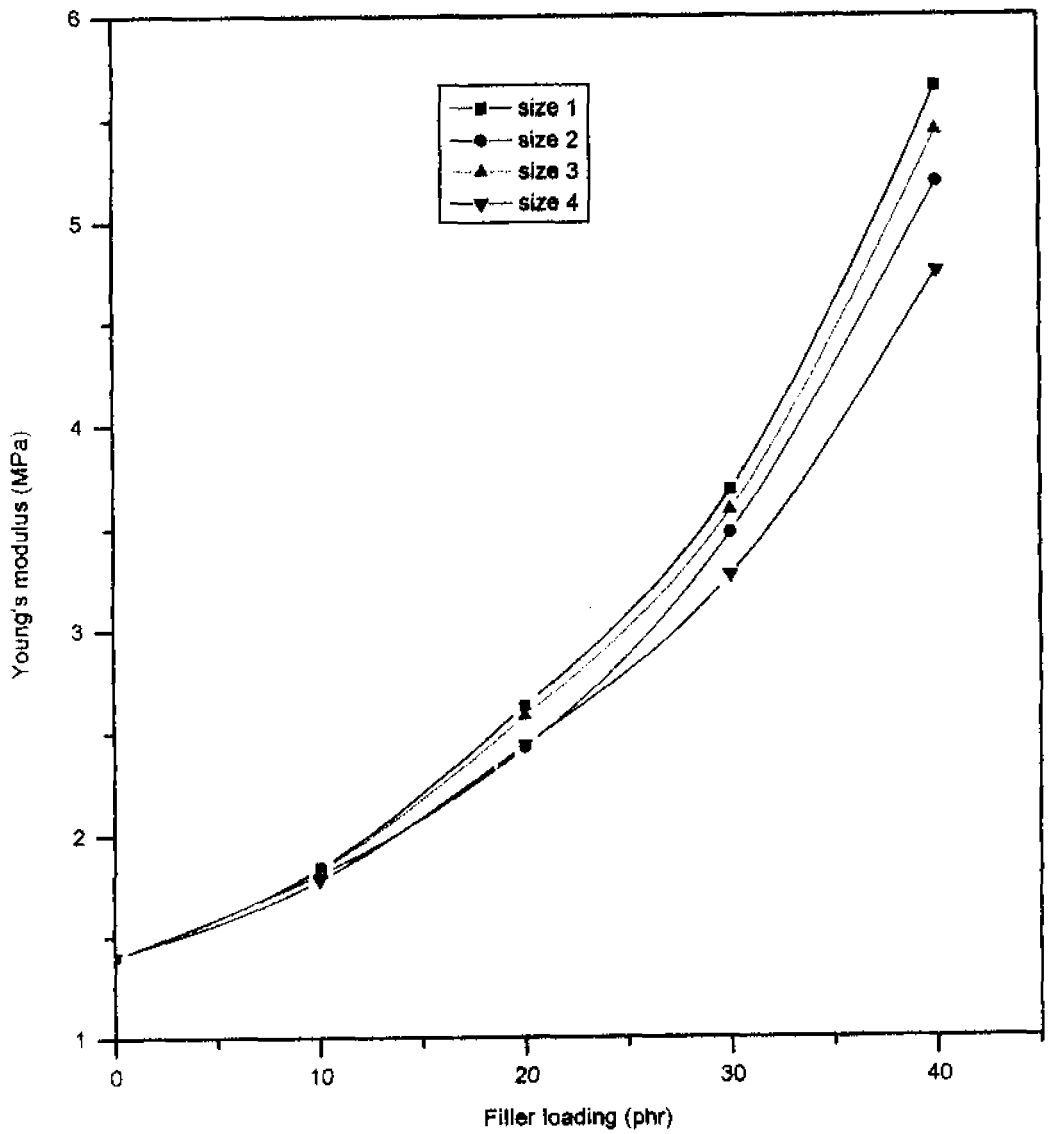

Fig. 19. Theoretical plots of tensile strength from Brodnyan's model (CV system).

the aspect ratio or shape factor, which is the length-to-width ratio of filler particles.

The values of p determined for different particle sizes are given in Table 3. It is clear from Eq. (12) that the modulus of the composite predicted by the equation will be the highest for the case with the maximum value of p. Among the theoretical plots obtained for the different size grades in Fig. 18, size 1 shows the most superior performance. The model is able to predict the order of modulus variation as the particle size decreases. It is assumed by the model that $p \gg 1$, which is not correct as far as our system is concerned. This is clear from the shape factor value given in Table 3. Therefore, deviations from the experimental values can be normally expected.

There is another approach to explain the superior performance of the finest filler in the conventional vulcanisation system. This can more clearly illustrate the expected behaviour when spherical particles are stretched to form rod-shaped particles. Kuhn and Kuhn in the literature [49] derived an expression for the viscosity of suspension of randomly oriented rod-like or cigar-shaped particles in the form of ellipsoids. This equation was modified by Brodnyan [55] for elongated ellipsoids as:

$$M_c = M_m \exp\{2.5V_f + 0.407(p-1)^{1.508}V_f\}/1 - S(V_f) \quad (13)$$

where M_c, M_m, V_f and S are the same as given earlier and p is the aspect ratio ($1 < p < 15$).

The theoretical plots for Young's modulus for the conventional vulcanisation system from the Brodnyan model are presented in Fig. 19. The steeply rising trend of the plots shown by the model compared to the Cohan model (Fig. 18) is observable here. The values of p are the same as

Table 6
Swelling index values

Filler loading (phr)	Gum	Size 1	Size 2	Size 3	Size 4	M
0	408					
10		411	416	422	428	430
20		417	421	427	430	436
30		420	425	429	435	441
40		424	429	436	439	454

already reported (Table 3) and this equation also is found to be successful in predicting the comparatively better reinforcement in the case of finer fillers. Still, deviations from theoretical values can be expected. This is because the model assumes random orientation of rod-shaped fillers, whereas in the present case they are found to be oriented. This orientation results from the shearing in the two-roll mixing mill. This is clear from Fig. 26a. This model predicts that the higher the concentration of rod-like particles, the higher the modulus value. However, it neglects the anisotropy in property associated with their alignment in the matrix. From these discussions it is clear that the models, namely the Cohan and Brodnyan models, can explain the relative order of performance of different size grades in the conventional vulcanisation system only. The trend in the EV system, where larger fillers are more reinforcing, cannot be explained unless these two models are modified appropriately. Moreover, from the theory of all the models described above, the rubber matrix must have the same properties as the unfilled vulcanisate ($V_f = 0$) if a direct experimental test is to be possible. This condition will never be met and, therefore, deviation from different models can be justified. For the present cases, these equations can only be considered as semiquantitative guides for predicting the modulus of composites containing less-rigid soft fillers in a soft matrix.

3.4. Solvent transport studies and cross-link density determination

The swelling index value, which is a measure of the swelling resistance of the rubber compound, is calculated using the equation:

$$\text{Swelling index}\% = A_s/W_1 \times 100 \quad (14)$$

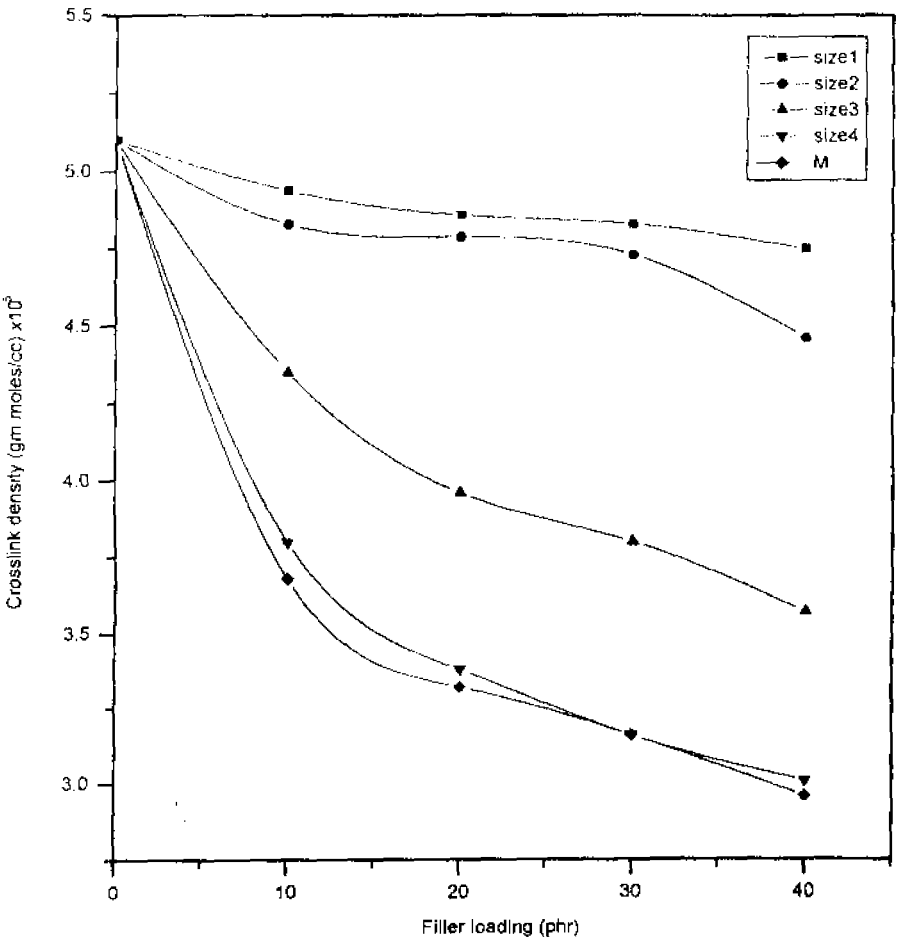

Fig. 20. Effect of filler loading and size on the cross-link density of ENR vulcanisates.

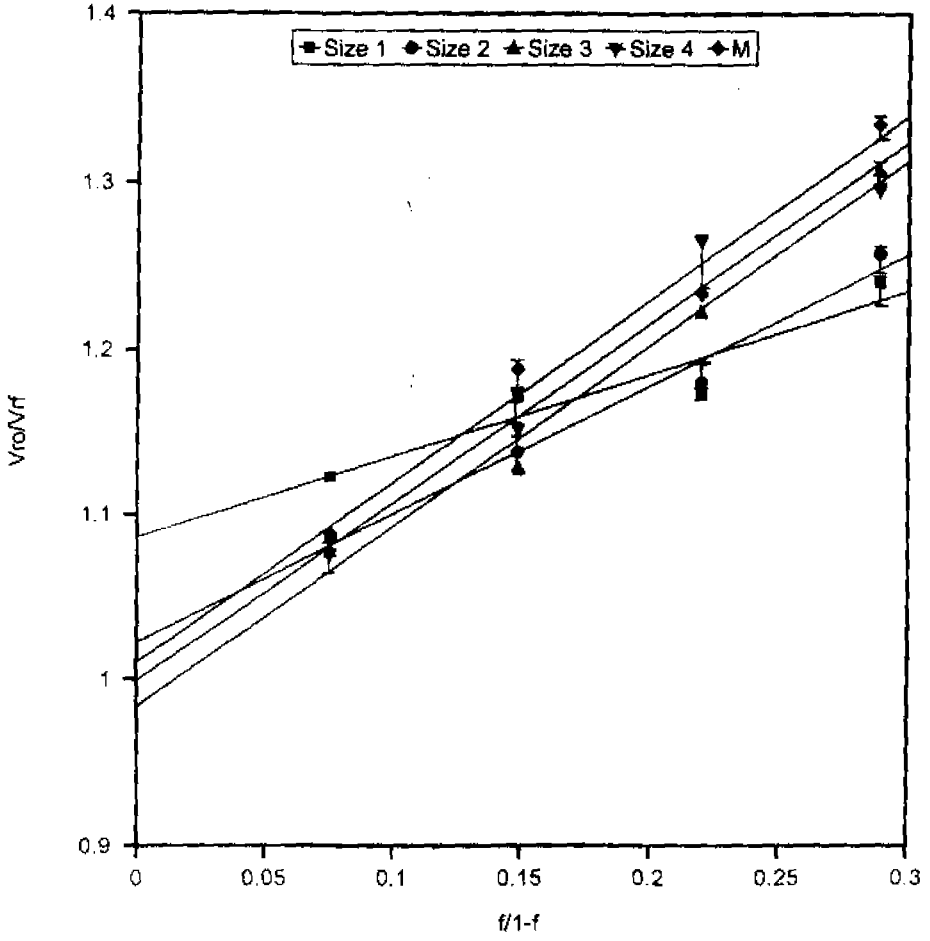

Fig. 21. Variation of V_{ro}/V_{rf} as a function of filler loading (Kraus plots).

where A_s is the amount of solvent absorbed by the sample and W_i is the initial weight of the sample before swelling.

It has already been reported in the literature [56,57] that in the case of various polymer solvent systems, differences in the solubility parameter (and hence interaction parameter) values can be used to characterise the sorption behaviour of the solvent. However, our analysis proved that such a correlation is ineffective since the diffusion behaviour of elastomer-filled elastomer systems are more dependent on the compact nature of the sample. This fact is strongly supported by the literature [58]. Since the compact nature of the ENR sample decreases with the addition of prophylactics, the diffusion of the solvent through the sample also increases. It has also been reported in the literature [59] that the diffusion mechanism in rubbery polymers is essentially connected with the ability of the polymer to continually provide opportunities for the solvent to progress in the form of randomly generated voids. Since the ease of void generation in the sample increases with the addition of prophylactics, the uptake of the solvent also increases. Therefore, as the filler content increases, the swelling index value increases for all size grades (Table 6). The solvent absorption by the latex filler particles is found to be minimum for the size 1 filler. This again confirms that in an ENR matrix cross-linked by a CV system, the size 1 filler shows good adhesion. This behaviour is supported by the cross-linked density values (Fig. 20). As the filler content increases, the cross-link density values are found to decrease. This effect can be explained using the basic equations used for swelling:

$$M_C = -\rho_r V_s V_{r_f}^{1/3} / \ln(1 - V_{r_f}) + V_{r_f} + \chi V_{r_f}^2 \quad (15)$$

where M_C is the molecular weight of the polymer between two cross-links ρ_r is the density of the polymer, V_s is the molar volume of solvent and χ is the interaction parameter, which is given by the Hildebrand equations [60,61]:

$$\chi = \beta + \frac{V_s}{RT}(\delta_s - \delta_p)^2 \quad (16)$$

where β is the lattice constant, V_s is the molar volume, R is the universal gas constant, T is the absolute temperature, δ_s is the solubility parameter of the solvent, δ_p is the solubility parameter of the polymer and V_{r_f} is the volume fraction of elastomer in the solvent swollen filled sample and is given

Table 7
Values of slopes and C

Particle size	Kraus equation slope (m)	C	Cunneen and Russell equation slope (a)	Lorenz–Park equation slope (a)
S1	0.4961	0.9946	0.6790	−1.3979
S2	0.7789	1.2070	−1.0532	1.5344
S3	1.0979	1.4467	−1.5003	−2.1026
S4	1.0833	1.4357	−1.5067	−2.1725
M	1.0956	1.4449	−1.5107	−2.2144

by the equation by Ellis and Welding [62]

$$V_r = \frac{(d - fw)\rho_p^{-1}}{(d - fw)\rho_p^{-1} + A_s\rho_s^{-1}} \quad (17)$$

where d is the deswollen weight of the sample, f is the volume fraction of the filler, w is the initial weight of the sample, ρ_p is the density of the polymer, ρ_s is the density of the solvent and A_s is the amount of solvent absorbed by the sample.

As the filler content increases, the amount of solvent absorbed by the sample (A_s) increases, which leads to lowering of V_r and this in turn reduces the cross-link density values as evident from Fig. 20. It is to be noted that the cross-link density decrease is minimum for finer filler sizes 1 and 2, which have comparatively more reinforcing action in ENR for the CV system and, therefore, they absorb a minimum quantity of solvent. So the cross-link density values (from swelling studies) presented here have good correlation with filler–matrix interface adhesion.

3.5. Extent of reinforcement

The extent of filler reinforcement can be analysed by

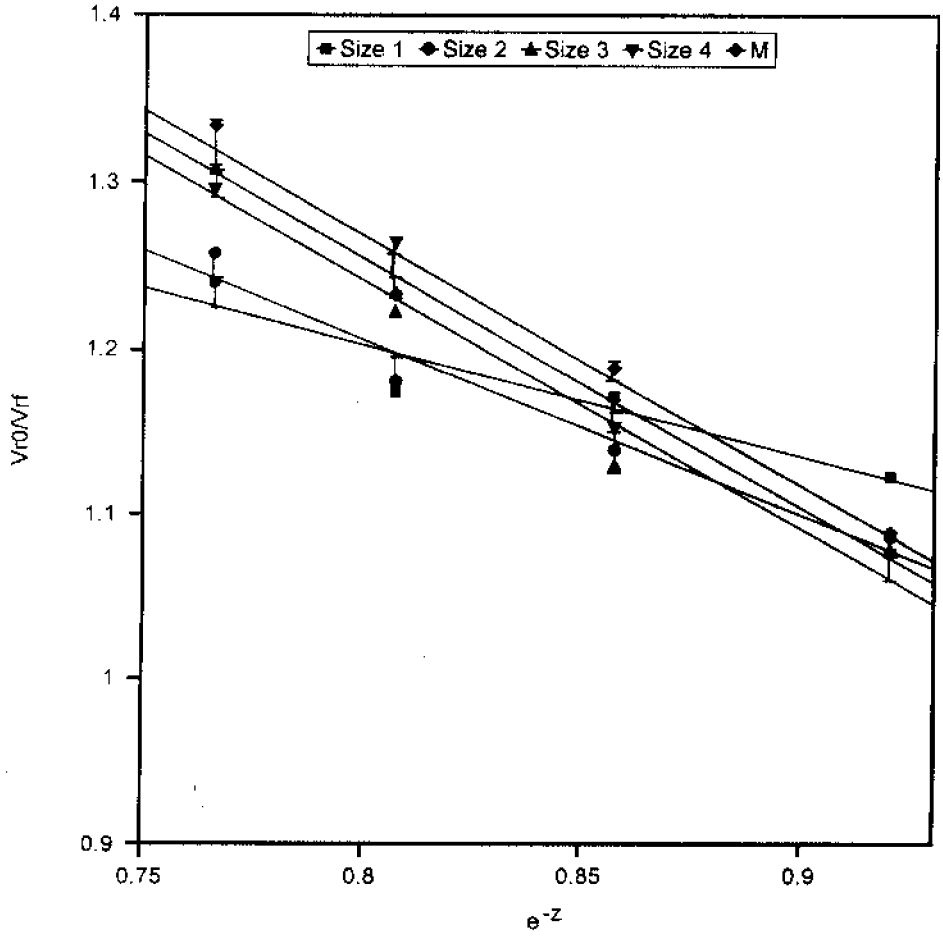

Fig. 22 Variation of V_{ro}/V_r as a function of filler loading (Cunneen–Russell plots).

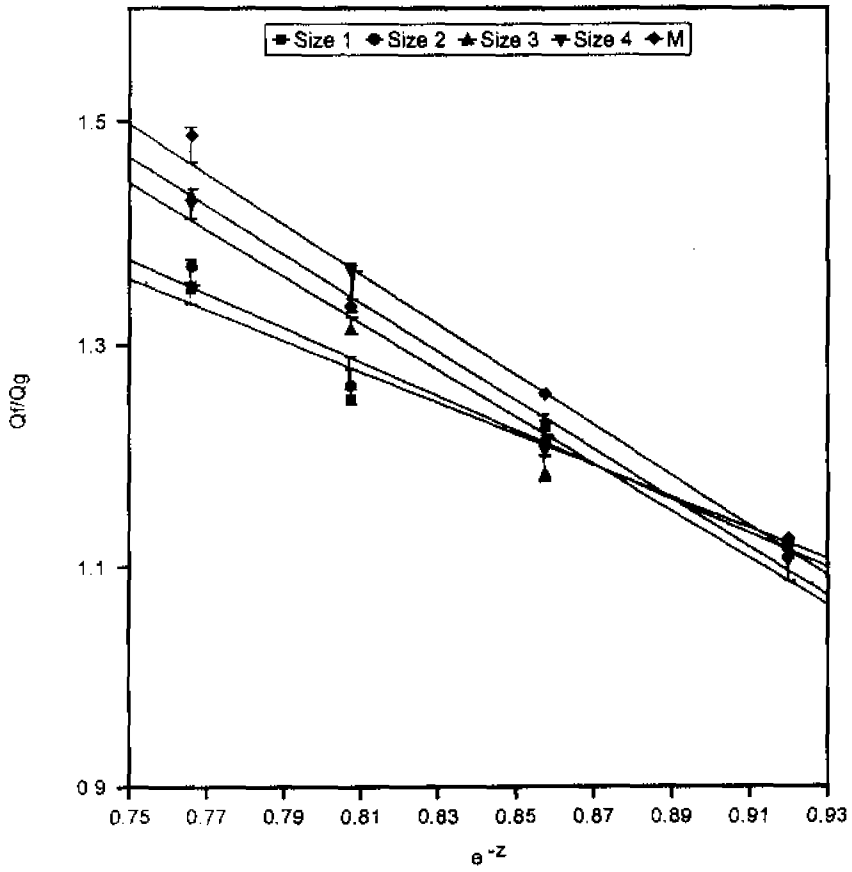

Fig. 23. Variation of Q_f/Q_g as a function of filler loading (Lorenz–Park plots).

using Kraus [35], Cunneen and Russell [36] and Lorenz–Park [37] equations. The Kraus equation is:

$$V_{r_0}/V_{r_f} = 1 - m(f/1-f) \tag{18}$$

where V_{r_f} is the same as explained above and V_{r_0} is the volume fraction of elastomer in the solvent swollen unfilled sample. Since the above equation is in the form of a straight line, a plot of V_{r_0}/V_{r_f} versus $f/1-f$ should give a straight line, whose slope (m) will be a direct measure of the reinforcement of the filler. The constant C given by the equation:

$$C = \frac{m + V_{r_0} - 1}{3(1 - V_{r_0}^{1/3})} \tag{19}$$

which is characteristic of the filler, is calculated also. The Kraus plots obtained are given in Fig. 21 and the slope values are presented in Table 7. According to the theory by Kraus, reinforcing fillers such as carbon black will have a negative higher slope. In the present case, we observed that as the filler loading increases, the solvent uptake of the sample also increases. As already explained, this will cause a reduction in V_{r_f} values, which will increase the ratio V_{r_0}/V_{r_f} since V_{r_0} is constant. This behaviour leads to a positive slope in every case. Since size 1 filler exhibits a minimum positive value of the Kraus slope, it is clear that its solvent absorption is minimum, thereby supporting its better adhesion with the ENR matrix in the CV system. Moreover, constant C is inversely related to filler agglomeration tendency. It is also clear from Table 7 that the finest filler size 1 has maximum tendency for agglomeration. The trend given by the C value in the Kraus equation is in agreement with S, the crowding factor given by Mooney [47]. It has also been experimentally proved [47] that the S value increases with reduction in particle sizes. This means an increase in the ratio of apparent volume occupied by the filler to true volume, which points to the case of filler agglomerations. Thus, the higher tendency of the size 1 filler for agglomeration can be justified.

The Cunneen–Russell equation is

$$V_{r_0}/V_{r_f} = a\,e^{-z} + b \tag{20}$$

where V_{r_0} and V_{r_f} are the same as explained earlier, z is the weight fraction of the filler, a and b are constants. Here a plot of V_{r_0}/V_{r_f} versus e^{-z} should give a straight line with negative slope (a). V_{r_0}/V_{r_f} is found to increase with increasing filler loading as clear from Fig. 22. This increase is extensive in the case of large-size fillers (size 4 and M). For finer fillers, sizes 1 and 2, which are comparatively highly reinforcing, the absorption of the solvent is minimum,

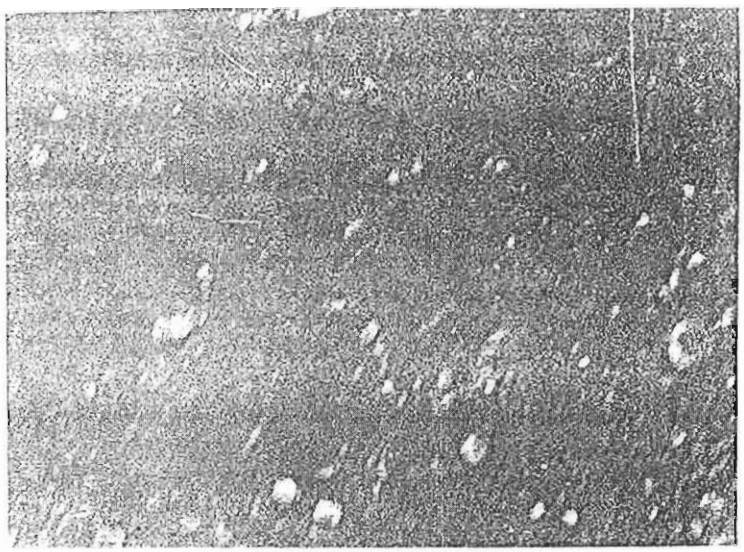

Fig. 24. SEM fractograph of tensile gum specimen.

which results in a lower V_f/V_g ratio and a smaller negative slope.

The Lorenz–Park equation is

$$Q_f/Q_g = a\,e^{-z} + b \tag{21}$$

where Q is defined as the amount of solvent absorbed/gm of rubber and is given by

$$Q = \frac{\text{Swollen weight} - \text{dried weight}}{\text{Original weight} \times 100/\text{formula weight}} \tag{22}$$

The subscripts f and g refer to filled and gum vulcanisates, respectively. z is the weight fraction of the filler. A plot of Q_f/Q_g versus e^{-z} gives a straight line with negative slope (Fig. 23). As explained earlier, here also finer fillers (sizes 1 and 2) exhibit lower slope, proving their better adhesion with ENR.

All the above previously established equations support the superior performance of the size 1 filler compared to large-size fillers when a CV system is used for the cross-linking of ENR.

3.6. Fractographic analysis

The improvement in tensile and tear performance with loading of filler is supported by the morphology of the fractured surfaces. These fractographs are presented in Figs. 24–30. Since the presence of filler particles is clearly visible in all the filled cases, this latex-filled ENR system can be considered only as a composite material. All the composite samples exhibit a two-phase morphology.

The fractograph of the gum vulcanisate is presented in Fig. 24. The smooth fractured surface observed here is

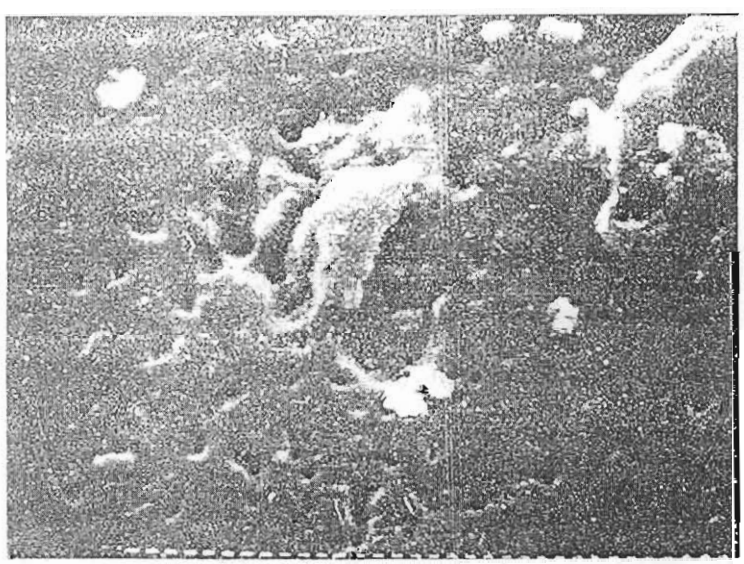

Fig. 25. SEM fractograph of tear gum specimen.

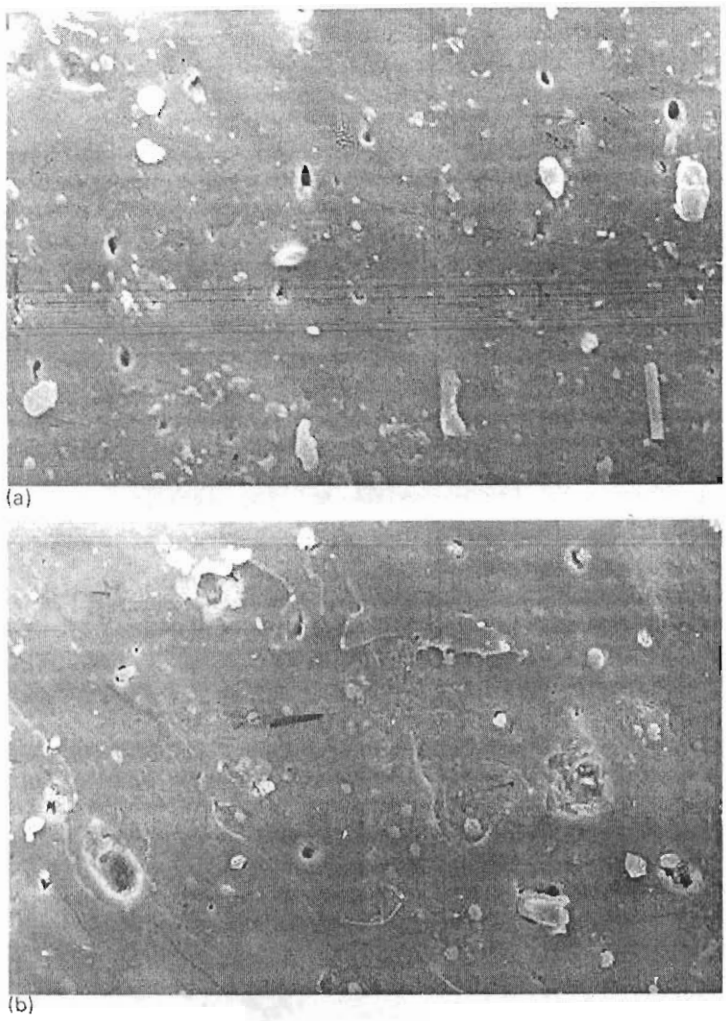

Fig. 26. (a,b) SEM fractograph of tensile specimen filled with 10 phr of size 1 filler.

Fig. 27. SEM fractograph of tensile specimen filled with 30 phr of size 1 filler.

(a)

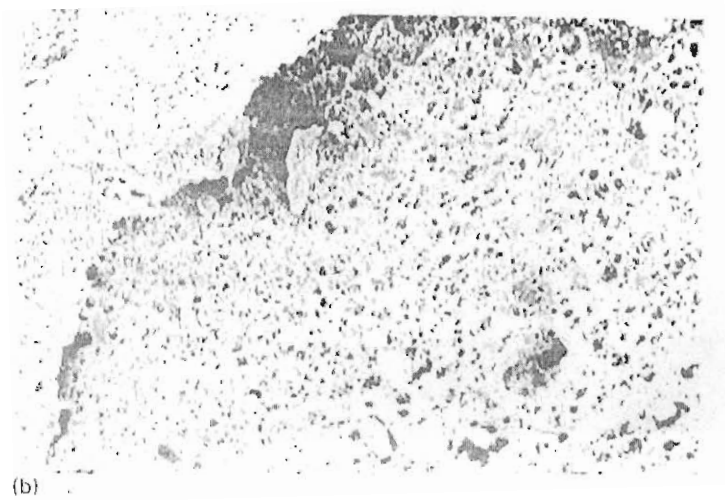

(b)

Fig. 28. (a,b) SEM fractograph of tear specimen filled with 40 phr of size 1 filler.

characteristic of low-strength vulcanised materials. In the case of torn surfaces of gum vulcanisates also, a similar morphology could be observed. The weak mechanical strength of the gum is clear from the undeviated cracks in Fig. 25.

In the case of ENR filled with 10 phr of size 1 filler, the fractography reveals the presence of fine filler particles (Fig. 26a). The presence of cigar-shaped particles aligned in a particular direction also is observable. Moreover, the fracture is found to deviate only slightly (Fig. 26b) presenting incomplete parabolic patterns. This confirms the comparatively high strength of the material. Still, dewetting is present in Fig. 26a. Fig. 27 is the tensile fractured surface of the ENR sample filled with 30 phr of size 1 filler. Here the cracks are extensive and much deviated. Such parabolic fractured surfaces support the high strength of the material. The role of filler particles in blocking the advancing crack also is observable. The torn surface of ENR filled with 40-phr size 1 filler is presented in Fig. 28a and b. Here also crack deviation is extensive. The portions from which the filler particles are debonded are visible as holes in the figure. The filler particles elongate to high strains and obstruct the tear (Fig. 28b). Thus, as explained above, the material filled with size 1 filler shows superior tear performance.

For fillers of higher sizes (size 4) at a loading of 10 phr, debonding is extensive. Also the cracks are again becoming smooth. Dewetting is clear from Fig. 29a and b and smooth fractures are visible in Fig. 29b and c. It can be seen from Fig. 29c that the particle size of fillers is not uniform. This is because large-size fillers undergo more size reduction during mixing.

Fig. 30 is the torn surface of ENR filled with 30-phr size 4 filler. The material shows cracks with slight deviations, which proves its good tear strength. The accumulation of filler particles on the crack path in an effort to prevent the advancing crack is visible in the figure. It is a general observation in Figs. 29c and 30 that the larger-size grade (size 4) filler particles are polydispersed in size owing to their breakage during mixing.

For most of the filled cases, the fractured surfaces are

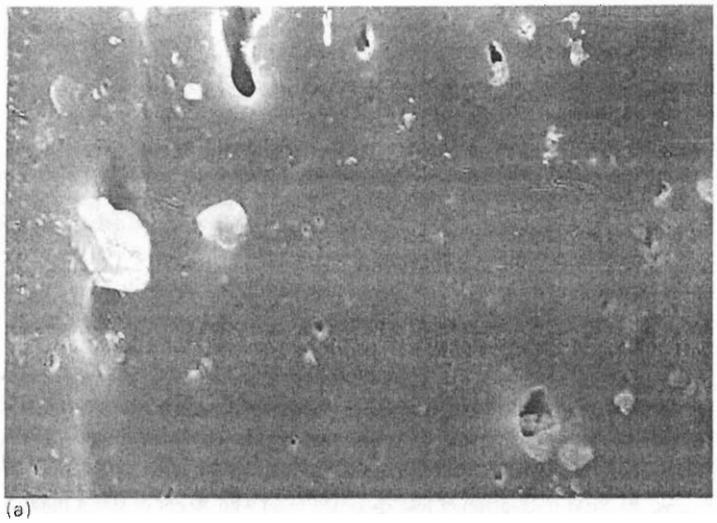

(a)

(b)

(c)

Fig. 29. (a–c) SEM fractograph of tensile specimen filled with 10 phr of size 4 filler.

Fig. 30. SEM fractograph of tear specimen filled with 30 phr of size 4 filler.

greatly crack deviated and present a series of parabolic lines distributed all over the surfaces. Such behaviour is due to the interaction of main fracture fronts with subsidiary fracture fronts and from the resistance in tear propagation by filler particles. Thus the superior mechanical performance of size 1 filler is strongly supported by the SEM fractographic studies.

4. Conclusions

The utilisation of cross-linked waste natural rubber as a potential filler in ENR deserves much attention. The cross-linked waste rubber has been powdered and sieved into different particle sizes. The morphology and size distribution of these particles has been analysed. It has been observed that, as the filler content increases, the curing characteristics like optimum cure time, scorch time and induction time decrease. The cure-activating nature of the filler is clear from the increase in cure rate index and rate constant values. The filler helps the compounder by reducing the sticky nature of epoxidised natural rubber compound during mixing. These observations are advantageous as far as processability and productivity are concerned. In the case of the conventional vulcanisation system, where sulphur migration is absent, finer filler shows superior tensile performance than size 4 and the mill-sheeted form of the filler. However, in efficient vulcanisation systems, where sulphur migration plays a role, the order of performance is inverted. The theoretical models such as those of Einstein, Mooney, Guth, Cohan, and Brodnyan are found to deviate from the experimental observations. Still the experimentally observed order of performance for different size grades of the filler could be correctly depicted by the Cohan and Brodnyan models. The three-layer model used here has been found to be completely successful in understanding the phenomena of sulphur migration in the efficient vulcanisation system and its extent in the case of different particle sizes of the fillers. As far as tear strength is concerned, size 1 filler has proved to be the best, but in every case, the property drops at 40-phr loading. The swelling index values register a constant increase with loading of filler and this increase is minimum for fine fillers such as size 1. In addition to this, the reduction in cross-link density with filler loading also is minimum for size 1 filler. The comparatively better adhesion between epoxidised natural rubber and size 1 filler is proved by previously established equations like the Kraus, Cunneen and Russell and Lorenz–Park equations. The scanning electron micrographs of fractured surfaces clearly support the good particle–matrix adhesion in the case of fine fillers. The non-compatible and phase-separated nature of the filler particles in the epoxidised natural rubber matrix cause these materials to be classified only as a filled epoxidised natural rubber composite, rather than as a blend system.

Acknowledgements

One of the authors (G.M.) is thankful to the Council of Scientific and Industrial Research, New Delhi, for the financial support.

References

[1] Debnath S, De SK, Khastgir D. J Appl Polym Sci 1989;37:1449.
[2] Debnath S, De SK, Khastgir D. J Mater Sci 1987;22:4453.
[3] Swor RA, Jensen LW, Budzol M. Rubber Chem Technol 1980;53:1215.
[4] Phadke AA, Bhattacharya AK, Chakraborthy SK, De SK. Rubber Chem Technol 1983;56:726.
[5] Rajalingam P, Sharpe J, Baker WE. Rubber Chem Technol 1993;66:664.
[6] Acetta A, Vergnaud JM. Rubber Chem Technol 1981;54:302.
[7] Drozdovskii VF. Int Polym Sci Technol 1992;19(11):T/57.
[8] Phadke AA, Chakraborthy SK, De SK. Rubber Chem Technol 1984;57:19.
[9] Phadke AA, Kuriakose B. Kautsch Gummi Kunstst 1985;38:694.

[10] Claramma NM, Thomas KT, Thomas EV. Paper presented at the Rubber Conference, Jamshedpur, 6–8 November 1986.
[11] Aziz Y. Paper presented at Polymer 90, Kuala Lumpur, Malaysia, 23 September 1990.
[12] Pittolo M, Burford RP. Rubber Chem Technol 1985;58:97.
[13] Air products Ltd, Appln 2, 022, 105, 12 December 1979.
[14] Dubaime JRM, Baker WE. Plast Rubber Compos Process Appl 1991;15(2):87.
[15] Oliphant K, Baker WE. Polym Engng Sci 1993;33(3):166.
[16] Tukachinsky A, Schworm D, Isayev AI. Rubber Chem Technol 1996;69:92.
[17] Levin VYu, Kim SH, Isayev AI, Massey J, Meerwall Evon. Rubber Chem Technol 1996;69:104.
[18] Isayev AI, Chen J, Tukachinsky A. Rubber Chem Technol 1995;68:267.
[19] Isayev AI, Yushanov SP, Chen J. J Appl Polym Sci 1996;59:803.
[20] Fujimoto K. Nippon Gomu Kyokaishi 1979;52:281.
[21] Creasey JR, Wager MP. Rubber Age 1968;100(10):72.
[22] Fujimoto K, Nishi T, Okamoto T. Int Polym Sci Technol 1981;8(8):T/30.
[23] Fujimoto K, Nishi T, Okamoto T. Int Polym Sci Technol 1981;8(8):T/65.
[24] Yasuda H, Marsh C, Brandt S, Reilly CN. J Polym Sci Polym Chem 1977;15:991.
[25] Zimmerman CJ, Ryde N, Kally N, Partch RE, Matijevic E. J Mater Res 1991;6:855.
[26] Blythe AR, Briggs D, Kendall CR, Rance DG, Zichy VJI. Polymer 1978;19:1273.
[27] Eaves JM. J Adhes 1973;5:1.
[28] Singh A. Potential modification of polyblends by irradiations. In: International Conference on Advances in Additives, Modifiers and Polymer Blends, Miami, Florida, 1992.
[29] Yu DW, Xanthos M, Gogos CG. Polym Mater Sci Engng 1992;67:313.
[30] Nasir M, Choo CH. Eur Polym J 1989;25(4):355.
[31] Baker CSL, Gelling IR, Newell R. Rubber Chem Technol 1994;58:67.
[32] Davis CKL, Wolfe SV, Gelling IR, Thomas AG. Strain crystallization on random copolymer produced by epoxidation of *cis*-1,4-polyisoprene. Polymer 1983;24:107.
[33] Grebenkina ZI, Zakharov ND, Volkova EG. Int Polym Sci Technol 1978;5(11):2.
[34] Gorton ADT, Pendle TD. NR Technol 1976;7(4):77.
[35] Kraus G. J Appl Polym Sci 1963;7:861.
[36] Cunneen JI, Russell RM. Rubber Chem Technol 1970;43:1215.
[37] Lorenz O, Parks CR. Rubber Chem Technol 1961;50:299.
[38] Sharapova LN, Chekanova AA, Zakharov ND, Borisova EYu. Int Polym Sci Technol 1983;10:4.
[39] Furtado CRG, Nunes RCR, De AS Siqueira Filho. Eur Polym J 1994;30(10):1151.
[40] Lewis, Nielsen LE. J Appl Polym Sci 1970;14:1449.
[41] Ahmed S, Jones FR. Composites 1988;19:277.
[42] Spanoudakis J, Young R. J Mater Sci 1984;19:487.
[43] Einstein A. Investigation on theory of Brownian motion. New York: Dover, 1956 (English translation).
[44] Edwards DC. J Mater Sci 1990;25:4175.
[45] Mathew G, Singh RP, Lakshminarayanan R, Thomas S. J Appl Polym Sci 1996;61:2035.
[46] Phadke AA, Bhowmick AK, De SK. Rubber Chem Technol 1985;58:4063.
[47] Mooney M. J Colloid Sci 1951;6:162.
[48] Payne AR. In: Krause G, editor. Reinforcement of elastomers. New York: Wiley-Interscience, 1965. p. 76.
[49] Nielson LE. J Comput Mater 1967;1:100.
[50] Guth E. J Appl Phys 1951;16:21.
[51] Bueche AM. J Polym Sci 1957;25:139.
[52] Wu TT. Int J Solids Struct 1966;2:1.
[53] Chow TS. J Polym Sci Polym Phys Ed 1978;16:959.
[54] Cohan LH. India Rubber World 1947;117:343.
[55] Brodnyan JG. Trans Soc Rheol 1959;3:61.
[56] Uragami T, Morikawa T, Okuno H. Polymer 1989;30:1117.
[57] Okuno H, Nishimoto H, Miyata T, Uragami T. Makromol Chem 1993;194:927.
[58] Rhim JIW, Yoon S, Kim SW, Lee KH. J Appl Polym Sci 1997;63:521.
[59] Amerongen GJV. Rubber Chem Technol 1964;37:1065.
[60] Hildebrand JH, Scott RL. The solubility of non-electrolyte. 3rd ed. New York: Van Nostrand Reinhold, 1950 (Dover, New York, 1964).
[61] Hildebrand JH, Scott RL. Regular solutions. Englewood Cliffs, NJ: Prentice-Hall, 1962.
[62] Ellis B, Welding GN. Techniques of polymer science. London: Society for Chemical Industry, 1964 (p. 46).